

Exploring streamer variability in experiments

PROEFSCHRIFT

ter verkrijging van de graad van doctor
aan de Technische Universiteit Eindhoven,
op gezag van de Rector Magnificus, prof.dr.ir. C.J. van Duijn,
voor een commissie aangewezen door het College voor Promoties
in het openbaar te verdedigen
op donderdag 6 december 2007 om 16.00 uur

door

Tanja Maria Petronella Briels

geboren te Weert

Dit proefschrift is goedgekeurd door de promotoren:

prof.dr. U.M. Ebert

en

prof.dr.ir. G.M.W. Kroesen

Copromotor:

dr.ir. E.M. van Veldhuizen

This work was financially supported by the Dutch Technology Foundation STW (project CMM. 6501) and by the Nederlandse Organisatie voor Wetenschappelijk Onderzoek, NWO (project 047.016.017).

CIP-DATA TECHNISCHE UNIVERSITEIT EINDHOVEN

Briels, Tanja M.P.

Exploring streamer variability in experiments / by Tanja M.P. Briels. - Eindhoven : Technische Universiteit Eindhoven, 2007. - Proefschrift.

ISBN: 978-90-386-1160-0

NUR 926

Trefwoorden: elektrische gasontladingen / gassen / hoogspanningspulsen / corona's / plasmadiagnostiek / optische meetmethoden / digitale fotografie

Subject headings: electric discharges / gases / pulsed power supplies / streamers / plasma diagnostics / plasma properties / high-speed optical techniques / digital photography

Copyright © 2007 T.M.P. Briels

All rights reserved. No part of this book may be reproduced, stored in a database or retrieval system, or published, in any form or in any way, electronically, mechanically, by print, photoprint, microfilm or any other means without prior written permission of the author.

Printed by Printservice Technische Universiteit Eindhoven, Eindhoven, The Netherlands.
Cover design by Verspaget & Bruinink. Figure 1.1, 3.4, 3.6, 5.1f and 6.5b of this thesis.
Background: 99.8% N₂ : 0.2% O₂, 1 bar, 34 kV, zoom to region 6.5-11 cm from tip in a 16 cm gap.

Contents

Summary	vii
1 Introduction	1
1.1 Streamers...	1
1.2 First view on streamers	1
1.3 State of the art of streamer observations	3
1.4 Motivation and scope of the thesis	10
1.5 Organization of the thesis	11
2 Physical mechanisms of streamer propagation and applications	13
2.1 Streamer initiation	13
2.2 Streamer propagation	14
2.3 Pressure dependence	17
2.4 Air and nitrogen	19
2.5 Typical length- and timescales, fields and densities	20
2.6 Applications	21
3 Stages of positive streamer evolution: time resolved measurements	23
3.1 Introduction	24
3.2 Experimental setup	24
3.2.1 MIPT-supply	25
3.3 Results	26
3.3.1 Streamer start	26
3.3.2 Streamer propagation	27
3.3.3 Other discharge processes	30
3.3.4 Other visual effects in photographs	33
4 Streamers of different widths	35
4.1 Introduction	36
4.2 Experimental setup and diagnostics	37

4.2.1	The two pulsed power supplies used	38
4.2.2	Diagnostic procedure	43
4.3	Results	45
4.3.1	The influence of voltage and gap spacing	45
4.3.2	The influence of the power supply	49
4.3.3	The velocity of different streamer types	52
4.4	Discussion and conclusions	53
4.4.1	Comparison of power supplies: the role of rise time and internal resistance	53
4.4.2	Thick and thin streamers, streamer branching	54
4.4.3	An estimate on the current density	55
4.4.4	Final remarks and theoretical challenges	56
5	Pressure dependence: an overview	59
5.1	Introduction	60
5.2	Experimental setup	60
5.3	Results	61
5.3.1	First observations	61
5.3.2	Scaling with $p \cdot d$	61
6	Streamers in air and nitrogen-oxygen mixtures	65
6.1	Introduction	66
6.2	Experimental setup	66
6.2.1	General information	66
6.2.2	Discussion on the setup	68
6.3	Diagnostics and data analysis	73
6.3.1	Camera	73
6.3.2	Spectrometer	74
6.4	Results	74
6.4.1	First observations	74
6.4.2	Spectral lines	79
6.4.3	Diameter and scaling with pressure	81
6.4.4	Velocity	83
6.4.5	Distance between branching events	86
6.4.6	Current and voltage	88
7	Streamers of different polarity	91
7.1	Introduction	92
7.2	Experimental setups and diagnostics	92

7.2.1	Point-plane gap	92
7.2.2	Plane-plane gap	93
7.2.3	Timing diagram C-supply	94
7.2.4	Power modulator	94
7.3	Results: point-plane gap	99
7.3.1	First observations	99
7.3.2	Negative streamer start	101
7.3.3	Diameter	104
7.3.4	Velocity	105
7.3.5	Current, voltage and energy	107
7.3.6	Nitrogen and air	109
7.4	Results: plane-plane gap	111
7.4.1	First observations	111
7.4.2	Current and voltage	114
8	Analysis and synthesis	117
8.1	Diameter	117
8.2	Velocity	124
8.3	Dissipated energy	126
8.4	Branching and multiple streamers	128
8.5	Streamer dependence on the oxygen:nitrogen ratio	131
8.6	Scaling with gas density or pressure	136
8.7	Start and propagation of streamers	139
8.7.1	The start of positive and negative streamers	139
8.7.2	Propagation of positive and negative streamers	142
8.8	Electric field and average electron energy	144
9	Conclusions and outlook	147
A	Overview of the parameter regimes in the setups	149
A.1	Experimental setups	149
A.2	Intensified CCD-cameras	149
	Bibliography	153
	Related publications	165
	Dankwoord	169
	Curriculum Vitae	171

Summary

Exploring streamer variability in experiments

The goal of this experimental investigation is to systematically explore differences in streamers under a large variety of conditions; this will form a basis on which theory can be tested and developed. Streamers are narrow, rapidly growing, weakly ionized channels. They can be created by applying a high voltage over a non-conducting medium such as air. Streamers are used in applications because highly reactive radicals are created in their ionizing front which are very suitable for cleaning purposes in water and gas (e.g. killing of bacteria, removal of phenol, NO_x, SO₂, fly ash, odor and tar). Also, in the ignition of so called high intensity discharge lamps streamers are found.

Although streamers show up in many desired or undesired places, especially at sharp tips where the electric field is enhanced, not many people have ever seen their wonderful appearance due to their low light intensity and short duration. They typically look like lightning but then with many more branches, like a tree. You can try to observe them in nature as sprite discharges high up in the atmosphere or as St. Elmo's fire on ships. The chances of hearing them are higher. They make a distinct hissing or buzzing sound as sometimes can be heard near high voltage lines.

This thesis focusses on the start and propagation of *primary* streamers. Parameters that are changed during the experiments are the streamer polarity (positive and negative), the electrode distance (10-160 mm) and shape (point-plane and plane-plane), voltage amplitude (1-96 kV) and rise time (12-150 ns), pressure (13-1000 mbar) and gas (air and nitrogen). An intensified CCD-camera with a time resolution of ~ 2 ns is used to photograph the discharge. Current and voltage are digitized on an oscilloscope.

A streamer is called positive (cathode directed) or negative (anode directed) depending on the polarity of the applied pulse (chapter 7). Time resolved photographs show that the positive and negative primary streamer propagation is built up of four stages: 1) a light emitting cloud at the electrode tip that evolves into 2) a thin expanding shell from which 3) one or more streamers emerge that 4) propagate through the gap. Positive streamers

go through stages 1 to 4 for voltages $V \geq V_{\text{inception}}$ (chapter 3). The negative streamer propagation needs a minimal critical voltage to go beyond stage 2 (chapter 7). This voltage appears to be around the DC-breakdown voltage in our experiments. The differences between positive and negative streamers disappear with increasing voltage as shown for streamers in a 40 mm point-plane gap in air at 1 bar:

- $5 \text{ kV} < V < 40 \text{ kV}$ ($\approx V_{\text{DC-breakdown}}$): The positive streamers are thin ($0.2\text{-}1 \text{ mm}^1$), bridge the complete electrode gap when $V \geq 20 \text{ kV}$ and branch. Their velocity ranges from 0.1 to 1 mm/ns . Negative streamers remain as a cloud near the electrode tip.
- $40 \text{ kV} < V < 56 \text{ kV}$: Positive and negative streamers have a similar thickness ($1\text{-}2 \text{ mm}$) only the negative streamers do not bridge the gap until a voltage of 56 kV is applied. The positive streamer velocity is $1\text{-}1.5 \text{ mm/ns}$.
- $56 \text{ kV} < V < 96 \text{ kV}$: Positive and negative streamers have a similar diameter ($2\text{-}3 \text{ mm}$) and energy ($20\text{-}50 \text{ mJ @ } 74\text{-}90 \text{ kV}$). Negative streamers are $\sim 20\%$ slower than positive streamers which have a velocity of $1.5\text{-}4 \text{ mm/ns}$.

The remainder of the summary is devoted to positive streamers since they are easier to create at sharp tips than negative ones because of their lower inception voltage.

Positive streamers become gradually thicker and faster with increasing voltage (chapter 4). For ease of comparison they are labelled type 1 to 4 based on their diameter. In a 40 and 80 mm electrode gap and voltages between $5\text{-}60 \text{ kV}$ in air these values are:

- Type 1 streamers are very thick with a diameter of about 2.5 mm , their velocity is just over 1 mm/ns and they carry currents of up to 12 A . Their current density is about 2.4 A/mm^2 . They are created when $V > 40 \text{ kV}$.
- Type 2 streamers are thick with a diameter of about 1.2 mm , a velocity of 0.5 mm/ns and currents of the order of 1 A . Their current density is about 2.4 A/mm^2 . They are created when $V \approx 40 \text{ kV}$ ($\approx V_{\text{DC-breakdown}}$).
- Type 3 streamers are the thinnest streamers found. Their diameter is 0.2 mm , their velocity is $\sim 0.1 \text{ mm/ns}$, their current $\sim 10 \text{ mA}$ and their current density is about 0.5 A/mm^2 . They are created when $V_{\text{inception}} \lesssim V < 40 \text{ kV}$.
- Type 4 streamers are late, they start to propagate after streamers of type 1 or 2 have crossed the gap, their diameter appears to be similar to type 3 streamers, their velocity and current could not be determined but are expected again to be similar

¹The first value corresponds to the lowest voltage in this range, the last value to the highest voltage.

to type 3 streamers. Type 4 streamers occasionally connect to the already existing streamer paths of type 1 or 2.

The number of streamers and branches increases up to the moment that approximately the DC-breakdown voltage is applied. At higher voltages the number of streamers and branches decreases with increasing voltage. Type 1 or 2 streamers can branch into thinner ones (type 2 or 3) provided that the electrode gap is long enough. Type 3 streamers branch often but they keep (approximately) the same diameter. In our small point-plane gaps (≤ 40 mm) the streamer diameter usually remains constant. Only at voltages higher than 40 kV the diameter seems to be slightly thinner near the electrodes. A thin streamer can arise via branching but it can also directly be created when a voltage just above the inception voltage is applied or when an impedance is added to the circuit such that the voltage pulse has a long rise time (> 60 ns) and the streamers start before the voltage has reached its maximal amplitude. In general, it seems that diameter and velocity are related since a certain diameter has a certain velocity regardless of where the streamer propagates in the gap. The streamer properties depend on the local electric field as is usually assumed in numerical models.

Differences between positive streamers in ambient air and nitrogen (N_2 , purity 99.9%) in a pressure range of 13-1000 mbar are investigated in a point-plane gap (chapter 6). Positive streamers in nitrogen are 1) thinner, 2) curlier, 3) more intense and 4) less diffuse than streamers in air. They also 5) branch more resulting in 6) a shorter distance D between branching events and 7) they propagate further down the electrode gap. The branches that deviate from the main channel however 8) die out closer to this channel.

The measurements are used to search for experimental evidence of the theoretical expectation that lengths and times scale with inverse pressure p (chapter 5 and 6). These results can be extrapolated to sprites at an altitude of 80 km in the atmosphere where the pressure is $\sim 10^{-2}$ mbar.

- For the minimal diameter d the relation $p \cdot d = 0.20 \pm 0.02$ mm·bar for air and $p \cdot d = 0.12 \pm 0.02$ mm·bar for N_2 is found. The estimated minimal value for sprites is 0.1-0.3 mm·bar.
- The ratio D/d gives a value of $D/d = 11.6 \pm 1.5$ for air and $D/d = 9.1 \pm 3.3$ for N_2 .
- The experiments in air and N_2 show that the streamer velocity v increases about 0.1-0.2 mm/ns with decreasing pressure while the scaling theory predicts that v is independent of p . Here it must be noted that the measurements are done on minimal, type 3 streamers and type 2 streamers.

In a 10 mm plane-plane gap, discharges are initiated by focussing and shooting a laser on the top plate (chapter 7) when a voltage near the DC-breakdown voltage is applied. On

the photographs only negative discharges that consist of a streamer and evolution to glow are seen; no positive discharges can be photographed except for sparks. This is unexpected since both polarities show a streamer peak in the current signal of similar amplitude (1-10 mA for pressures of 100-1000 mbar). In the negative current pulse the evolution to glow is also visible while this does not exist for positive discharges. Perhaps the streamer light is too faint compared to the laserspot and only the glow is seen on the pictures. It must be noted though that primary streamers in a point-plane gap are not overexposed by laserlight when the laser is shot to the needle tip. Current and voltage evolutions in the plane-plane gap furthermore show that positive and negative streamers in N₂ and air at different pressures are created at a similar reduced electric field of 20 ± 5 kV/(cm·bar).

This thesis gives insight into streamer start, propagation and branching behavior. Its measurements are in good agreement with various experimental results reported in the literature which makes the broad parameter study reliable and suitable for comparison with results from analytical theory and numerical simulations.

The conclusion of this thesis is that there is *one* kind of streamer whose properties vary gradually with voltage, pressure and circuit impedance as long as measurements are done in *one* gas and with *one* polarity, where it must be noted that the differences between positive and negative streamers decrease with increasing voltage. When measurements are done in different gases, different minimal diameters, velocities, distances between branching events, breakdown voltages, etc. are found. The experiments have verified that lengths scale with inverse pressure even when streamers are ignited at an electrode at (near) atmospheric pressure: conditions that according to theory will break the scaling law since the electrode is not scaled with pressure and the nitrogen states that emit the photons that are used for photoionization are quenched at pressures above ~ 40 mbar. A last conclusion is that streamers made in different setups show similar patterns and diameters as long as the voltage rise time, peak voltage and internal resistance are similar.

Chapter 1

Introduction

1.1 Streamers...

Streamers are a phenomena that most people have never heard of or seen but they occur frequently in every day life. Streamers - usually invisible by eye - prepare the path of sparks of all sizes; from the static electric shock when you touch someone to the beautiful large scale spectacle of lightning. With luck they are seen as the so-called sprite discharges in the region of 40-90 km altitude above thunderclouds. In industry streamers are found in applications that are based on the deposition of electrical charge or on molecular excitations in the streamer head that initiate chemical processes. The coupling of moving space charge regions to gas convection is under investigation for possible applications.

Although streamers are formed on many desired or undesired occasions they are still not fully understood and usually their appearance is just considered a fact.

1.2 First view on streamers

When a high voltage is applied over a non conducting gas volume the gas will become ionized. The ionization will typically not occur homogeneously but in the form of extending channels, so called streamers (figure 1.1). These streamers are narrow and grow rapidly. An ultrafast, high resolution camera is needed to visualize them.

Figure 1.1 shows four pictures taken by such a camera with different exposure times of positive streamers that emerge from a point electrode at the upper left corner of the photographs¹ and propagate towards a plate electrode at the bottom of the pictures. The left picture with an exposure time of 300 ns shows the filamentary structure of the frequently branching streamers. The right picture with an exposure time of 2 ns shows that not the complete channels emit light but only the actively growing heads. The light trace that

¹Most photographs are shown in false color in the digital version.

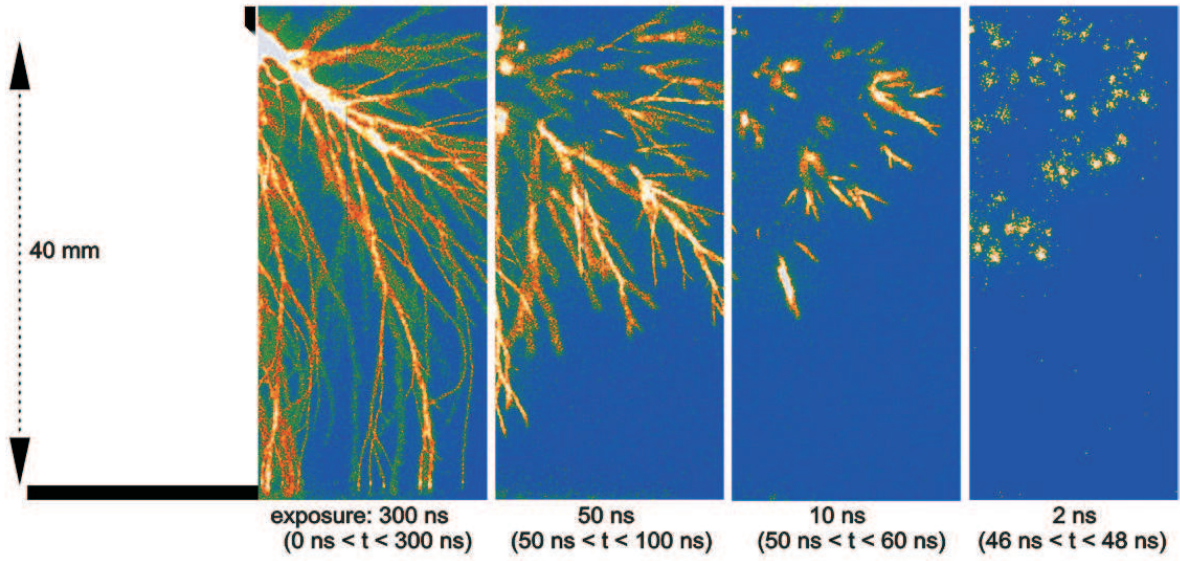


Figure 1.1: *Intensified CCD photographs of positive streamers in ambient air in a 40 mm gap between a point (top) and plate (bottom) electrode. Applied voltage 28 kV. The exposure times are 300, 50, 10 and 2 ns; the actual time intervals are given in brackets where $t = 0$ is the approximate time when the streamers emerge from the upper electrode.*

is seen on photographs must thus be interpreted as the path that the streamer head has followed during the exposure time of the camera. Then it can also be concluded that the streamers in figure 1.1 need more than 100 ns but less than 300 ns to cross the 40 mm electrode gap. The fact that only the streamer head emits light tells us that at that place highly energetic electrons are present which can ionize and excite neutral gas molecules since it is the light emitted by the decay of the excited states (within 1-2 ns, section 1.4) that is visible on the photographs. A crucial element in streamer propagation is the enhancement of the electric field at the streamer head. This concept was originally proposed in the 1940's [57; 65; 89] where it was assumed that the space charge was smeared over the complete head. Later simulations [25; 26; 33; 68; 70; 121] however have shown that the space charge can be concentrated in a thin space charge layer that leads to screening of the electric field from the streamer interior and a much stronger field enhancement immediately in front of a strongly curved head.

The enhanced electric field at the tip makes it also possible for the streamer to propagate into regions where the background electric field is too low for efficient ionization and thus propagation. In this way the streamer can be compared to fractures in solid media where the mechanical force is focussed at the tip of the fracture line.

1.3 State of the art of streamer observations

Experiments found in literature show that streamers created under different circumstances (different experimental setups and/or investigators) have different diameters, velocities and/or branching behavior as will be elaborated below. Industry uses these different streamers to optimize their product. In simulations authors use different models with e.g. different boundary conditions on the electrode and different initial electron distributions which results in different streamer properties. Because of all these different observations, it is desired to have a unifying approach to systematically explore differences due to e.g. applied voltage, the polarity of the streamer head, pressure, gas and distance between electrodes and/or electrode configuration in *one* setup and compare if streamers are reproducible in other setups. This will be the topic of this thesis.

Polarity

A streamer can be positive (cathode directed) or negative (anode directed). About 90% of cloud-to-ground sparking is preceded by negative streamers and leaders [116]. Man-made discharges are positive or negative depending on their application. In dust precipitators negative discharges are used to charge the dust which then can be removed from the gas by applying a low electric field [104]. In gas and water cleaning and in ozone generation positive streamers are used since in earlier work these streamers gave the best results [104]. Recent investigations however show that negative streamers can have a higher oxygen radical yield, necessary for ozone generation [119]. Most experiments are done on positive streamers since they are emitted from strongly curved electrodes at a much lower voltage than negative ones. In this thesis also mainly positive streamers are discussed unless indicated otherwise.

Voltage

Different streamer diameters have been reported in literature which are created in different experimental setups at different voltages. Two examples are shown in figure 1.2. In figure 1.2a thin, frequently branching streamers at 25 kV with a diameter of 0.2 mm in a 25 mm point-wire electrode gap at 1000 mbar are shown [106]. Figure 1.2b is a top view picture of thick streamers at 100 kV with a diameter of 10 mm in a wire-cylinder electrode configuration with a diameter of 290 mm at 480 mbar [9]. The streamers start at the wire in the middle of the picture and propagate outward to the cylinder wall which they have almost reached. The photograph is taken 40 ns after the voltage pulse is applied with an exposure time of 5 ns.

The velocity of the streamers also varies with voltage. Because it is only the streamer head

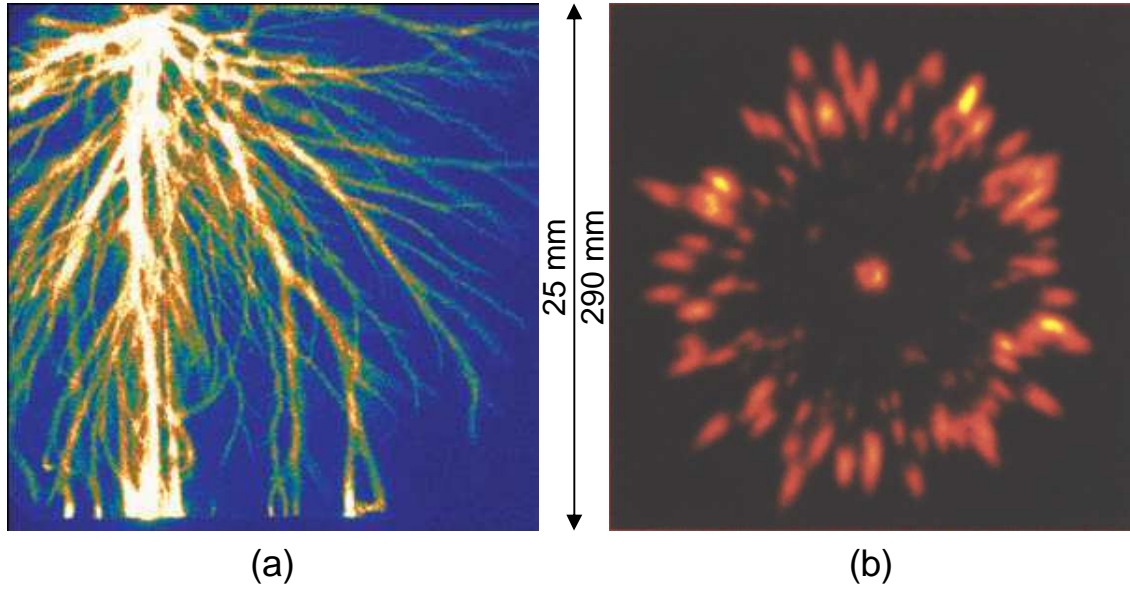


Figure 1.2: a) *Positive streamers of 0.2 mm in diameter in a 25 mm point-wire gap at 25 kV at 1000 mbar in air. Photograph is taken from [106].* b) *Thick positive streamers with a diameter of 10 mm in a wire-cylinder gap with a diameter of 290 mm at 100 kV and 480 mbar in air. Photograph b) is taken from [9].*

that emits light, figures that show complete channels must be interpreted as the trace that the streamer head has followed during the exposure time of the camera. In this way the velocity can be calculated by dividing the length of the light trace of the streamer by the exposure time. In figure 1.1 this means that the thin streamers have a velocity of ~ 0.6 mm/ns while the thick streamer velocity in figure 1.2b is ~ 4.5 mm/ns.

Electrode gap length

Also the electrode gaps used in experiments vary a great deal; either small gaps of ≤ 30 mm [80; 100; 106; 108; 109] or large gaps of ≥ 100 mm [9; 119; 123] are used for streamer studies. Hardly any studies of intermediate gaps are found. For leaders and lightning studies the gap will be in the order of meters [18; 91]. Usually thin streamers of ~ 0.2 mm appear in a small gap (figure 1.2a) and thick streamers, with diameters larger than 1 mm, in a large gap (figure 1.2b).



Figure 1.3: *Streamers in a 25 mm a) protrusion-plane gap and b) point-wire gap at 12.5 kV, 1000 mbar air, both pictures are taken from [106].*

Shape of electrodes

The shape of the electrodes alters the propagation of the streamers, as can be seen in figure 1.3. The streamers in the protrusion-plane gap² (figure 1.3a) propagate less outward than the streamers in the point-wire gap (figure 1.3b). This is due to the local electric field. From the plotted equipotential lines in figure 1.4a it can be concluded that the local electric field in the protrusion-plane gap is rather homogeneous except very close to the protrusion. Since the streamers follow the electric field lines - thus propagate perpendicular to the equipotential lines - they hardly spread. It must be noted though that the streamers do not need to follow the field lines exactly since the space charge can modify the background field. In the point-wire gap the electric field lines spread outward, just like in the point-plane gap, and thus the streamers spread outward as shown in figure 1.3b. Other electrode configurations that are often used, especially in gas and water cleaning, are the wire-cylinder [9; 20] and wire-plate [20; 40; 110; 119]. Theory and simulations are often performed in a homogeneous electric field, e.g. [33; 69; 84]. In experiments a homogeneous electric field is created between parallel plates (plane-plane gap). The spontaneous ignition of streamers is facilitated with increasing sharpness of the starting electrode.

²A protrusion-plane gap is a plane-plane gap with a sharp needle sticking out of one of the electrodes to facilitate the streamer inception, figure 1.4a.

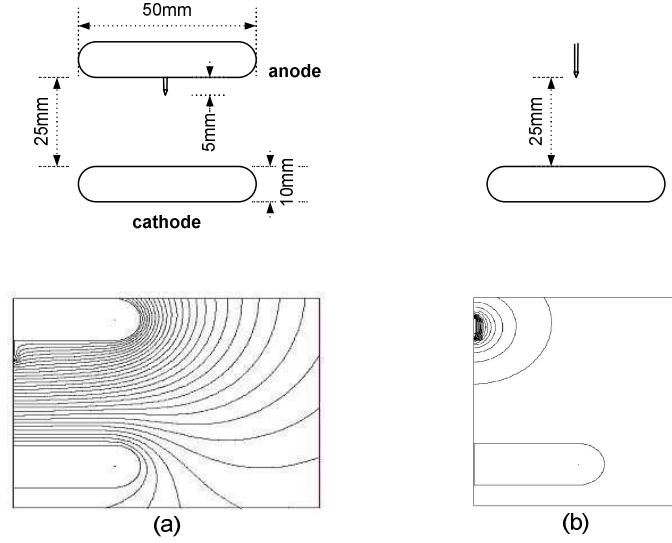


Figure 1.4: a) *Protrusion-plane* and b) *point-plane* electrode configuration. Below each gap an indication is given of the equipotential lines. This figure is taken from [108].

Electric circuit

Another aspect that can influence the streamer diameter is the electric circuit. Elements in the electric circuit like the length of the connecting wires (self inductance) or resistors can change the voltage rise time [106]. When the rise time is long compared to the inception and transit time between the electrodes the streamers might already start when the voltage is still rising and thus are created at a lower instantaneous voltage than the saturation value.

Pressure

Streamers become thicker with decreasing pressure. This is a result of the electron mean free path which determines the streamer scales. Theoretically, it scales inversely proportional with the gas particle density. The gas particle density can be substituted by pressure via the ideal-gas equation provided that the temperature is constant. Because of this scaling law, sprites (figure 1.5, [35; 36]) with a diameter of ~ 50 m at ~ 80 km altitude can be regarded as an upscaled version of laboratory streamers at 1 bar with a diameter of 0.5 mm at 30 kV in a 40 mm point-plane gap [82]. When comparing the photograph of sprites in figure 1.5b with a photograph of streamers in figure 1.2a the discharge channels have a remarkably similar structure.

A consequence of scaling with pressure is that at low pressure the electrode gap has to be enlarged to see the complete streamer structure because *all* length scales within the discharge scale with pressure (and not only the diameter). Else only a thick glowing channel

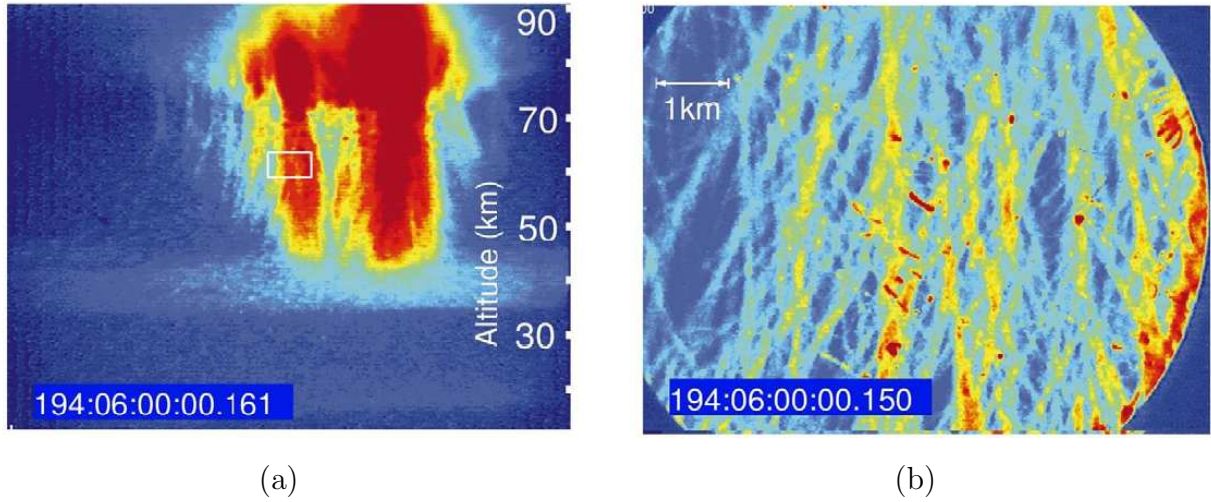


Figure 1.5: *Telescopic image of a sprite discharge. The right photograph zooms into the white rectangle of the left photograph. These pictures are taken from [35].*

without any structure (figure 1.6a) or a spark³ (figure 1.6b) can be seen. These phenomena arise more frequently at low pressure where less voltage is needed to create overvolted gaps⁴. When then the pulse duration is long, the streamer can evolve into a glow and via glow evolve into a spark. So, when the gap is not enlarged at low pressures one may conclude that streamers are different with varying pressure while actually different temporal stages of the discharge are shown: a streamer, a glowing channel or a spark.

For completeness, in figure 1.7 a current voltage evolution of the streamer, glow and spark in an overvolted gap are shown. In the current signal the different phases are clearly distinguishable:

- 1) a capacitive peak (the result of how the voltage is set over the electrode gap), nothing is visible on the camera
- 2) a short streamer current peak
- 3) a long glow
- 4) a spark.

In the voltage signal the streamer propagation can show a small dip depending on current through and internal resistance of the discharging circuit but usually it remains unnoticed. The glow gives a noticeable decrease in voltage which shows that the channel is conducting

³The main difference between a streamer and a spark is that a spark is significantly hotter than a streamer and has a much better electrical conductivity.

⁴An overvolted gap is created when the applied voltage is higher than the DC-breakdown voltage. The DC-breakdown voltage is the voltage at which a spark is formed when a DC-voltage is applied.

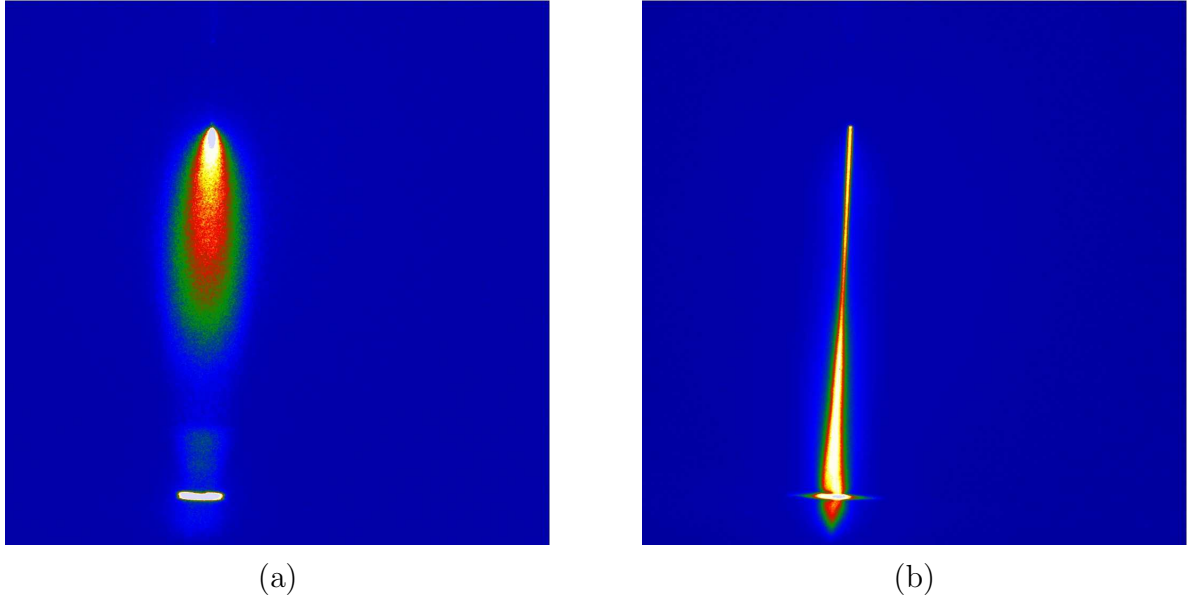


Figure 1.6: *Positive discharge in ambient air in a 17 mm point-plate gap. a) Streamer and glow at 100 mbar, applied voltage 3 kV. b) Spark at 200 mbar, applied voltage 7 kV. The pictures are taken from [13].*

where the decay of the voltage signal depends on the conductivity of the channel. A spark is a highly conducting channel and therefore the voltage drops almost immediately to zero while the current increases rapidly to the maximum that the power supply can deliver.

Gas

The composition of the gas can also alter the streamer's appearance. Most experiments are done in air since all natural discharges occur in air and it is mostly used in applications. The streamers then propagate in channels as can be seen in most figures in this section. In figure 1.8a Yi and Williams [123] show that streamers in pure nitrogen propagate as a "cloud". Apparently streamers propagate in channels when 15% oxygen is added to the pure nitrogen, figure 1.8b. Differences are observed when a composite gas is used (e.g. air) or a pure gas, which can either be molecular (e.g. pure nitrogen) or a atomic (e.g. pure argon). This is due to processes such as photoionization, electron attachment or the excitation of rotational and vibrational states [109].

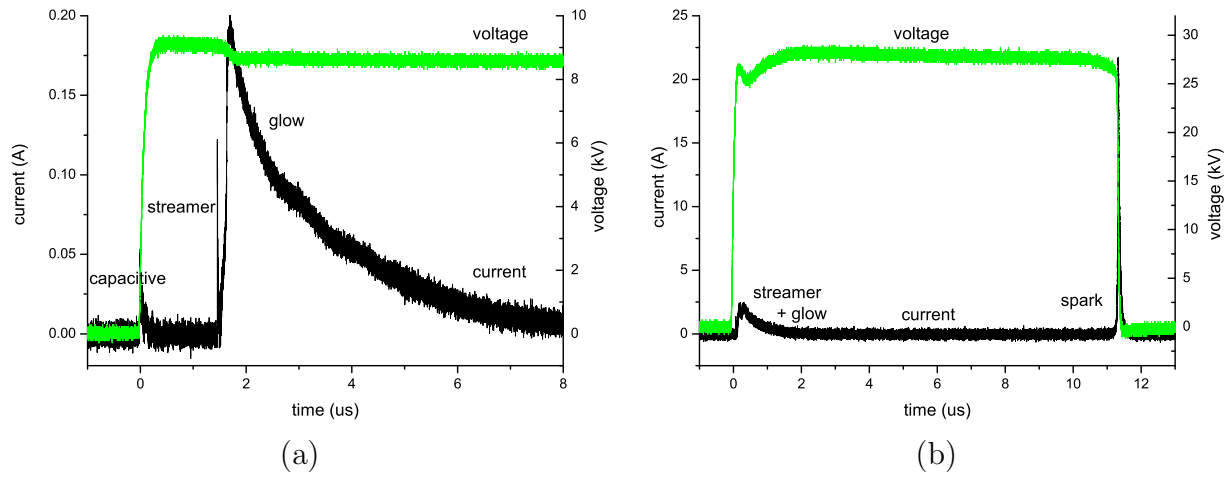


Figure 1.7: *Current voltage evolution of discharges in air in a 40 mm point-plane gap. a) Streamer and glow at 9 kV, 200 mbar and b) streamer, glow and spark at 29 kV, 400 mbar.*

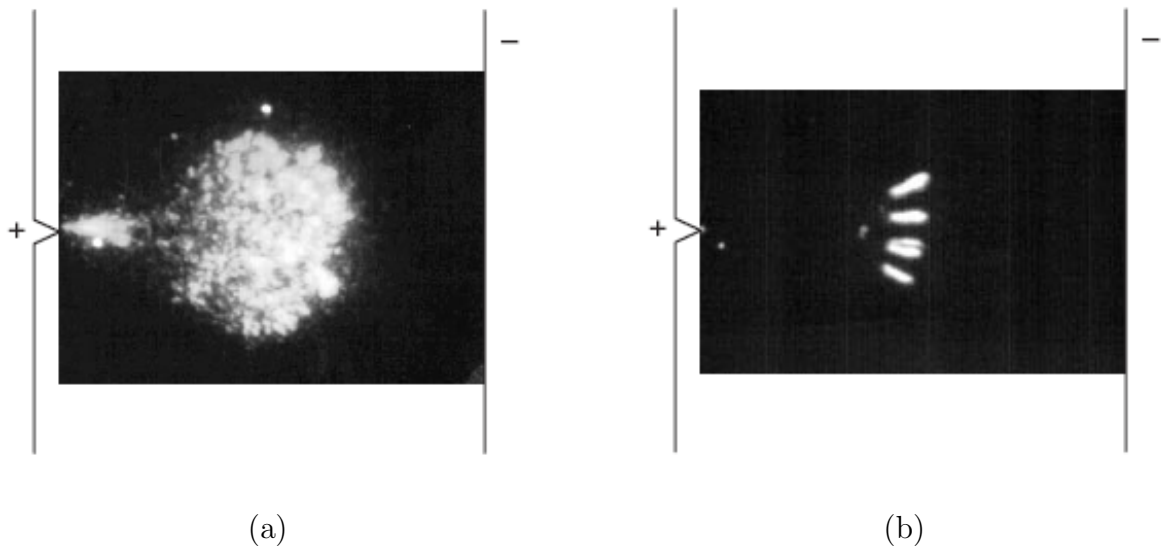


Figure 1.8: *Positive streamers in a 130 mm gap in a) pure N_2 and b) $N_2:O_2$ mixture containing 15% O_2 . The pictures are taken from [123].*

1.4 Motivation and scope of the thesis

Many measurements and observations are done under (extreme) conditions in which only a few parameters can be varied: e.g. a very high voltage applied over a large gas volume (gas cleaning), in very small electrode gaps at low voltages (experiments), at very low pressure (sprites), etc. To investigate the transitions of one regime to another an experimental setup has been built in the Physics Department of the Eindhoven University of Technology (TU/e). On this setup extra parts can easily be mounted or removed to switch between interesting streamer regimes. The measurements remain comparable since it stays the same setup.

- (1) The large vacuum vessel gives the opportunity to investigate all inter-electrode distances from a small 10 mm gap to a large 160 mm gap to see the full development of the streamer even when the pressure is decreased.
- (2) The voltage across the gap is applied as a short pulse to be able to work in overvolted gaps without creating a spark. Sparking must be avoided since it can damage the light sensitive camera (due to the bright light) or the setup equipment (due to the large currents and power input in the setup components). The pulse duration can be changed from one μs to several ms.
- (3) The voltage rise time can be varied from 25 to 150 ns. When the voltage rise time is large compared to the evolution of the streamer, streamers can initiate in the rising slope of the voltage pulse. These streamers have different properties than streamers that start when the total applied voltage is already set across the gap. The rise time is kept as short as possible to maintain a clear physical picture.
- (4) The electrode configuration, which in experiments usually is an inhomogeneous point-plane configuration can be changed to a homogeneous plane-plane configuration triggered by a laser, which makes the discharge independent of voltage rise time. By using a laser the electrode tip which still distorts the electric field in the protrusion-plane gap can be removed. The plane-plane configuration is more convenient for comparison with theory.
- (5) The pressure can be varied between 13 mbar and 1000 mbar to test scaling with pressure, which can be extrapolated to sprites at 80 km altitude, i.e. a pressure of $\sim 10^{-2}$ mbar. Because of the scaling law, pressure can also be used as a magnifying glass and slow motion player to zoom into streamer parts that need extra attention, e.g. the start of (branching of) the streamer.
- (6) The voltage pulse amplitude can be changed from 1 kV to 60 kV to study thin and thick streamers and a possible transition regime between them.
- (7) Differences between gases can be investigated. Here we focus on air and nitrogen because air is the gas that is most common in nature and mostly used for applications; nitrogen is studied since it is the main component of air but also because it is a simple non-attaching molecular gas and measurements can ease comparison with theory.

(8) A fast intensified CCD camera with an exposure time down to ~ 2 ns in combination with low jitter in the setup (≤ 10 ns) can be used to examine the temporal streamer development. This camera can resolve the short time structure of streamers in air and nitrogen at atmospheric pressure down to the physical limit because in air and nitrogen the C-B transition of N_2 dominates the streamer light emission. The lifetime of the C-state is of the order of 1-2 ns at atmospheric pressure. Therefore further improvement of the temporal resolution of the camera does not improve the temporal resolution of the picture.

(9) The polarity of the streamer can be changed by reversing certain components in the setup. There is especially a lack of experiments on negative streamers since these are more difficult to generate.

Additional measurements are done in a 40 mm point-plane electrode gap without surrounding vacuum vessel at the Electrical Engineering Department of TU/e to examine positive and negative streamers in a voltage range of 40 kV to 96 kV and a fast voltage rise time of 15 ns. At the Moscow Institute for Physics and Technology (MIPT) several of the above conditions are tested to see whether streamers are reproducible when done in another setup.

All these measurements should give us insight into streamer behavior, propagation and branching over a large range of parameters so that predictions can be made for regimes in which it is not possible to do measurements (e.g. sprites) or that industry does not have to test by trial and error what adjustments they have to make for e.g. the most efficient gas cleaning. They form a standard on which theory can be tested and developed.

1.5 Organization of the thesis

In chapter 2 the physical mechanisms that are necessary to comprehend streamer propagation are described. Chapter 3 visualizes the start and propagation of the positive streamer by using time resolved measurements and zooming in to the discharge by decreasing pressure. It also shows qualitatively that voltage can be used to play with streamer thickness. Also phenomena that appear on photographs but do not belong to the primary streamer propagation are bundled and given in this chapter. Chapter 4 studies quantitatively the positive streamer diameter by varying the voltage amplitude and rise time of the electric circuit. Chapter 5 visualizes differences in positive streamer appearance when the pressure is varied. Also scaling of the positive streamer diameter with pressure is introduced which will be quantified in chapter 6 where differences and similarities between positive streamers in air and nitrogen are discussed. Chapter 7 studies positive and negative streamers which are mainly created at atmospheric pressure in air. This chapter also contains measurements on streamers between parallel plane electrodes. All other chapters show streamers

in a point-plane electrode configuration. In chapter 8 an analysis and synthesis of the results are given. In chapter 9 the main conclusions are drawn.

The thesis does not contain a separate chapter about experimental setups. These details are described in the chapters where that specific setup configuration is used. The main setup at the Physics Department, that is used to generate and visualize the positive streamer dependence over the large parameter range as given in section 1.3, is thoroughly described in chapter 4. Additional measurements for positive and negative streamers at voltages between 40 to 96 kV are done at the Electrical Engineering Department of the Eindhoven University of Technology. This point-plane setup without surrounding vacuum vessel is described in chapter 7. To see whether the comprehension of the streamers in the Physics Department can be used universally, test measurements are done at the Moscow Institute for Physics and Technology (MIPT) in Moscow. This setup, with a small vacuum vessel and fast (12 ns rise time) voltage pulse shape, is described in chapter 3. Although the setup is very different, the streamers show similar, predictable behavior compared to our own streamers; the streamers are reproducible. A complete overview of the possibilities of the different setups is given in Appendix A.

The values of the variables and dimensions used in this thesis are given such that most values are between 0 and 100. It is tried as much as possible to keep the same dimension for one variable throughout the thesis. In general the following dimensions are used: electrode gap in mm, pressure in mbar, diameter in mm, velocity in mm/ns, voltage in kV, electric field in kV/cm, current in A and energy in mJ.

Chapter 2

Physical mechanisms of streamer propagation and applications

2.1 Streamer initiation

The creation of a streamer starts with the acceleration of free electrons through an electric field between two electrodes in a non conducting gas. These free electrons can be liberated from a cathode tip but they can also be present in the background gas as a result of cosmic radiation, radioactivity or detachment from negative ions. The normal level of this background ionization is $n_e = 10^3 \text{ cm}^{-3}$ at STP¹ [77]. When such a free electron propagates through an electric field, it gains energy which can be used to free another electron from its molecule by electron impact ionization if the ionization threshold energy is reached. When assuming that an electron travels $\sim 3 \text{ }\mu\text{m}$ at 1000 mbar before colliding with a molecule and it needs $\sim 10 \text{ eV}$ to ionize it, the electric field has to be $\sim 33 \text{ kV/cm}$ to obtain impact ionization. In practice the electric field in air is sufficient for ionization at $\sim 30 \text{ kV/cm}$ [90] where a balance between generation and absorption is obtained. Then two electrons propagate through the electric field, gain energy and ionize two other molecules resulting in a total of four free electrons and so on. In this way an electron avalanche is created, as was first described by Townsend [91; 101; 104]. The avalanche regime can go over into a space charge dominated streamer regime. Experiments and derivations indicate that the transition from avalanche to streamer occurs frequently when the number of free ions or the electrons in the electron avalanche is in the order of $10^8 - 10^9$ (Raether-Meek criterion) [57; 65; 89]. However, this derivation does not take electron diffusion into account which will suppress streamer formation in low electric fields [68; 69]. Simulations show that when diffusion is taken into account the criterion saturates to 10^6 at 1 bar in overvolted gaps

¹STP = standard temperature and pressure, i.e. 293 K and atmospheric pressure. The particle density of the background gas is $n_g = 2.5 \cdot 10^{25} \text{ m}^{-3} = 2.5 \cdot 10^{19} \text{ cm}^{-3}$.

($V_{\text{applied}} > V_{\text{DC-breakdown}}$ ²) and reaches values larger than 10^{16} in undervolted gaps, where the propagation is diffusion dominated [68; 69]. When the criterion is reached the space charge electric field, generated by the separation of the electrons and their ions, is similar to the applied background electric field and the streamer can start propagating as a result of its own generated electric field.

2.2 Streamer propagation

Townsend's avalanche theory turned out to be unsuitable to explain the further propagation of the streamer since experiments showed that streamers would also run in much lower applied electric fields of ~ 5 kV/cm, where the field is too low for ionization. Raether, Loeb and Meek [57; 65; 88; 89] suggested then that a plasma channel propagates through an electrode gap by ionizing the gas in front of its charged head owing to a strong field at the head itself (higher than ~ 30 kV/cm), the space charges here being smeared out over the complete streamer head. Later simulations [33; 68; 70] show that there is indeed an enhanced electric field at the streamer head which takes care of the propagation of the streamer through low fields. But they show that the space charge is not in the complete head but in a thin layer at the front of the streamer. Therefore field enhancement can be stronger.

Streamers can be positive (cathode directed) or negative (anode directed). Since their propagation mechanism is different a distinction must be made between both polarities.

Negative streamers

Negative discharges are created when the electric field at the cathode is enhanced due to its sharp tip. The electrons necessary for streamer propagation come from the cathode tip (when the applied voltage is larger than the work potential of the cathode material) or are created in the streamer head: a thin shell of space charge. The electric field is enhanced directly ahead of the space charge [33; 68] and the free electrons are accelerated towards the anode.

Here a distinction must be made most likely based on the voltage applied to the needle. Streamer channels are found in a 130 mm protrusion-plane gap at a voltage of 123 kV in N_2 [123] and in a 37 mm wire-plane gap at 61 kV in air [119] but not in a 25 mm point-plane gap at 12.5-25 kV in air [107]. In the first two cases the streamers propagate in the same direction as the electrons (figure 2.1a). In the last case the discharge remains as a cloud (with a height of 2 mm) near the tip.

²The DC-breakdown voltage is the voltage at which a spark is formed when a DC-voltage is applied.

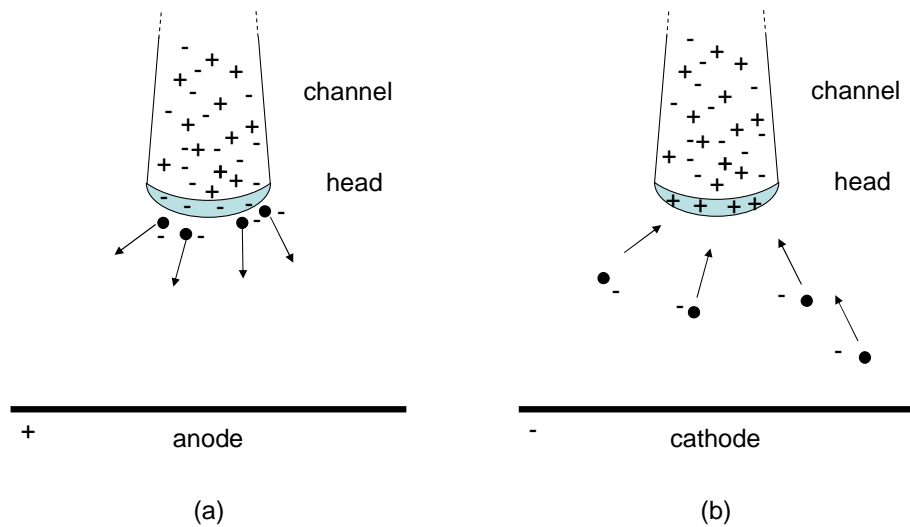


Figure 2.1: a) Negative and b) positive streamer propagation from point to plane at some distance from the point electrode (not shown).

Positive streamers

Positive streamers are created when the electric field at the anode is enhanced. In this case electrons propagate towards the positive streamer tip (figure 2.1b). As the electrons are absorbed into the streamer, continuously new electrons need to be generated ahead of the streamer. These new electrons are provided by the streamer itself. For streamers in air-like mixtures it is generally believed that photoionization of oxygen is the electron source, e.g. [104; 116]. Besides ionizing molecules, energetic electrons in the streamer head can excite molecules. Some of these excited states can decay directly upon radiating a photon. Ionization of oxygen directly through photons is possible at wavelengths ≤ 102.5 nm. Nitrogen absorbs radiation with a wavelength < 98 nm [126]. Therefore, photons must have an energy between 12.1 and 12.7 eV for photoionization (figure 2.2). These photons come from the excited states of nitrogen. The so created electrons can start an avalanche which will move towards the positive tip leaving new positive ions behind. Note that the process of photoionization can also take place in negative streamer propagation only it is not required since there is no "electron loss" as in the positive streamer propagation. Note furthermore that electron detachment and background ionization are other mechanisms to provide electrons next to photoionization. This is still under debate in the literature.

Additional considerations concerning propagation

Residues stay behind like ions or metastables when streamer discharges follow each other up fast. This pre-ionization can facilitate subsequent discharges. Simulations by Pancheshnyi [79] suggest that a discharge in air can be considered as a single shot discharge for frequencies $< 10^{-2}$ Hz at 1000 mbar or frequencies < 0.1 Hz at 100 mbar for a 20 mm point-plane electrode gap. The influence of the repetition rate can be suppressed by gas flow as shown in experiments by Winands [119] in a ~ 60 mm wire-plane gap where no visual differences in streamer pattern are found between the first shot and the n^{th} shot when measurements are performed up to a pulse repetition rate of 400 Hz and a gas flow rate of 30 m³/h in a volume of ~ 0.02 -0.04 m³. Simulations furthermore show that in nitrogen-oxygen mixtures the "background" pre-ionization by cosmic radiation or accumulation of charged particles (up to 10^7 cm⁻³) can be neglected when photoionization is taken into account [77]. When there is no photoionization an inexplicably high "background" pre-ionization of 10^7 cm⁻³ is necessary to obtain similar values for the streamer velocity, reduced electric field and conductivity current as with photoionization.

It is observed in many experiments at STP that electric fields higher than the so called stability field³ of 4.4 - 5 kV/cm are necessary for the positive streamer to propagate in point-plane and plane-plane gaps in air with an interelectrode distance varying between 5 - 600 mm [4; 90] (and references therein) and ~ 1.5 kV/cm in nitrogen (up to 2% oxygen) [90]. According to [90], the value of the stability field is very sensitive to attachment. Since electrons are removed from the process in electronegative gases higher energies and electric fields are necessary to obtain the same amount of free electrons as in an electropositive gas. For negative streamers the stability field is two to three times higher [6]. Also the applied electric field must be higher to ignite negative streamers [90]. According to calculations in [6] the differences between positive and negative streamers decrease with increasing electric field strength.

The light emitted by the excited particles in the streamer head in air and nitrogen that is visible on the intensified CCD camera mainly comes from the so called Second Positive System (SPS) and First Negative System (FNS) of nitrogen (figure 2.2) [20]. These systems send out light in a wavelength band centered at 337 nm and 391 nm, respectively [20; 81; 85]. Since the degree of ionization is low, in the order of 10^{-5} , the electron energy distribution function is often approximated by either a Maxwellian or a Druyvesteyn distribution. Since the energy level of the $N_2^+(B)$ state is higher than that of the $N_2(C)$ state (figure 2.2), the density of the $N_2^+(B)$ state will be much lower than the density of the $N_2(C)$ state. Hence the SPS is in favor of the FNS.

³The stability field is the lowest applied electric field that is necessary for streamer propagation once the streamers are created.

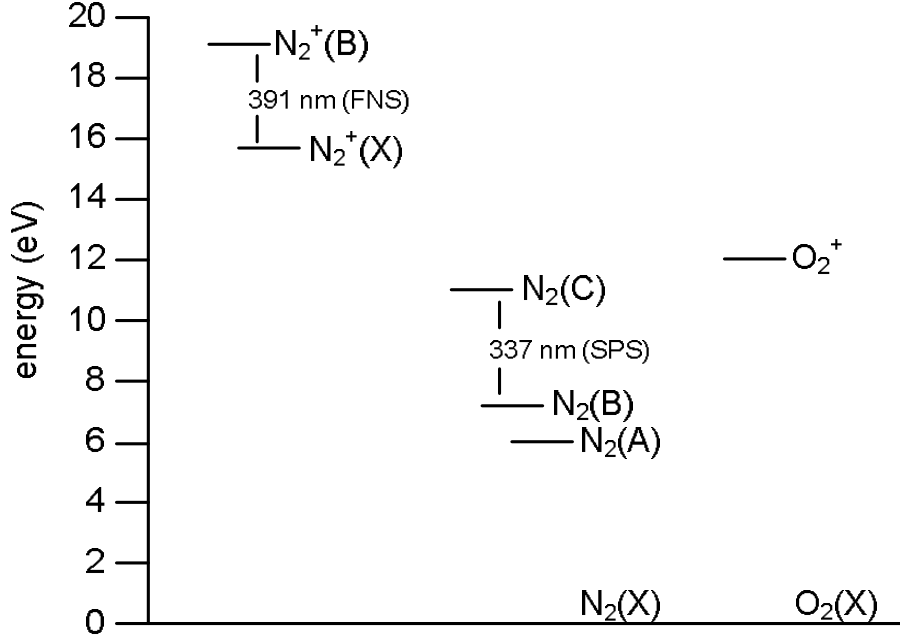


Figure 2.2: Part of the energy diagram of $N_2^{(+)}$ and $O_2^{(+)}$ [43; 85]. Shown are the First Negative System (FNS) and Second Positive System (SPS). Excited states of N_2 between 12.1 and 12.7 eV emit photons that can be used for photoionization.

2.3 Pressure dependence

The propagation of streamers depends on the propagation of electrons and ions through the gas. The distance between particle collisions can be calculated by the mean free path of a particle, given by

$$\ell_{\text{mfp}} = \frac{1}{4\sigma n_g} = \frac{kT}{4\sigma p}, \quad (2.1)$$

in which ℓ_{mfp} is the mean free path, σ the collision cross section, n_g the gas particle density, k the Boltzmann's constant, T the temperature and p the pressure. This relation shows that the mean free path is inversely proportional to the gas particle density and to pressure, provided that the temperature remains constant. In our measurements the temperature is around 20°C and therefore in this thesis scaling with pressure is discussed instead of scaling with gas particle density.

With this knowledge other reduced or "similar" parameters can be derived [56; 95; 100]:

- (1) All lengths scale with $l \sim \ell_{\text{mfp}} \sim 1/p$.
- (2) Electric field $|\mathbf{E}| \sim p$: When ℓ_{mfp} is so small that the electric field $|\mathbf{E}|$ over this region can be assumed constant, the streamer properties are dominated by the local electric field. This is typically the case in streamers, except possibly very close to a point electrode. It

is expected that similar discharges can be obtained if the energy gain over the relevant length $q_e \cdot |\mathbf{E}| \cdot \ell_{\text{mfp}}$ (and thus $\sim |\mathbf{E}|/n_g$) is constant.

(3) Streamer velocity v remains constant: The streamer velocity is determined by the drift of the electrons $v_d = \mu \cdot |\mathbf{E}| \sim 1/p \cdot p$, where the $\mu \sim 1/p$ is the mobility.

(4) Reduced time $t \sim 1/p$: When $v = \text{constant}$ (item 3), $l \sim 1/p$ (item 1) and $v = l/t$, then $t = l/v \sim 1/p$.

(5) Reduced electron density $n_e \sim p^2$ and current density $j \sim p^2$: The Poisson equation states that $\nabla \cdot \mathbf{E} \sim q$ in which $q = n_+ - n_e$ is the space charge. From $|\mathbf{E}| \sim p$ (item 2) and $\nabla \sim p$ (item 1) follows that $q \sim p \cdot p = p^2$, so that $n_e \sim p^2$ and $j \sim p^2$ since $j = n_e \cdot q_e \cdot v_d$ in which q_e is the electron charge.

(6) A consequence of these parameters is that the voltage V and current I remain constant with pressure since $V = \int \mathbf{E} \cdot d\mathbf{x} \sim p \cdot 1/p$ is constant and $I = j \cdot A \sim p^2 \cdot 1/p^2$ is constant, where A is the area through which the current flows.

Since the mean free path and the local energy gain between two collisions must be the same everywhere at the same reduced distance the geometrical electrode shapes must also be changed to obtain the same geometrical field in which the discharge which will be launched [2]. For the inception of a streamer, electrons can be liberated from the tip. When this occurs via ion impact the tip must be scaled to obtain similar discharges. When they are created via field emission (a form of quantum tunneling), the scaling law is broken locally. Furthermore, in experiments electrodes always have surface roughnesses where the electric field can be as high as 10 MV/cm. Since streamers usually start at these roughnesses, scaling of the needle probably has less influence on the streamer pattern than would follow from the arguments above.

When photoionization effects are not taken into account, the above listed set of similarity relations works very well for describing characteristics of short streamers (i.e. when three body attachment, recombination, gas heating and thermal conduction processes are negligible) at near and lower than atmospheric pressures [55]. When the photoionization effects are included in numerical simulations, streamers at pressures lower than several mbar preserve similarity but similarity laws do not hold at higher pressures [55]. Modelling results emphasize that the quenching of molecular nitrogen emitting photoionizing radiation is responsible for this non similar behavior. There is some uncertainty about this value above which quenching takes place. Some authors prefer 80 mbar and others 40 mbar (altitudes higher than ~ 24 km) [56; 59] (and references therein). At ground pressure (1000 mbar) the photoionizing radiation level is reduced by a factor of $p_q/(p + p_q) \sim 20$ in comparison with cases of streamers at 15 and 0.07 mbar [56] where p is the pressure and p_q is the quenching pressure.

2.4 Air and nitrogen

Although air consists for the main part of nitrogen, both gases have different properties due to the presence or absence of oxygen. One difference between the gases is that N_2 is electropositive and O_2 is electronegative. Thus, O_2 attaches free electrons from the gas which otherwise could be used by the streamer propagation. This can occur via two reactions:

1) $O_2 + e \rightarrow O^- + O$: The rate constant of dissociative attachment $k_{att} = 3.5 \cdot 10^{-17} \text{ m}^3/\text{s}$ at an electron temperature $T_e = 3 \text{ eV}$ and gas temperature $T_g = 300 \text{ K}$ [99]. At 1 bar air this gives a typical timescale for attachment of $\tau = (k_{att} \cdot n_{O_2})^{-1} \approx (10^{-17} \cdot 10^{24})^{-1} = 10^{-7} \text{ s}$.

2) $O_2 + e + X \rightarrow O_2^- + X$: where $k_{att} = 4.8 \times 10^{-42} \text{ m}^6/\text{s}$ at $T_e = 3 \text{ eV}$ and $T_g = 300 \text{ K}$ [64]. At 1 bar air this gives a typical timescale for attachment of $\tau = (k_{att} \cdot n_{O_2} \cdot n_X)^{-1} \approx (10^{-42} \cdot 10^{24} \cdot 10^{25})^{-1} = 10^{-7} \text{ s}$.

The streamer head propagates in typical time scales of 10^{-9} s . Therefore attachment is not important in the streamer head. The processes after the primary streamer propagation such as secondary streamers or the evolution to glow and/or spark (time scales of 10^{-6} s) can be affected by attachment.

The other difference is that direct photoionization, which is assumed to be necessary for positive streamer propagation, can only take place in air and not in nitrogen since oxygen is necessary for this process.

Relating this knowledge to streamer polarity:

Air: Already before the streamer starts, a part of the free background electrons are attached to oxygen and thus removed from the gas. Therefore, photoionization is assumed to be the main source of free electrons in the gas when the streamer propagates. This process creates enough electrons so that positive streamers (and also negative streamers) can propagate in air.

Nitrogen: Since oxygen is absent, there is no attachment in the gas and the photoionization mechanism that is available in $N_2:O_2$ mixtures (such as air) cannot occur. Therefore, it is assumed that the free electrons, available for the propagation, are only the background electrons. It is unknown whether in pure nitrogen the number of background electrons is too small for positive streamer propagation and only negative streamer propagation is possible. In experiments a pollution of several ppm O_2 in pure N_2 may already result in direct photoionization. However no literature data about this subject is found. The actual propagation of positive streamers in pure nitrogen is a matter of current investigation.

2.5 Typical length- and timescales, fields and densities

The streamer can be considered to be built up by a fast moving ionizing head and a recombining channel behind it. Therefore, different processes on different timescales take place. The intrinsic parameters depend on pressure p and are given below.

Streamer head

In the streamer head the following processes occur.

- (1) The generation of electrons and ions in regions of high electric field by impact of accelerated electrons on neutral particles and by photoionization.
- (2) Drift and diffusion of the charged particles in the local electric field between abundant neutral particles. The electrons are much faster than the heavy ions. They take care of the impact ionization and the excitation of the molecules whose decay is seen on the photographs.
- (3) The modification of the externally applied electric field by the generated space charges.

For negative streamers in nitrogen, a dimensional analysis determines the characteristic scales. The ion density in the streamer head will be of the order of $10^{14} \cdot (1 \text{ bar}/p)^2 \text{ cm}^{-3}$. The typical ionization length in simulations is $\ell_{\text{mfp}} \approx 2.3 \cdot (1 \text{ bar}/p) \mu\text{m}$ and the typical field $E_0 \approx 200 \cdot (1 \text{ bar}/p) \text{ kV/cm}$ [30]. The streamer velocity is determined by the drift velocity. This drift velocity varies in air from 0 - $90 \cdot 10^{-3} \text{ mm/ns}$ for $|\mathbf{E}|/p = 0 - 30 \text{ kV}/(\text{cm} \cdot \text{bar})$ and in nitrogen from 0 - $70 \cdot 10^{-3} \text{ mm/ns}$ for $|\mathbf{E}|/p = 0 - 27 \text{ kV}/(\text{cm} \cdot \text{bar})$ [57]. These drift velocities v_d can be scaled for values at higher electric fields via the electron mobility μ given by $v_d = \mu \cdot |\mathbf{E}|$. At an electric field $E_0 = 200 \text{ kV/cm}$ the drift velocity in nitrogen is $\approx 0.76 \text{ mm/ns}$, as is used in e.g. [30].

Streamer channel

In the streamer channel the following processes are present:

- (1) Drift and diffusion of electrons and positive ions in the quasi-neutral channel. The ion density approaches a steady-state value of $10^{14} - 10^{15} \text{ cm}^{-3}$ in nitrogen at 1 bar [25].
- (2) A current will flow through the channel to sustain the discharge. The strength of the field established by the current flow is relatively low and is called the stability field. This field is 4.4 - 5 kV/cm [4; 90] in air and $\sim 1.5 \text{ kV/cm}$ in nitrogen (up to 2% oxygen) [90] for positive streamers at 1 bar. The stability field for negative streamers in air at 1 bar is 2 to 3 times higher than the stability field of positive ones [6]. However, in contrast to the textbook discussion [90], other situations are possible where the field behind a group

of streamers is screened completely and no current flows in the channel [60].

(3) The loss of electrons and ions by recombination (formation of molecules) and attachment (electrons sticking to oxygen molecules). Typical timescales of recombination and attachment are $\sim \mu\text{s}$ [103] and $\sim 100\text{ ns}$ at 1 bar.

2.6 Applications

The highly energetic electrons in the enhanced electric field at the streamer head can collide with other gas particles resulting in ionization, excitation and dissociation of these particles. Apart from ions and excited states also highly reactive radicals can be created. These radicals can break large molecules apart and are used in pollutant removal processes. Research of pulsed discharges has been carried out to the treatment of polluted water [1; 3; 38; 40]. Pollutants in gases that can be removed include VOC's (Volatile Organic Compounds), NO_x , SO_2 , fly ash, odor and tar [17; 27; 73; 104; 118]. Small dust particles can be charged by negative dc corona's and drawn out of a gas stream in so called dust-precipitators [46; 104]. Corona charging is also utilized in electrophotography, copying machines and printers. Ozonizers, used for disinfection purposes, are also based on streamer processes [104]. A new field in which streamers are used is the combination of chemical and hydrodynamic effects which can be used in plasma-assisted combustion [94] and flame control [48].

Chapter 3

Stages of positive streamer evolution: time resolved measurements

The positive primary streamer propagation is studied with an intensified CCD-camera at different voltages, gap distances and pressures. By lowering the pressure and enlarging the electrode gap it is possible to zoom into the discharge since the processes then occur over a longer distance and time. Measurements at 62.5 mbar in a 160 mm gap show that the primary positive streamer propagation consists of 4 stages: a) a light emitting cloud at the anode tip that evolves into b) an expanding shell. From this shell c) one or more streamers emerge that d) propagate towards the cathode plate. The number of streamers and their diameter changes with applied voltage. At a given pressure and a voltage just above the inception threshold there are a few streamers which are thin, branch little and die out while propagating towards the cathode plate. At an intermediate voltage there are many streamers that are a little bit thicker, branch a lot and bridge the complete electrode gap. Above a critical voltage, which in our experiments appears to be around the DC-breakdown voltage, there are again only a few streamers but this time they are thick, bridge the electrode gap and hardly branch. Events that do not belong to the primary streamer propagation but are visible on photographs are also summarized in this chapter.

setting	gap (mm)	R_1	R_2	R_3	shunt or R_4	CC or C	switch
a	40	25 M Ω	2 k Ω	1 M Ω	2.75 Ω	1 nF	Behlke HTS 651
b	160	25 M Ω	1 k Ω	8 k Ω	8.5 Ω	1 nF	sparkgap
c	40	25 M Ω	1 k Ω	25 M Ω	2.75 Ω	250 pF	Behlke HTS 361

Table 3.1: *Values of the components used in the C-supply.*

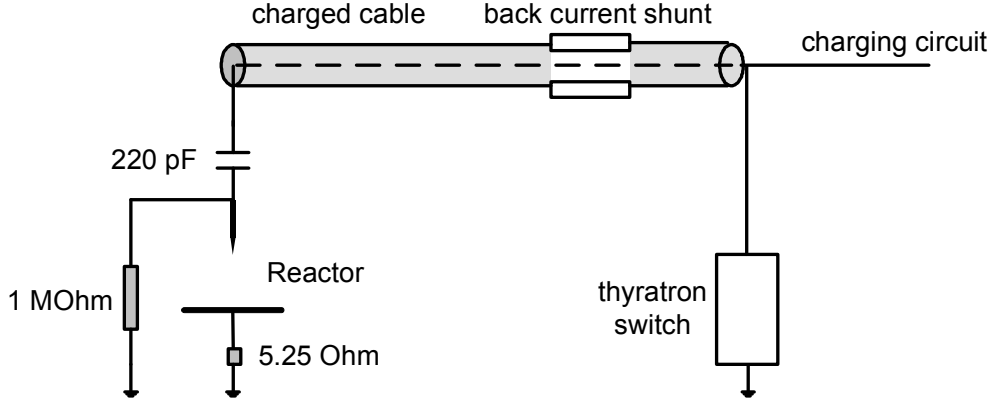
3.1 Introduction

A complete discharge starts with the rise of the voltage pulse and ends when the voltage pulse has died out. During this time interval the discharge can go through several stages depending on the applied voltage pulse amplitude and duration, e.g. primary streamer propagation, return stroke, secondary streamer propagation and late streamers, glow, spark. The primary streamer propagation itself also consists of several stages like the ignition at the high voltage electrode, the propagation through the gap and reaching the opposite electrode. In section 3.3.1 and 3.3.2 the start and propagation of the positive primary streamer is visualized with an iCCD-camera since the primary streamer propagation is the process we are interested in. Section 3.3.3 shows the events that can occur after the primary streamer propagation. In section 3.3.4 other events that can occur on photographs are given.

3.2 Experimental setup

Two different supplies are used which will be called the C-supply and the MIPT-supply. The C-supply is thoroughly discussed in chapter 4. The value of the components in the C-supply are given in table 3.1. For the photographs of streamers in the C-supply with setting *a* and *b* a digital 4QuikE camera from Stanford Computer Optics is used while photographs with setting *c* are made with an Andor Technology ICCD-452. A point-plane electrode configuration is used in which the needle is made from pure tungsten (setting *a* and *b*) or thoriated tungsten (setting *c*) and the plate from stainless steel. No differences in streamer pattern are observed when using the two needles. Both needle tips have a radius of $\sim 15 \mu\text{m}$ and diameter of 1 mm.

As shown in figure 4.2d and discussed in section 4.2.1 there is a fixed time delay in the C-supply between the pulse of the function generator ($t_1 = 0$) and the start of the high voltage pulse (t_2) of at least $1.2 \mu\text{s}$ when the sparkgap switch is used. When a Behlke semiconductor switch is used this fixed delay becomes shorter because of different trigger electronics but it remains at least $0.35 \mu\text{s}$. No streamer propagation is possible before this

Figure 3.1: *Scheme of the MIPT-supply.*

time is due. Since the camera is also triggered by the function generator this means that the combination of preset camera delay T and exposure time Δt must exceed $1.2 \mu\text{s}$ or $0.35 \mu\text{s}$, respectively, to obtain an image on the photograph. Depending on the streamer inception time and variable jitter in the sparkgap the delay can become (much) longer. The combination of camera delay and exposure time must be adjusted accordingly to capture the discharge.

3.2.1 MIPT-supply

The MIPT-supply at the Moscow Institute for Physics and Technology consists of a small cubic vacuum vessel with an edge of 220 mm [76]. The measurements are done in an inhomogeneous point-plane electrode gap. The needle with a radius of $\sim 15 \mu\text{m}$ and diameter of 1 mm is made of thoriated tungsten. The bottom plate is a brass disk, 80 mm in diameter which is connected to the vacuum vessel via a current shunt of 5.25Ω . The electrode gap is varied between 30 and 40 mm. The windows of the vacuum vessel are 100 mm in diameter and made of quartz.

A scheme of the MIPT-supply is given in figure 3.1. A coaxial cable is charged to high voltage and when the hydrogen filled thyatron switch closes, the cable discharges over the point-plane gap. The difference with voltage pulses created in the C-supply is that here the voltage pulse is almost rectangular where the length of the cable determines the pulse duration. The C-supply has an exponential rise- and decay time where the rise time depends on the series resistance (R_2 , figure 4.1), the geometric capacitance (C_g) and the inductance of the circuit. The decay time depends on the parallel resistance (R_3) and the charged capacitor (C). The voltage pulse duration of the MIPT-supply is 400 ns. The voltage rise time is 12 ns.

The voltage pulse amplitude is measured by the back current shunt in the coaxial cable. The relation between the shunt voltage (Y) and the cable voltage (X) is $X/Y = 321.5 \pm 0.3\%$ [74]. The voltage pulse measured by the back current shunt is diminished by 20 dB before putting it on the oscilloscope, a Tektronix TDS3054 (500 MHz, 5 GSamples/s). Furthermore, the voltage is doubled on the high voltage electrode due to the pulse reflection in the coaxial line. Only positive streamers are created.

A PicoStar HR12 intensified CCD-camera from La Vision with an Industar 61L/3 lens is mounted on the setup to take the photographs. This camera can take stroboscopic images but generally it is used to take one exposure per discharge.

The gases used are ambient air and synthetic air (20% oxygen, 80% nitrogen) in a pressure range of 465 mbar to atmospheric pressure. The vessel is flushed two times before filling it with synthetic air. No gas flow is maintained. The room temperature varies between 18 - 22 °C, the humidity is 50 - 60 % and the atmospheric pressure is in the range of 985 - 1004 mbar. For more information about the MIPT-supply see [76].

3.3 Results

3.3.1 Streamer start

Streamers that are usually shown in publications are positive streamers in air at atmospheric pressure at an intermediate voltage as shown in figure 3.2a. This picture shows that the streamers start at the anode tip and propagate towards the cathode plate and underway they branch. At low pressure the streamers typically look like figure 3.2b. Here the streamers are thicker and emerge from a light emitting cloud at the tip. They hardly branch. In both pictures the streamers can reach the plate electrode but they are photographed during their transit.

To investigate the start of the streamer at the tip it is best to zoom into this region by using low pressures and a large gap since then the start has a longer intrinsic time and length scale as discussed in chapter 2. The applied voltage is chosen such that only one streamer forms. The moment that the camera switches its intensifier on is denoted with T where $T = 0$ is the moment that the camera is triggered by the function generator. This time T is also called the camera delay. The exposure time of the camera, also called gate width, is given by Δt . Figure 3.3a shows a time integrated picture of a complete discharge in a 160 mm gap at 15 mbar and 5 kV for an $N_2:O_2$ mixture with 0.2 vol% O_2 . The time resolved photographs in figure 3.3b-g show that this discharge starts at $T = 1.4 \mu s$ with a light emitting cloud or sphere at the tip with a height of ~ 5 cm and width of ~ 9 cm (b) which evolves into a thin expanding shell with a diameter of ~ 12.5 cm and thickness of ~ 2 cm (c). While this shell propagates towards the cathode (d) a streamer emerges (e) that propagates towards (f) and reaches (g) the cathode. In (h) all processes

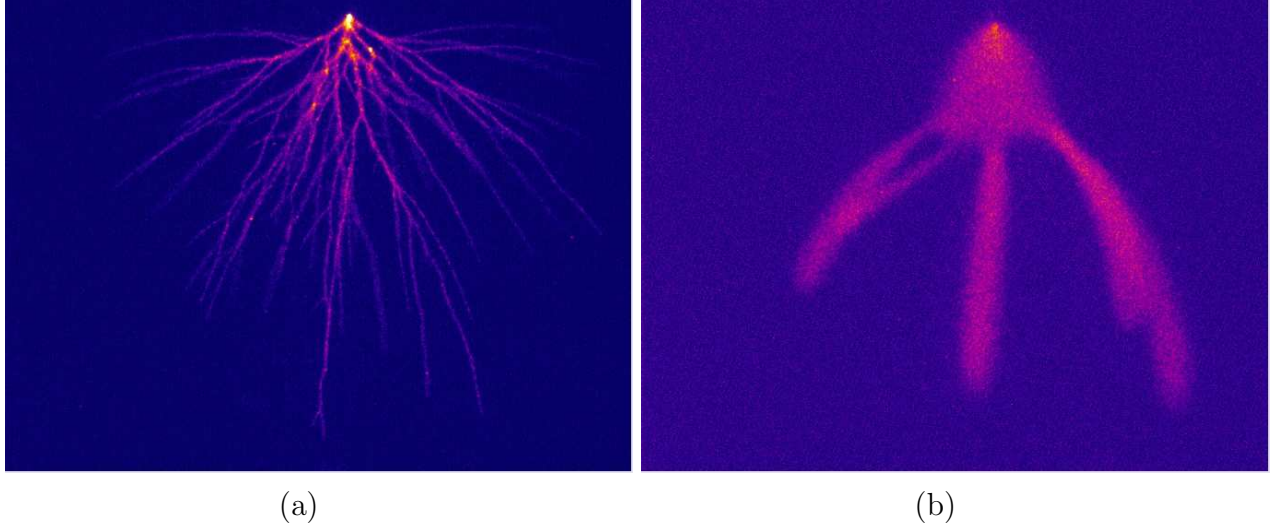


Figure 3.2: *Positive streamers in a 40 mm gap in air at a) 21 kV, 1000 mbar and b) 6 kV, 100 mbar. Setting a in table 3.1. The camera's delay is 0 ns and exposure time is a) 0.6 μ s and b) 0.7 μ s.*

are photographed that arise after the primary streamer has bridged the electrode gap. A similar set of pictures can be made in air in a 40 mm gap at 100 mbar and 10 kV as shown in figure 3.4. In both situations the discharge velocity is ~ 0.2 mm/ns. The discharges show a similar pattern since the electrode gap is too small compared to $\ell_{\text{mfp}} \sim 1/p$ for the discharges to develop into more than one streamer.

3.3.2 Streamer propagation

When a high voltage pulse with an amplitude of 40 kV at 613 mbar is applied very fast over a 30 mm point-plane gap (i.e. a voltage far above the DC-breakdown voltage) a primary streamer that is as thick as the cloud propagates towards the cathode. This is shown in the time resolved photographs of figure 3.5a and 3.5b for a positive streamer which is made in the MIPT-supply with a voltage duration of 400 ns and rise time of 12 ns. Its reduced diameter is 1.9 mm·bar and its velocity is 1.5 mm/ns. When it has reached the cathode a return stroke moves back towards the anode tip (figure 3.5c). When it has stretched back to close to the needle it forms the glow as seen in figure 3.5d. Late streamers (see also section 4.3.1) are seen around the glow. Furthermore, in figure 3.5c and 3.5d also light at the needle is visible. This usually occurs after the primary streamers have bridged the gap. The dark region between the plate and the glow can be decreased by increasing the voltage. A more extensive set of photographs is given in [75].

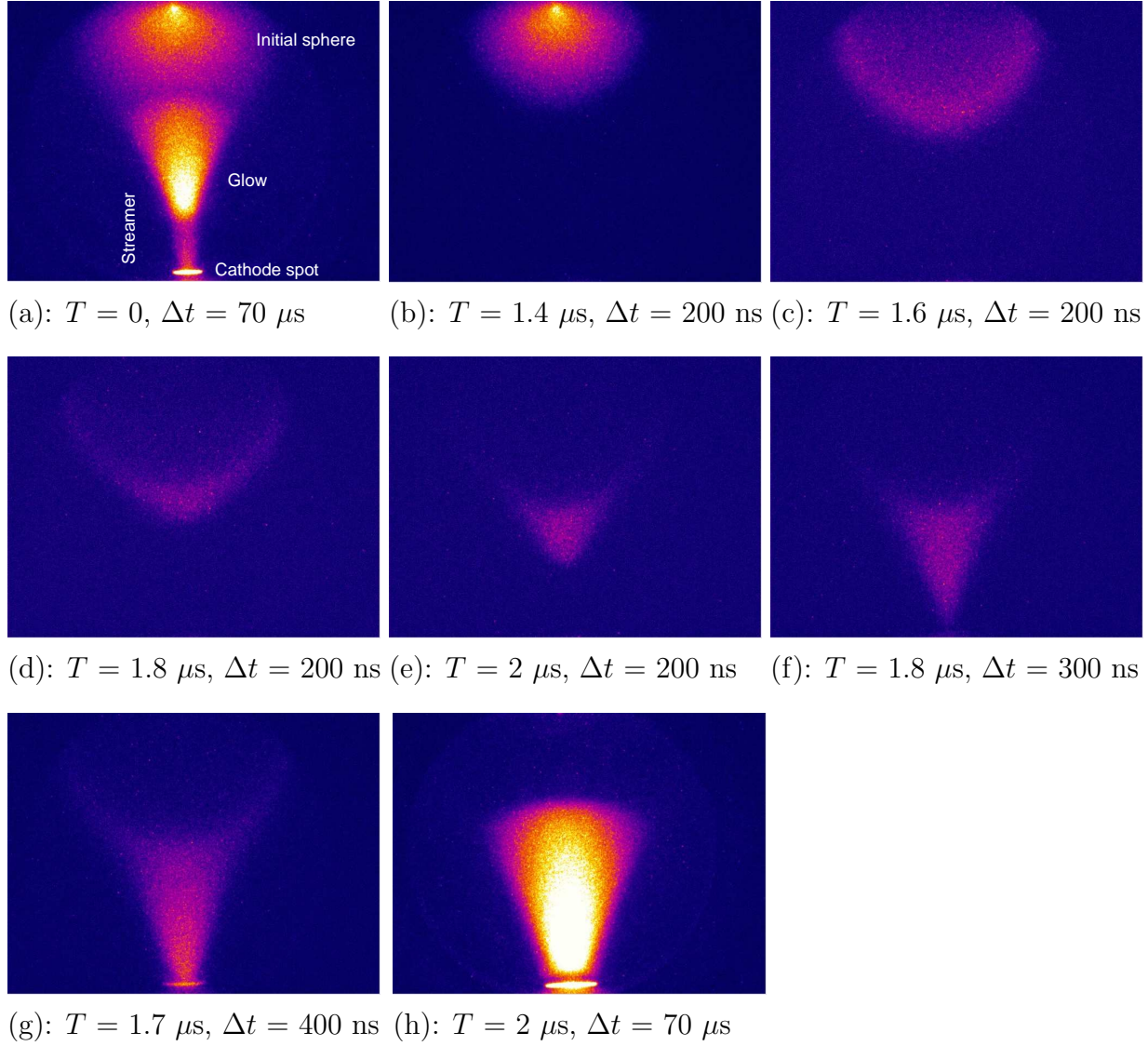


Figure 3.3: *The start of a streamer in a 160 mm gap at 15 mbar and 5 kV in 99.8%N₂:0.2%O₂. Setting b, table 3.1. The camera's delay T and exposure time Δt are given.*

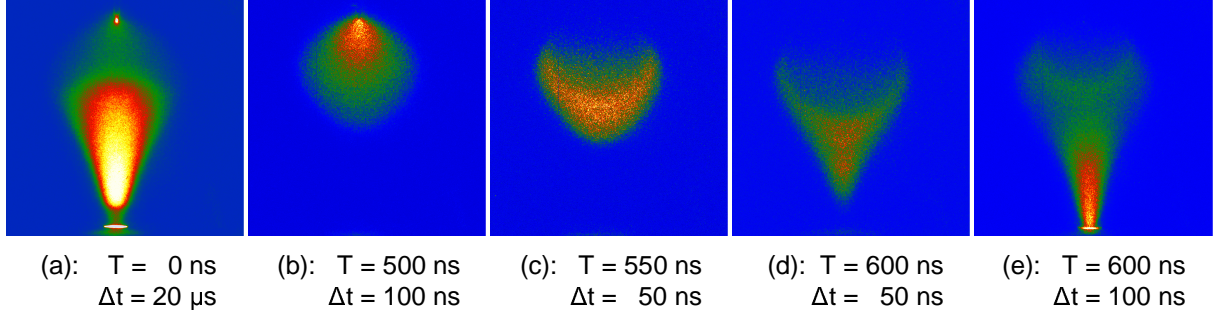


Figure 3.4: *The start of a streamer in a 40 mm gap at 100 mbar and 10 kV in air. Setting c in table 3.1. The camera's delay T and exposure time Δt are given.*

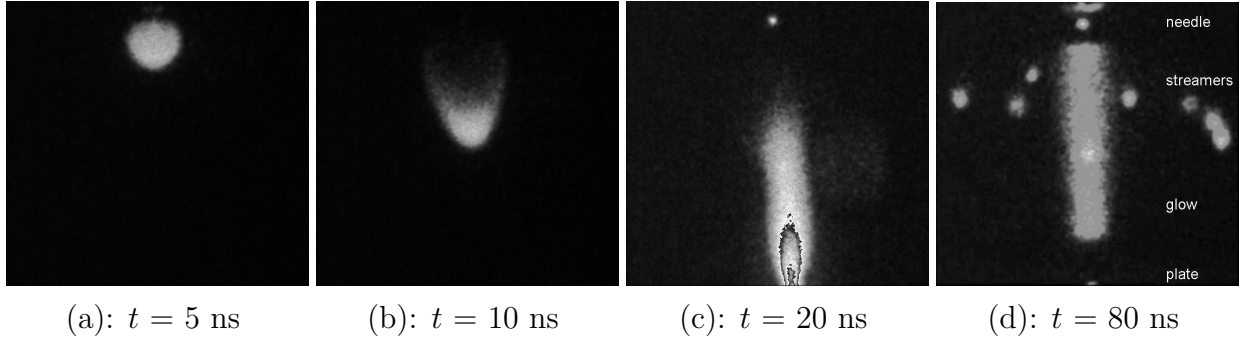


Figure 3.5: *The start and propagation of a streamer in a 30 mm point-plane gap at 613 mbar in synthetic air with the MIPT-supply with a rise time of 12 ns and pulse frequency of 1 Hz. The voltage is 40 kV. The exposure time is 5 ns. The actual time is given by t where $t = 0$ is the approximate start of the discharge.*

When a voltage is applied at approximately the DC-breakdown voltage ($V \gtrsim V_{\text{DC-breakdown}}$) a set of photographs as in figure 3.6 can be made. The discharge starts at $T = 485 \text{ ns}$ with a smaller cloud at the tip (figure 3.6a) which evolves into a shell from which several streamers emerge whereafter the shell disappears (figure 3.6b,c). The streamers propagate towards the cathode (figure 3.6d). The difference in streamer position in the gap while T and Δt are the same, as shown in figure 3.6c and 3.6d, is caused by jitter in the sparkgap and streamer inception.

When the pressure is increased and/or the voltage is decreased ($V < V_{\text{DC-breakdown}}$), the cloud becomes smaller until it eventually is not visible anymore (figure 3.2a). Also the streamers start to branch. The streamers die out in the 40 mm gap when the voltage is decreased further to just above the inception voltage - the minimal voltage necessary for the discharge to start. This is only observed at 1000 mbar since at lower pressures of 400,

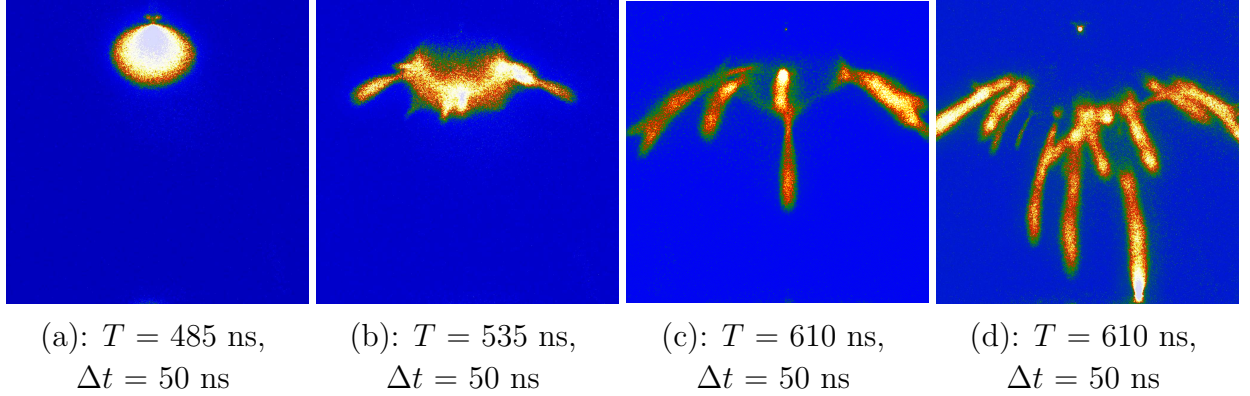


Figure 3.6: *The start and propagation of a streamer in a 40 mm gap at 400 mbar and 25 kV in ambient air. Setting c in table 3.1. The camera's delay T and exposure time Δt are given.*

200 or 100 mbar the discharge is enlarged by a factor 2.5, 5 or 10 (pressure scaling law) and the opposite electrode is reached at a similar applied voltage.

The findings described above are summarized in table 3.2. The values in this table are given for a 40 mm point-plane electrode gap in which the streamers are made using the C-supply. The table shows that voltage can be used to go to regimes of few streamers and branches or many streamers and many branches. This observation also holds for different gap sizes. It is not meaningful to give a value of the average applied electric field instead of the applied voltage since for the strong local field variation the average field has no physical meaning, as is also shown in [11].

3.3.3 Other discharge processes

As said before, in this thesis a complete discharge cycle starts by the rising of the voltage pulse and it ends when the voltage pulse has died out. This one discharge can consist of several stages depending on voltage pulse duration and amplitude: primary streamer start - primary streamer propagation - return stroke - secondary streamers and late streamers - glow - spark. Important events that can occur during the discharge but do not belong to the primary streamer propagation are summarized below.

1. When the primary positive streamer reaches the plate, cathode spots arise (e.g. figure 3.3a and 7.14). So, when there is a cathode spot then it is sure that the primary streamer has crossed the complete gap and events that can occur after the primary streamer propagation may have influenced the image on the iCCD-camera. Therefore, we tried to use pictures without the cathode spot if possible. Negative streamers that have crossed the electrode gap show anode spots.

pressure (mbar)	V just above $V_{\text{inception}}$ ($\lesssim 15$ kV at 1000 mbar) ($\lesssim 5$ kV at 100 mbar)	intermediate V	$V \geq V_{\text{DC-breakdown}}$ ($\gtrsim 40$ kV at 1000 mbar) ($\gtrsim 10$ kV at 100 mbar)
1000 400	<ul style="list-style-type: none"> - < 10 streamers - thin streamers - fade halfway gap - little branching - figure 5.2a, 6.2 	<ul style="list-style-type: none"> - ~ 100 streamers - become thicker - reach cathode - branch often - figure 3.2a, 1.2a 	<ul style="list-style-type: none"> - < 10 streamers - thick streamers - reach cathode - little branching - small cloud at tip - figure 3.6
200 100	<ul style="list-style-type: none"> - < 5 streamers - small cloud at tip - reach cathode - branch once/twice - figure 5.1g, j 	<ul style="list-style-type: none"> - < 10 streamers - cloud expands - reach cathode - no branching - figure 3.2b, 5.2c 	<ul style="list-style-type: none"> - 1 streamer - cloud+glow fills gap - reach cathode - no branching - rarely cloud <i>and</i> streamers - figure 3.3, 5.1i, l

Table 3.2: Description of the streamer pattern visualized in figure 5.1 for a 40 mm gap in air. Setting c of table 3.1.

2. When the streamer reaches the plate electrode a return stroke starts to move back towards the needle electrode (e.g. figure 3.5c).
3. When the applied voltage exceeds the DC-breakdown voltage a short voltage pulse is necessary else a glow or spark will arise, figure 1.6. Note that the strong light emission of a spark might damage the intensifier of the camera. Therefore the creation of sparks is avoided as much as possible.
4. After the fastest positive or negative streamer has bridged the electrode gap a light spot arises at the needle tip (e.g. figure 3.5 and 3.6). It can also be visible before the streamers have reached the plate (e.g. figure 7.3 or figure 4.6a) but then the voltage must be sufficiently high so that there is a large field enhancement at the tip.
5. When the primary streamer has crossed the electrode gap, a new set of streamers can start at the needle tip or edges of the (disappeared) cloud and propagate over the *same* path as the primary streamer, see figure 3.7a. In time integrated photographs it is usually seen as a white overexposed region (e.g. in figure 4.6d). These streamers are called *secondary* streamers. They usually do not cross the complete gap but fade before reaching halfway the gap. They arise due to the rearrangement of the electric

field at the tip after the primary streamers have bridged the electrode gap. Maybe the glow in figure 3.3 is also a secondary streamer, just like the light spots in figure 6.6d. Note that the *late* streamers of chapter 4 propagate in *new* channels (the very thin streamers in figure 4.6d), probably because the electric field changed due to charges deposited in the electrode gap by the primary streamers.

6. Late streamers are very thin streamers that ignite at surface roughnesses higher up at the anode needle than the primary streamers or at existing streamer paths (e.g. figure 4.6c and 4.6d). They can appear at a surface roughness before the primary streamers have crossed the gap but then they remain short (as in figure 4.6c) until the gap has been crossed and the electric field has had time to rearrange. Then it becomes crowded with late streamers as in figure 4.6d. Usually the late streamers start after the primary streamers have bridged the gap. It appears as if they start at the same moment or a little later than the secondary streamers since secondary streamers are always visible when the picture is crowded with late streamers (figure 4.6d) or when there are no late streamers at all (figure 3.7a). Late streamers are only observed when thick, type 1 or 2 streamers (chapter 4) are created with voltage pulse durations longer than the time needed for the primary streamers to cross the electrode gap. We have not found them at pressures below 1 bar. In contrast, secondary streamers are also found at low pressures.
7. Streamers are 3-dimensional phenomena. Therefore, spatial information gets lost when they are projected onto a 2D photograph. Care must be taken when processing 2D images because two (thin) streamers that in 3D propagate behind each other can appear as one (thicker) streamer on a 2D photograph. This is shown in figure 3.7b where two photographs under an angle of $\sim 8^\circ$ are made of the same discharge (stereo photography). Here it is seen that streamer 1 and 2 in the left figure overlap while in the right figure they do not.
8. Streamers can connect to each other (e.g. figure 4.6c). This is only seen to happen after the primary streamer has transited the electrode gap. Most likely the primary streamer reaches the plate electrode and a late streamer bends toward the primary channel. Time integrated photographs of positive and negative streamers in the PM-supply (chapter 7) at voltages larger than 56 kV (positive) or 66 kV (negative) support this hypothesis. They show thin streamers (in a region of thick streamers) that connect to the thick streamers. In such a case the thin streamers usually are late streamers; the thick streamers are the primary ones.

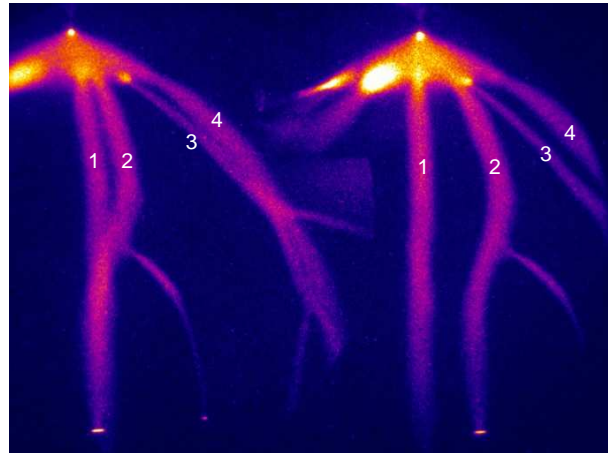
(a): $T = 760$ ns, $\Delta t = 50$ ns(b): $T = 0$ ns, $\Delta t = 30$ μ s

Figure 3.7: a) Secondary streamer in a 40 mm gap at 400 mbar and 25 kV in air. Setting c in table 3.1. This is the subsequent photograph of the discharge in figure 3.6. b) A recent stereo photograph of streamers in nitrogen at 61 mbar in a 160 mm gap at 10 kV and 10 Hz. Setting b in table 3.1. The numbers on the left and right side of the photograph identify the same streamer. The delay is given by T and the exposure time by Δt .

3.3.4 Other visual effects in photographs

Besides all processes that can occur during a discharge other effects may also be visible on photographs. These effects are summarized below.

1. In the 160 mm gap (e.g. figure 3.3 or figure 6.7) the photographs shows a dark circle at the outside of the picture. This is the border of the viewing port that contains the quartz window ($\varnothing = 155$ mm) through which the camera takes the photograph of the discharge.
2. When a laser is used to trigger the discharge in a parallel plate gap (chapter 7) material can be sputtered away from the electrode by the laser (figure 7.13). This is seen as bright paths of light, which are reflected in the upper plate.
3. Light reflections can be seen in different places. In figure 7.13 the laser light and the paths of the sputtered material are reflected in the top plate. The laser light is also reflected in the bottom plate and the shine of light in the middle of the photograph comes from reflections in the windows or the lens of the camera. In other photographs mainly reflections of the streamers in the bottom plate are visible. The real streamer starts at the tip and ends at its cathode spot, so all light that is seen from below

the cathode spots is a reflection (e.g. figure 7.5c,e,f and 7.12). Note that half of the cathode spot is also a reflection because the cathode acts as a mirror. In the middle of figure 3.7b the stand on which the fiber of the spectrometer was mounted is still visible as a vague white cylinder.

4. The streamer paths near the point electrode are usually overexposed. This can not be avoided since the small streamer channels further down the gap become invisible or immeasurable compared to the background noise when the gain of the camera is decreased.

Chapter 4

Streamers of different widths

Diameter and branching structure of positive streamers in ambient air are investigated with a fast iCCD-camera. We use different pulsed power circuits and find that they generate different spatial streamer structures. The electrodes have a point-plane geometry and a distance of 40 or 80 mm, and the peak voltages over the discharge gap are up to 60 kV. Depending on circuit and peak voltage, we observe streamers with diameters varying gradually between 0.2 and 2.5 mm. The streamer velocity increases with the diameter, ranging from 0.07 to 1.5 mm/ns, while the current density within the streamers stays almost constant. The thicker streamers extend much further before they branch than the thinner ones. The pulsed power supplies are a switched capacitor supply with an internal resistance of 1 k Ω and a transmission line transformer supply with an impedance of 200 Ω ; additional resistors change the impedance as well as the voltage rise time in the case of the capacitor supply. We observe that short rise times and low impedance create thick streamers near the pointed electrode, while a longer rise time as well as a higher impedance create thinner streamers at the same peak voltage over the discharge.

This chapter is published in a slightly altered form as [T.M.P. Briels, J. Kos, E.M. van Veldhuizen and U. Ebert, *Circuit dependence of the diameter of pulsed positive streamers in air*, J. Phys. D.: Appl. Phys. **39** (2006) 5201-5210.]. It contains some changes based on new insight. For diameters at voltages above 60 kV, see chapter 7.

4.1 Introduction

Electric breakdown in gases over large distances occurs in several stages. The first stage is the build up of an avalanche. Then when space charge starts to influence the applied field, the streamer discharge creates a weakly ionized channel. At very high fields this streamer branches. As realized already more than half a century ago [65; 88], streamers are difficult to visualize and to describe, due to their rapidity as well as due to their internal multiscale nature [33]. The aim of this chapter is in particular to clarify the experimental findings on different streamer patterns, diameters and velocities, and their relation to the external electric circuit.

A variety of streamer diameters under different experimental conditions has been reported. Photographic observations were made forty years ago by Waters and Jones for a voltage of 270 kV over a 2 m gap. They show a streamer with a diameter near the anode of roughly up to 20 mm, decreasing further on in the gap to ~ 2 mm [114]. On such photographs, however, one easily overestimates the size because the center of the channel can be overexposed. The experimental conditions of [114] are far from the small gaps that are studied nowadays for pulsed corona applications [104]. On the other hand, the photos in [114] show that a pulse with a relatively long voltage rise time of the order of $1 \mu\text{s}$ can create thick and thin streamer channels and pronounced branching.

Corona streamers created by pulsed positive voltages have been studied mainly in small gaps. Diameters reported in the literature are e.g. 0.040 mm in pure oxygen at 500 mbar in a gap of 10 mm and a voltage of about 11 kV [7]. Values obtained for streamers in air are e.g. 0.2 mm in a wire-plane gap of 35 mm at 30 kV [19] and 0.5 mm in a point-plane gap of 20 mm at 25 kV [80]. In larger gaps limited information is available. Ref. [8] reports diameters of 10 mm in a wire-cylinder gap of 290 mm diameter using a voltage pulse of 100 kV (figure 1.2b). The recent publication [37] shows a very abrupt change from 4 mm to ≤ 0.5 mm in a wire-plane discharge of 35 mm with a short voltage pulse with a maximum of 45 kV; the thin streamers probably occurred after the voltage had collapsed. We will show below that errors in diameter measurements can occur not only due to photographic overexposure, but also due to insufficient resolution of CCD-cameras. On the other hand, they will not explain diameters varying by two to three orders of magnitude at normal pressure.

High altitude discharge phenomena also show interesting effects. They have become a subject of study since their discovery in 1989, see e.g. [83; 97]. These transient luminous events are referred to as sprites, elves, blue jets etc. Sprites, in particular, are thought to be a type of streamer discharges and their larger diameter of up to 100 m [35] corresponds to the much lower air density at high altitudes. This scaling with air density follows from simple streamer models taking only impact ionization into account [33] and relates experiments at low or high pressure to each other, the results are somewhat modified by

photoionization [55; 59; 126].

The question of the streamer diameter also has played a classical role in streamer theory. Dawson and Winn [24] were the first to perform so-called 1.5D dynamical streamer computations that used a constant value for this diameter. A value of 0.060 mm was thought to be an optimal value at the time. Later a fixed streamer diameter was predicted by minimization arguments by D'yakonov and Kachorovskii [29] and Simakov and Raizer [92], for a discussion see [33]. In 2D computations the diameter is not an input, but a result of the computation. Recent computations in gaps longer than 5 mm [50; 55; 56; 59; 70; 71; 78] show that the diameter of both positive and negative single streamers can depend on the applied voltage. Streamer diameters up to 16 mm are reported in [50] in a point-plane gap. Simulations in a homogeneous field show that streamers can expand in overvolted gaps [5; 55; 56; 59; 70; 71; 93]. Calculations and measurements are still difficult to compare as they use different voltage pulse parameters and initial and boundary conditions. A recent attempt to compare measurements and calculations for single positive streamers in air shows that this is still not a straightforward task [80].

In this chapter, our goal is to set a basis for such a comparison by performing well defined experiments that determine how experimental streamer properties and, in particular, the optical diameter depend on applied voltage and gap length. We investigate positive streamers in a point-plane geometry in ambient air. The experiments are performed in the same experimental setup, but with different power supplies. We find that the applied voltage is a key parameter but that the internal resistance and the rise time of the power supply have a distinct influence as well.

This chapter is organized as follows: in section 4.2, the experimental setup and diagnostics are described. Section 4.3 contains the experimental results and section 4.4 further discussion and conclusion.

4.2 Experimental setup and diagnostics

Streamers are made in a large cylindrical stainless steel vacuum vessel with an internal diameter of 500 mm and an internal height of 300 mm. The vacuum vessel has three viewing ports with an inner diameter of 155 mm that can be closed by glass, stainless steel or quartz windows. The viewing port through which the camera looks at the streamers is always closed by a quartz window to be able to photograph also the UV-light coming from the discharge. The setup is shielded from the camera by a Faraday cage. This Faraday cage contains an ITO-window to keep the cage intact but allows the camera to photograph the discharge (figure 6.1). Two power supplies can be mounted on this vacuum vessel.

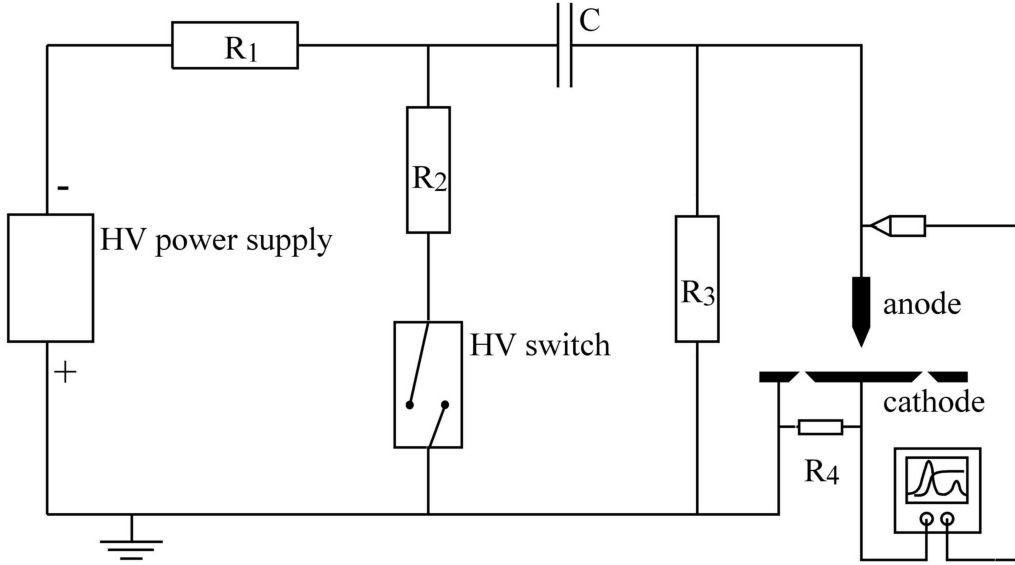


Figure 4.1: *The electric circuit to be called 'C-supply'.*

4.2.1 The two pulsed power supplies used

Two different power supplies are used to generate pulsed positive streamers. In both supplies first a capacitor is charged and then a switch is closed. However, the consecutive discharging of this capacitor over the needle-plate gap differs.

The first power supply (called C-supply) is sketched in figure 4.1, it is similar to the supply used previously [106]. The capacitor C (250 pF) is charged negatively through the resistor R_1 (25 M Ω). Closing the homemade, triggered spark gap puts the potential on the needle-plate electrode gap, with the negative polarity applied to the plate. Details about the homemade sparkgap switch can be found in [47]. In this way a positive corona is emitted from the needle. The resistor R_2 can be used to limit the current through the gap and the switch, its value is either 0 or 1 k Ω . Resistor R_3 determines the duration of the voltage pulse and is 4 k Ω in a 40 mm gap and 25 M Ω in a 80 mm gap. A resistive-capacitive divider (Tektronix P6015) is used to measure the voltage at the anode. The voltage rise time depends also on the series resistor R_2 . The current through the corona gap is obtained via a so called divided cathode¹. The divided cathode consists of a stainless steel inner plate of 100 mm in diameter and a stainless steel grounded outer ring of 180 mm. The plate and the ring are connected through 12 equally spaced resistors of 33 Ω , resulting in a resistance of $R_4 = 2.75 \Omega$. The outer ring around the cathode ensures a well defined,

¹Throughout the thesis this will be called "divided cathode" even though in the case of negative streamers it is actually a divided anode.

low stray capacity and therefore a fast rise time of the current measurement [41]. All signals are digitized using 0.2 ns sampling time (LeCroy Waverunner 6100A). The energy is determined as the time integral over voltage times current, after the capacitive part of the total current is subtracted [106]. Noise is filtered out of the signals before integration [41].

Figure 4.2a-c shows the measured voltage, current and energy of the discharge when the DC voltage is set to $V_{DC} = 60$ kV. The resistors R_2 and R_3 here are 1 k Ω and 4 k Ω . This leads to a rise time of the voltage pulse of ~ 60 ns, while when using $R_2 = 0$ k Ω the rise time becomes ~ 30 ns as is discussed in more detail in section 4.4.1. The decay of the voltage is controlled by resistor R_3 . In the 40 mm gap a rather low value of 4 k Ω is chosen to limit the time during which the voltage is at its maximum. This prevents the transition of the corona discharge into a spark. It also means that the voltage V_{DC} applied on the capacitor is not reached on the gap since the capacitor rapidly starts to discharge through resistor R_3 . With the DC voltage set to 60 kV, the maximum or peak V_P of the voltage pulse on the discharge gap is here 42 kV; in general, it will depend on the value of R_3 and the discharge current. The measured current consists of a capacitive part and a discharge part. The geometric capacity of the current measurement system is determined to be 350 fF at 3 kV. At 42 kV this capacitive part has a negligible influence on the energy content of the corona pulse which is ~ 6 mJ for the case of figure 4.2.

We estimate that roughly 50% of this energy is used for the primary streamer propagation. This estimate is based on the assumption that the maximum current is achieved when the primary streamers reach the cathode. Figure 4.2 shows that at this point the energy is halfway, i.e. 3 mJ of the total 6 mJ. This fraction, however, very strongly depends on the pulse duration and the gas composition. The other half of the energy is consumed after the streamers reach the cathode, in the so-called secondary streamer. In the figure, the corona current reaches its maximum I_P at time $t = 1.4$ μ s. At that moment, a small dip can be seen in the voltage. This voltage drop of about 2 kV is in agreement with the voltage drop across R_2 and an internal resistance in the supply at the measured current of 1 A. The peak current I_P is an almost pure particle current, as the displacement current is negligible near the maximum of the voltage.

Figure 4.2d shows the timing diagram for the control of the CCD camera. At t_1 , a function generator creates the starting pulse. This pulse is mostly a single shot, manual pulse but it can also be one from a steady pulse train. The pulse goes to the trigger unit of the spark gap. The trigger circuit creates an optical signal which enters through a fiber into the shielded high voltage box where it is converted and amplified to an 8 kV pulse. The total delay of the trigger unit t_2 has a fixed value of 1.2 μ s. The spark gap follows 10-20 ns after this 8 kV pulse and then the high voltage pulse starts. The start of corona streamers is at t_{ss} , the value of $t_{ss} - t_2$ (also called inception delay) strongly depends on the voltage level and rise time. In figure 4.2 it is about 50 ns, but it can be much longer if the peak

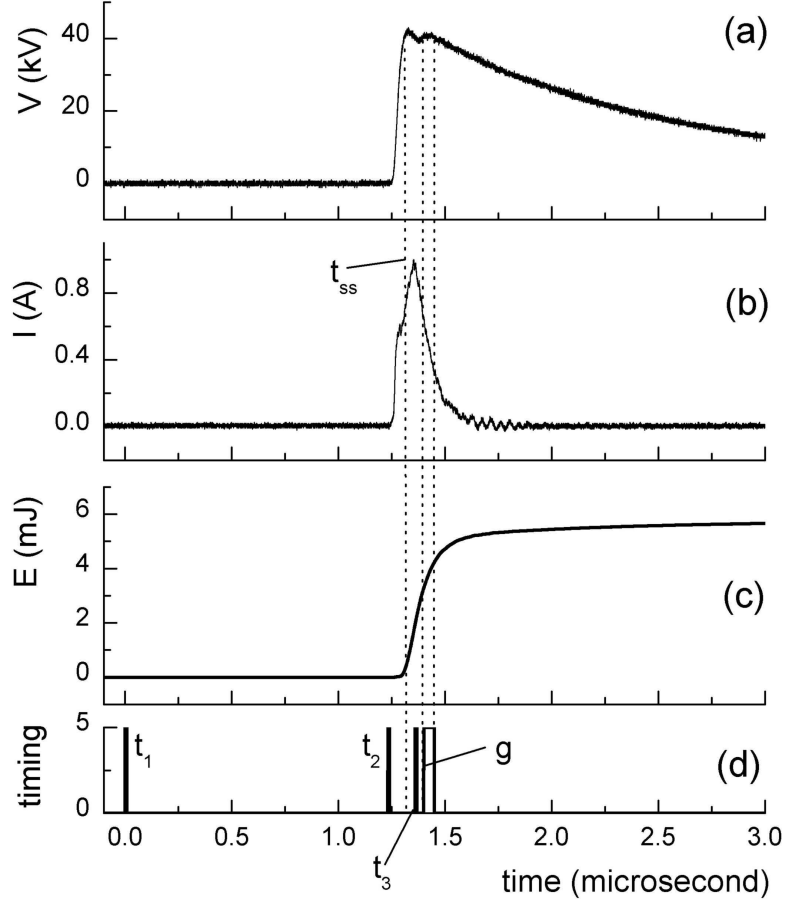


Figure 4.2: Evolution of voltage (a), current (b) and energy in the corona gap (c) obtained with the C-supply and a charging voltage of $V_{DC} = 60$ kV, $R_2 = 1$ k Ω and $R_3 = 4$ k Ω . The peak current and voltage on the 40 mm gap are $I_P = 1$ A and $V_P = 42$ kV. A total time interval of $3 \mu s$ is shown. The voltage rise time is ~ 60 ns and the decay time is $5 \mu s$. In (d) the timing of the measurement is indicated as described in the text: t_1 is the initial starting pulse for the trigger unit of the complete experiment, t_2 is the actual trigger for the high voltage pulse, t_3 is the trigger for the camera with an adjustable delay, t_{ss} is the moment at which the streamers start — this time can jitter considerably —, and g is the actual opening gate (i.e. exposure time) of the CCD-camera, here it is 50 ns.

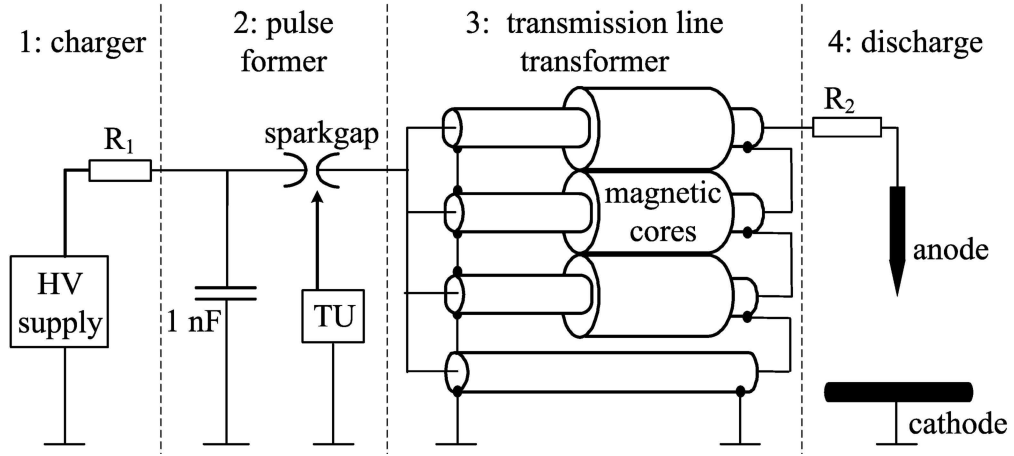


Figure 4.3: The electric circuit to be called 'TLT-supply'. Parts 1–4 are explained in the text. TU: trigger unit.

voltage is only just above inception. In that case the jitter of $t_{ss} - t_2$ can be up to several microseconds. The signal t_1 has simultaneously been sent to a delay generator that gives a pulse to the CCD-camera at t_3 . The camera opens its gate 35 ns after t_3 with an adjustable duration or "gate" g . In the figure the value of the exposure time g is set to 50 ns, the camera allows settings from 2 ns to "infinite". With low discharge jitter, t_3 and g can be chosen in such a way that the streamers cross only a part of the gap during the exposure time of the camera, an example of such a snapshot is shown in figure 4.6a. If the jitter is high, it is unlikely that the camera observes the streamers with a short exposure time g . In that case photos are taken mostly with very long exposure times, as in figure 4.6d.

The second power supply (called TLT-supply) is shown in figure 4.3. Here again a capacitor (1000 pF) is charged (part 1 of the figure), but in this case to a positive polarity. It discharges when the spark gap is closed (part 2) via a Transmission Line Transformer (part 3) over the electrode gap (part 4 of the figure). This supply in principle transforms the voltage up by a factor of 4. Note that this supply is not inverting because the positions of capacitor and spark gap are exchanged in comparison to figure 4.1. The TLT provides $12.5 \, \Omega$ load impedance to the pulse former, but $200 \, \Omega$ to the discharge [122]. Therefore it is able to create high current pulses with better matching than a C-supply. Voltage and current are measured here with a Tektronix high voltage probe (P6015) and a Pearson current monitor (6585). The magnetic cores are inserted to damp reflections when the load is not well matched to the source.

Typical waveforms of voltage, current and energy are shown in figure 4.4. A series resistor of $R_2 = 0$ or $1 \, \text{k}\Omega$ is used again to probe its effect on the discharge. The voltage rise time

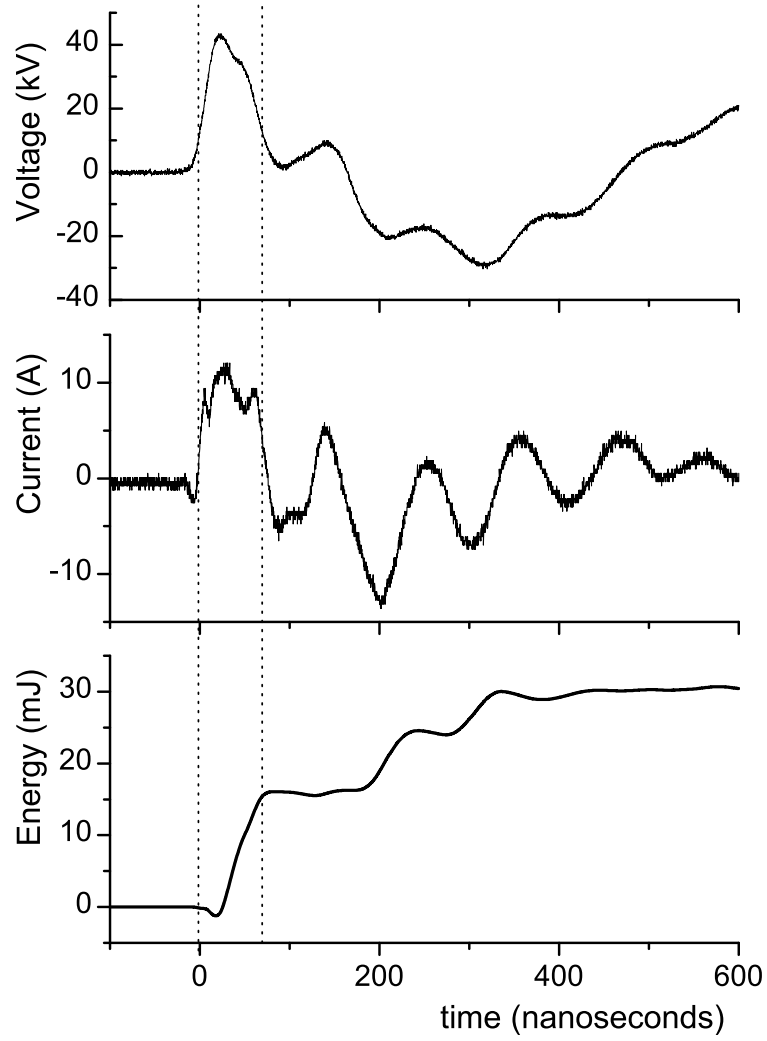


Figure 4.4: *Evolution of voltage, current and energy on the TLT-supply with a charging voltage of 14 kV in an 80 mm gap with $R_2 = 1 \text{ k}\Omega$. The peak current and voltage are $I_P = 12 \text{ A}$ and $V_P = 40 \text{ kV}$. The voltage rise time is $\sim 24 \text{ ns}$, the corona pulse duration is $\sim 50 \text{ ns}$.*

is ~ 25 ns, and it is independent of the series resistor R_2 . Figure 4.4 shows a current of ~ 12 A with $R_2 = 1$ k Ω obtained at 14 kV charging voltage. When taking an additional voltage drop of 12 kV across R_2 into account, this amounts to a transformation ratio of 3.8. In another case with $R_2 = 0$ a peak voltage of 41 kV is obtained at 11.3 kV charging voltage, so the transformation ratio is 3.6. Probably the higher current in this case leads to more losses in the TLT.

The pulse shape appears to be independent of the value of R_2 for the values used here because the rise time in the TLT-supply is determined by the output impedance of the TLT and the capacitance of the discharge for as long as the resistance of the discharge is of the same order as the output impedance (when stray inductance and capacitance is neglected). Changing the resistance then hardly influences the rise time.

The width of the corona pulse is indicated in the figure with two dotted lines that are 70 ns apart (the first peak is capacitive, the actual corona current peak is ~ 50 ns). The energy content, as shown in figure 4.4, is ~ 15 mJ up to the second dotted line. The oscillations after 100 ns show that the impedance of the corona discharge does not match to the power supply. The energy from these oscillations anyway does not contribute to the primary streamer propagation. The matching of TLT-supplies to a corona discharge can be almost perfect in long wire-cylinder discharges at very high currents [122].

4.2.2 Diagnostic procedure

In all measurements reported here, a point-plane electrode configuration is used, and the distance between the electrodes is adjustable. The anode tip is made of thoriated tungsten and has a radius of ~ 15 μm . The round cathode inner plate is 100 mm in diameter, the outer ring of the divided cathode has an outer diameter of 180 mm. All measurements are performed in ambient air at normal pressure.

Photographs of the discharge are taken with an analogue intensified CCD-camera, a 4QuikE from Stanford Computer Optics with 736 x 572 pixels with 8.6×8.3 μm pixel size. The camera is sensitive in the optical wave length range of 300 to 800 nm; the figures are actually dominated by emission of the $\text{N}_2(\text{C-B})$ transition that has a decay time of about 1 ns. In the figures within this chapter, the focal depth is about 20 mm.

The streamer diameter is determined from iCCD-photographs like in figure 4.5. When measuring the diameter, care is taken that measurements are done on a single streamer at a place without return stroke, multiple streamers, anode glow or ‘out-of-focus’- effect. To avoid measuring effects of the return stroke, the camera’s exposure time is chosen in such a way that only the primary streamer during its flight is photographed, i.e., the exposure time is less than 100 ns. Voltage oscillations as in figure 4.4 then do not influence the images. Occasionally a long integration time of several μs is used to show the later evolution after the streamers have reached the cathode. This is in particular done for the

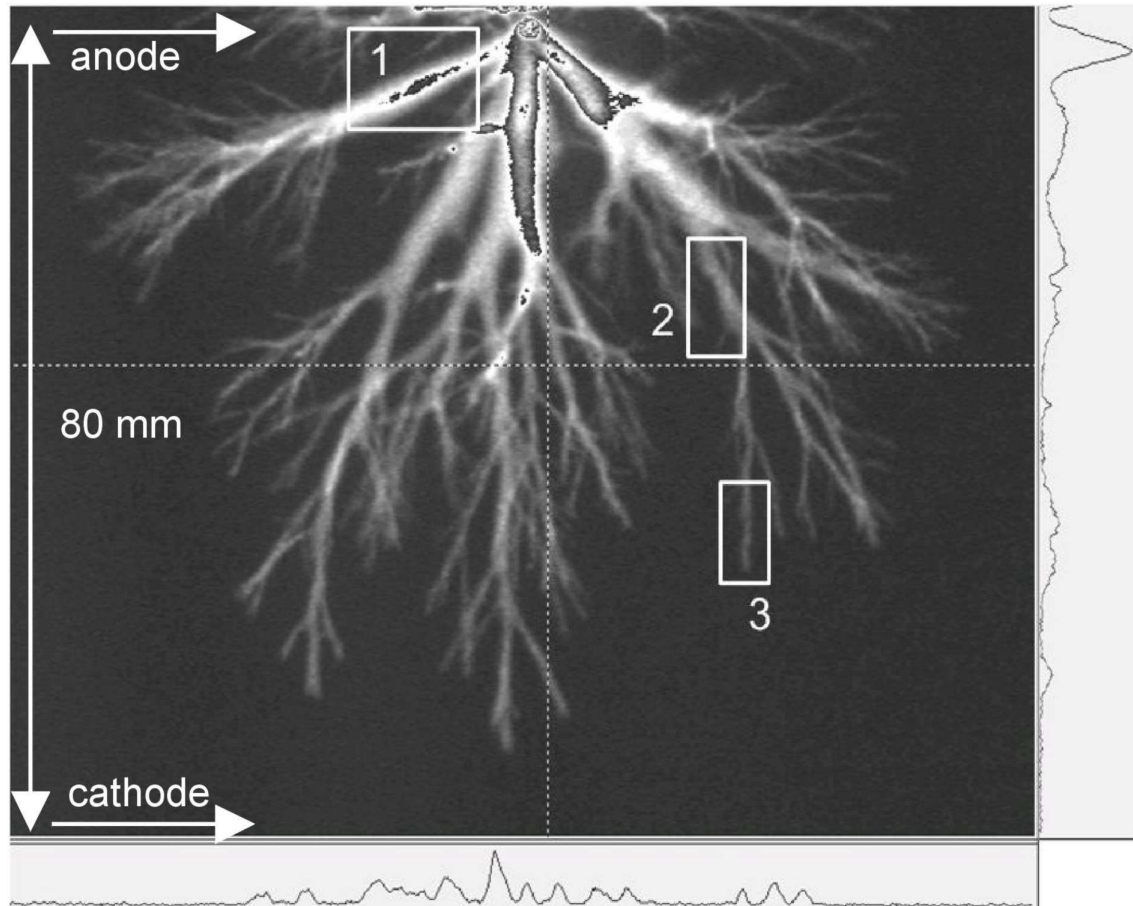


Figure 4.5: Streamers obtained with the C-supply in an 80 mm gap with $R_2 = 0$, $V_P = 60$ kV and $I_P = 10$ A. Profile bars at the positions indicated by the dotted lines are shown at the right and at the bottom. The optical exposure time for this photo is ~ 80 ns, during this time the streamers have not crossed the gap yet. The boxes indicate very thick (type 1), thick (type 2) and thin (type 3) streamers. For further discussion, we refer to section 4.3.

C-supply where the voltage decays slowly.

The dotted lines in figure 4.5 indicate the positions of the cross-sections shown in the profile bars below and beside the picture. Each peak in the profile corresponds to a streamer. The streamer diameter is measured as the full width at half maximum (FWHM) in the profile of the respective peak. At this point, we want to warn the reader that these diameters can deviate from the visual impression of the converted and plotted images: in the plotted images, bright channels will appear wider than faint channels when the FWHM diameter is the same.

4.3 Results²

4.3.1 The influence of voltage and gap spacing

Figure 4.5 shows a typical streamer pattern at atmospheric pressure in a gap of 80 mm under a voltage pulse of 60 kV. Near the anode three streamers with a large diameter can be seen. The clearest one is indicated with a box labelled 1. The FWHM diameter of this streamer is ~ 2.5 mm according to the prescription of section 4.2.2. The diameter is more or less constant while the streamers propagate towards the cathode. After ~ 20 -30 mm these thick streamers branch and several thinner streamers emerge with a diameter of ~ 1.2 mm. One such streamer is again indicated with a box, labelled 2. Then after shorter travel distances of the order of 5 to 10 mm, the streamers branch again in even thinner channels. Again, such a thin streamer is indicated by a box and labelled 3. The streamers from now on will be referred to as type 1, 2 or 3 according to the box number shown in figure 4.5 though we stress that there seems to be a continuous transition between streamers of different diameter, therefore the types should not be misunderstood as a classification of distinct propagation modes.

Reading the diameter of the type 3 streamers from figure 4.5 leads to a value of ~ 0.7 mm. In this situation, however, one pixel of the CCD camera corresponds to 0.15 mm. Taking into account that there is always some cross-talk between adjacent cells of a CCD array, one could suspect that these 0.7 mm are an overestimation. Indeed, when the CCD camera zooms in into the lower part of the discharge with a factor 2 or a factor 4, always at least 4 pixels in a row transversal to the streamer are illuminated, as summarized in table 4.1. It is clear that the diameter of the thin streamer is broadened due to instrumental effects when a large gap is imaged onto our CCD camera. When the total view of the camera is decreased to 20 mm, additional broadening sets in with now 5-6 pixels illuminated; this measured result of about 0.2 mm probably approaches the real streamer diameter.

²For extra information on the influence of voltages above 60 kV on diameter and velocity and the difference between power supplies, see chapter 7.

total view (mm)	FWHM width (# pixels)	apparent size (mm)
80	4 – 5	0.62 – 0.77
40	4 – 5	0.29 – 0.38
20	5 – 6	0.19 – 0.23

Table 4.1: *Diameters of streamers of type 3 in a gap of 80 mm obtained with different zoom factors.*

Zooming in further gives problems with focal depth and finding a streamer that meets all requirements for a correct determination of the FWHM. This value of 0.2 mm is also close to values reported earlier [12; 80; 106]. The measured diameters of the wider streamers of type 1 and 2 are, within experimental errors, not affected by zooming in.

First observations in a 40 mm gap using the TLT-supply have been given in [37] and in [33]. When compared to the photographs of e.g. [106], these pictures appear to give the idea of completely different streamer types, that would be distinguished by different propagation modes and separated by phase transitions. At that time the different appearance was essentially attributed to the TLT-supply with its low internal impedance. Here it will be shown that thick streamers with almost no branching also occur with the C-supply at sufficiently high voltage.

Figure 4.6 shows four streamer patterns in a shorter gap of 40 mm with a voltage pulse of 54 kV using the C-supply. (Because spark formation had to be prevented, higher voltages could not be explored in this short gap.) Figure 4.6a is taken with a camera exposure time $g = 4$ ns and such a delay t_3 that the observed streamers are in the middle of the gap. As shown previously [33; 105], not the complete streamer emits light, but only the actively growing heads of the channels. The image shows the path that the streamer heads have crossed within the exposure time, hence the velocity can be determined. In figure 4.6a, the travelled distance is $\Delta y = 6$ mm and the exposure time is $g = 4$ ns, therefore the local velocity at this part of the gap is 1.5 mm/ns. Note that there is some ambiguity in this determination as some streamers propagate towards or away from the camera and are therefore optically shortened. For our velocity measurements, we choose streamers that stay in focus and that we believe to propagate within the image plane.

Figure 4.6b is taken with an exposure time of the CCD intensifier of 50 ns. The streamers have not yet reached the cathode during this time interval because the gate opened some time before the streamers started. Several thick streamers of type 1 start at the anode, their diameter remains constant or even seems to increase and very few thinner branches are just appearing. The overall pattern in this photo is quite similar to the pattern of the thickest streamers in figure 4.5 when the different sizes (40 versus 80 mm) of the gaps are taken into account.

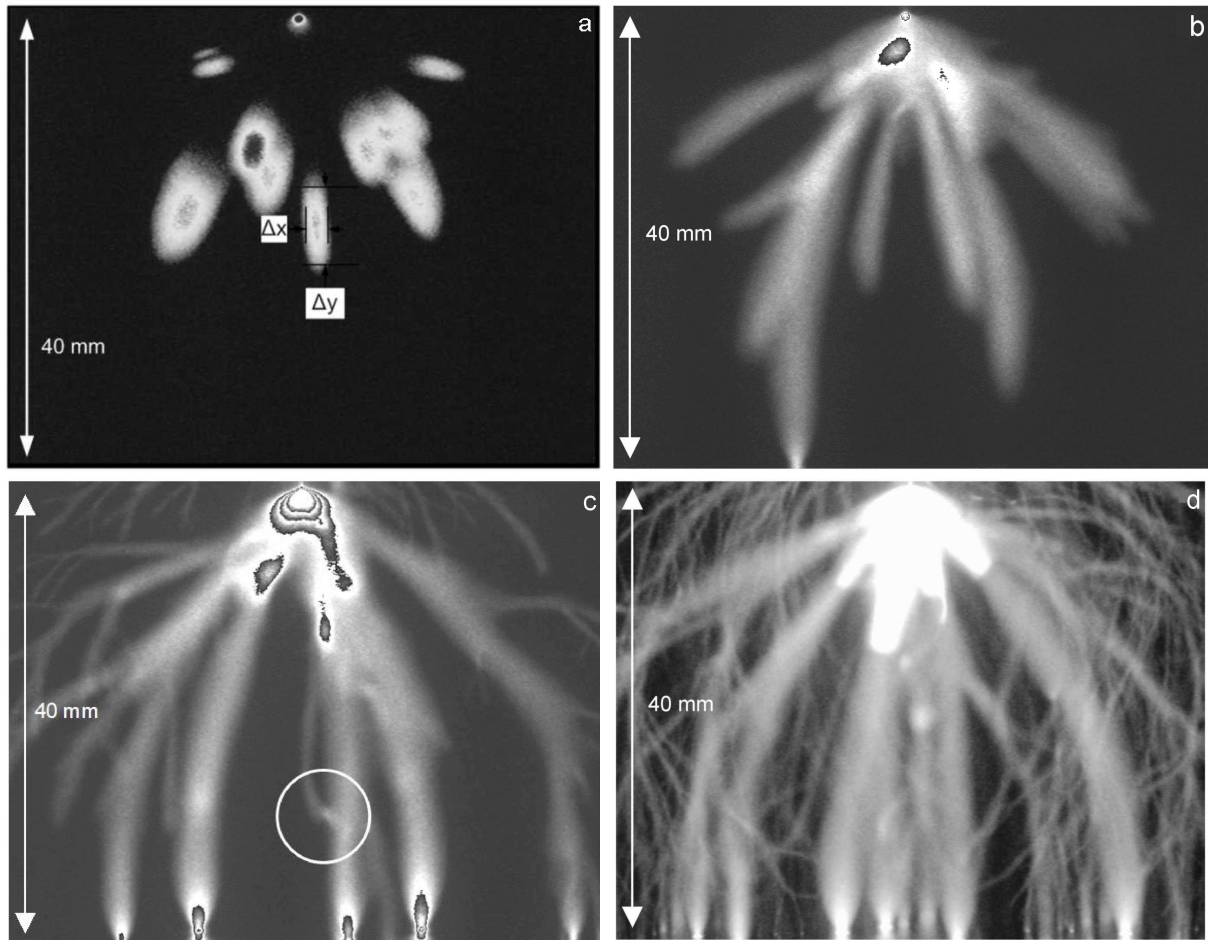


Figure 4.6: *Streamers in a 40 mm gap exposed to 54 kV with the C-supply. ($R_2 = 0$, $V_{DC} = 60$ kV, $V_P = 54$ kV and $I_P = 11$ A.) Camera exposure time: a) 4 ns, b) 50 ns, c) also 50 ns, d) 1.8 μ s.*

Figure 4.6c shows the discharge development taken with the same exposure time of 50 ns. But due to some jitter in the spark gap and the discharge inception, this picture shows a somewhat later stage of the development than figure 4.6b. The figure shows that the type 1 streamers can fully bridge the gap within these 50 ns as also observed in [33] and [37]. A new interesting feature appears: streamers with a diameter similar to those of type 3 in figure 4.5 start in the neighborhood of the point. These thin streamers will be called type 4. They mostly start after the thick streamers have reached the cathode. They seem to start at some surface roughness higher up on the anode or somewhere along an existing streamer path. When the integration time of the camera is longer, the thin streamers cross the whole gap. Figure 4.6c is chosen here particularly because it is not overcrowded with streamers and because it shows how late streamers have emerged from the anode but have not reached the cathode yet. Figure 4.6d shows how many thin late streamers cross from anode to cathode when a longer exposure time is used. Late streamers of type 4 are not observed when using the TLT-supply because the pulses of this supply are much shorter in time (see table 4.2).

Another remarkable event is observed in the circle drawn in figure 4.6c. A late streamer does not continue its way to the cathode but appears to bend towards an existing streamer path and seems to connect to it. This effect can, of course, not clearly be concluded from 2D photographs of a 3D event, but it is observed on many photos that a streamer bends towards another straight one and precisely stops at the straight streamer and practically never just before or just after. A plausible explanation for this observation is that a ‘return stroke’ changed the polarity of the early thicker streamer after it connected to the cathode, and that it therefore became electrically attractive for the late streamer. This effect was observed before [37; 106]; a similar event, but probably without prior connection to an ‘electrode’, was recently observed in sprites [22].

Now the behavior in the wider gap of 80 mm as in figure 4.5 is studied. For this gap length, pulses of 60 kV are strong enough to let the streamers bridge the gap. First, figure 4.7a shows streamers in an 80 mm gap at an applied voltage of 40 kV using the TLT-supply. These streamers die out roughly halfway the gap. They start as thick streamers at the anode with a diameter corresponding to type 2. They branch into type 3 streamers after ~ 10 to 40 mm.

In figure 4.7b the voltage is increased to 60 kV. The exposure time of the photograph is taken so short that the streamers have not reached the cathode yet. At the anode four streamers of type 1 diameter can be seen that branch into streamers of type 2 after ~ 20 mm. The streamer pattern in this figure, after branching into type 2 streamers, is very similar to the streamer pattern in figure 4.7a starting right at the anode. A possible conclusion is that the end of the type 1 streamer in the 60 kV discharge plays a similar role as the electrode needle for the 40 kV discharge: it supplies a similar current and voltage for the further streamer evolution.

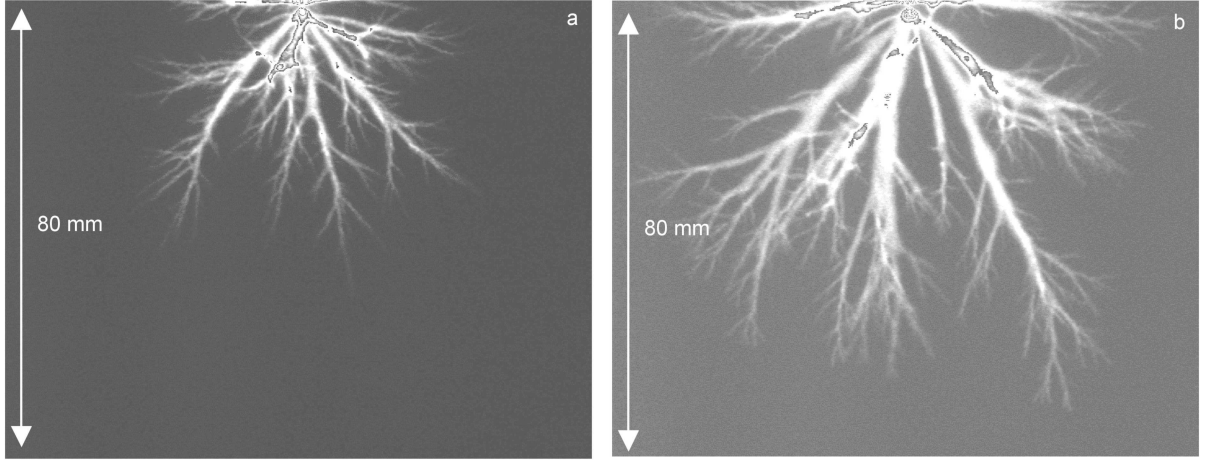


Figure 4.7: *Streamers in an 80 mm gap with the TLT-supply and $R_2 = 0$. a) $V_{DC} = 11$ kV, $V_P = 40$ kV, $I_P = 19$ A. b) $V_{DC} = 16$ kV, $V_P = 60$ kV, $I_P = 48$ A. In figure b, the voltage pulse of 60 kV is high enough and the pulse duration is long enough for the streamers to bridge the gap, as other observations show. However, the exposure time in this particular picture is chosen so short that the primary streamers have not crossed the gap yet during the camera exposure time.*

Figure 4.7b shows frequent streamer branching that creates many type 3 streamers in practically the whole gap, but in the most pronounced way further away from the anode. These thin streamers do reach the cathode, as is observed on pictures with longer optical exposure times. However, type 4 streamers have not been observed in the 80 mm gap, neither with the short pulse of the TLT-supply nor with the C-supply.

4.3.2 The influence of the power supply

The C-supply and the TLT-supply have both been operated with a peak voltage V_P on the gap of 40 and 60 kV and with R_2 set to zero or 1 k Ω . The maximum of the DC supply is 60 kV so the peak voltage of the pulse is lower if there is a considerable current pulse across R_2 . The parameters of the electrical pulses used in this chapter are summarized in Table 4.2.

Table 4.2 is not complete because some current measurements were considered to be unreliable due to oscillations. Nevertheless, the table does show several remarkable effects:

1. For given peak voltage the peak current slightly decreases with increased gap spacing.
2. The series resistor R_2 of 1 k Ω reduces the peak current by a factor $\sim 0.1 - 0.3$ in the case of the C-supply and by a factor $\sim 0.4 - 0.6$ for the TLT-supply.

	gap (mm)	V_{DC} (kV)	R_2 (k Ω)	V_{peak} (kV)	I_{peak} (A)	T_R (ns)	dt (ns)	E (mJ)
C-supply	40	40	0	40	1.7	30	80	6.4
		60 ^a	0	54	11	30	70	59
		60 ^a	1	42	1	60	120	5.5
	80	60	0	60	$\sim 10^b$	27		
		60	1	57	$\sim 3^b$	51		
TLT-supply	40	11.3	0	40	22	25	25	19
		17.2	0	60	55	26	35	95
	80	11.3	0	40	19	24	35	22
		16	0	60	48	23	25	72
		14	1	40	13	24	50	17
		22	1	60	$\sim 20^b$	23		

Table 4.2: *Electrical properties of the pulses.* V_{DC} is the voltage of the source and R_2 a resistance in the circuit, see figures 4.1 and 4.3. V_P and I_P are peak voltage and peak current at the discharge. T_R is the voltage rise time, dt the halfwidth of the current peak and E the integrated energy of the total peak. The values indicated with ^a are measured with $R_3 = 4$ k Ω ; for the rest $R_3 = 25$ M Ω . The values indicated with ^b are an estimate.

3. For $R_2 = 0$ the TLT has a transformation ratio of 3.6 ± 0.1 between peak voltage V_P on the corona gap and V_{DC} of the power source, and for $R_2 = 1$ k Ω this ratio goes down to 2.8 ± 0.1 . When the voltage across R_2 is added the ratio becomes 3.7 ± 0.1 .
4. The rise time of the C-supply depends on R_2 . The rise time of the TLT-supply does not depend on R_2 .
5. The peak currents with the TLT-supply are 5-10 times larger than those with the C-supply for identical pulse voltages V_P and gaps.
6. The pulse duration of the TLT-supply is shorter.
7. The energies per pulse are a factor 2 to 3 higher for the TLT-supply. This comparison is troublesome because the incompleteness of the dataset is most obvious here. Further, the longer duration of the pulses of the C-supply contain energy of the secondary streamers and the energy of the TLT-supply pulses can be inaccurate due to the oscillations of the TLT.

Now the branching patterns obtained with both power supplies will be compared. The streamer patterns created with both power supplies are not very different when R_2 is zero, see figures 4.5 and 4.7b. The main difference is that the thick streamers propagate further

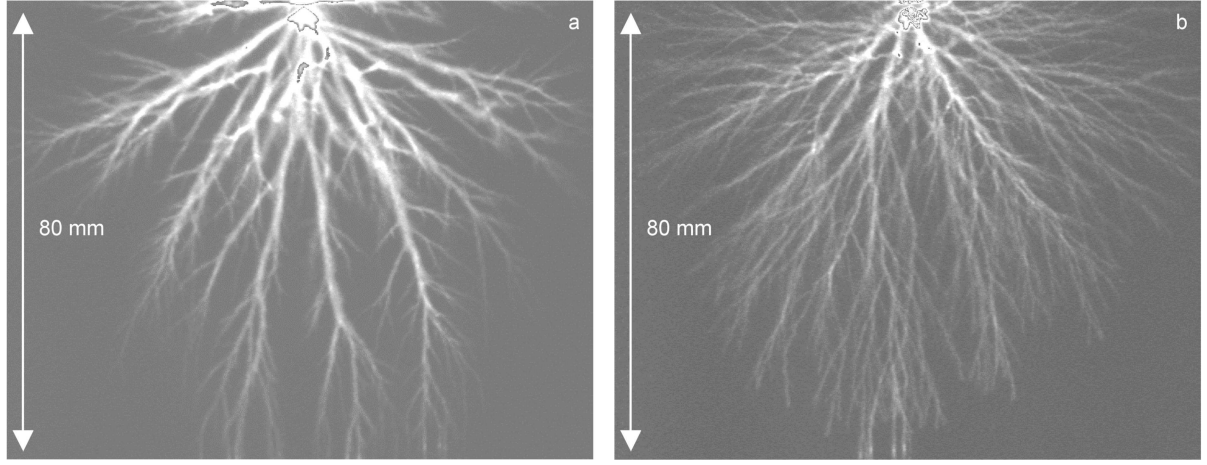


Figure 4.8: *Streamers in an 80 mm gap with $R_2 = 1 \text{ k}\Omega$. a) TLT-supply with $V_{\text{DC}} = 22 \text{ kV}$, $V_{\text{P}} = 60 \text{ kV}$, $I_{\text{P}} = 20 \text{ A}$, optical exposure time $50 \text{ }\mu\text{s}$. b) C-supply with $V_{\text{DC}} = 60 \text{ kV}$, $V_{\text{P}} = 57 \text{ kV}$, $I_{\text{P}} = 3 \text{ A}$, optical exposure time $1.4 \text{ }\mu\text{s}$.*

in the gap in the case of the TLT-supply. Table 2 shows that there is a difference of a factor ~ 4 in current between figures 4.5 and 4.7b.

Figure 4.8a shows a picture of the 80 mm gap in the case when the resistor $R_2 = 1 \text{ k}\Omega$ is added to the TLT-supply circuit. The current through the discharge decreases from 48 A (figure 4.7b) to $\sim 20 \text{ A}$ (for $V_{\text{P}} = 60 \text{ kV}$) while the rise time remains the same. No type 1 or type 4 streamers can be seen. The branching of type 2 streamers into type 3 streamers occurs in figure 4.8a closer to the anode than in figure 4.7b. So, the current and the streamer thickness is limited here by the impedance.

When the resistor R_2 is added to the C-supply, not only the maximum current is reduced with a factor three in the 80 mm gap, but also the rise time of the voltage pulse becomes a factor 2 longer. Figure 4.8b shows the streamer pattern in this situation (figure 4.5 shows the case with $R_2 = 0$). Also here there are no type 1 and 4 streamers, and the type 2 streamers are even shorter than in figure 4.8a. The type 3 streamers fill up the larger part of the gap and branch many times.

The rise time of the voltage in the last case becomes comparable to the gap crossing time of the streamers. So what probably happens is, that the streamers initiate from the needle before the voltage has reached its maximum; therefore initially they form a pattern of thinner streamers corresponding to this lower voltage. Apparently, the streamer diameter cannot increase substantially during the later evolution, while streamers can branch into thinner streamers. A future theoretical study of electric currents and potentials within the streamer pattern will have to shed more light on this evolution.

	V_{DC} (kV)	R_2 (k Ω)	velocity (mm/ns) per streamertype		
			1	2	3
C-supply	40	0	—	0.4	0.1
		1	—	—	—
	60	0	1.5	0.5	—
		1	—	1	—
TLT-supply	40	0	—	0.35	0.07
		1	—	—	—
	60	0	1.5	0.4	—
		1	—	0.5	<0.3

Table 4.3: *Streamer velocities obtained in the 80 mm gap.*

4.3.3 The velocity of different streamer types

The streamer velocity at various places in the electrode gap can be obtained from time resolved measurements as demonstrated, e.g., in figure 4.6a for type 1 streamers or in figure 1.1 for type 3 streamers. The travelled distance is measured as the full width half maximum length of the streamer head path and this is divided by the exposure time which typically ranges from 4 to 50 ns. This measurement is complicated by several circumstances. First, the spark gap switches have considerable jitter, therefore the time t_2 in figure 4.2d has a jitter of the order of several tens of nanoseconds. So it is a matter of trial and error to obtain a suitable piece of streamer on a photo in a wanted position in the gap. For this reason table 4.3 could not be completed. A second cause for incompleteness of this table is that not all types of streamers occur under the conditions indicated.

Furthermore, as already said above, there are not really distinguishable streamer types, and a streamer can continuously change from type 1 to type 2 and further to type 3. The table contains measurements on short streamer parts that clearly fall into one particular ‘type’. The shortness of the streamers leads to larger errors in the determined velocity. Therefore the velocities in table 4.3 have errors and should be understood as representing a broad distribution with widths of 20 – 50 %. Late type 4 streamers appear with considerably more jitter in time. This makes it virtually impossible to determine their velocity with the method used here.

Table 4.3 shows that thick streamers travel faster than thin ones; they also occur closer to the point electrode where the instantaneous local background fields are higher — however, the local background field in the absence of streamers should not be confused with the actual local field when the streamers are present. In ambient air at atmospheric pressure, streamers of type 1 are the fastest with velocities of more than 1 mm/ns. Streamers of type

2 have velocities of ~ 0.5 mm/ns and streamers of type 3 have velocities of ~ 0.1 mm/ns. The velocity range found here is in the same range as in other experiments [19; 80] and calculations [19; 50; 80].

A general trend is that type 2 and type 3 streamers are faster when the applied voltage is higher, but further quantification is not possible at the present stage. For type 1 streamers, the limited amount of data available does not allow conclusions.

4.4 Discussion and conclusions

4.4.1 Comparison of power supplies: the role of rise time and internal resistance

In our point-plane gaps of 40 and 80 mm, with pulse amplitudes in the range of 40 – 60 kV, currents are obtained in the range of 1 to 55 A, see table 4.2. This demonstrates the well-known strongly non-linear relation between peak voltage and peak current of the pulsed corona discharge that in addition are strongly influenced by the different power supplies with their different voltage rise times and internal resistances.

In the C-supply for $V_{DC} = 40$ kV, the voltage rise time increases from 30 to 60 ns when the series resistance $R_2 = 1$ k Ω is added. Assuming that this is an RC charging time, the internal resistance of the power supply, R_C also has to be ~ 1 k Ω . This agrees with a dip of ~ 2 kV when the peak voltage of $V_P = 42$ kV as seen in figure 4.2; here the peak current is $I_P = 1$ A and the series resistance is $R_2 = 1$ k Ω , see table 4.2. With $R_2 = 0$ the current almost doubles to 1.7 A. This implies that the discharge adapts to the power supply and changes its internal resistance with almost the same factor of 1.7. So the consequence of adding R_2 in the C-supply is both a limitation of the current and an increase of the voltage rise time. Under these conditions, the streamers are considerably thinner and carry less current.

The output impedance of the TLT-supply is 200 Ω . For a peak voltage $V_P = 60$ kV in the 80 mm gap, the peak current is $I_P = 48$ A when $R_2 = 0$. This corresponds to an internal loss in the power supply of $48 \text{ A} * 200 \Omega = 9.6$ kV. For this peak, 17.2 kV charging voltage was used, so ideally the TLT-supply should produce 69 kV with a transformation ratio of 4. Therefore the peak voltage at the gap should be 59.4 kV, very close to the measured value of 60 kV. With $R_2 = 1$ k Ω , the current drops to ~ 20 A and a charging voltage of 22 kV is required. This leads to a peak voltage on the gap of $4 * 22 \text{ kV} - (1 \text{ k}\Omega + 200 \Omega) * 20 \text{ A} = 64$ kV, again close to the measured value of 60 kV. For the TLT-supply, the resistor R_2 limits the current, but has no influence on the voltage rise time.

The hypothesis that the internal resistance of the power supply determines the streamer pattern when peak voltage and rise time are identical, can be tested by comparing exper-

iments with the C-supply and $R_2 = 0$ to experiments with the TLT-supply and $R_2 = 1$ k Ω . This is because the C-supply has an internal resistance of ~ 1 k Ω as derived from its change in rise time while the TLT-supply with R_2 added has 1.2 k Ω resistance in total. Indeed, when applying these two power supplies to the 80 mm gap at $V_P = 60$ kV, the C-supply delivers 10 A and the TLT-supply the very similar value of 13 A. Furthermore the streamer patterns in these two cases are quite similar as figures 4.5 and 4.8a show. We conclude that power supplies will create similar streamer patterns if their voltage rise time, peak voltage and internal resistance are similar, and that the internal resistance plays a decisive role.

4.4.2 Thick and thin streamers, streamer branching

For ease of discussion, streamers of different width are characterized here as four different "types", though they do not seem to be distinguished by phase transitions or different propagation modes:

- Type 1 streamers are very thick with a diameter of about 2.5 mm, their velocity is just over 1 mm/ns and they carry currents of up to 12 A.
- Type 2 streamers are thick with a diameter of about 1.2 mm, a velocity of 0.5 mm/ns and currents of the order of 1 A.
- Type 3 streamers are thin, their diameter is 0.2 mm which can only be properly determined by zooming in sufficiently with the camera (cf. table 1), their velocity is ~ 0.1 mm/ns and their current ~ 10 mA.
- Type 4 streamers are late, they start to propagate after streamers of type 1 or 2 have crossed the gap, their diameter appears to be similar to type 3 streamers, their velocity and current could not be determined but are expected again to be similar to type 3 streamers. Type 4 streamers occasionally connect to the already existing streamer paths of type 1 or 2.

A qualitative explanation of these different streamer diameters is that high local electric fields, in particular, fields that exceed the breakdown threshold [69] close to the needle electrode, create wide streamers. Similar observations of increasing negative streamer diameters in increasing fields can be found in the simulations presented in [59; 70; 71]. On the other hand, if the voltage rise time is comparable to streamer formation and propagation time, streamers can initiate near the needle while the local field is still lower, and the streamers are then more narrow. Therefore one could expect that a voltage rise time of 10 ns or less for a 60 kV voltage pulse would create even thicker streamers. This

is consistent with streamers of 10 mm diameter in [8] that are created in a larger dV/dt (pulses of 140 kV with 30 ns rise time) in a wire-cylinder gap of 145 mm radius.

In the present point-plane electrode geometry, streamers approximately keep their initial diameter between branching events, though in a wire-plate electrode geometry recently streamer diameters were observed to grow [117]. The streamers characterized as type 3 and 4 might be streamers of *minimal* diameter. Such a minimal diameter is necessary for the specific mode of streamer propagation by local field enhancement [33]; it requires the streamer diameter to be larger than the thickness of the charged ionization front in the streamer head [33].

In contrast to these streamers of probably minimal diameter ("minimal streamers"), the thick streamers of type 1 and 2 propagate faster and in higher background fields. They seem to come with a continuous variety of diameters. It is surprising to note that the average distance between branching is much larger for thick streamers than for thin streamers. An explanation for this fact is presently not at hand.

Another intriguing phenomenon is that late (type 4) streamers can bend towards earlier channels as shown, e.g., in figure 4.6b. Similar phenomena have recently been observed in sprites [22]. However, in the present setup, it is likely that the streamer channels change polarity after reaching the electrode and therefore attract later streamers; this mechanism is unlikely for sprites in high layers of the atmosphere.

4.4.3 An estimate on the current density

We observe that the current density in streamers seems to be rather unchanged in quite different streamer patterns generated by different circuits. The estimate is based on the fact that the peak current lasts about as long as the streamers propagate.

The highest current peak measured is 48 A in figure 4.7b. When one assumes that this current initially near the electrode is carried by four thick streamers with a diameter of 2.5 mm, the current density in such a streamer is ~ 2.4 A/mm². In figure 4.8a 7 streamers of type 2 can be identified near the tip. The measured current peak is 20 A. With a diameter of 1.2 mm this gives a current density of ~ 2.4 A/mm². Figure 4.8b shows the measurement with the largest number of thin streamers, namely more than 200. Here the current is 3 A in total, i.e., ~ 0.015 A per streamer. The diameter of this type 3 streamer is 0.2 mm, therefore the current density is 0.5 A/mm².

According to this very rough estimate, the current density within the streamer varies by a factor of ~ 5 while the current within a single streamer varies by a factor ~ 800 .

4.4.4 Final remarks and theoretical challenges

Pulsed positive corona discharges in air show a large variety of streamer diameters and consecutive branching patterns. We suggest that this is determined by three properties of the external electric circuit: the peak voltage, the voltage rise time and the internal resistance.

We have presented our experimental results. It appears that all streamer photographs known to us fit in the presented frame of different diameters under the indicated conditions, such as gap size and pulse parameters. Obviously they ask for theoretical explanation: can theory reproduce streamer diameters, current, current density and velocity as a function of the external circuit? Which additional insight does theory give into the inner structure of the streamer that is experimentally not accessible? The recent progress in numerical simulations of streamer dynamics, e.g. in [56; 59; 70; 71; 78; 80], appears to make it possible to address the questions raised here in the near future.

A detailed understanding of the generated streamer structures requires us to distinguish different stages of the dynamics, namely *(i)* the inception and nucleation process next to the pointed anode, *(ii)* the streamer propagation and branching dynamics, and *(iii)* the late stages of evolution after the first streamers have crossed the gap. These are clearly distinct processes and should be analyzed separately. *(i)* The first step is the streamer inception. Our experiments show that a fast rise to a high voltage together with a low impedance of the circuit favor the formation of thick streamers next to the pointed electrode; these streamers are fast and can carry a high current. For the formation of these streamers, the source of free electrons and the anode processes in the instantaneous local field need to be modelled appropriately. An ionization seed is formed in the high field region around the pointed electrode that then propagates outwards and destabilizes into a number of streamer branches. This nucleation process determines the number and size of the emerging streamers. *(ii)* In the second phase each streamer carries a given charge, enhances the local field and propagates outwards. Here the challenge lies in understanding the diameter, velocity and branching process of a streamer head that is characterized by a certain head potential and charge content. We stress our conviction [33] that the electric potential alone is an insufficient characterization, and that different streamer diameters need to be related to different amounts of electric charge carried by the respective streamer heads. The splitting of one thick into several thinner streamers is then understood also as a splitting of the charge content of the original streamer over several new streamers — where we emphasize that electric charge is a conserved physical quantity. Note that numerical simulations about streamers in literature only deal with this second phase. *(iii)* After the streamer has reached the cathode, return stroke and electric recharging determine the further current flow and electric interaction of the channel.

We conclude with remarking that recently it was shown that the thick streamers created by

very short pulses are very efficient for ozone productions [39; 117]. They also use the power supply in the most efficient way [122]. The present study therefore not only increases our fundamental knowledge on streamer discharges, but is also very relevant for applications.

Chapter 5

Pressure dependence: an overview

Streamer patterns at pressures below one bar are visualized with an iCCD-camera for positive streamers in a point-plane gap in air. In a fixed electrode gap and at a fixed voltage, the streamer diameter increases with decreasing pressure, the cloud at the electrode tip enlarges and the distance between branching events increases. The electrode gap has to be enlarged to see streamer structures. The results show that lengths scale approximately as $1/p$.

5.1 Introduction

In this chapter we will take a qualitative look on streamers at pressures below one bar before showing the quantitative details in chapter 6. In chapter 3 about the evolution of streamers it is already mentioned that pressure can be used to zoom into the structures and evolutions of the discharge because lengths and fields are expected to approximately scale with inverse pressure p (chapter 2). Other motivations to study the influence of pressure are that streamer concepts are applied to so-called sprite discharges [33; 35; 83; 97] that occur at heights of 40 to 90 km in the atmosphere; the pressure at 80 km height is about 10^{-5} bar. Here the verification of similarity laws is vital for predictions. And furthermore, pressure variation is a natural extension of the range of measurements.

5.2 Experimental setup

The measurements are done on positive streamers in a point-plane gap with the C-supply, as described in chapter 4, with voltages up to 40 kV in gaps up to 160 mm. The components are given in table 5.1. Two different high voltage switches are used, a low inductance semiconductor Behlke HTS 651-03-LC switch ($V_{\max} = 65$ kV, $I_{\max} = 30$ A) and a sparkgap switch, which both can be inserted at "HV-switch" in figure 4.1. The difference between the switches is their internal resistance and capacitance: the semiconductor circuit (C-SC-supply) has a resistance of 60 - 1000 Ω and a capacitance of 30 pF, while for the sparkgap (C-SG-supply) these parameters are estimated to be 1 pF and ~ 10 Ω [106]. This can result in differences in streamer appearance [106]. However, the addition of the 2 k Ω series resistance in the circuit dominates the current and determines the streamer pattern (chapter 4). Therefore, photographs from both setups can be compared. The combination of R_3 and C determines the decay time of the voltage pulse and has no effect on the streamer pattern.

All measurements are done in air with a tungsten needle (diameter = 1 mm, tip radius = 15 μm) and the stainless steel divided cathode plate. The voltage is measured by a Northstar PVM4 voltage divider just above the anode (figure 4.1). The photographs are taken with a digital 4QuikE camera from Stanford Computer Optics. The fixed time delay between the pulse of the function generator ($T = 0$) and the start of the high voltage pulse is at least 1.2 μs when the sparkgap is used and 0.35 μs when the Behlke switch is used. Depending on the streamer inception time and jitter in the setup the delay can become (much) longer. Since the streamer propagation starts after this delay the combination of camera exposure time and delay must exceed ~ 1.2 μs or ~ 0.35 μs , respectively, to obtain an image on the photograph. The discharges are pulsed single shot unless indicated otherwise. No differences are observed between streamers that are pulsed single shot (at least 10 seconds between the discharges) or 1 Hz.

gap (mm)	R_1	R_2	R_3	R_4	C	switch
10, 20, 40	25 M Ω	2 k Ω	1 M Ω	2.75 Ω	1 nF	Behlke HTS 651
160	25 M Ω	2 k Ω	25 M Ω	8.5 Ω	1 nF	sparkgap

Table 5.1: *Values of the components used in the C-supply.*

5.3 Results

5.3.1 First observations

A first observation of streamers as a function of voltage and pressure is given in figure 5.1 for a 40 mm point-plane gap. The transition from thin to thick streamers with increasing applied voltage as discussed in table 3.2 is nicely shown. It also shows that when the pressure decreases the streamer diameter increases, the number of streamers and branches decreases, the cloud at the tip becomes larger and the distance between branching events becomes longer. At 1000 mbar and voltages just above the inception voltage, the streamers fade during the transit, as in figure 5.1a. At other conditions, i.e. at 1000 mbar and higher voltages or at lower pressures (100, 200 and/or 400 mbar), streamers either cross the complete electrode gap or do not ignite at all. Streamers in figure 5.1b-l that do not reach the cathode are photographed during their transit. The photographs at 100 and 200 mbar show that the cloud at the tip grows with increasing voltage. In figure 5.1l the discharge (cloud + glow, chapter 3) fills the complete interelectrode distance. Here and in figure 5.1i, extra streamers are visible beside the cloud+glow. Measurements show that also a cloud+glow without these extra streamers can appear at these settings, as shown in figure 3.3. When then the voltage amplitude or duration is increased a spark arises.

When comparing these measurements with those in a 17 mm gap [13], where the figures show a maximum of four streamers at 400 mbar down to one streamer at 100 mbar, it is clear that streamers need space to develop. It is experimentally found that an electrode gap of at least 20 mm is necessary when using the C-supply to see streamer structures of more than one channel at a pressure of 100 mbar. The observation that streamers die out in the gap at $V \approx V_{\text{inception}}$ ¹ and 1000 mbar while they do not fade at similar voltages but lower pressures of 400, 200 and 100 mbar is because all lengths scale with $1/p$ (chapter 2) and thus the streamers become large enough to reach the opposite electrode.

5.3.2 Scaling with $p \cdot d$

Figure 5.2 shows streamers at a fixed voltage (10 kV) and gap (40 mm) and decreasing pressure to test if lengths scale as $1/p$. In the upper line it is shown that with decreasing

¹ $V_{\text{inception}}$ is the lowest voltage at which streamer channels are observed.

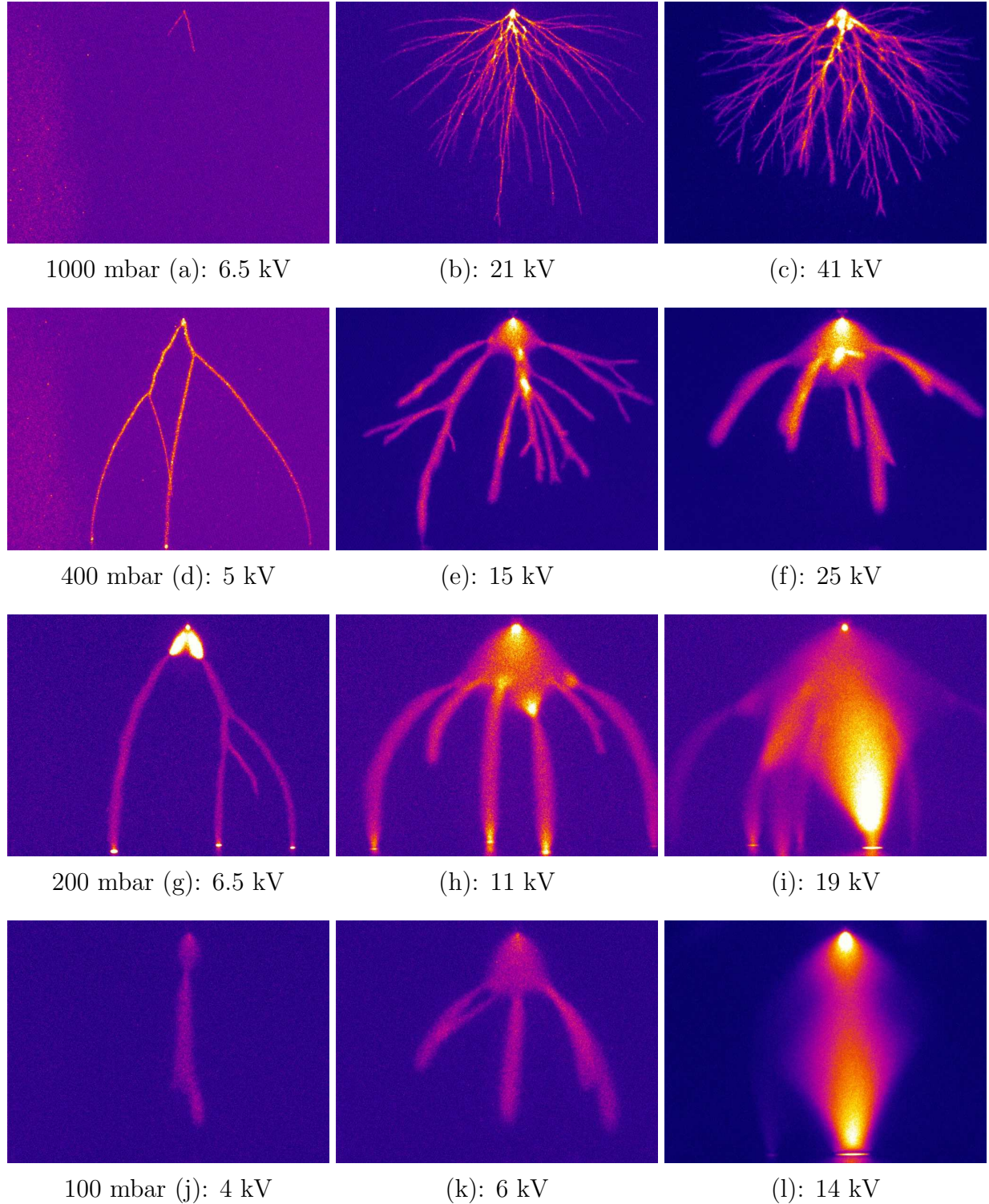


Figure 5.1: Measurements in a 40 mm gap in air at a-c) 1000 mbar, d-f) 400 mbar, g-i) 200 mbar and j-l) 100 mbar. The delay = 0; the exposure times are a) 60 μ s, b) 0.6 μ s, c) 0.44 μ s, d) 60 μ s, e) 0.6 μ s, f) 0.43 μ s, g) 15 μ s, h) 1 μ s, i) 0.5 μ s, j) 10 μ s, k) 0.7 μ s and l) 0.5 μ s. The streamers at j+k) are pulsed at 1 Hz.

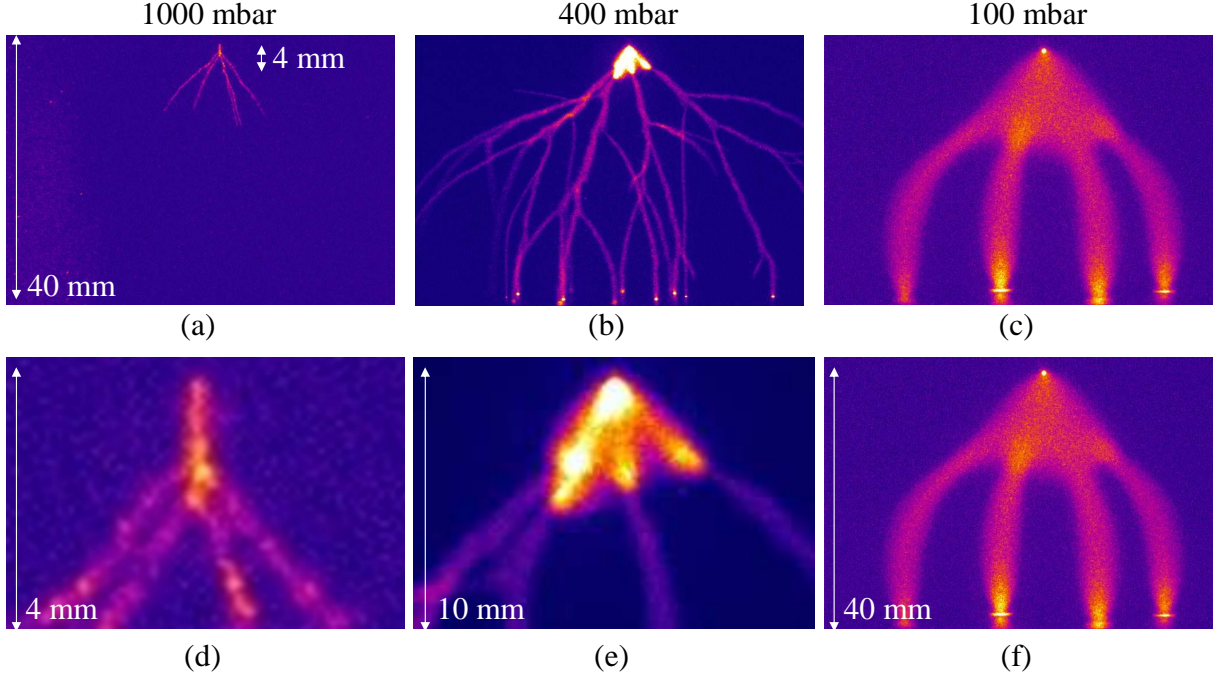


Figure 5.2: *Streamers in a 40 mm gap in air at ~ 10 kV at a+d) 1000 mbar, b+e) 400 mbar and c+f) 100 mbar, 1 Hz. Figure d-f) are zoomed photographs of a-c) such that pressure \cdot height = 4 mm \cdot bar. The delay = 0; the exposure times are a) 60 μ s, b) 10 μ s and c) 0.5 μ s.*

pressure the streamers start to cross the electrode gap, the streamer diameter increases and the distance between branching events increases. Also the cloud at the tip arises.

When zooming in to the region of the needle tip such that pressure \cdot zoomed height = 4 mm \cdot bar, i.e. a zoom of $\frac{1000\text{mbar}}{100\text{mbar}} = 10\times$ for the picture at 1000 mbar, we see that the presence of the tip breaks the scaling but that the streamer diameters scale away from the tip. All three discharges start with four streamers, with approximately the same diameter and do not branch.

Figures like figure 5.2 support the idea that lengths scale with $1/p$ rather well, especially when it is considered that the scaling law holds for discharges in which electrode processes and starting conditions can be neglected, which is certainly not the case near the electrode. It must also be noted that all measurements are done with the same needle with a radius of ~ 15 μ m while actually the needle tip radius (a length scale) has to be scaled with pressure too for true comparison.

The quantitative data of the variation in streamer diameter, velocity and distance between branching events with pressure will be given in section 6.4.3, 6.4.4 and 6.4.5, respectively, where it will directly be compared with measurements in nitrogen.

Chapter 6

Streamers in air and nitrogen-oxygen mixtures

Positive streamers are created in ambient air, nitrogen ($\sim 99.9\%$ pure) and a nitrogen-oxygen mixture with 0.2 vol% oxygen in a point-plane electrode gap. The streamers in air show a very different propagation pattern than the streamers in nitrogen and the mixture. In nitrogen the streamers are 1) thinner, 2) curlier, 3) intenser and 4) less diffuse than streamers in air. They also 5) branch more resulting in 6) a shorter distance between branching events and 7) they propagate further down the electrode gap. The branches that deviate from the main channel however 8) die out closer to this channel. The difference in intensity can be ascribed to the difference in average electron energy which is higher for nitrogen. The pressure scaling law is tested for minimal streamers over the pressure range from 13 to 1000 mbar. For the diameter a constant pressure times diameter is found of 0.20 ± 0.02 mm·bar for air and 0.12 ± 0.02 mm·bar for nitrogen. The branching parameter for the thinnest streamers, given by the ratio of distance between branches D and diameter d , is independent of pressure resulting in a value of 11.6 ± 1.5 for air and $D/d = 9.1 \pm 3.3$ for N_2 . This ratio appears to decrease with increasing voltage giving a value of $D/d = 7.6 \pm 3.6$ for very thick and thick streamers together, at 1000 mbar air. The streamer velocity increases with decreasing pressure. A final difference is the longer current pulse duration of the streamer- and glow-regime of the nitrogen discharge with respect to air (factor 30 at 1 bar) due to the absence of attachment in nitrogen.

6.1 Introduction

This chapter deals with differences between positive streamers in ambient air and nitrogen. Ambient air is used since it is the most commonly used gas in applications, experiments and nature. A complication of air is that it is a compound gas (78% N₂, 20% O₂, 0.97% H₂O, 0.03% CO₂ and 1% noble gases, mainly Ar [125]) in which many processes can occur. Nitrogen, the main component of air, is a simple single molecular gas which eases comparison with theory. At first glance one might think that differences between these gases are small. However, due to the amount of oxygen in air the differences are substantial. Oxygen in air gives the possibility of photoionization which is assumed to be necessary for creating positive streamers. Furthermore, oxygen is an electronegative gas that attaches electrons which results in quenching of the discharge in air. Since in a single molecular gas like nitrogen less processes occur than in a compound gas as air it is less complex to simulate streamer propagation in nitrogen in numerical models. However, a complication of nitrogen is that 100% pure nitrogen cannot be obtained in experiments. Therefore, always some impurities will be present in the gas that may influence the streamer behavior.

6.2 Experimental setup

6.2.1 General information

The measurements are done on positive streamers in a point-plane gap using the C-supply, as described in chapter 4 with voltages up to 45 kV in gaps up to 160 mm. The components are given in table 6.1. The voltage is measured with a Northstar PVM4 and the current is measured via a divided cathode (≤ 40 mm gap) or current shunt (160 mm gap). To obtain the total streamer current care is taken that the distance between anode and cathode is less than twice the plate's diameter [115]. Therefore, when measuring in the 160 mm gap the stainless steel divided cathode is replaced by a stainless steel disk of 340 mm in diameter, see figure 6.1. Since this disk is close to the walls of the vacuum vessel, no outer ring is used. It is connected to the bottom of the vessel by 4 equally spaced resistors of 33 Ω resulting in a resistance of 8.25 Ω . The current is measured over this resistance. Since the cathode can be descended/elevated only a few centimeters in the vertical direction, the anode needle has to be moved to obtain the right distance between the electrodes. To avoid sparking between the needle and the upper lid of the vacuum vessel in the 160 mm gap, an erthalite disk is suspended to the upper lid of the vessel (figure 6.1). The needle is made from tungsten and has a diameter of 1 mm and tip radius of ~ 15 μm .

The camera must be able to move over a distance up to ~ 1.5 m from the needle to image the complete 10 mm to 160 mm electrode gaps on the camera. For electrode gaps ≥ 40 mm the camera (including the lens) can stay outside the Faraday cage and look through the

gap (mm)	R_1	R_2	R_3	shunt or R_4	CC or C	switch
10, 20, 40	25 M Ω	2 k Ω	1 M Ω	2.75 Ω	1 nF	Behlke HTS 651
160	25 M Ω	1 or 2 k Ω	8 k Ω , 1 or 25 M Ω	8.25 Ω	1 nF	sparkgap

Table 6.1: Values of the components used in the C-supply.

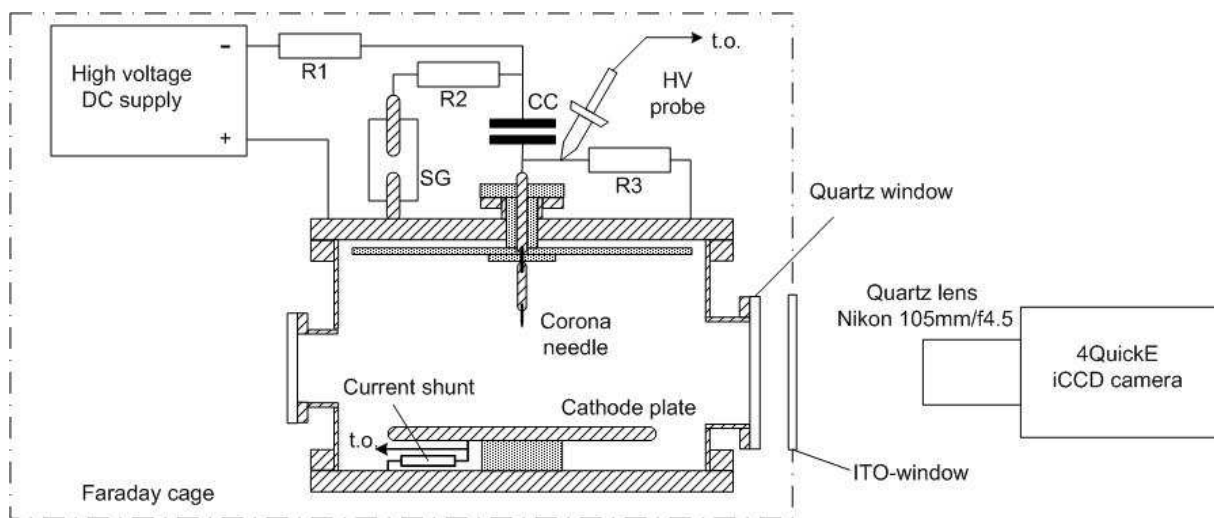


Figure 6.1: Scheme of the stainless steel vacuum vessel with the sparkgap C-supply for a 160 mm electrode gap. For other gap lengths a divided cathode is used (figure 4.1). SG = spark gap, CC = coupling capacitor, R_1 = charging resistor, R_2 = rise time determining resistor, R_3 = decay time determining resistor, t.o.= to oscilloscope.

ITO-window, just like in chapter 4 or figure 6.1. For gaps ≤ 40 mm the lens moves (partly) into the vacuum vessel. A copper tube with a BK7-window at its end is mounted to the Faraday cage (to keep the cage intact). The copper tube slides into a stainless steel tube that is mounted on the vacuum vessel. This stainless steel tube, which is situated inside the vacuum vessel, contains a quartz window. Both the ITO-window (gaps ≥ 40 mm) as the combination BK7 – quartz windows (gaps ≤ 40 mm) block light with wavelengths of less than 300 nm.

Gases

The gases used are ambient air, nitrogen (purity $\sim 99.9\%^1$) and a nitrogen-oxygen mixture (of 0.218 vol% O_2), hereafter called air, N_2 and $N_2:O_2$, respectively. They are used in a pressure range of 13 mbar to atmospheric pressure that is measured by the Pfeiffer CMR261. The pressure can be set on the Pfeiffer RVC300 control unit and is regulated by the Pfeiffer EVR 116 control valve. The gases flow via Brooks Massflow Meters (5850 TR series) in the vacuum vessel. The ambient air is the laboratory room air of that specific moment. The room air is as follows: The atmospheric pressure is between 996 - 1004 mbar, the temperature is regulated at 21.7 ± 0.5 °C and the relative humidity is 60%. Experiments in a point-plane gap showed that the effect of fluctuations of the air humidity on the streamer is limited [109]. When measuring with ambient air at atmospheric pressure, the front viewing window is taken off to ensure sufficient ventilation. At lower pressures all vessel windows are closed and there is no air flow into the vessel.

The vacuum vessel is pumped down by a Speedvac ED 150 rotary vane pump to 10 mbar and flushed three times before using nitrogen. The nitrogen comes from a cylinder with a purity of 99.999%. However, the nitrogen is led through (polluted) copper tubes into the building and via plastic tubes to the vacuum vessel. Besides impurities picked up (mainly) in the copper tubes, there are also impurities in the vessel due to components used like the tungsten needle, erthalite disk, glue and the perspex feedthrough. The vessel cannot be baked out to remove the water in the walls. Therefore, the purity of the nitrogen is expected to be only to $\sim 99.9\%^1$ and is supposed to contain mainly water vapor and oxygen. A gas flow is set on the Brooks Instrument (Readout & Control Unit 0154) with a refreshment rate of 6 slm² at 1000 mbar which corresponds to a complete refreshment of the vessel in ~ 10 minutes. This refreshment rate is adjusted with pressure to keep a refreshment time of ~ 10 minutes, e.g. 0.6 slm at 100 mbar.

The nitrogen-oxygen mixture is taken from a cylinder that contains nitrogen with 0.218 vol% oxygen. It is led directly to the vacuum vessel via plastic tubes. Before using this mixture the vessel is pumped down to 10 mbar and filled with N_2 . Thereafter it is pumped down again and filled with the mixture. Here also a gas flow is maintained with a refreshment rate of 6 slm at 1000 mbar. At lower pressures the refreshment rate is adjusted, just like for nitrogen.

6.2.2 Discussion on the setup

In the measurements different setup components and/or settings are used. The effect hereof on the streamer pattern is discussed in this section.

¹At the time of the measurements the purity was expected to be $\sim 99.999\%$.

²1 slm = 1 l/min at STP.

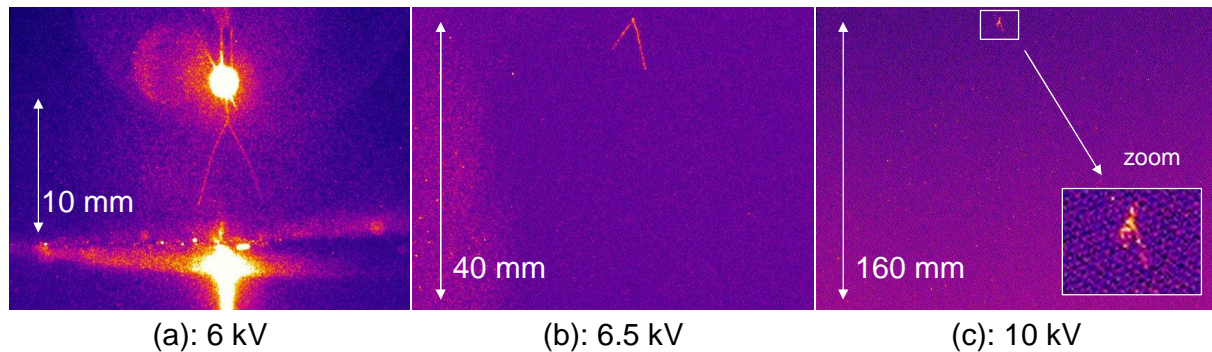


Figure 6.2: *Streamers at 1000 mbar in air in different gaps at their inception voltage. The delay = 0 ns and the exposure times are a) 70 μ s, b) 60 μ s and c) 2 μ s. In all three pictures the whole propagation is photographed.*

Needle shape

The sharpness of a needle degrades with increasing number and strength of applied pulses. Test measurements are done with a sharp (tip radius of 15 μ m), a round (tip radius of 0.5 mm) and a flat (edges of 90°) thoriated tungsten tip to investigate the influence of degradation on the streamer pattern. The discharge with the sharp needle ignites and sparks at ~ 2 kV lower voltage than the other two. It also induces considerably less jitter in the setup. No significant differences in streamer appearance are found when using the three tips. Therefore, no difference in streamer pattern is expected due to degradation of the tip. Since time resolved photographs can only be made with the sharp tip, this tip is used throughout the measurements.

Electrode gap

Figure 6.2 shows that when a rather similar voltage is applied at the needle tip the discharge is also rather similar regardless of the position of the bottom plate (provided that the streamer has enough space to develop): two streamers are observed that propagate approximately 10 mm towards the plate. These measurements show that the local electric field at the tip determines the streamer pattern and that an averaged electric field in the point-plane gap has no physical meaning. This is also shown in [11] for a 10, 17 and 25 mm point-plane electrode gap. In figure 6.2a a laserspot at the needle tip is visible. The laser will be explained in chapter 7. No differences are observed in streamer pattern with and without the laser.

Frequency

The discharges are pulsed single shot to be able to measure in a gas without electrons and ions from a previous discharge. However at very low voltages and pressures a pulse frequency of 1 Hz or 10 Hz is sometimes necessary to keep the discharge going. Differences in streamer pattern between single shot ("frequency" ≤ 0.1 Hz) and 1 Hz are not found. At 10 Hz the discharge pattern is usually similar to a single shot pulsed discharge at a little lower voltage (~ 3 kV) but compared to changes due to pressure or larger voltage differences this can be neglected. All data is from single shot pulsed measurements unless indicated otherwise.

Series resistance R_2

The internal resistance of the circuit limits the current and elongates the voltage rise time. When the voltage rise time is long compared to the streamer inception and propagation time, the streamers can start propagating when the voltage is still rising and are thus created at a lower voltage than the maximum applied voltage. In this way the internal resistance can influence the streamer diameter (chapter 4). The dependence of the streamer pattern on the 1 and 2 k Ω series resistance is tested by investigating streamers at a low pressure of 62.5 mbar because then the influence of the resistance on constraining the diameter is expected to be easiest to detect (a decrease in diameter of e.g. 1 pixel at 1000 mbar will be a decrease of 16 pixels at 62.5 mbar because all lengths scale with $1/p$). Figure 6.3 shows that the 1 or 2 k Ω series resistor hardly changes the streamer diameter at 62.5 mbar in the 160 mm gap at 6 kV because the values are well within the error bars. In fact, the difference between the averaged diameters is ~ 0.15 mm which is even less than one pixel on the camera, corresponding to 0.168 mm. Since no relevant difference in diameter is found, also no relevant difference in velocity (chapter 4) or in the branching rate is expected.

High voltage switches

Two different high voltage switches are used to close the circuit: a low jitter, fragile Behlke HTS651 ($V_{\max} = 65$ kV, $I_{\max} = 30$ A) semiconductor switch and a large jitter, robust homemade sparkgap (details see [47]). Different switches may give differences in streamer appearance when their internal resistance and capacitance differ [106]. Here again no differences are expected in streamer diameter since a large seriesresistance is used during the measurements that dominates the streamer pattern (chapter 4).

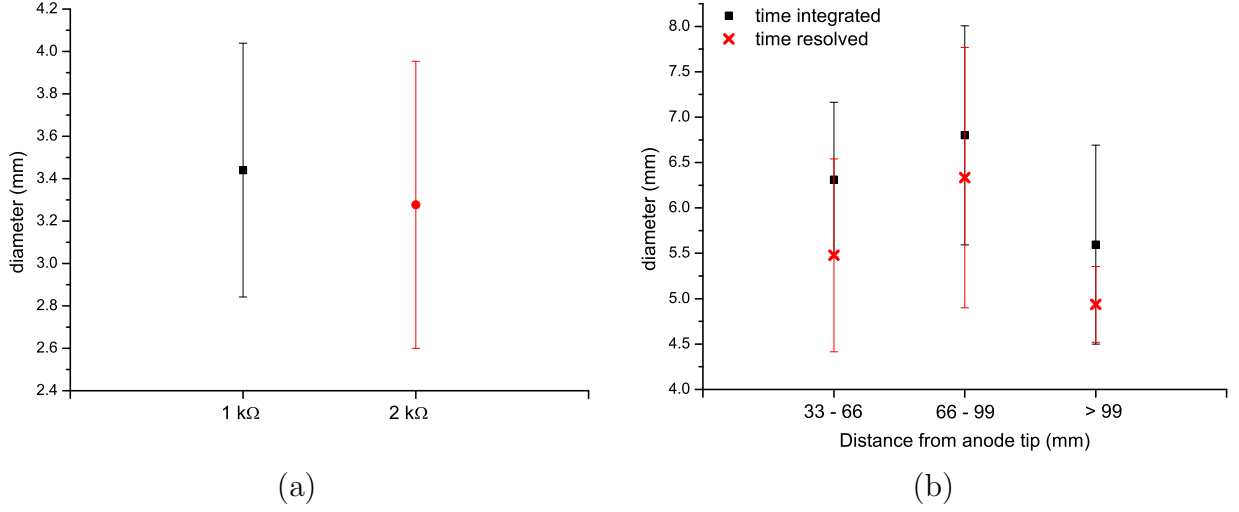


Figure 6.3: a) The diameter of N_2 streamers at 62.5 mbar in a 160 mm gap with series resistor $R_2 = 1\text{ k}\Omega$ or $2\text{ k}\Omega$ at 6 kV. b) The diameter of time resolved and time integrated measurements of streamers in N_2 at 63 mbar and 12 kV in a 160 mm gap. $R_2 = 1\text{ k}\Omega$. Note that the different average diameter value in a) and b) is due to the difference in voltage resulting in a $p \cdot d = 0.2\text{ mm}\cdot\text{bar}$ (type 3) streamer in a) and $p \cdot d = 0.4\text{ mm}\cdot\text{bar}$ in b), section 6.4.3.

Jitter and time resolved measurements

The jitter in the setup must be as short as possible, but at most $\sim 100\text{ ns}$, to be able to make reliable time resolved measurements. This jitter depends on the high voltage switches, the electrical-optical signal conversion in the optical fiber and on the stochastic behavior of the streamer ignition itself. The jitter in the optical fiber is less than a ns. The jitter in the streamer inception can be less than several ns when measurements are done at pressures $\geq 400\text{ mbar}$ and/or \geq intermediate voltages (chapter 3) but it becomes much larger, up to tens of μs , when the pressure is low and/or the voltage is just above the inception threshold. The two high voltage switches each have their own jitter. The sparkgap switch has a minimal jitter of $\sim 10\text{ ns}$. This jitter depends on the fine-tuning of the gas flow and pressure through the sparkgap, the polarity of the sparkgap and the high voltage in the streamer circuit. The semiconductor switch has a jitter of $\sim 0.1\text{ ns}$. This makes the semiconductor switch more suitable for taking time resolved photographs.

Since it is sometimes not possible to take photographs of primary streamers during their gap transit also photographs that include later events, after the primary streamer propagation, are used to examine the streamer pattern. Due to these events, such as secondary streamer propagation, return stroke, etc., the channels can be broadened. The diame-

ters of these photographs are compared in figure 6.3b where "time resolved" stands for photographed-during-transit (e.g. figure 4.5 or 4.6a) and "time integrated" includes also later events (e.g. figure 4.6c or 4.6d). On the horizontal axis the position of the streamer in the 160 mm gap is given whose diameter is determined. The graph shows that the streamer diameters in the time resolved photographs are thinnest but still fall within the error bars of the time integrated ones. Furthermore, the maximal difference in averaged diameter is 1 mm at 63 mbar which will be 0.063 mm at 1000 mbar: a difference that can just be resolved when zoomed in to $\sim \frac{1}{4}$ th of the 160 mm gap where the camera resolution becomes 0.045 mm/pixel. Therefore, preferably time resolved measurements are used but when this is not possible time integrated photographs are used.

Timings and jitter

The minimal time delay between the pulse of the function generator ($T = 0$) and the start of the high voltage pulse is $\sim 1.2 \mu\text{s}$ when the sparkgap is used and $\sim 0.35 \mu\text{s}$ when the Behlke switch is used because of differences in the trigger electronics (see also chapter 4). Streamer propagation starts after this delay. Therefore, the combination of camera exposure time and delay must exceed $\sim 1.2 \mu\text{s}$ or $\sim 0.35 \mu\text{s}$, respectively, to obtain a good photograph.

Which stage of the discharge is shown on a photograph depends to a great extend also on the jitter. When the jitter is large ($\geq 100 \text{ ns}$), it is difficult to open the camera at the same moment as the streamers propagate since this moment is uncertain. Therefore, it might be possible that the streamers start before the camera is opened and (depending on exposure time) do not show up, fade halfway the gap or reach the other electrode. It is also possible that the discharge starts when the camera already closes and no discharge at all is captured. Especially for exposure times of 1 - 5 μs the value of the exposure time does not necessarily tell whether the complete discharge is imaged onto the iCCD-camera. Exposure times of $\geq 10 \mu\text{s}$ (usually) show the complete discharge, even when the voltage pulse decay time is longer (pulse duration can be set from 1 μs to 25 ms). When the streamer is not connected to any electrode on time resolved measurements, it is certain that the illuminated path represents the trace of the streamer head within the exposure time and velocities can be obtained. Unless indicated otherwise, all streamers shown in the figures below reach the cathode. If they do not do so they are photographed during their flight.

6.3 Diagnostics and data analysis

6.3.1 Camera

The photographs are taken with a digital 4QuikE intensified CCD-camera. The streamer diameter and velocity can be measured for streamers travelling in all directions but it is described for a propagation perpendicular to the plate in chapter 4. Since the velocity can change when a streamer branches and changes diameter (see chapter 4), measurements are done on streamer parts that show no splitting of the channel. Mostly exposure times of 10 or 50 ns are used. Only the velocity of the fastest and longest streamer parts are measured to avoid measuring on streamers that propagate outside the plane of view. The determination of the distance between branching events is given below. Velocities and distance between branching events are measured when the complete gap is imaged onto the camera. For diameter measurements of streamers in the 160 mm gap, the camera has zoomed to ~ 45 mm to avoid the broadening of the diameter due to instrumental effects (chapter 4). The small gaps (≤ 40 mm) are not zoomed into.

Distance between branching events

Figure 4.5 shows that the distance between branching events is not constant. Near the electrode tip, where the streamers are thick, this distance is larger than near the plate where the streamers are thin. In general, the branching distance is measured between the starting point of the streamer channel or branch and the place where the next branch deviates from this channel. Occasionally, the branching distance is measured between the tip and the next branch, so possibly including the cloud at the tip. Actually the evaluations should be done between the edge of the cloud and the next branch, since the streamers start from the cloud. However, frequently the region of the tip is overexposed and it is not certain whether there is a cloud or not. Therefore, data containing a cloud or overexposed regions are avoided as much as possible. When streamers propagate toward the plate electrode without branching, especially at low pressures, they are not used for data analysis. This however can influence the statistics making the average distance between branching events shorter than in reality. The distance between branching events is obtained by measuring the distance between the observed starting point and end point of the channel; no full width at half maximum of the intensity is used. The streamer diameter is measured just before the branching of the channel. Typical exposure times used are shorter than the time the streamer needs to bridge the gap. This way measuring in processes that occur after the primary streamer propagation is avoided.

In N_2 the branches are very short. Therefore, only measurements can be done on streamers with sharp, bright branches because else a blurry surrounding, scattered light or accidentally overexposed pixels can be regarded as a branch. This limits the number of evaluations

that can be done.

6.3.2 Spectrometer

An Ocean Optics USB2000 plug-and-play spectrometer with a resolution of 0.35 nm/pixel is used to record the discharge spectrum in the wavelength range of 200-850 nm. A pulse frequency of 10 Hz is needed to obtain a good signal to noise ratio. The spectra are recorded by integrating the light, collected by an optical fiber close to the anode tip, over 60 s and averaging this 3 times. This means that with a pulse frequency of 10 Hz, the plotted spectrum is built up from 1800 discharges.

6.4 Results

6.4.1 First observations

A first overview of the differences between positive streamers in N_2 and air (also called N_2 (streamers) and air (streamers)) in a 40 mm gap at 400 mbar is given in figure 6.4. In these two photographs the differences are clearly visible. The N_2 streamer pattern shows more and thinner streamers that branch more often and have a zigzag-structure (as we reported previously in [14; 111]). The branches themselves die out closer to the main channel than the branches in air. Simulations based on fluid theory have evaluated that photoionization makes a negative streamer smoother [59]. This may explain some observed differences between streamers in air and nitrogen since a smooth streamer probably also branches less since its head becomes less perturbed. This explanation however still needs to be verified in a particle model. Furthermore, N_2 streamers show a better contrast between sharp and out-of-focus streamers. Air has a light emitting cloud at the tip (see also chapter 3) while N_2 shows this light cloud only at lower pressures. The streamer tips are also different. The air streamers are round and stop abrupt (figure 6.5a) while the N_2 streamers have more diffuse tips (figure 6.5b). The distance of the tip over which the intensity drops to 50% of its maximum is measured to be ~ 4 times longer in N_2 .

Figure 6.6 and 6.4 show that at 1000 mbar and 400 mbar the streamer pattern of N_2 and air differ while at 62.5 mbar they are more alike, i.e. the streamers are smooth and branch only once. This is most likely due to the sizes of the vacuum vessel which are too small for the discharge to develop at low pressures.

In figure 6.7, streamers are made in all three gases with exactly the same setup and camera settings (apart from the gas composition). The exposure time is 70 μ s, which is longer than the voltage pulse duration, so that if the streamers bridge the gap it is always shown

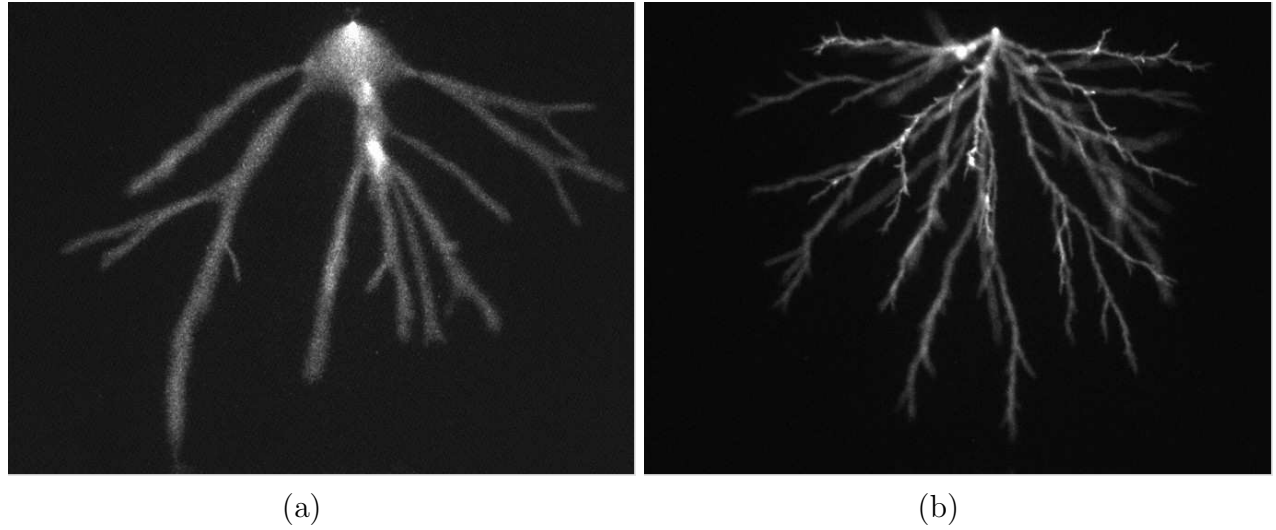


Figure 6.4: *Streamers in a 40 mm gap at 400 mbar and 16 kV in a) air and b) N_2 . Camera delay is 0, exposure time is a) $0.6 \mu s$ and b) $2 \mu s$.*

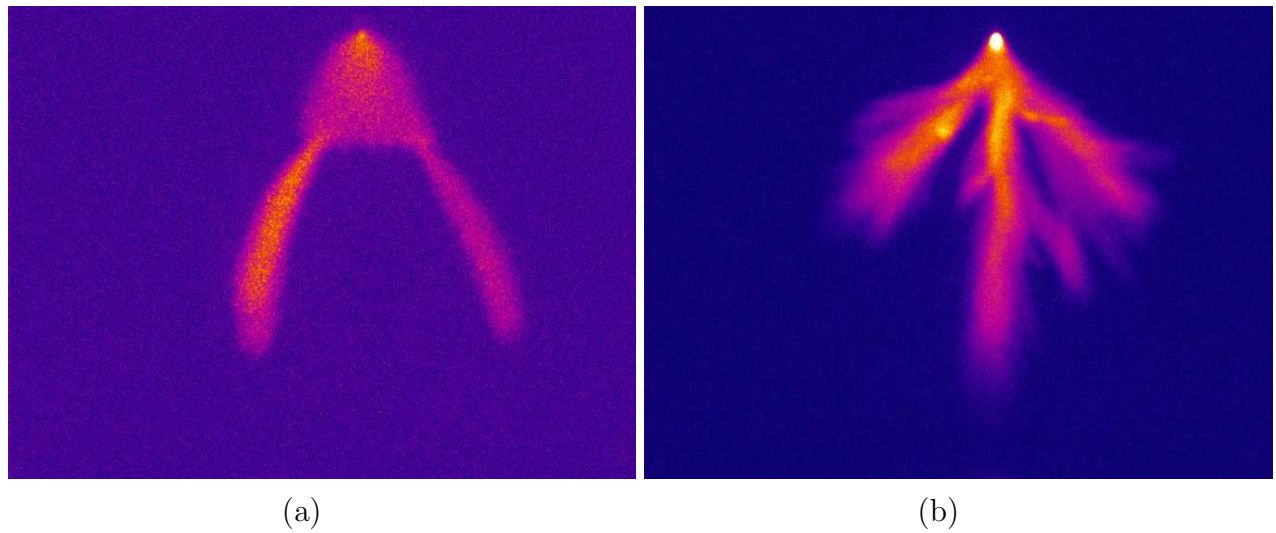


Figure 6.5: *Streamers in a 40 mm gap at 100 mbar a) air, 5 kV and b) N_2 , 15 kV. Camera delay is 0, the exposure time and pulse frequency are: a) $0.7 \mu s$, 1 Hz and b) $0.37 \mu s$, 10 Hz.*

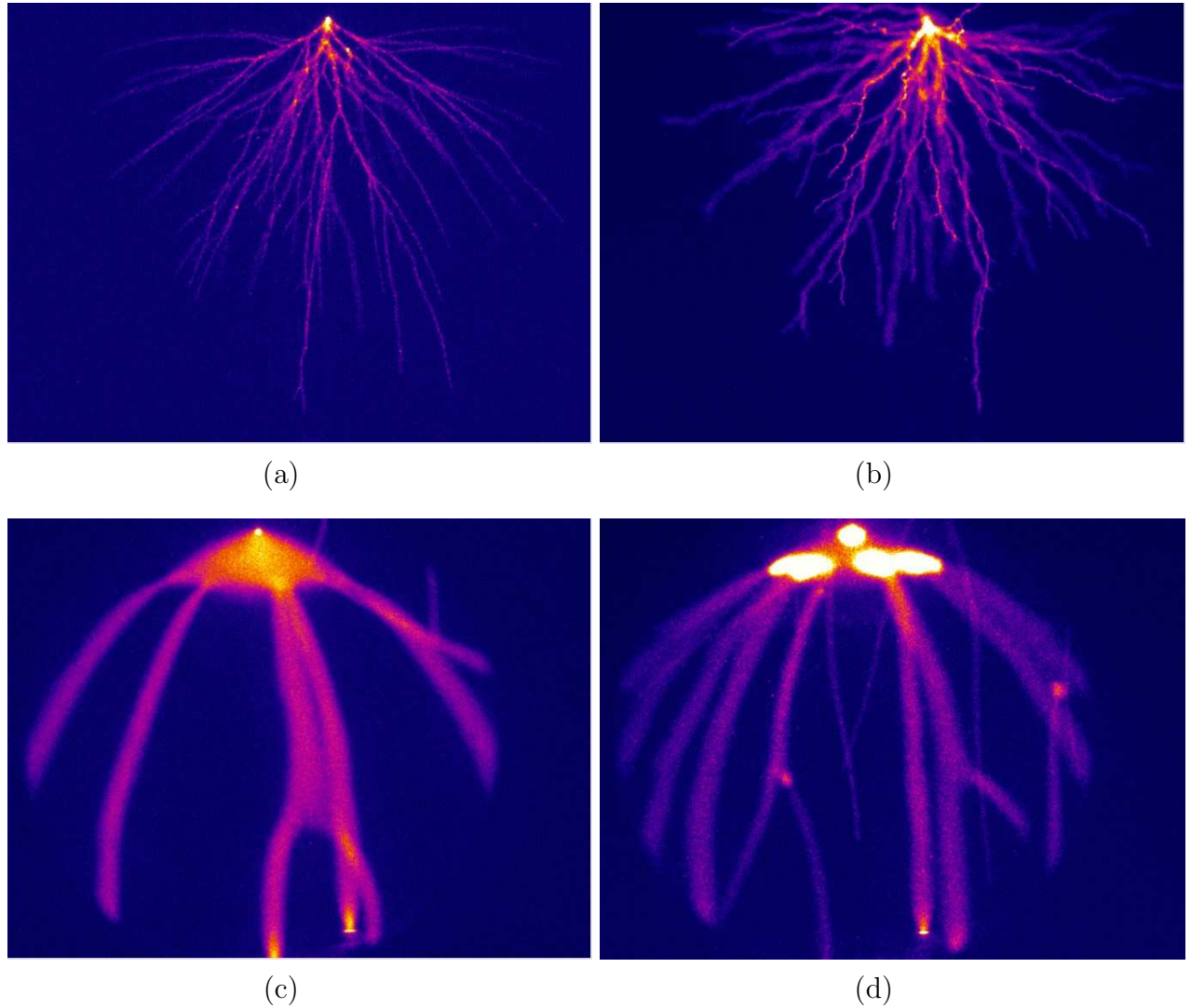


Figure 6.6: Upper line: streamers in a 40 mm gap at 1000 mbar, 20 kV in a) air and b) N_2 . The delay is 0 and exposure times are a) $0.6 \mu s$ and b) $1.2 \mu s$. Lower line: streamers in a 160 mm gap at 62.5 mbar, 10 kV, in c) air and d) N_2 . Camera delay $1 \mu s$ and exposure time $1.5 \mu s$.

gap (mm)	gas	pressure (mbar)	start (kV)	bridge gap (kV)	spark (kV)
10 / 40	air	1000	5 ^a / 5	5 ^a / 20	15 / 40
40	air	400	5	5	25
40	air	200	5 ^a	5 ^a	20
40	air	100	2 ^a	2 ^a	15
10 / 40	N ₂	1000	5 ^a / 15 ^{a,*}	5 ^a / 15 ^{a,*}	12.5 ^a / 30
40	N ₂	400	5 ^b	5 ^b	16
40	N ₂	200	4 ^b	4 ^b	10 ^a
40	N ₂	100	2.5 ^b	2.5 ^b	15 ^a
160	air	1000	10	> 48	> 50
160	air	400	4	30	> 40
160	air	62.5	5	5	> 22
160	air	13	5	5	30
160	N ₂ :O ₂	1000	10	35	> 40
160	N ₂ :O ₂	400	10	10	> 30
160	N ₂ :O ₂	62.5	9	9	> 10
160	N ₂ :O ₂	15	5 ^a	5 ^a	> 5 ^a
160	N ₂	1000	10	35 – 40	> 50
160	N ₂	400	10	10	> 40
160	N ₂	62.5	6 ^a	6 ^a	> 12
160	N ₂	13	3 ^a	3 ^a	> 10

Table 6.2: Approximate values of the minimal voltage at which the streamers start, bridge the gap and go over to a spark in a 40 mm and 160 mm gap. When a pulse frequency is used instead of manual triggering this is indicated in the table by $a = 1$ Hz and $b = 10$ Hz. The value indicated by * is very unlikely, therefore also the value in the 10 mm gap is given.

on the photograph. It shows that nitrogen(like) streamers propagate further down the gap and are more intense than the air streamers at the same voltage. This intensity difference is also present at other pressures and voltages where the nitrogen(like) streamers have not yet bridged the gap (not shown). Here it is also visible that the streamers in nitrogen(like) gas branch more. The black ring at the outside of the photographs is the border of the viewing port that contains the quartz window through which the camera takes the photograph.

The difference in minimal voltage at which the streamers start, bridge the gap and turn into spark are given in table 6.2. For the measurement indicated with a * also the values

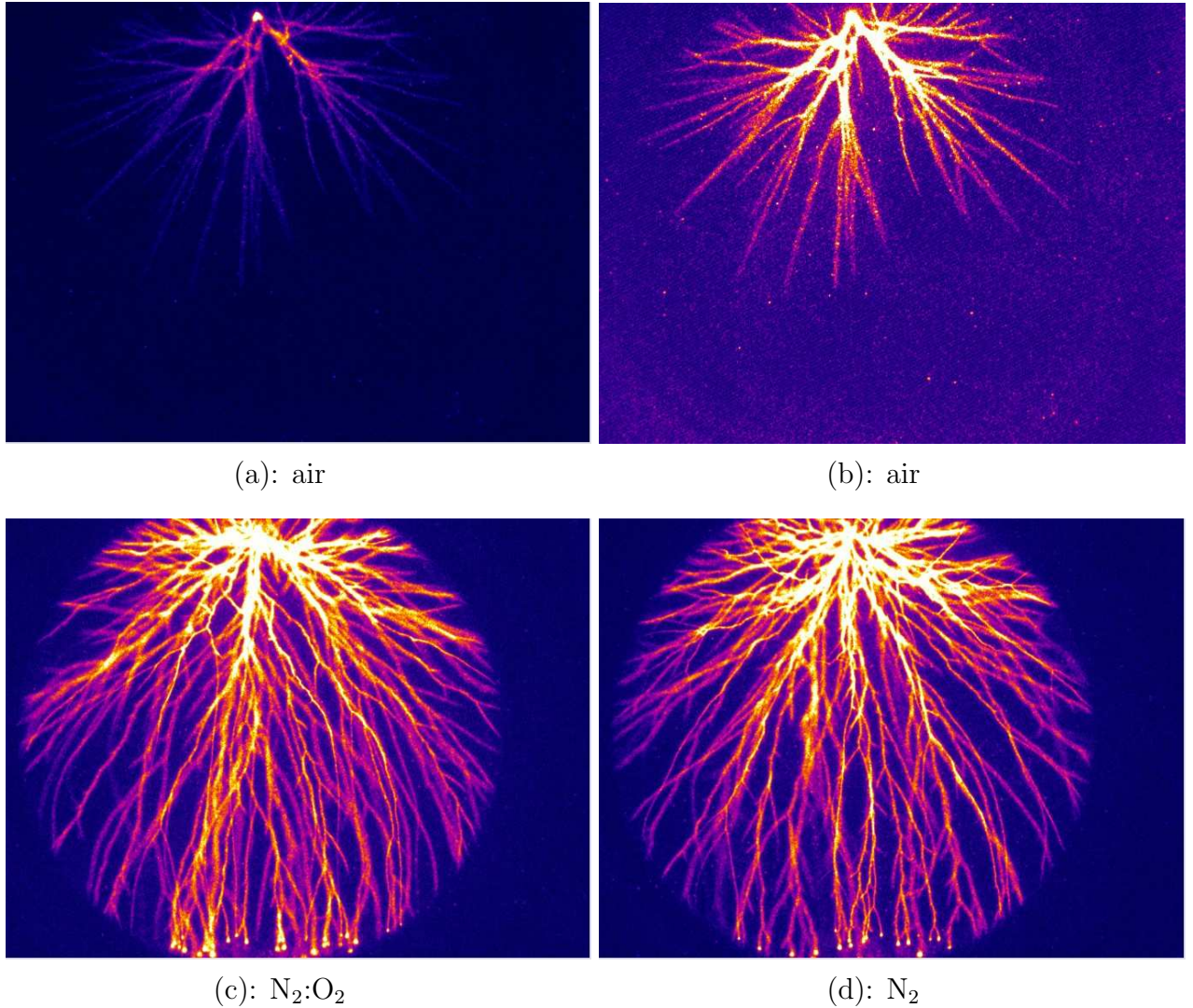


Figure 6.7: *Streamers in a 160 mm gap at 400 mbar and 20 kV in a+b) air c) $\text{N}_2:\text{O}_2$ mixture and d) N_2 . a+c+d) are on the same intensity scale, b) has a different scale to show the streamer structure. The camera's delay is 0, exposure time is 70 μs . The streamers in figure a+b) cannot reach the plate electrode at this applied voltage.*

in the 10 mm gap are given since it shows a surprisingly high start value of 15 kV in the 40 mm gap. It is very likely that this start value should be 5 kV. The results show that the air and N₂ streamers have roughly the same starting voltage and that at pressures ≤ 400 mbar the streamers always cross the complete gap once they ignite (except for the 160 mm gap at 400 mbar air). The minimal voltage at which streamers bridge the gap (data 160 mm gap) and the breakdown voltage (data 40 mm gap) are lower for N₂. The stability field³ in air is approximately 5 kV/cm since the streamers at 1000 mbar transit the 40 mm gap at 20 kV applied voltage. This is consistent with the empirical observation that the electric field along the streamer channel decreases with 5 kV/cm [4; 90]. For N₂ and N₂:O₂ the measurements give a stability field of ~ 2 -3 kV/cm at 1000 mbar which is close to the 1.5 kV/cm as given in [90] for N₂ with up to 2% O₂. The table also shows that the starting voltage in the 40 and 160 mm gap is roughly the same. The current pulse duration for discharges in N₂ is longer than in air (see also section 6.4.6) due to the absence of attachment, therefore the N₂ streamers develop into a glow or spark at lower voltages than air streamers. The breakdown voltage in the 160 mm gap cannot be obtained because of sparking between the high voltage feedthrough of the vacuum vessel and the needle.

The observed properties of air and N₂ will be discussed in more detail in the next sections.

6.4.2 Spectral lines

In figure 6.8 the spectrum of the light emitted by streamers in air and nitrogen at a pressure of ~ 60 mbar and 10 kV in a 160 mm point-plane gap is shown for the wavelength interval of 300-400 nm. The light is collected at the needle tip and it is integrated over 1800 complete voltage pulses (see also section 6.3). It therefore consists also of light from events that occur after the primary streamer propagation, such as secondary streamers. Via the curves of intensity ratio of the SPS- and FNS-wavelengths ($R_{391\text{nm}/337\text{nm}}$ and $R_{391\text{nm}/394\text{nm}}$) versus field strength in [81] the field strength in plasmas can be estimated if the nitrogen molecules are excited dominantly from the ground state directly by electron impact. These curves are experimentally obtained by using a non-self-sustaining dc discharge in a parallel-plane gap for the excitation of the gas molecules and by varying the reduced field strength in the range of $(150\text{-}5000) \cdot 10^{-20}$ kV·m² where it is also noted that in air the excitation mechanism of examined states of nitrogen is the same for pulsed and steady state conditions [81].

The time available for excitations in the streamer head is estimated to be several ps; a time interval in which only one-step processes can occur. Therefore, it is assumed that the nitrogen molecules are excited dominantly from the ground state and the curves of [81]

³The stability field is the lowest electric field which the streamers need to keep propagating once they are created.

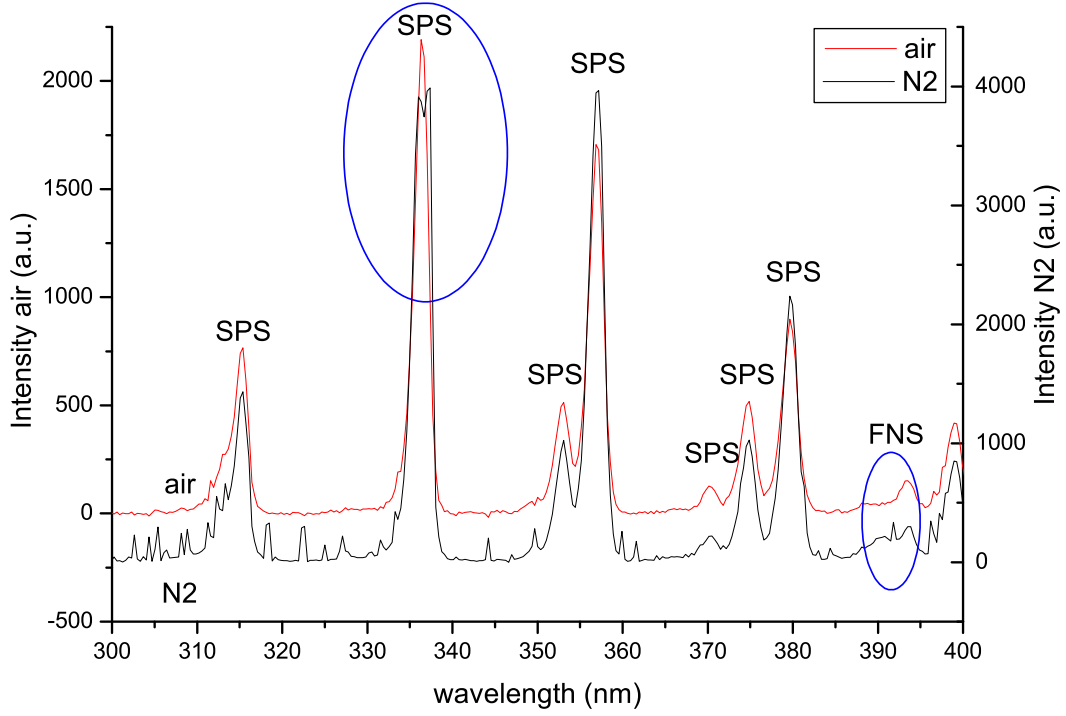


Figure 6.8: The spectrum of streamers in air (55 mbar) and N_2 (61 mbar) in a 160 mm gap at 10 kV and 10 Hz in the wavelength interval of 300-400 nm.

can be used.

In figure 6.8 the central wavelength of the SPS and FNS are indicated by the ellipses. The 391 nm spectral line is clearly visible in N_2 while it appears to be absent in air. Therefore, for air the value of the plateau is taken. This gives as ratios $R_{391\text{nm}/337\text{nm}} = 0.08 \pm 0.01$ for N_2 and $R_{391\text{nm}/337\text{nm}} = 0.03 \pm 0.01$ for air. Via the measured curves⁴ of [81], a reduced electric field is found of $|\mathbf{E}|/p \approx 125 \pm 13 \text{ kV}/(\text{cm}\cdot\text{bar})$ and $|\mathbf{E}|/p \approx 88 \pm 13 \text{ kV}/(\text{cm}\cdot\text{bar})$ for the light emitting part of the streamerheads in N_2 and air, respectively. These values are checked by also measuring the ratio $R_{391\text{nm}/394\text{nm}}$. This gives for N_2 a value of $R_{391\text{nm}/394\text{nm}} = 1.13 \pm 0.2$ resulting in an $|\mathbf{E}|/p \approx 128 \pm 25 \text{ kV}/(\text{cm}\cdot\text{bar})$ and for air $R_{391\text{nm}/394\text{nm}} = 0.3 \pm 0.1$ resulting in an $|\mathbf{E}|/p \approx 75 \pm 12 \text{ kV}/(\text{cm}\cdot\text{bar})$. Both ratios give consistent results.

⁴These curves are given for $|\mathbf{E}|/n_g$ as function of $R_{391\text{nm}/337\text{nm}}$ or $R_{391\text{nm}/394\text{nm}}$. The values of $|\mathbf{E}|/n_g$ can be converted to $|\mathbf{E}|/p$ when the temperature is constant (chapter 2). Since the temperature in one primary streamer channel increases only 13 K (chapter 7) the temperature is assumed constant at room temperature.

The obtained reduced electric fields can be used to estimate the average electron energy. In [124] an electron energy distribution function is calculated by solving the Boltzmann equation from which an average electron temperature follows that can be related to an electric field. Note that corrections to this approximation are found and discussed in [54]. The average electron temperature is related to an electric field in e.g. [20] for positive streamers in air where detachment and recombination are neglected. When it is assumed that this curve can also roughly be applied to streamers in N_2 the following values are found via the calculated curves of $|\mathbf{E}|/n_g$ versus average electron energy (figure 4.10 in [20]): an average electron energy of $\sim 11 \pm 2$ eV for N_2 and $\sim 8 \pm 2$ eV for air. These values are in agreement with simulations of negative streamers in N_2 [54] that show that the average electron energy in the high field region of the streamer tip in a parallel plane gap can vary between 5 eV and 15 eV for fields between 50 kV/cm and 200 kV/cm.

Note that these values are only given as a rough estimate to show that streamers in nitrogen are more energetic than in air. The higher average electron energy in N_2 may explain the more intense streamer pattern in N_2 compared to air.

Note that the intensity scale of air and N_2 in figure 6.8 cannot be compared since the construction, on which the optical fiber that collects the streamer light was mounted, slightly moved when the vacuum vessel was flushed with air or N_2 . Hence it cannot be guaranteed that the fiber was in exact the same place during both measurements.

6.4.3 Diameter and scaling with pressure

Figure 6.9 shows that streamers become thicker with increasing voltage and decreasing pressure. The increase in diameter with decreasing pressure is related via the pressure scaling law which states that all lengths scale approximately with $1/p$ (chapter 2).

This relation is calculated for the minimal diameter (chapter 4) at different combinations of pressure (13 – 1000 mbar), voltage and gap distance since these streamers are away from the electrodes, where the scaling law is most valid. The results are plotted in figure 6.10. The error bars indicate the standard deviation of about 10 different measurements of streamer diameters in each gap of 10, 20, 40 and 160 mm. Systematic errors are minimized as much as possible by the measurement procedure of chapter 4 and it is estimated that they are less than the stochastic errors due to noise, etc. The data shows indeed a scaling with pressure resulting in an average value of $p \cdot d = 0.12 \pm 0.02$ mm·bar for N_2 and $p \cdot d = 0.20 \pm 0.02$ mm·bar for air. The value in air is however more reliable than the one in N_2 since the average value for N_2 is just outside four of the six error margins shown in figure 6.10. This is most likely due to the concentration of impurities picked up in the copper tubes (section 6.2.1), which may vary per experiment. The scaling of streamer diameters

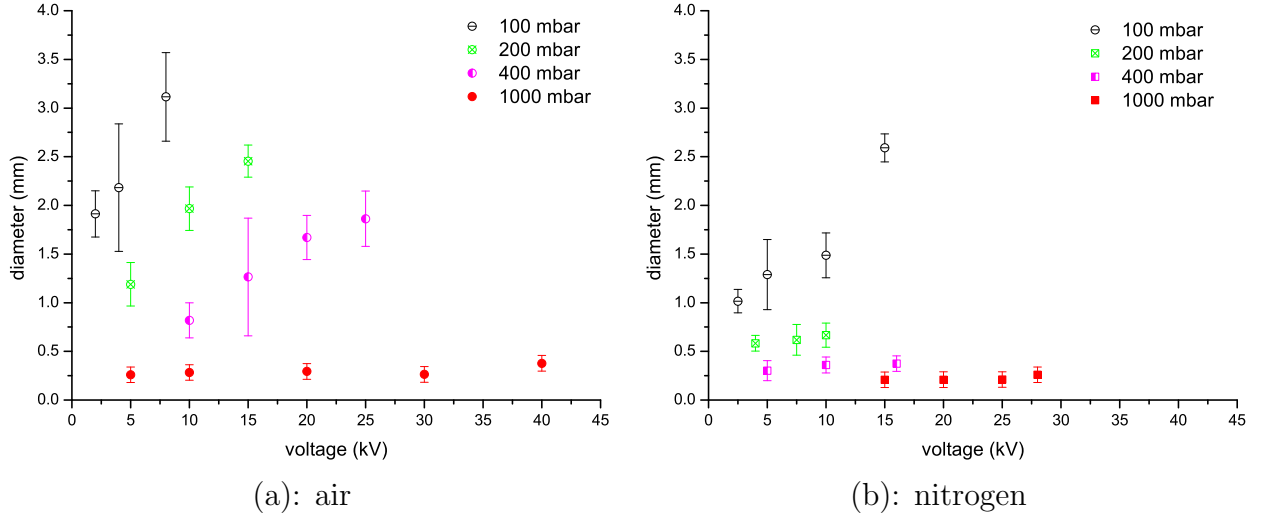


Figure 6.9: *Streamer diameters as a function of voltage in a 40 mm gap at different pressures in a) air and b) N_2 .*

at near and atmospheric pressure is unexpected since photoionization becomes increasingly suppressed for pressures above 40 mbar because the excited states of N_2 lose their energy via collisions which breaks the scaling law.

The green triangles give an estimate for sprite discharges which have a minimal diameter of 20-50 m (± 13 m) at an altitude of 75-80 km (± 5 km) [35] which is at about 10^{-5} bar, giving a minimal diameter of $p \cdot d = 0.2 - 0.5$ mm·bar. The minimal diameter values are slightly higher than the average values found for air in the laboratory experiments. This can be due to instrumental broadening since it is difficult to capture spatially resolved sprites on a camera. Another possibility is that sprites are a large scale phenomenon which propagates over a distance of ~ 40 km, i.e. in different pressure regimes. Therefore, the diameter of a sprite will vary with altitude and it may be difficult to find the real minimal diameter. Furthermore, scaling with pressure is only allowed at a fixed temperature (chapter 2). The temperature at sprite altitudes varies between $\sim 7^\circ\text{C}$ at 50 km to $\sim -83^\circ\text{C}$ at 80 km altitude [112], so it is not even near the room temperature of $+20^\circ\text{C}$ in the laboratory. Since the temperature decreases by $\sim 35\%$, also ℓ_{mfp} and thus the diameter decreases by 35% resulting in a pressure·diameter = 0.1-0.3 mm·bar at laboratory conditions.

The dimensions of the light emitting cloud near the tip in air (as e.g. in figure 6.5a) are measured where the cloud is highest and widest and the intensity has decreased to $\sim 20\%$ of its maximum value. The evaluations are mainly done when no streamers have yet emerged from the cloud. The dimensions are given in table 6.3. The height and width can vary by a

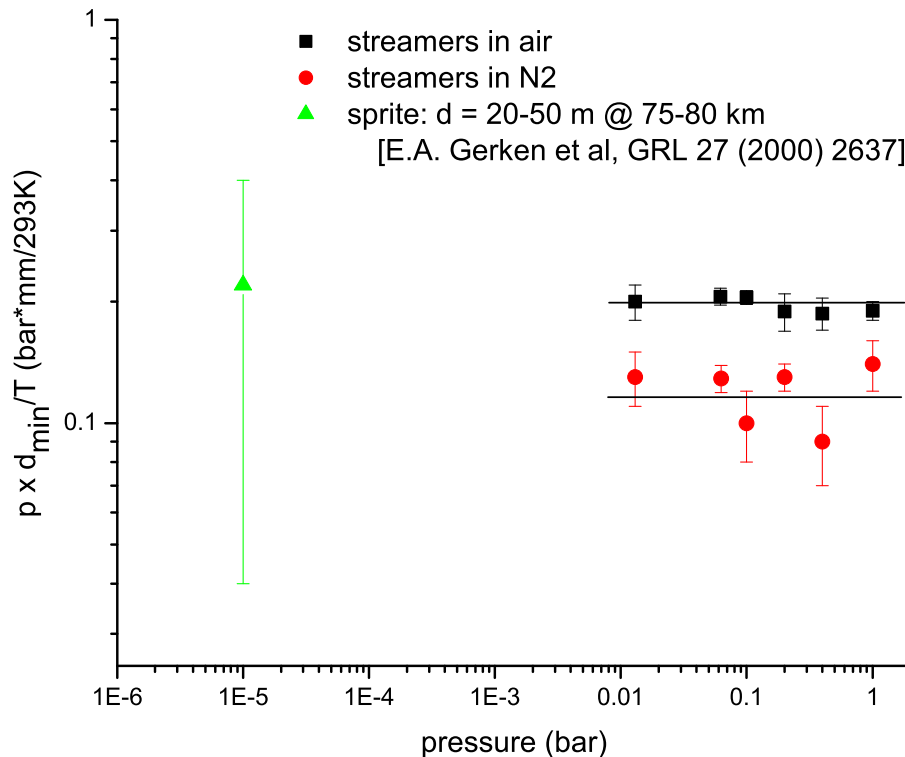


Figure 6.10: *Scaling of the minimal diameter with pressure for N₂ and air streamers . An estimate of the sprite diameter at 75-80 km altitude, scaled to 20°C, is also shown.*

factor 2 between measurements done at the same parameter settings of the setup. Typical order of magnitudes are given in table 6.3. The table shows that the dimensions increase with decreasing pressure for the same voltage, as is also shown in figure 5.1. Furthermore, the cloud is usually 15-50% wider than high, except at the inception voltage in the 40 mm gap where the opposite is found. Occasionally, the cloud is two times wider than high. It is observed that when a fast voltage rise time of 12 ns is used the cloud does not break up into several streamers but propagates as a whole to the other electrode, as shown in figure 3.5 and [75].

6.4.4 Velocity

The velocities of type 2 and type 3 streamers in N₂, air and N₂:O₂ at 400 mbar and 30 kV are given in figure 6.11. The streamer channels in air at voltages below 20 kV die out very close to the anode so that no reliable velocity evaluations can be done. Therefore these values are not plotted. Figure 6.11 shows that the transition in velocity of type 3 streamers

gap (mm)	p (mbar)	V (kV)	height (mm)	width (mm)
160	13	2	30	45
		3	45	73
		4	38-50	75-90
40	100	2	5	3
		5	4-9	5-10
		8	8-9	10-16
	200	5	3	2
		10	5-8	9-15
		20	20	24-28

Table 6.3: Overview of the width and height of the cloud at the tip in air. The error in the values can be as high as 50%.

at 10 kV ($p \cdot d = 0.3 \text{ mm} \cdot \text{mbar}$, figure 6.9a) to type 2 at 40 kV ($p \cdot d = 0.8 \text{ mm} \cdot \text{mbar}$, figure 6.9a) is gradual. The velocities of the streamers in the different gases are almost equal at low voltages but slowly deviate with increasing voltage (figure 6.11). The streamers in N_2 become faster. The figure shows data of 400 mbar because at this pressure a complete set of measurements can be made from velocities measured near the tip, halfway the gap and near the plate. The error bars of these velocities overlap, e.g the velocity in $\text{N}_2:\text{O}_2$ at 20 kV is $0.16 \pm 0.02 \text{ mm/ns}$ at 50 mm from the tip while it is $0.14 \pm 0.04 \text{ mm/ns}$ at 130 mm from the tip. The velocities and error bars are therefore plotted as one average value with error bars that stretch from the lowest possible value to the highest one. Note however that the highest velocities are generally found near the tip while the lowest ones are generally found near the plate.

Measurements at 1000 mbar show that the streamers in air are faster than in N_2 . They have a velocity from 0.1-0.2 mm/ns over a voltage range from 30-50 kV while in N_2 the velocity ranges from 0.02-0.05 mm/ns in a voltage range of 20-40 kV (figure 6.12). These measurements however are less suitable for comparison because the air streamers are shorter than the N_2 streamers and therefore the velocity is measured closer to the needle where the electric field is higher. Even though this problem can be circumvented by also measuring the velocity in N_2 near the tip, a second problem is that only very short exposure times can be used for air to be certain that the streamer has not stopped before the camera closes. During this short exposure time the streamer travels with many other (overlapping) streamers close together over a small distance. At lower pressures, e.g. 100 mbar, only a small voltage range of 10 kV can be measured which does not give an accurate trend.

It is unexpected with the present theory that the velocities are almost equal since the positive streamer propagation in air is assumed to be dominated by photoionization, while

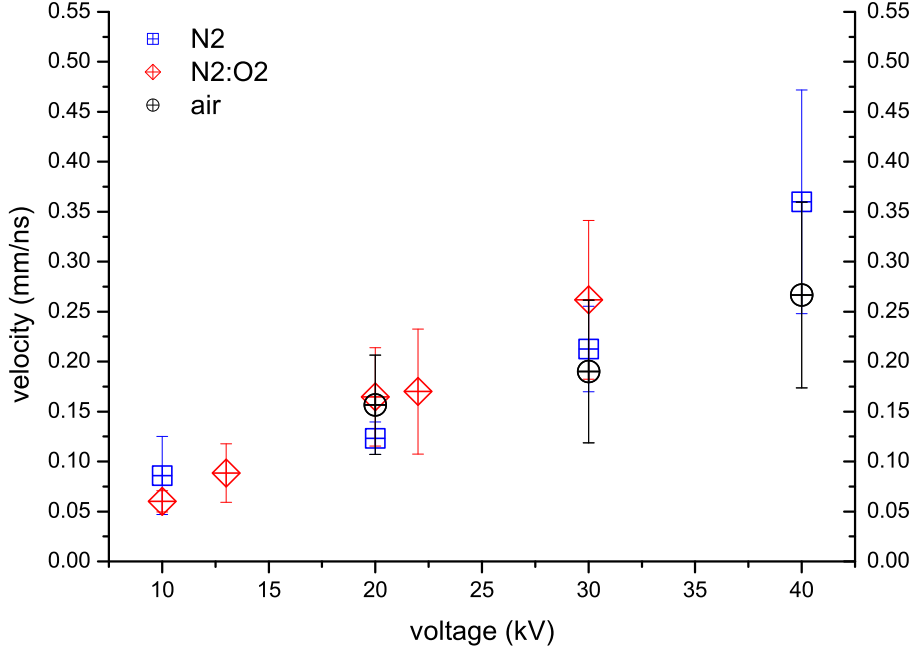


Figure 6.11: *Velocity of type 2 and type 3 streamers in air, N_2 and $N_2:O_2$ in a 160 mm gap at 400 mbar.*

this process can not occur in N_2 (chapter 2). In N_2 the propagation is assumed to be dominated by background electrons (which in air become attached to oxygen and are thus removed from the gas). A possible explanation for this result is that the N_2 used is not pure enough and therefore the streamers in N_2 can use the same propagation mechanisms as the ones in air.

Figure 6.12 shows that the velocity of type 2 and 3 streamers (chapter 4) in air and N_2 increases with decreasing pressure. These data points are also measured near the electrode tip, halfway the gap and near the plate resulting in the error bars (cf. figure 6.11). In an ideal situation, the velocity v should be independent of pressure according to the scaling law (chapter 2). Although the velocity is seen to increase with decreasing pressure it can be regarded as constant around 0.2 mm/ns in air as a first approximation (figure 6.12a). This can be done because the variation in velocity due to pressure is much smaller than the variation due to voltage (section 4.3.3): a thick streamer in air at low pressure (e.g. 2 mm at 100 mbar) still has a $p \cdot d = 0.2$ mm·bar which is equal to the minimal value of 0.20 ± 0.02 mm·bar. Therefore, this streamer will still have a type 3 velocity of about 0.1-0.2 mm/ns, which is in agreement with figure 6.12a. The thick streamers at atmospheric pressure as given in chapter 4 have a $p \cdot d = 2$ mm·bar which are type 1 streamers which have much higher velocities of more than 1 mm/ns.

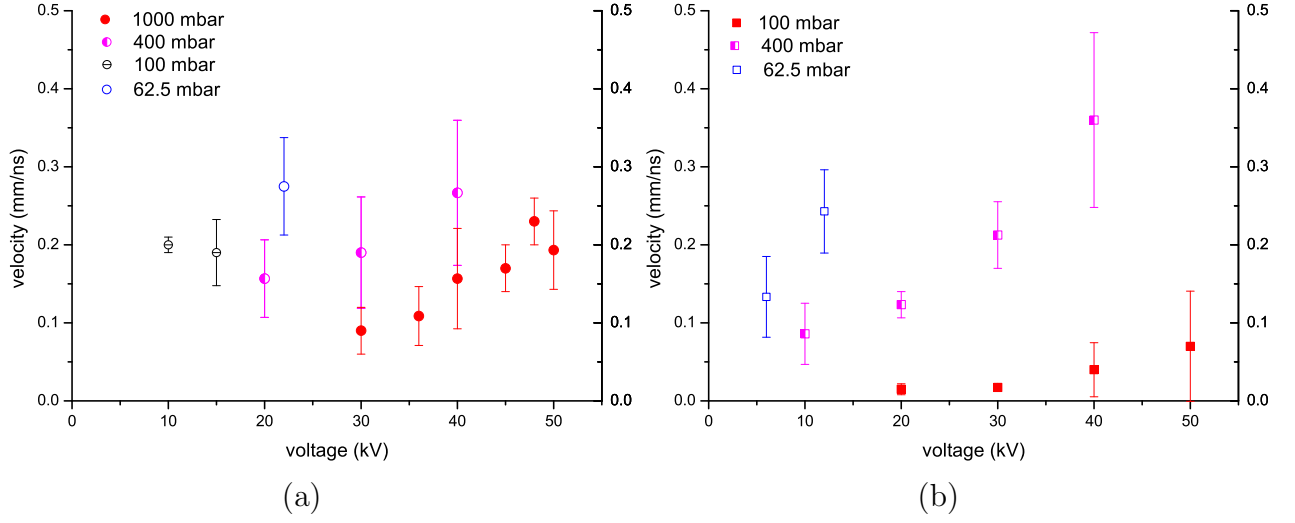


Figure 6.12: *Velocity of type 2 and type 3 streamers in a 160 mm gap at different pressures in a) air and b) N₂.*

The measurements in N₂ are too far apart to give an average velocity (figure 6.12b).

6.4.5 Distance between branching events

In figure 6.13a the branching distance of minimal, type 3 streamers in air, N₂ and N₂:O₂ at 30 kV and 400 mbar are plotted where the diameters in N₂ and air are measured at 40-160 mm from the tip and in N₂:O₂ between 45-90 mm from the tip. This figure shows that streamers in N₂ and N₂:O₂ have similar diameters but that in N₂:O₂ the branching distance is larger. In air the streamers have a larger diameter and branching distance than in N₂ and N₂:O₂. Roughly speaking it seems that the distance between branching events increases with increasing oxygen concentration. This can also be concluded from figure 6.13b where the number of branches per streamer in a 40 mm gap is plotted. The streamers in N₂ at 400 mbar and 16 kV branch approximately 9 times in 40 mm (which is generally every 4 to 5 mm) while in air they branch every 12 to 13 mm at 400 mbar and 15.5 kV. Figure 6.13b also shows that with decreasing pressure the number of branches per streamer decreases. This is consistent with the fact that at lower pressures all length scales become larger and thus the distance between the branches increases resulting in less branches over the same distance.

The ratio of distance between branching events, D , and minimal diameter, d , is given for different pressures in air and N₂ in figure 6.14a. The evaluations are based on the same

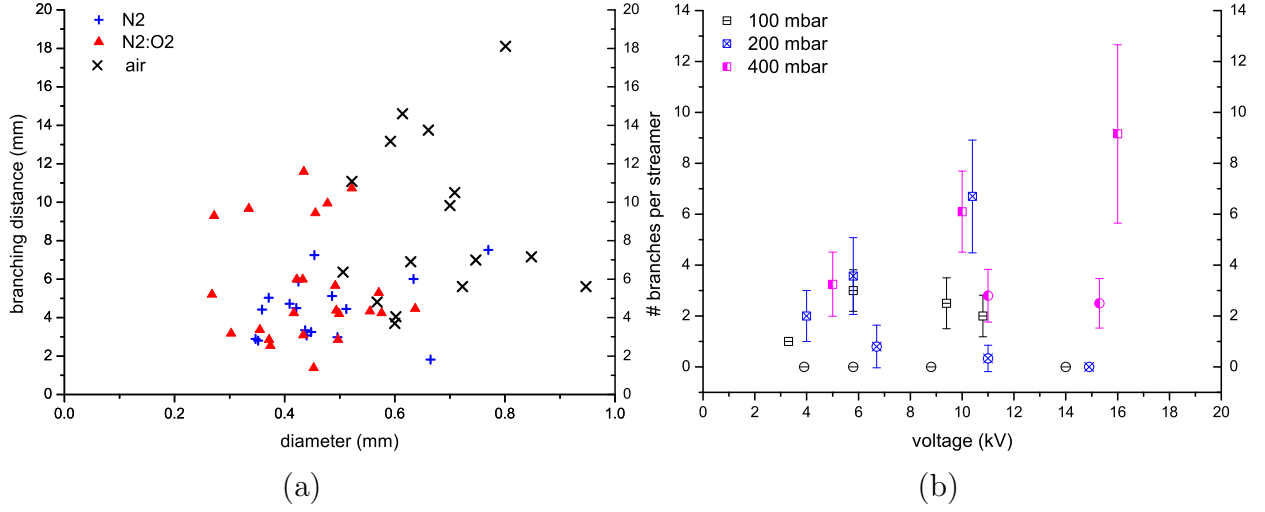


Figure 6.13: a) Distance between branches in N₂, N₂:O₂ and air in a 160 mm gap at 400 mbar and 30 kV. b) The number of branches per streamer that bridges the 40 mm gap for different pressures of N₂ (squares) and air (circles).

measurements in a 40 mm gap as shown in figure 6.9. When at the respective pressure no minimal diameter is found, diameters of streamers at the lowest voltage at that pressure are used (hence $V \leq 10$ kV). Since the ratio D/d has some extreme values per pressure a median is used instead of an average. The figure shows that the ratio remains rather constant over the investigated pressure range and thus appears independent of pressure as is expected from the scaling law. When a horizontal line is fitted through the data points it gives a ratio of $D/d = 11.6 \pm 1.5$ for air and $D/d = 9.1 \pm 3.3$ for N₂. So, when the streamers are equally thick the streamers in N₂ have less distance between the branches and thus branches more during the gap transit. This is in agreement with the observations in figure 6.4.

Streamers also become thicker with increasing voltage as shown in chapter 4 where thick, type 1, streamers near the electrode tip branch less than thin, type 3, streamers near the plate. When the diameter and distance between branching events of those measurements⁵ are plotted it shows that the branching distance indeed increases with increasing voltage and increasing diameter, figure 6.14b. When a line is fitted through the data points an average $D/d = 7.6 \pm 3.6$ is found at 1000 mbar in air. When this data is compared to the minimal streamer data of figure 6.14a for voltages below 10 kV, it appears that the

⁵Thus measurements with the C- and TLT-supply as given in chapter 4 for an 80 mm gap while $R_2 = 0$.

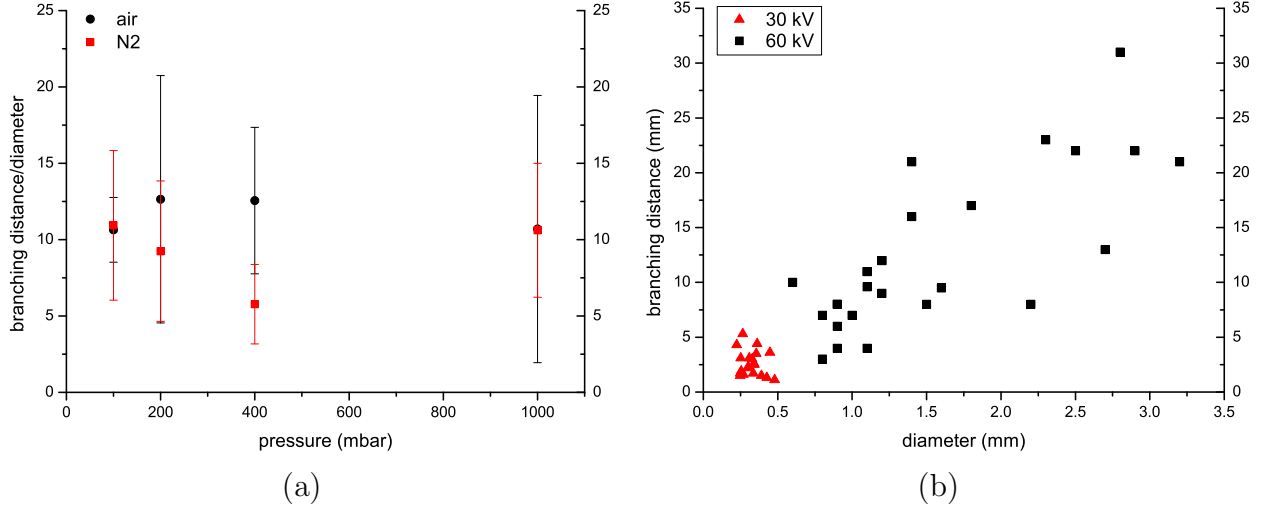


Figure 6.14: a) The ratio of branching distance by diameter for minimal streamers at different pressures in a 40 mm gap. b) The distance between branches as function of the voltage in an 80 mm gap in 1000 mbar air.

ratio D/d decreases with increasing voltage. This means that the radial expansion of the streamer increases faster with voltage than the axial distance between branching events. In other words, thick streamers propagate over a shorter distance with respect to their diameter before branching than thinner ones.

6.4.6 Current and voltage

A typical current and voltage evolution of a discharge in air and N₂ at 1 bar is shown in figure 6.15. The figure shows that the current pulse of air and N₂ consists of a capacitive current peak and a streamer peak. N₂ also shows a glow peak (chapter 1). This glow peak starts at latest 400 ns after the start of the streamer peak, since then the streamers have bridged the electrode gap (as is calculated via the velocity). The total current duration in N₂ is a factor 30 longer than the current pulse in air where the glow-stage does not exist or is much shorter (figure 6.15a). The difference in current duration can be explained by the electronegativity of oxygen in ambient air. The oxygen molecules attach the electrons that are necessary to sustain the discharge and hence the discharge fades. In N₂ this process is not available and therefore the discharge keeps going. This is most likely the reason that sparking occurs at lower voltages in a gap filled with N₂ than with air (table 6.2): the gas returns to its unperturbed stage much later and the ionized streamer channel has time to evolve to a glow (typically at pressures ≤ 200 mbar) and/or a spark.

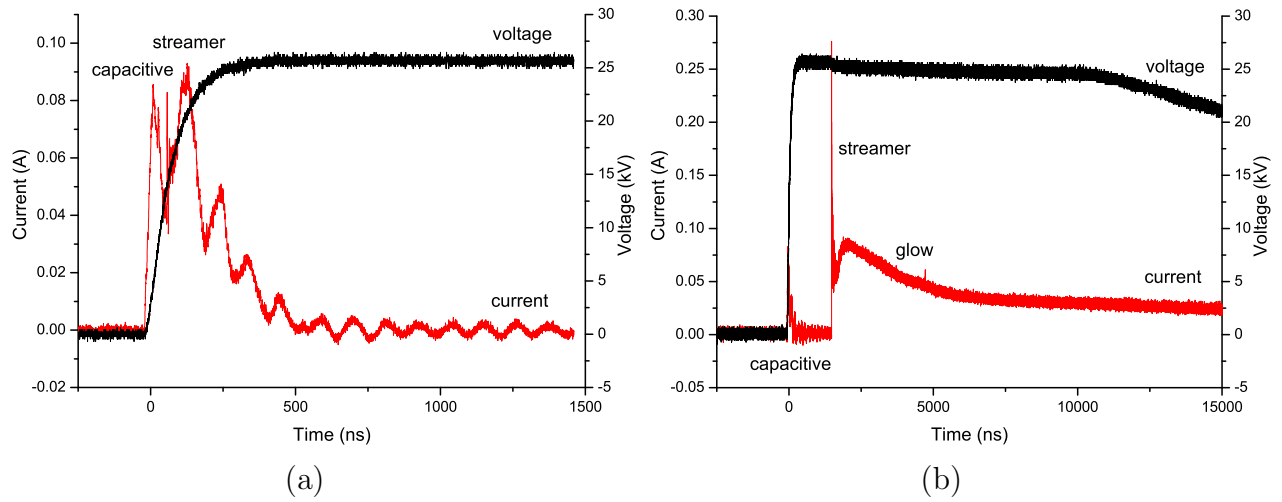


Figure 6.15: *Current and voltage at 25 kV in a 40 mm gap at 1000 mbar in a) air and b) N₂.*

The current density of streamers in N₂ is estimated as $\sim 0.3 \text{ A/mm}^2$. This estimate is based on the discharge of figure 6.15b in which the maximum of the streamer current is 0.28 A for approximately 50 streamers (halfway the 40 mm gap) with a diameter of 0.16 mm. The current density of the discharge in air of figure 6.15a is estimated as $\sim 0.1 \text{ A/mm}^2$ since the current peak is 0.09 A for 35 streamers with a diameter of 0.2 mm. The oscillations shown in figure 6.15a are also present in figure 6.15b only there they are invisible because of the larger current and time axis. The oscillations could not be removed from the signal.

Chapter 7

Streamers of different polarity

Negative and positive streamers created in a 40 mm point-plane gap in air at 1 bar are compared in a wide range of pulse amplitudes from 5 to 90 kV. The streamer propagation consists of: 1) a light emitting cloud at the tip that 2) evolves into a thin expanding shell from which 3) one or more streamers emerge that 4) propagate towards the plate. Negative streamers need $V \gtrsim 40$ kV ($\approx V_{\text{DC-breakdown}}$) to proceed beyond stage 2. Positive streamers go through stages 1 to 4 when $V \geq V_{\text{inception}}$ (≈ 5 kV). They show thin channels (≤ 1 mm in diameter) that bridge the electrode gap and branch when $V \leq 40$ kV.

When $V \gtrsim 40$ kV positive and negative streamers become more alike with increasing voltage. First they both show thick channels (1-2 mm) but the negative ones still die out in the gap during transit as long as $V < 56$ kV. At $V \geq 75$ kV both polarities show thick streamers (2-3 mm) that carry the same energy (~ 50 mJ), bridge the gap and hardly branch. Still, positive streamers are $\sim 25\%$ faster and remain slightly thicker.

In a plane-plane gap of 10 mm at different pressures only negative discharges can be photographed that consist of a streamer that has evolved to glow; no positive discharges are photographed except for sparks. In the current signals both positive and negative streamer currents of about the same magnitude are seen. The streamer evolution to glow is only observed in the negative current signal. In gaps larger than 10 mm no discharges at all are visible on the camera. Therefore it cannot be verified if the single channel cannot develop in the small 10 mm electrode gap (cf. the point-plane gap) or that the single channel is a result of the fast streamer evolution in a high reduced electric field. Positive and negative discharges in air and N_2 can only be created at a reduced electric field of ~ 20 kV/(cm·bar).

supply	gap	R_1 (M Ω)	R_2 (k Ω)	R_3 (M Ω)	R_4 (Ω)	C (nF)	rise time (ns)	polarity	switch
C	point-plane	25	0	0.004	2.75	0.250	30	+	SG
C	point-plane	25	2	1	2.75	1	150	+ and -	SC
TLT	point-plane	25	1	—	—	1	25	+	
PM	point-plane	—	—	—	—	2	15	+ and -	
C	plane-plane	25	2	0.008	2.75	1	—	+ and -	SG

Table 7.1: *The supplies used. SG = sparkgap, SC = Behlke HTS 651.*

7.1 Introduction

In many industrial applications positive streamers are used since positive (cathode directed) streamers are easier to create around sharp tips than negative (anode directed) ones [90]. They are also used in gas cleaning and for ozone production in ozonizers since they have a higher efficiency than negative streamers [104]. Negative streamers on the other hand usually precede lightning channels [116] and recently it is found that at certain conditions negative streamers have a better efficiency for ozone production [119]. Furthermore, negative DC-corona is used in dust precipitators to charge small particles that thereafter can be drawn out of a gas stream by an electric field. In this chapter both polarities are studied to get a good picture of differences and similarities of these discharges. Since the discharge ignition is influenced by the electrode shape also measurements are done in a parallel plate electrode gap. These measurements will also be more suitable for comparison with theory that preferably uses a homogeneous electric field to study streamers since it limits the complexity of the models [33; 69; 84].

7.2 Experimental setups and diagnostics

7.2.1 Point-plane gap

Positive and negative discharges are made in the voltage range of 5 to 60 kV using the C-supply which is described in chapter 4. For extra comparison with thick positive streamers, measurements using the TLT-supply (chapter 4) are added. The values of the components used are given in table 7.1. The polarity of needle and plate (and thus the streamer) is changed by reversing the polarity of the DC-power supply and the high voltage switch so that the needle and the plate remain at their original position. Photographs of the streamers using the C-supply with $R_2 = 0$ k Ω and the TLT-supply are made with an analogue 4QuikE camera from Stanford Computer Optics. The current is measured via

the divided cathode and the voltage via a Tektronix P6015. The needle is made from thoriated tungsten. The streamers made when using the C-supply with $R_2 = 2 \text{ k}\Omega$ are photographed by a digital 4QuikE Stanford Computer Optics camera. The current is again measured via the divided cathode but the voltage via a Northstar PVM4. The needle is made from pure tungsten. The discharges do not show any differences in appearance, inception voltage, sparking voltage or current signals due to the different needles.

The positive and negative streamer measurements are extended with discharges generated in the voltage range of 40 to 96 kV in the Pulsed Power Modulator supply (PM-supply), as described in section 7.2.4. See [117; 119] for more details.

All measurements are done in ambient air at atmospheric pressure in a 40 mm point-plane electrode gap, except for section 7.3.2 where the negative streamer start is investigated in a 160 mm gap and section 7.3.6 where differences between negative streamers in nitrogen and air are shown. Then the electrode gap is 10 mm.

Photograph analysis

Figure 7.5 shows that the streamers in the 40 mm gap generally have one width while propagating through the gap. At voltages (far) above the DC-breakdown voltage they can be slightly thinner near the tip and plate as is seen in chapter 4, figure 7.5e,f or [15]. They do not branch from thick into thinner ones as the streamers in the 80 or 160 mm gap in chapter 4 or grow 200% in diameter as in the wire-plane gap in [117]. Therefore, in the gap of 10 or 40 mm it is possible to talk about *the* streamer diameter and *the* streamer velocity (since diameter and velocity are related, chapter 4) when away from the electrodes. Most diameter evaluations are done halfway the gap. Velocity evaluations are made throughout the gap. The methods are described in chapter 4 when using the C- and TLT-supply and in section 7.2.4 for the PM-supply.

In figure 7.12a,b a laserspot at the needle and several reflections in the bottom plate are visible. No differences in streamer pattern or inception time are observed in the point-plane gap whether the laser is fired or not; the discharge still starts spontaneously.

7.2.2 Plane-plane gap

In section 7.4 measurements are described between two stainless steel parallel plates in air and N_2 using the sparkgap-C-supply (C-SG-supply, chapter 4). First a pulsed voltage is applied over the electrode gap. Thereafter a laser is fired such that the discharge is ignited when the voltage is at its maximum. In this way it is avoided that streamers start in the rising slope of the voltage as can occur in a point-plane gap where streamer inception occurs spontaneously. The upper plate has a Rogowski profile, the bottom one is the divided cathode. Both disks have a diameter of 100 mm. Tests are done with two Rogowski disks

since then the electric field in the central part is most close to homogeneous [102] but no difference in streamer pattern is observed compared to the case with the divided cathode. The discharge is ignited by focusing and shooting a laser on the top plate (the divided cathode is the bottom plate). This laser is a Quantel Ultra UL422411 laser from Big Sky Laser Technologies. It emits a beam with an energy of 4.8 mJ at a wavelength of 266 nm with a pulse width at full width at half maximum of less than 8 ns. From literature data it is estimated that a hole of 1 μm depth and 60 μm in diameter is drilled per shot. This corresponds to an order of 10^{10} metal atoms that are released per shot [44; 58; 87]. Further, the energy density of the focussed laser beam is also high enough to create a tiny plasma cloud.

The polarity of the electrodes (and thus of the streamer) is changed by reversing the polarity of the sparkgap switch and the DC-power supply. The electrode gap is 10 mm. In larger gaps no streamer discharges are visible for applied voltages in the range of 1-60 kV. Photographs are made with the digital 4QuikE camera. The voltage and current are measured by the PVM4 and divided cathode, respectively.

7.2.3 Timing diagram C-supply

In figure 7.1 the timing diagram of the setup is shown when the C-SG-supply is used with the YAG-laser and the camera. The laser receives a signal from the "function generator" (Agilent 33250A, 80 MHz) and prepares for lasing. The output signal from the laser's "lamp-synch" is used to trigger the "CCD-camera" and the delay generator. The delay between the "lamp synch" and the "laser pulse" is $\sim 135 \mu\text{s}$. Therefore, the delay generator (Stanford Research Systems Inc. Model DG535) sends a signal to the "pulsed power supply" after $\sim 134 \mu\text{s}$, so that the "voltage pulse" is maximal when the "laser pulse" is fired. The timing of the camera has to be adjusted such that the camera opens at the same time that the streamers propagate.

When the YAG-laser is not used, the time delay between the pulse of the "function generator" and the start of the "high voltage pulse" of the "power supply" is decreased to 1.2 μs when using the C-SG-supply and 0.35 μs when using the C-SC-supply. The difference between C-SG- and C-SC-supply is caused by different trigger electronics.

7.2.4 Power modulator

Experimental setup

The measurements on positive and negative streamers in the Pulsed Power Modulator (PM-supply) at Electrical Engineering of the Eindhoven University of Technology are done in a fixed 40 mm inhomogeneous point-plane electrode gap *without* a surrounding vacuum vessel. The setup is thoroughly explained in [117; 119]; here only the most important

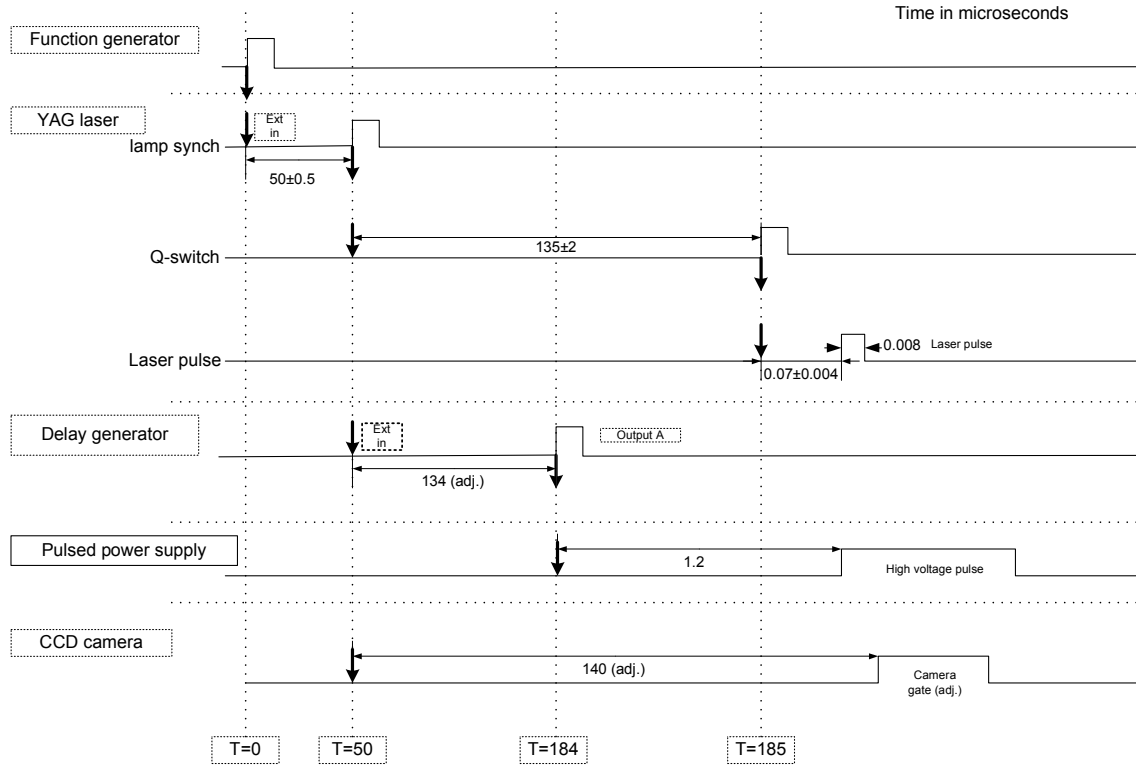


Figure 7.1: *Timing diagram of the experimental setup with the YAG-laser and the iCCD-camera using the C-SG-supply. Time axis is not on scale.*

aspects are given (also given in [16]). The tungsten needle has a tip radius of $\sim 15 \mu\text{m}$ and a diameter of 1 mm . The square plate electrode of roughly $0.5 \text{ m} \times 0.5 \text{ m}$ is made from aluminum. A Princeton Instruments 576G/RB intensified CCD-camera with a Sigma lens ($f = 180 \text{ mm}$) takes photographs of the discharge. This camera can make one photograph every $\sim 30 \text{ s}$.

The principle of the pulsed power modulator is to charge a pulse forming line (PFL) to high-voltage and subsequently to discharge it over the needle-plate electrode gap (figure 7.2, [117; 119]). The PFL consists of two 50Ω coaxial high voltage cables of 10 m that are connected in parallel resulting in a capacitance of 2 nF . The advantage of charging and discharging a PFL instead of a capacitor (as in the C-supply) is that the voltage pulses are short (100 ns) with an almost rectangular shape and a fast voltage rise time of 15 ns (cf. MIPT-supply). The LCR trigger circuit ($10 \mu\text{H}$, $30 - 80 \text{ pF}$, $400 \text{ k}\Omega$) takes care of reliable switching of the sparkgap switch. It causes the switch to close shortly after the PFL charging has been completed. The 2-stage TLT transforms the voltage a factor of 1.98 up to compensate for the factor 2 drop in voltage due to the PFL. The TLT also takes care of the 75 ns time-delay that is necessary for the camera to get itself ready for

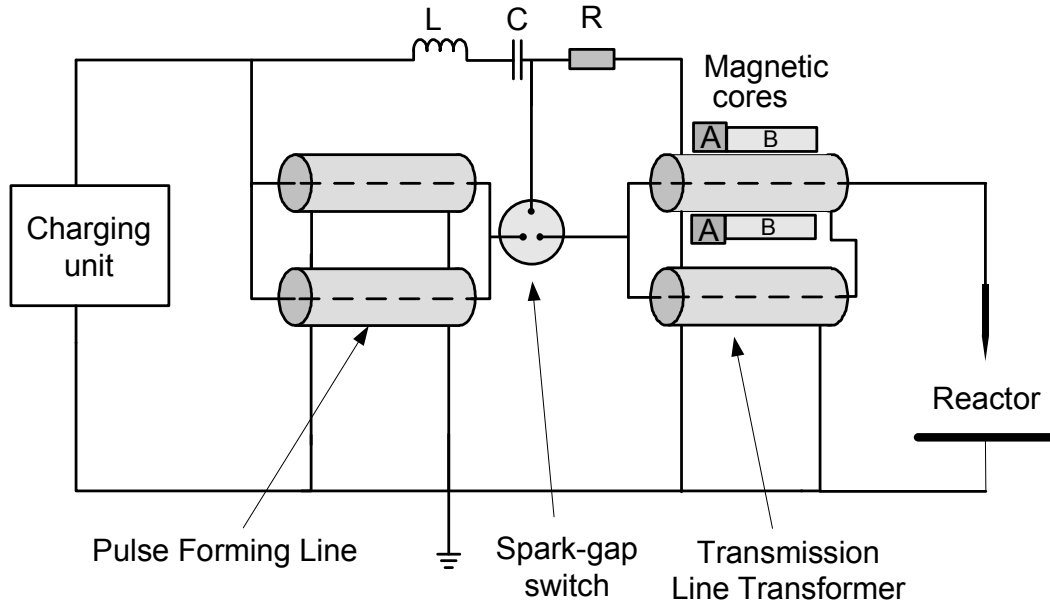


Figure 7.2: *The pulsed power modulator. The picture is a simplified version of the picture in [119]. $L = 10 \mu H$, $C = 30 - 80 pF$, $R = 400 k\Omega$, The magnetic cores A and B damp the reflecting wave when the load and the source are not well matched.*

the photograph (for the actual trigger scheme see [119]). The streamer polarity is reversed by making changes in the circuit which in figure 7.2 are bundled in "Charging Unit". The needle and plate electrodes therefore remain in their original position. In this setup the impedance of the PFL (25Ω), the TLT (PFL side 25Ω , discharge side 100Ω) and the discharge are better matched than when using the C-supply (see also TLT-supply, chapter 4), especially when high currents are drawn. The matching results in less oscillations on the signals and a good energy transfer from the circuit into the discharge.

A differentiating-integrating measuring system is used to be able to measure fast, high amplitude voltage (40 - 96 kV) and current waveforms [45; 119]. The advantage of this system is that the high frequency components of the signal (including the noise) are decreased with respect to the lower ones resulting in a better signal to noise ratio. Both signals are digitized on a LeCroy Waverunner 2 oscilloscope (1 GHz, 4 GSamples/s).

The ambient air is regulated between 20 - 24 °C and 35 - 60 % humidity [120]. The pressure is the prevailing outside pressure, which is around 1000 mbar. The discharges are pulsed at 10 Hz, but according to [120] the photographs are taken from the first discharge. The discharges made when using the C-supply and the TLT-supply are pulsed single shot with a "frequency" of less than 0.1 Hz.

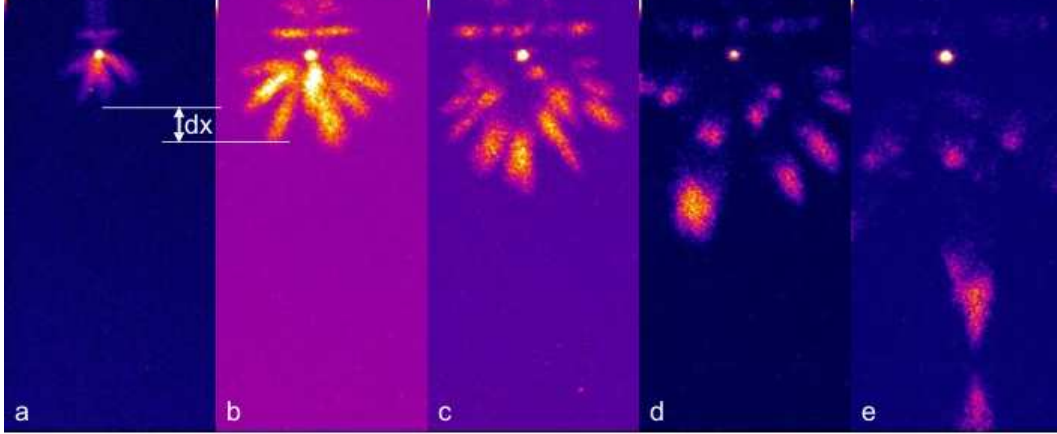


Figure 7.3: *Negative streamers in a 40 mm gap at 56 kV in ambient air at 1000 mbar with the PM-supply. The exposure time is ~ 5 ns. The gate delay is a) 4.4 ns, b) 9.3 ns, c) 14.3 ns, d) 19.6 ns, e) 28.8 ns. The light at the bottom of figure e) is a reflection of the streamer that reaches the anode plate.*

Photograph analysis

The positive and negative streamer diameters are measured as described in chapter 4. The measurements are done on primary and secondary streamers (chapter 3) since the secondary streamers have the same diameter as the primary ones [119] but a better contrast with the background which facilitates the evaluations. Only time resolved photographs are used for the evaluations.

The velocity is obtained from the propagation distance between photographs (dx in figure 7.3) divided by the difference in delay time of the photographs [119] because the jitter in streamer inception is small and the exact exposure time of the camera is unknown. Approximately five photographs are used of the whole propagation from needle to plate to obtain more accuracy. This method can be used since the velocity remains constant through the complete gap¹. The distance of the streamers and delay time are plotted and a line is fitted through the data points. The slope of this line gives the average velocity. Only the fastest streamers are used since they are the ones that propagate most parallel to the camera's focal plane. The error in the obtained velocity is $\leq 10\%$.

Energy calculations

A typical current-voltage evolution of the PM-supply is shown in figure 7.4a,b. The current in figure 7.4a shows a peak (the capacitive current peak) followed by a plateau and then

¹Note that in the wire-plane gap by [119] the velocity is constant in the gap but increases near the plate.

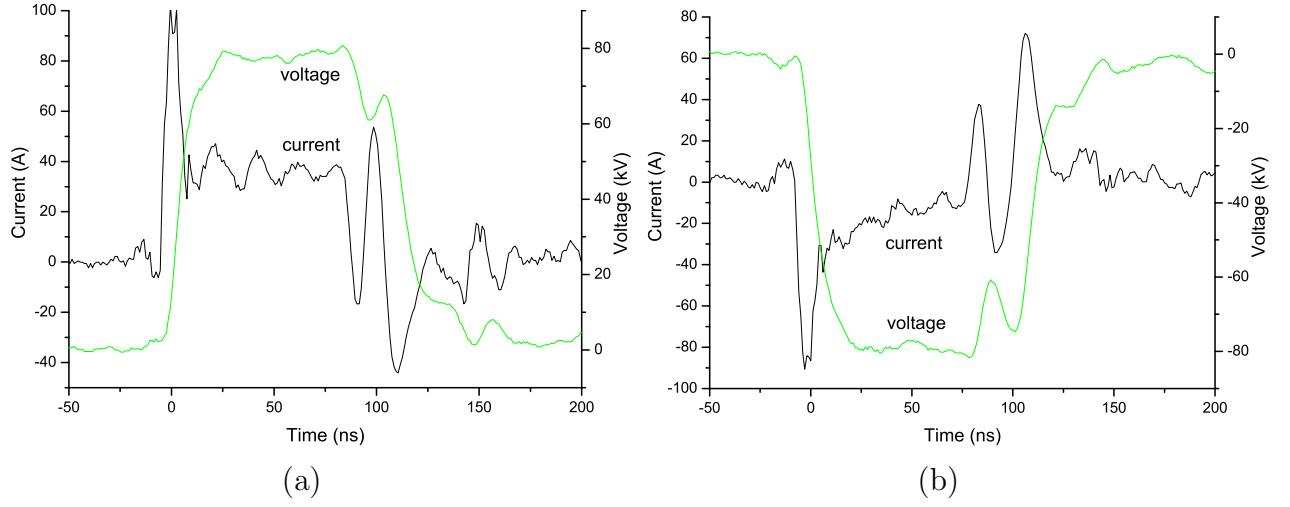


Figure 7.4: *Current-voltage evolution at ~ 82 kV in a 40 mm gap at 1000 mbar from a) positive streamers and b) negative streamers. The current and voltage lines are smoothed by adjacent averaging over 5 points.*

a negative peak. The two peaks arise from the capacitive current and add up to zero. Therefore, by integrating the data with equation

$$E_{\text{corona}} = \int V \cdot I \cdot dt \quad (7.1)$$

to $t = 200$ ns the capacitive current is eliminated from the energy and only the total corona energy is obtained. The energy is measured from a single discharge. It is not averaged over 100 discharges as in [119]. The error is estimated to be 10 - 20% [120].

The total corona energy however not only contains energy from the primary streamers but also from events that occur after the primary streamer propagation since the primary streamers transit the 40 mm electrode gap in 10 – 80 ns, depending on velocity (section 7.3.4). The primary streamer energy can be estimated by subtracting the capacitive current peak from the total current signal and then integrating the remaining signal with equation (7.1) to the estimated moment that the primary streamers reach the plate. The capacitive current can be calculated via

$$I_{\text{capacitive}} = C_{\text{geometry}} \cdot \frac{dV}{dt} \quad (7.2)$$

in which C_{geometry} is the capacitance of the electrode gap and t is the time. C_{geometry} must be obtained at voltages where no discharge takes place, since then $I_{\text{measured}} = I_{\text{capacitive}}$. Here the data for a negative discharge at 28 kV is used as a rough estimate since lower voltages

could not be obtained. At this voltage the discharge is still confined in a small region at the tip. It gives a value of $C_{\text{geometry}} = 12 \text{ pF}$. When C_{geometry} is known, measurements can be done at higher voltages where streamers ignite. Then $I_{\text{capacitive}}$ is known and can be subtracted from I_{measured} , resulting in an I_{corona} .

7.3 Results: point-plane gap

7.3.1 First observations

In figure 7.5 positive and negative discharges in a 40 mm gap at 20 kV (undervolted gap), $\sim 46 \text{ kV}$ (slightly overvolted) and $\sim 80 \text{ kV}$ (far overvolted gap) in air at 1 bar are shown. The differences between positive and negative discharges in undervolted gaps ($< 40 \text{ kV}$) are remarkable. The lowest possible voltage at which positive streamers start in a 40 mm gap is $\sim 5 \text{ kV}$ (figure 5.1a), while this is $\sim 20 \text{ kV}$ for a negative discharge (figure 7.5b). As shown in figure 7.5a the positive streamers are very thin ($\leq 1 \text{ mm}$), branch and bridge the complete electrode gap at 20 kV (see also chapter 6) while the negative discharge remains more like a cloud around the tip. At 46 kV both polarities show thick channels (1-2 mm) but the negative ones die out halfway the gap and hardly branch. They cross the electrode gap at 56 kV (figure 7.3). When the voltage increases the differences between positive and negative discharges slowly disappear. At voltages above 75 kV the streamers are much alike, i.e. they are thick (2-3 mm), bridge the gap and hardly branch. The positive streamers still branch a little more than the negative ones (figure 7.5e and 7.5f). Here it must be noted that part of the branching can also come from late streamers (chapter 4) and not only from the primary streamer itself since in figure 4.6, at roughly the same conditions as in figure 7.5c, not much branching is observed, except for late streamers.

The stability field of a negative streamer can be estimated from figure 7.5d where the streamer propagates approximately 30 mm at -47 kV. This gives a value of $\sim 15 \text{ kV/cm}$ which is $3\times$ the stability field of a positive streamer (5 kV/cm, chapter 6). This value is in agreement with simulations performed by [6] who modelled streamers in air at atmospheric pressure in a setting where the point-plane gap is approached by a sphere with radius 0.1 cm at 115 kV/cm that is placed in a uniform electric field (with values of 0 to 35 kV/cm). Raizer indicates that a minimal average field of $\sim 10 \text{ kV/cm}$ is necessary for negative streamer propagation in a 1-2 m electrode gap [90].

A possible reason why positive and negative streamers propagate in a different way at low voltages and are more similar at high voltage is the following. In the positive case, the electrons propagate towards the needle or streamer tip. The electrons thus go from a large volume to a small region where the electric field is high and thus the ionization is enhanced.

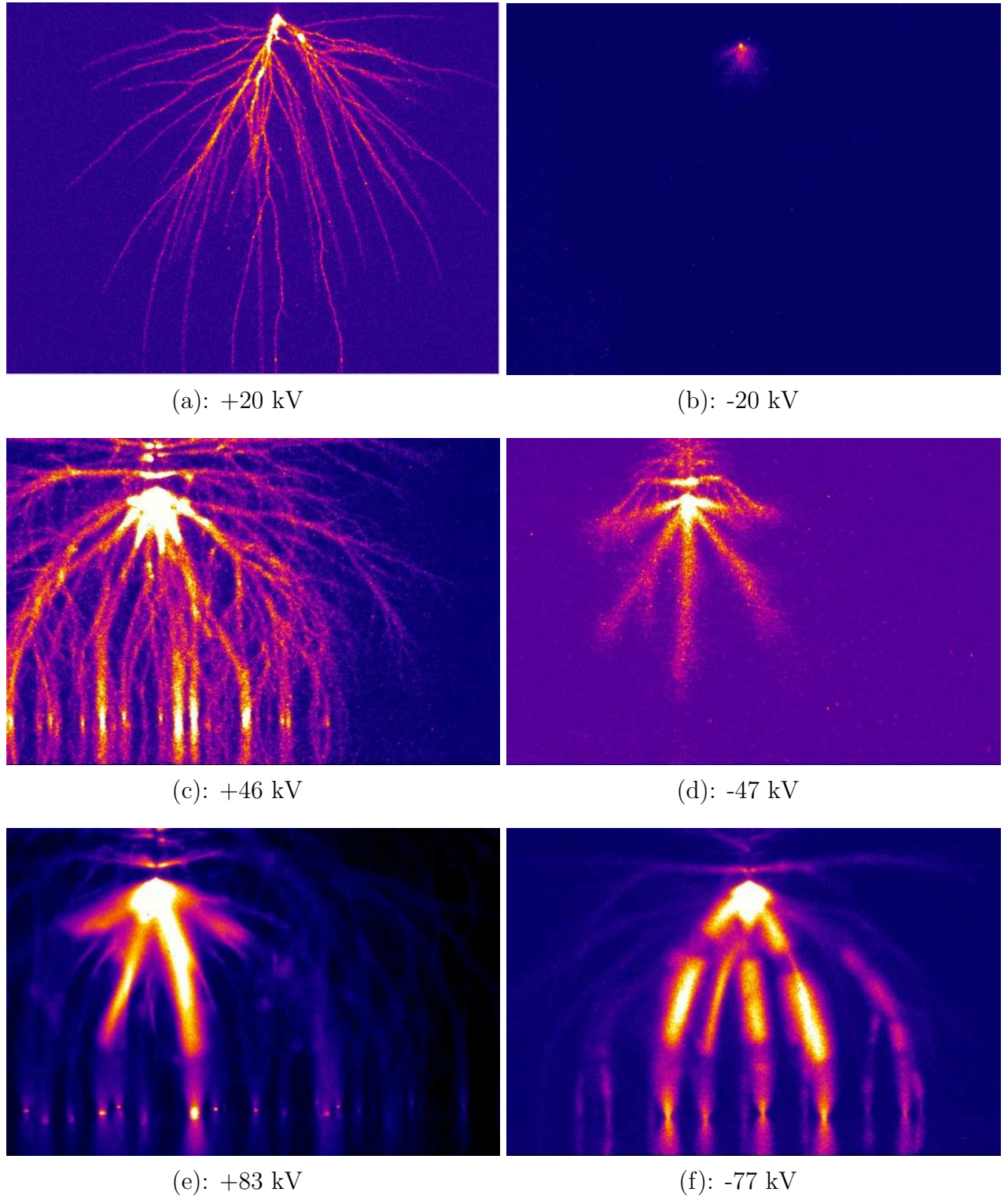


Figure 7.5: Time integrated photographs of positive (left) and negative (right) streamers in a 40 mm gap in air at 1000 mbar. The delay is 0 ns, the exposure time and supply are a) 1 μ s, C-SC-supply with $R_2 = 2$ k Ω , b) 100 μ s, C-SG-supply with $R_2 = 2$ k Ω and c-f) 160 ns with the PM-supply.

In this way enough electrons are created for the positive streamer to keep on going. In the case of negative streamers, the electrons start at the small needle and propagate into the large background volume. The electric field decreases and the avalanche, which runs through a low electric field, dies out. In very high overvolted gaps the applied electric field in the volume of the gap is high enough to keep also the negative discharge going and therefore the positive and negative streamer look more alike.

In figure 7.5f an overexposed region halfway the streamer is shown with a darker region near the tip and near the plate. This region increases with increasing voltage from 16 mm via 18 mm to 23 mm at 64 kV, 75 kV and 82 kV, respectively, and arises after the primary streamers have bridged the electrode gap. It is unknown why this large region forms in the middle of the gap, since usually such a region stretches out from the tip and is regarded as a secondary streamer (as in figure 7.5e). Perhaps the higher stability field of the negative streamers confines the secondary streamer to the middle of the gap. The observation that a glow-like channel is loose from the electrodes is also shown in figure 3.5d but then for positive streamers at 613 mbar. Striated or subdivided secondary streamers are reported in [98], however no photographs are shown that can be used for a comparison.

7.3.2 Negative streamer start

Figure 7.6 and 7.8 show the start of the negative discharge². In figure 7.6a a time integrated photograph of the discharge at 400 mbar in a 160 mm gap with the C-supply is shown. It manifests itself as a light emitting cloud around the tip. The other light rays seen on the photographs are reflections since they are also observed in figure 7.6b,d at exactly the same location. The negative discharge starts as a cloud with some structure in it at the tip (figure 7.6b) from which a shell evolves (figure 7.6c). No streamers however are seen to emerge from the shell. This is most likely due to the fact that in these photographs the voltage is below the critical voltage for negative channel formation, which in our experiments appears to be around the DC-breakdown voltage, see section 7.3.1. The shell arises and disappears somewhere between $T = 1900$ ns and 2200 ns. The shell's velocity is at least 0.1 mm/ns since it is uncertain whether the vertical length corresponds to 100 ns or less since no photographs with a shorter exposure time than 100 ns are made. After $t \sim 2200$ ns, only a little glowing ball at the tip is visible (figure 7.6d). The shell in figure 7.6c appears to be further away from the tip than the edges of the complete time integrated discharge in figure 7.6a. This is because the intensity scale between both figures is different to show the interesting regions without over- or underexposing the figures. In figure 7.7a a photograph of the positive streamer start is shown under the same conditions as the measurement series of figure 7.6, i.e. 160 mm gap, 400 mbar and 30 kV in N_2 . The streamers can reach the

²The positive streamer start is shown in chapter 3.

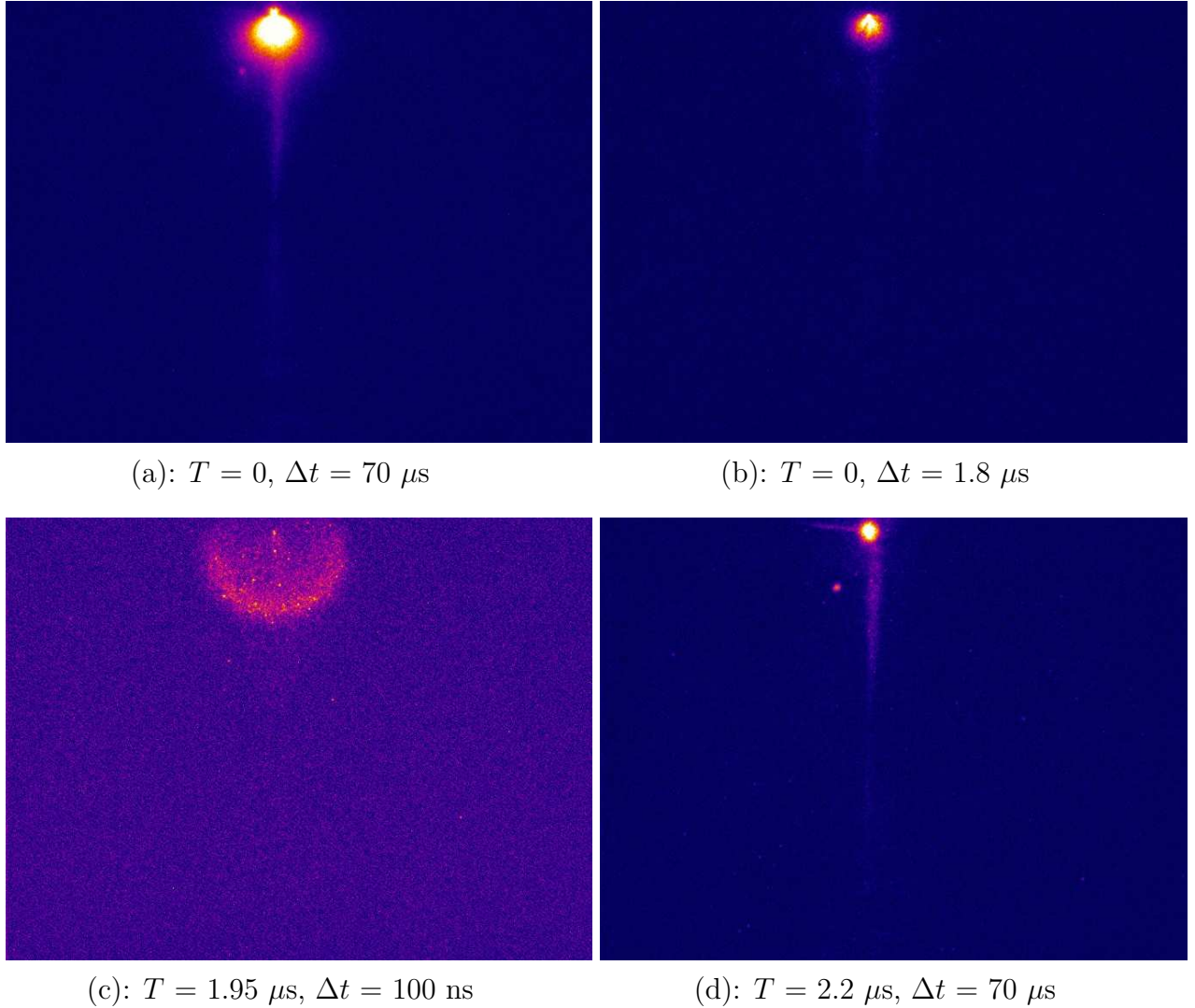


Figure 7.6: *The start of a negative streamer in a 160 mm gap at 400 mbar and 30 kV in N_2 (settings table 3.1). The camera's delay T and exposure time Δt are given.*

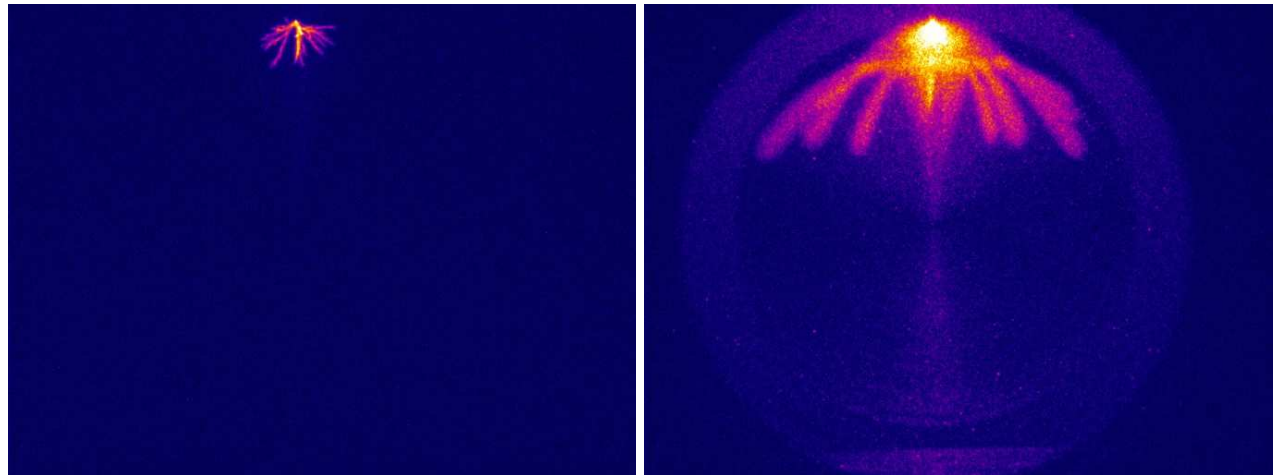
(a): $T = 1.7 \mu\text{s}$, $\Delta t = 50 \text{ ns}$ (b): $T = 0$, $\Delta t = 2 \mu\text{s}$

Figure 7.7: *Positive streamers in a 160 mm gap a) at 400 mbar and 30 kV in N_2 (settings table 3.1) and b) at 62.5 mbar and 22 kV in air (settings table 3.1). The camera's delay T and exposure time Δt are given. The streamers in a) and b) can reach the plate electrode but the exposure time is chosen such that they are photographed during their propagation.*

plate electrode but are photographed during propagation. The cloud at the tip from which the streamers start is not visible. Furthermore the streamers branch frequently. This is not clearly visible in figure 7.7a but this can be observed in the time integrated photograph of figure 6.7d which is taken at a lower voltage of 20 kV but shows a similar branching pattern only a little bit less crowded.

In figure 7.8 a time resolved series of negative streamers is seen at 62.5 mbar. Figure 7.8a shows the time integrated photograph. In dimensions it looks like the positive discharge in chapter 3 at 13 mbar. Figure 7.8b shows that the discharge starts again with a light

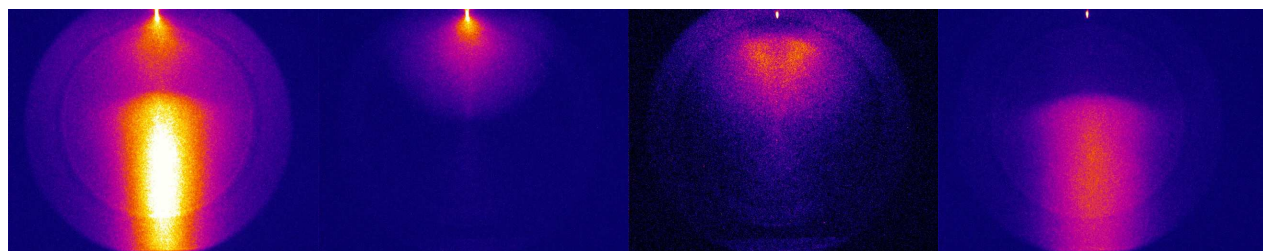
(a): 0, $6 \mu\text{s}$ (b): 0, $2 \mu\text{s}$ (c): $2 \mu\text{s}$, $2 \mu\text{s}$ (d): $4 \mu\text{s}$, $2 \mu\text{s}$

Figure 7.8: *The start of a negative streamer in a 160 mm gap at 62.5 mbar and 20 kV in air (settings table 3.1). The camera's delay T (first value) and exposure time Δt (second) are given.*

emitting cloud at the tip. Figure 7.8c shows that the cloud becomes loose from the tip but no real shell is visible. Note that this is not similar to the overexposed region in figure 7.5f since this occurs during the primary streamer propagation while the region in figure 7.5f arises after the primary streamer propagation. In figure 7.8d a glow arises just as in figure 3.3h. When a photograph with $T = 6 \mu\text{s}$, $\Delta t = 2 \mu\text{s}$ is taken the glow is still visible, at the exact same location, but less intense. A difference that is observed compared to figure 3.3 is that here the glow is more straight while in figure 3.3 it is more cone shaped with a transition to streamer. In figure 7.7b a photograph of the positive streamer start is shown under the same conditions as the measurement serie of figure 7.8, i.e. 160 mm gap, 62.5 mbar and 22 kV in air. The streamer pattern for positive and negative streamers appears different: positive streamers are observed to emerge from the cloud that propagate towards the plate. The positive streamers can reach the plate electrode but the exposure time is chosen shorter than the time that is needed to bridge the complete gap.

Negative streamer channels are only observed when using the PM-supply which has a fast, 15 ns, rise time and can apply high voltages from 40 to 96 kV.

7.3.3 Diameter

The diameters of positive and negative streamers in the voltage range from 5 - 96 kV in a 40 mm gap in atmospheric pressure air are shown in figure 7.9. Three different power supplies are used to have an overlap in voltage. This is allowed since in chapter 4 it is shown that when the total impedance in the discharging circuit is similar, measurements can be compared. The main measurements are done with the PM-supply, TLT-supply and C-supply without seriesresistance. The measurements with the C-supply and $R_2 = 2 \text{ k}\Omega$ are plotted as well, they show only very thin, type 3 streamers. They are thin since they start propagating while the voltage is still rising, thus ignite at a lower voltage than the maximum (chapter 4).

Figure 7.9 shows that 5 kV is the lowest voltage at which positive streamers ignite. Their diameter is 0.2 mm (i.e. the minimal diameter). At 20 kV they have a diameter of 0.4 mm and bridge the 40 mm gap for the first time. Their diameter increases rapidly further to a maximal diameter of $\sim 2.8 \text{ mm}$ at an applied voltage at the tip of 96 kV. The diameter of positive streamers increases even by a factor of 10 (from 0.2 to 2 mm) when the applied voltage is only varied a factor ~ 2 (from 25 to 55 kV) as can be seen in figure 7.9. The negative discharge starts at 20 kV but then the diameter is immeasurable since no real channels are formed (figure 7.5b). The diameter of the negative streamers can be measured at voltages higher than 40 kV. Then the minimal diameter is 1.2 mm. The negative streamers bridge the gap for the first time at $\sim 56 \text{ kV}$ (figure 7.3) with a

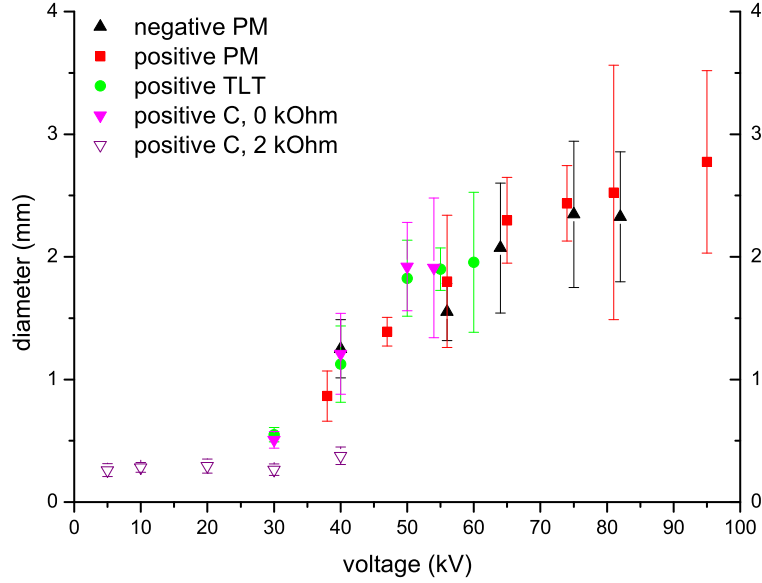


Figure 7.9: *Diameter of positive and negative streamers in air at atmospheric pressure in a 40 mm gap with three different supplies. On the horizontal axis the absolute voltage is given.*

diameter of 1.5 mm. Their diameter increases with applied voltage to a maximal diameter of ~ 2.3 mm for applied voltages between 76-82 kV. On average, the positive streamers are $\sim 10\%$ thicker than the negative ones but still within the error margins. The figure also demonstrates that the diameters obtained when power supplies are used with similar rise times are indeed close together and that the diameters obtained with the supply with a long rise time (C-supply and $R_2 = 2$ k Ω) are much thinner, as was expected from chapter 4.

7.3.4 Velocity

In figure 7.10a the velocities of positive and negative streamers are shown. Here again data from different supplies are used to have the overlap in the voltage range from 5 to 96 kV. A fit through the data points is given in table 7.2. It shows that the velocity of both streamer polarities increases with applied voltage. The positive streamer velocity increases rapidly from ~ 0.5 mm/ns at 30 kV to ~ 4 mm/ns at 96 kV. The negative streamers are $\sim 25\%$ slower than the positive ones. Their velocity increases from ~ 1.2 mm/ns at 56 kV to ~ 2.5 mm/ns at 83 kV. Velocities of negative streamers at voltages below 56 kV could not be measured because the streamers did not propagate far enough into gap to make reliable time resolved measurements. Here again the data from the supplies with low rise time are similar; they have approximately the same velocity growth with voltage (i.e. a

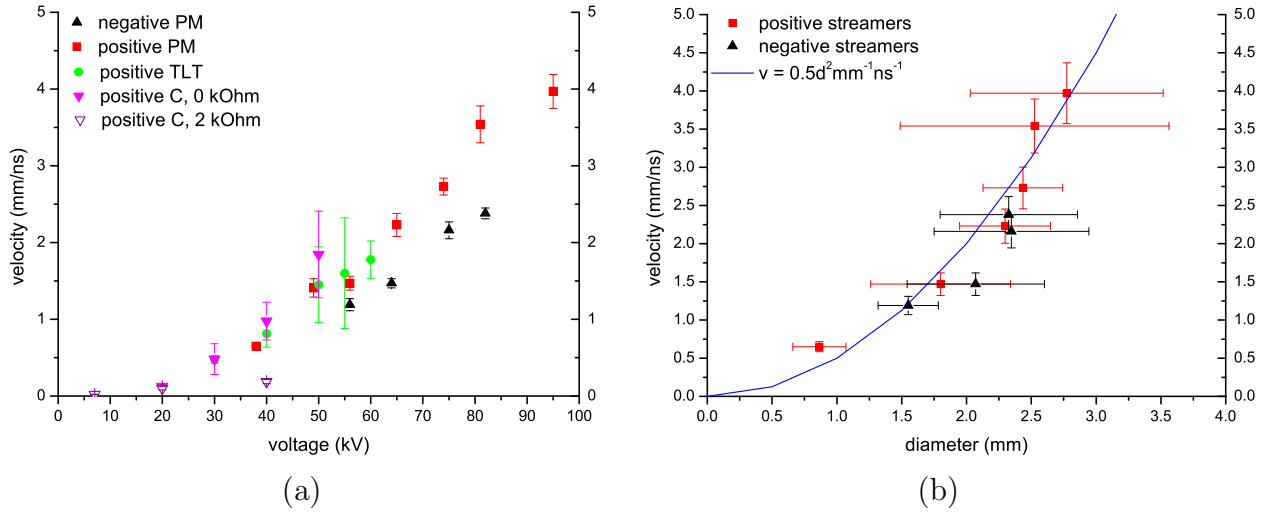


Figure 7.10: *a) Velocity of positive and negative streamers in air at atmospheric pressure in a 40 mm gap. On the horizontal axis the absolute value of the voltage is given. b) Velocity plotted as function of diameter in the PM-supply.*

similar slope, see table 7.2). The increase in velocity of the positive streamers created with a voltage rise time of 150 ns is limited, just like their increase in diameter (figure 7.9). The propagation time through the 40 mm gap can be calculated from the velocity. This ranges from ~ 80 ns at 30 kV to ~ 10 ns at 96 kV for positive streamers and from ~ 27 ns at 56 kV to ~ 15 ns at 83 kV for negative ones. Table 7.2 furthermore shows that the positive streamer velocity increases faster with increasing voltage than the negative one. This is surprising since calculations by [6] predict that differences between polarities disappear with increasing voltage which is also found experimentally in [119] for a wire-plane gap.

Figure 7.10b is made by plotting the diameter of figure 7.9 against the velocity of figure

polarity	supply	fit (mm/ns)	error (mm/ns) y-intercept	error (mm/ns) slope
negative	PM	$v = -1.55 + 0.048V$	0.27	0.004
positive	PM	$v = -1.56 + 0.058V$	0.13	0.003
positive	TLT	$v = -0.81 + 0.043V$	0.08	0.002
positive	C, 0 k Ω	$v = -0.77 + 0.045V$	0.11	0.005
positive	C, 2 k Ω	$v = -0.02 + 0.005V$	0.004	4.45e-4

Table 7.2: *Fit through the data points of figure 7.10.*

7.10a at the same voltage to test whether the diameter and velocity are related (chapter 4). Only the measurements with the PM-supply are used. The velocity measurements are given an error bar of 10% of the average velocity as an upper limit. This figure shows indeed that the velocity v increases with increasing diameter d , roughly as $v = 0.5 \cdot d^2 \cdot \text{mm}^{-1} \text{ns}^{-1}$.

7.3.5 Current, voltage and energy

A typical current and voltage evolution for positive and negative streamers is given in figure 7.4. The maximum current at 83 kV for both cases is ~ 45 A when disregarding the capacitive current peak in the first ~ 10 ns. The positive streamer current remains at this level for the duration of the voltage pulse (a plateau of ~ 80 ns). The negative streamer current does not have this plateau but slowly decreases to 10 A before the voltage pulse drops back to zero. For positive streamers, this plateau is clearly visible for voltages at 56 kV and higher. For negative streamers this slightly elevated current level appears for applied voltages above 66 kV. This difference indicates (again) that there is a difference in stability field for positive and negative streamers since the negative streamers need a higher applied electric field to obtain a similar current through the discharge.

The total energy for positive and negative discharges is shown in figure 7.11. The total energy for the negative discharges at voltages ≤ 40 kV give a small negative output due to the noise on the signal and is therefore not plotted. The reason for the negative values is because the setup is built for voltages > 40 kV and the measurements are not averaged [120]. The figure shows that the total energy for positive discharges is higher than for negative discharges. This is a result of the difference in current shape; the plateau is longer for positive streamers than for negative ones. In these current evolutions the difference in stability field is found back: at the same applied voltage or field, the negative discharge finds it more difficult to sustain its channels than a positive discharge. This is because the surrounding field is closer to the stability field of negative streamers than to the one of positive streamers, which is a factor 2 to 3 lower. Therefore, the negative streamer will die out sooner than the positive one resulting in a shorter current pulse.

The moment that the primary streamers start propagating is estimated from the moment that the calculated capacitive current is lower than the measured current. This is found to be around 12-13 ns which is close to the 15 ns rise time so the primary streamers start propagating when the voltage has (almost) reached its maximum. This start moment is used to calculate the primary streamer energy which is also shown in figure 7.11. Although these values must be regarded as an estimate the data gives similar values for positive and negative streamers. These values are maximal 50 mJ and thus are considerably lower

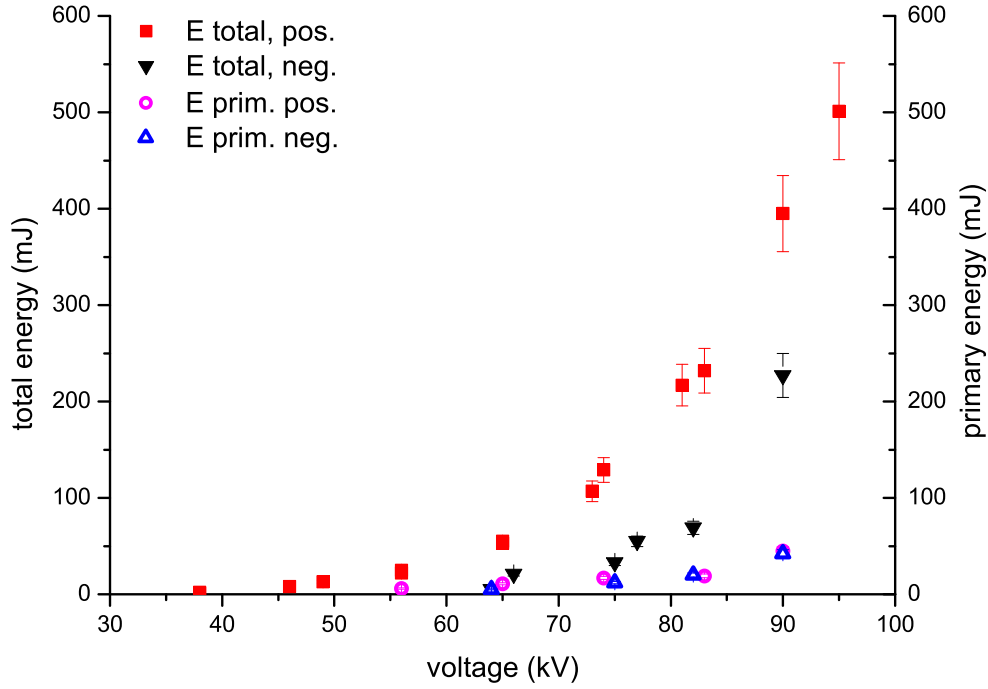


Figure 7.11: *Total and primary energy of positive and negative streamers in air at atmospheric pressure in a 40 mm gap with the PM-supply.*

than the total energy³ which is maximal 400 mJ for a positive discharge and 220 mJ for a negative one at 90 kV. In a wire-plane gap [119] it is also observed that the energy transfer efficiency of positive and negative streamers becomes more similar with increasing voltage.

The heating of a primary streamer channel can be calculated via the energy. By assuming that the discharge at 90 kV consists of 10 streamers with a diameter of 3 mm the gas in one primary streamer channel heats up ~ 13 K when conduction to the surrounding is neglected and when all dissipated electrical energy is thermalized. The temperature of the gas thus remains close to room temperature. The total positive discharge heats up one channel by ~ 110 K. Still the increase in average gas temperature is small. It is estimated to be ~ 5 K.

³Note that the total energy depends on the duration of the voltage pulse, which in these measurements is 100 ns.

7.3.6 Nitrogen and air

In the previous sections measurements on positive and negative streamers are mainly performed in a 40 mm electrode gap at atmospheric pressure in air with the fast rise time PM-supply. Since this setup does not contain a surrounding vacuum vessel measurements of both polarities in N₂ (purity 99.9%, chapter 6) must be done in the setup that contains the large vacuum vessel and the C-supply. Since in this setup negative channels are only observed in a 10 mm gap, so that voltages higher than the critical voltage for negative channel formation can be applied, all measurements in air and N₂ shown here are done in this small gap.

Photographs of the discharges are shown in figure 7.12 at the lowest voltage where they can reach the plate. The positive streamers in air and N₂ at 1000 mbar show two thin channels that propagate towards the plate. The streamers are very similar since the zigzag structure of N₂ is hardly visible. The negative discharge in air shows some structure near the tip but away from the tip the discharge is rather diffuse. At lower voltages only the structure near the tip is visible. The negative discharge in N₂ shows four channels from which two become a diffuse channel after ~ 5 mm. When this photograph is made at -10 kV instead of -12.5 kV the four very short channels near the tip remain but the (transition to) diffuse channels are not visible anymore. Whether these diffuse channels arise after the primary streamer propagation is unknown since only time integrated photographs could be made due to the large jitter in the negative discharge initiation. The stability field for negative streamers in air and N₂ is obtained from figure 7.12c and 7.12d. Since the streamers have already bridged the complete gap an upper value of this field is found of 18 kV/cm for air and 12.5 kV/cm for N₂. The value for air is ~ 3 kV higher than found in section 7.3.1.

At a lower pressure of 100 mbar and a 10 mm gap the negative discharges show only one or two channels (figure 7.14c+d) which are very similar to the positive discharges under the same conditions (figure 7.14e+f).

When positive and negative discharges at approximately the same voltage of 15 kV are compared the observed differences for positive and negative streamers in air in section 7.3.1 are also found for N₂: less channels and less branching for negative discharges. For negative discharges in air and N₂ the same differences are observed as for positive streamers (chapter 6): in N₂ there are more channels that bridge the electrode gap and they appear more intense. The difference in intensity is however difficult to verify because the discharge is diffuse and only time integrated photographs can be made. The difference in intensity can therefore also come from events that occur after the primary streamer propagation. The zigzag structure is not observed in the negative N₂ discharge. This is possibly due to the voltage just above inception since in the positive streamer of figure 7.12b, where

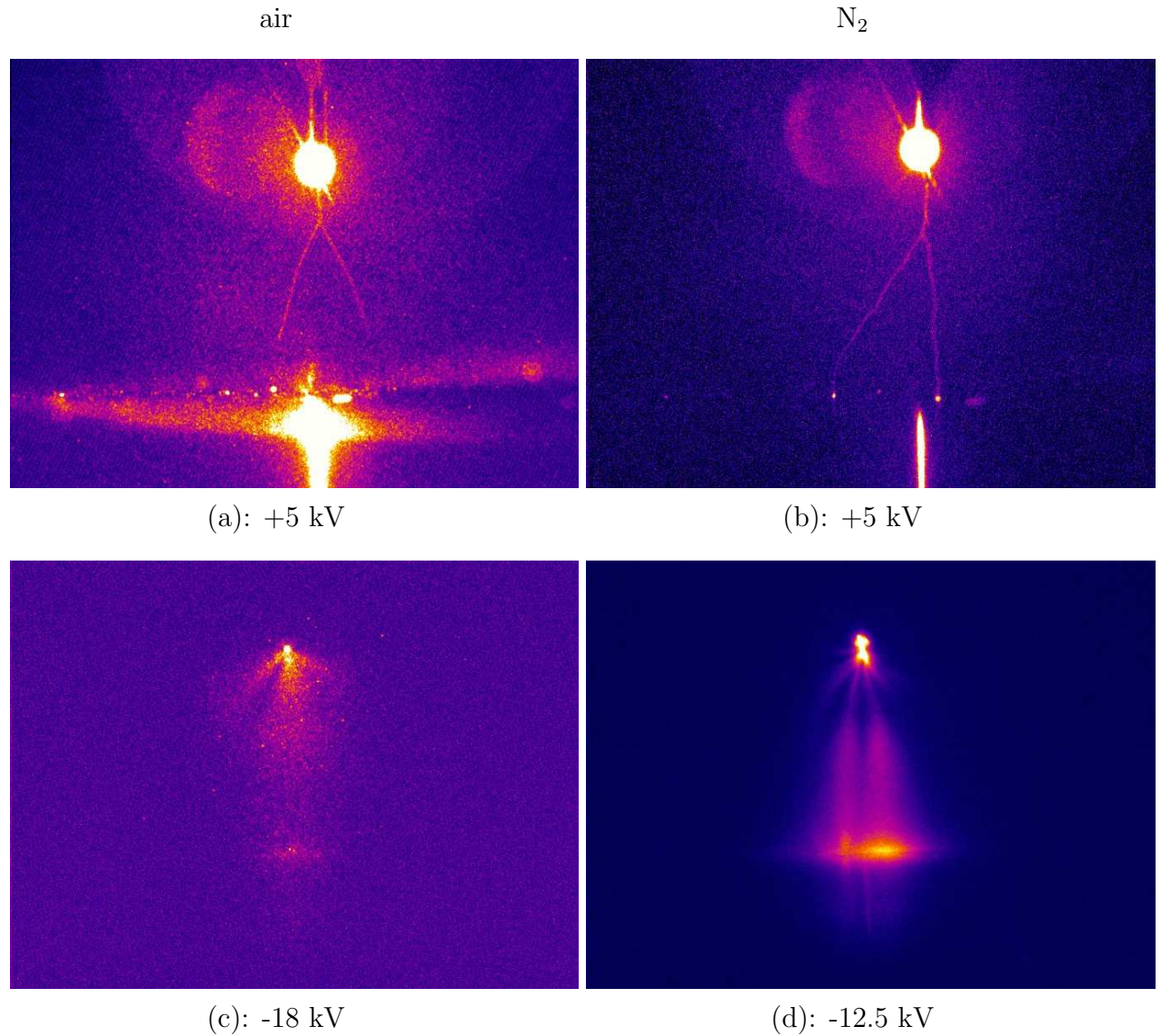


Figure 7.12: *Positive (top) and negative (bottom) discharges in air (left) and N_2 (right) at 1000 mbar in a 10 mm point-plane gap at the lowest voltage where the plate can be reached. The delay is 0 ns, the exposure time is a) 70 μ s, b) 4 μ s, c) 10 μ s and d) 100 μ s. In a+b) the laser is used.*

$V \approx V_{\text{inception}}$, only two zigzags are seen.

7.4 Results: plane-plane gap

Measurements in a homogeneous electric field are done in a 10 mm parallel plane electrode gap at 1000, 400 and 100 mbar. The measurements are triggered by a laser that is aimed at the upper plane through a quartz window on the vacuum vessel. The spot where the laser hits the upper plane is still visible in all pictures. Furthermore, the discharges are reflected in the bottom plane.

7.4.1 First observations

Lasers are well implemented in the triggering of sparkgaps where the laser creates a small plasma that is amplified by the electric field until a conductive path is created via an electron avalanche and streamer that closes the switch [28; 42; 62]. The laser beam usually is parallel to the gap axis and strikes an electrode.

It was therefore expected that streamers in parallel plane gaps could be created by using a laser to trigger the discharge. However, it is noticed that triggering the discharge with a laser is less easy than expected since the applied voltage must be close to the static breakdown voltage and the laser must be well focussed to the center of the upper plate to obtain a discharge. We observed spontaneous breakdown in a 14 mm plane-plane gap at a DC-voltage of 40 kV and 1000 mbar in air which is at 28 kV/(cm·bar) (not shown). The use of the laser decreased the breakdown voltage to 36 kV, so to a reduced electric field of 26 kV/(cm·bar) (not shown).

Figure 7.14a,b shows negative discharges in air and N_2 which appear quite similar to the streamer that has evolved to glow at low pressures in a point-plane gap (figure 7.14c-f). The photographs in the parallel plane gap however show a glow for all pressures investigated. Furthermore, only negative discharges can be seen on the CCD-pictures. Positive discharges do not show up on the photographs; either no discharge at all or a spark emerges. This is unexpected since in the point-plane gap positive streamers are easier to create because of their lower inception voltage. The possibility of bad laser focussing can be excluded since the surface of the upper electrode is damaged by the laser. In half of the photographs taken also the trajectories of metal parts that are shot out of the upper electrode are seen (figure 7.13). Perhaps the bright spot, caused by the laser, overexposes the primary streamers. Here it must be noted that when a laser is shot at the needle tip in a 10 mm point-plate gap, the positive streamers still are visible as can be seen in figure 7.12a,b. Possibly the negative discharge is more intense than the positive one but this can not be concluded from the photographs.

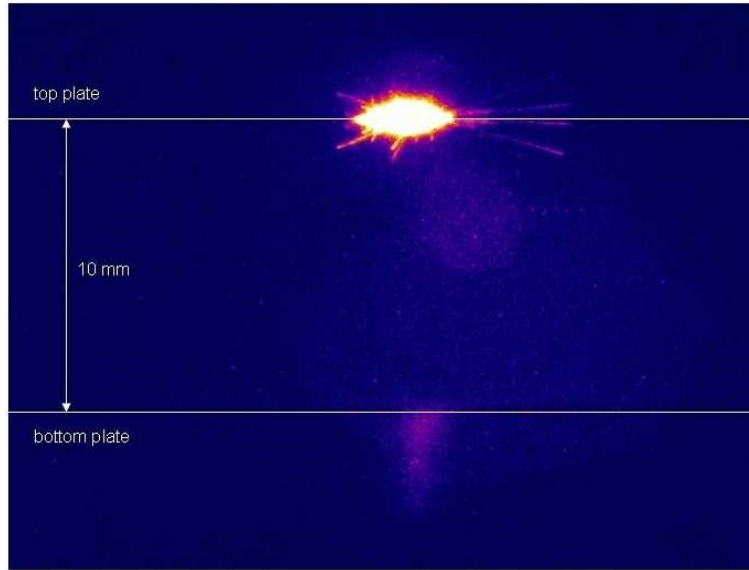


Figure 7.13: *Laser sputters electrode material away from the upper electrode plate at -32 kV. A reflection of the sputtered material can be seen in the upper electrode. Also a reflection of the laserlight is seen in the bottom plate. The other two faint light spots are reflections of the laser in the windows of the vacuum vessel. $d = 500$ ns, $gw = 70$ μ s.*

Figures 7.14a,b show that the discharge in air has its brightest part near the bottom plate while the discharge in N_2 has its brightest part near the upper electrode. This effect is better visible when the anode spot is brighter. It is unknown if this an effect of events that occur after the primary streamer has bridged the gap since it is not possible to make time resolved photographs without anode spots.

Time resolved photographs with a short exposure time (~ 50 ns) in air at 400 mbar show a similar discharge as in figure 7.14a,b only less intense. This indicates again that after the primary streamer propagation a glow arises that emits light for several microseconds until the complete discharge dies out. This evolution is much like the thick streamer (as thick as the cloud) that propagates towards the plate in figure 3.5 in a high applied electric field. Both discharges can evolve quickly and are barely restricted by the voltage rise time which is absent in the plane-plane gap (since the discharge is triggered when the voltage is already high) and only 12 ns in figure 3.5. In figure 3.5d also late streamers are seen around the glow. This is not seen in the plane-plane gap measurements. Another possibility for observation of the streamer that has evolved to glow is that the plane-plane streamers do not have enough space to develop, especially at 100 mbar, and therefore show only one channel just like in the point-plane gap where positive and negative discharges (figure 7.14c-f) also consist of a few channels. This possibility could not be verified since

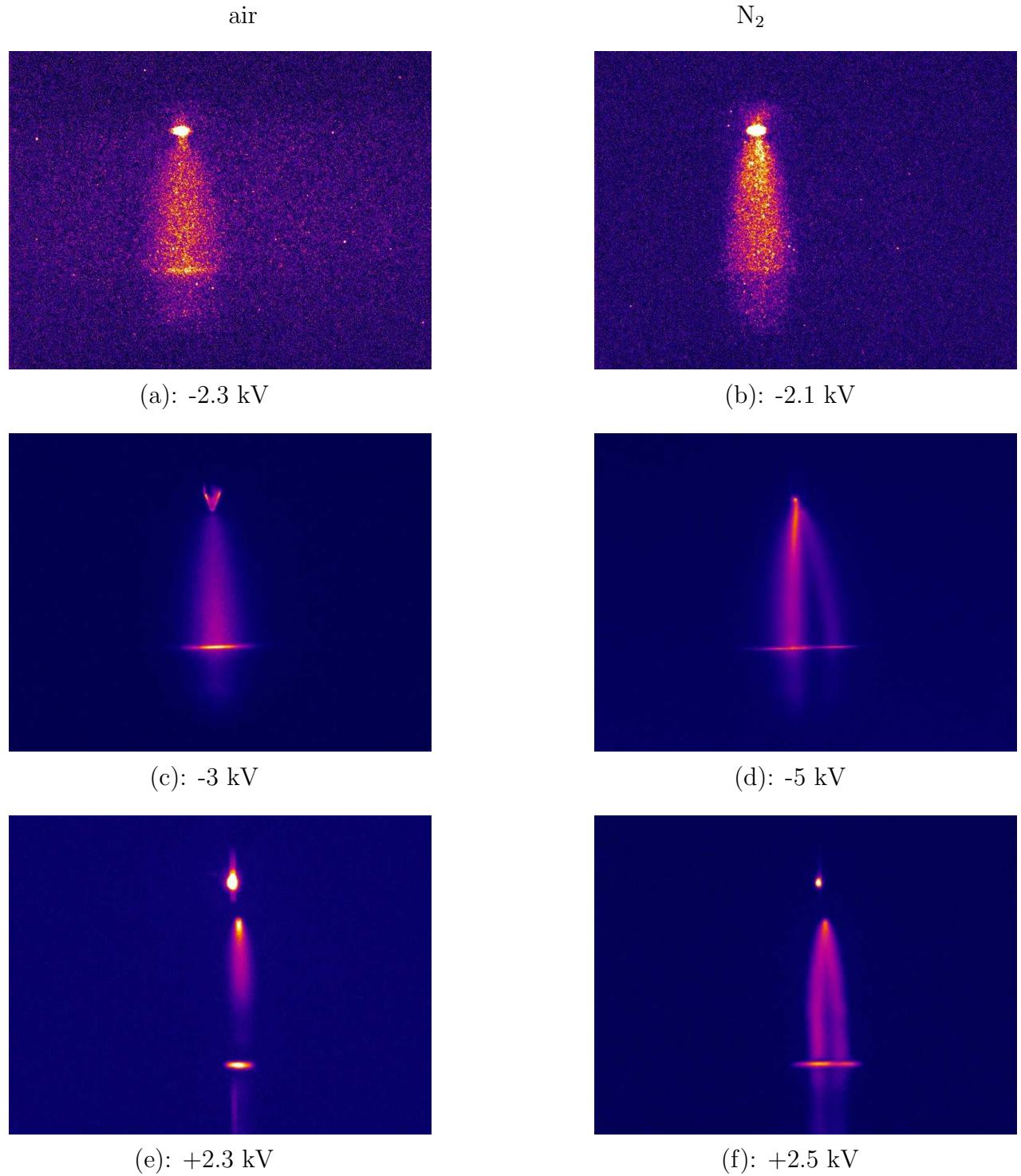


Figure 7.14: Discharges in a 10 mm gap at 100 mbar in air (left) and N₂ (right). a+b) Plane-plane gap, $d = 500$ ns, $gw = 70$ μ s. c+d) Point-plane gap, $d = 0$ ns and $gw =$ c) 100 μ s and d) 10 μ s. e+f) Point-plane gap, $d = 0$ ns and $gw = 4$ μ s.

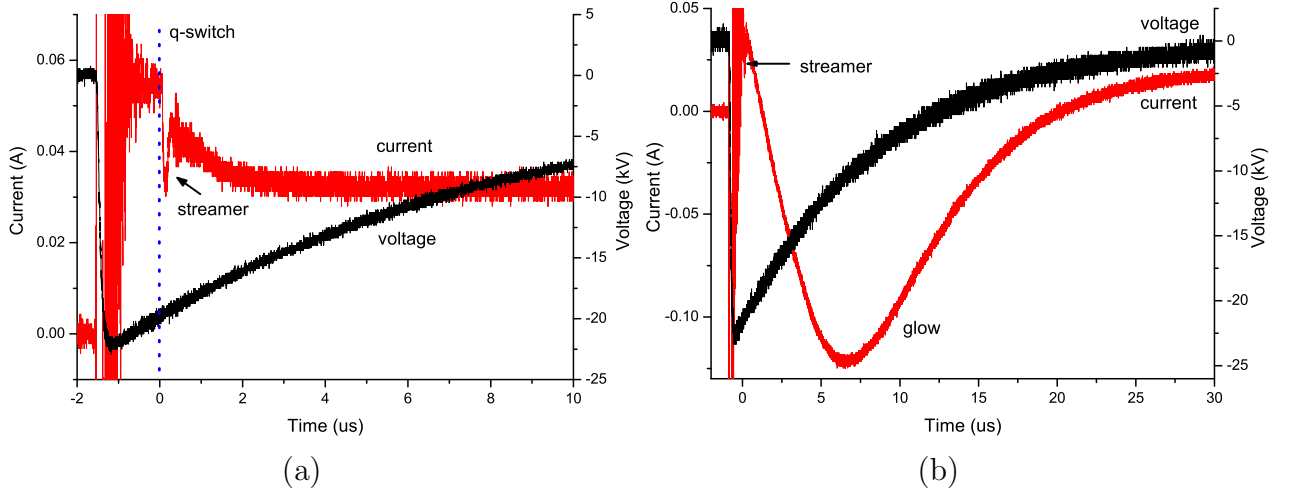


Figure 7.15: *Current voltage evolution of negative streamers at 1000 mbar in N_2 in a 10 mm gap. a) The streamer dip, at 19.5 kV b) The streamer dip (hardly visible) that grows out to glow at 21.3 kV.*

no discharges have been observed in gaps larger than 10 mm.

7.4.2 Current and voltage

In figure 7.15a,b the current and voltage evolution is shown for negative discharges. The large oscillations at $-1 \mu s$ are caused by the switching of the sparkgap. In figure 7.15a a dip in the current is visible at 19.3 kV. The dip arises in all measurements 70 ns after the q-switch of the laser is fired ($t = 0$ in figure 7.15), so at the moment the actual laser pulse hits the electrode (figure 7.1). It is likely that this dip is the streamer current since it has a halfwidth of roughly 150 ns which is in the order of the gap-transit time and it has an amplitude of 10 mA which is similar to the current that flows through one thin streamer as calculated in chapter 4. As mentioned above the streamer evolves into a glow. This transformation is also seen in figure 7.15b where the streamer dip in the current enlarges and evolves into a glow. The streamer dip is also visible in positive streamer current signals and is in air of the same order as for negative streamers (~ 10 mA at 1000 mbar, ~ 7 mA at 400 mbar and ~ 2 mA at 100 mbar). In N_2 the negative streamers carry more than a factor 2 more current than the positive ones but then their current pulse duration is shorter. The energies of positive and negative streamers in N_2 and air are of the same order: ~ 0.1 mJ at 1000 mbar, ~ 0.01 mJ at 400 mbar and ~ 0.001 mJ at 100 mbar. Here it must be noted that these numbers are only given as a rough estimate since only a few evaluations could be done. The grow-to-glow is not observed in positive current signals.

The glow regime in figure 7.15b is very long ($\sim 20 \mu\text{s}$) and heating of the gas may occur. An estimate of this is made when a channel diameter of 3 mm is assumed with an (glow) energy of $\sim 10 \text{ mJ}$. This gives a heating of the glowing channel of $\sim 340 \text{ K}$ which is $30\times$ more than the heating of a thick streamer in section 7.3.5.

The streamers usually start in the decaying voltage slope since the laser fire and the maximum of the voltage can not be matched well due to the μs jitter in the setup. This jitter is caused mainly by the laser (section 7.2.3) and the streamer inception itself. Since the moment of laser fire with respect to the voltage pulse is uncertain, the voltage at which the discharge is triggered can only be determined afterward. In air and N_2 the inception voltages are similar where for positive streamers they are $\leq 3 \text{ kV}$ higher than for negative ones. The values are found to be around 20 kV at 1 bar, 8 kV at 400 mbar and 2.5 kV at 100 mbar. This gives for all pressures an approximate reduced electric field of $|\mathbf{E}|/p \approx 20 \pm 5 \text{ kV}/(\text{cm}\cdot\text{bar})$. The observation that the streamers ignite at a similar reduced electric field over the whole pressure range is in agreement with the similarity law for discharges with the same $|\mathbf{E}|/p$ (chapter 2).

What part of the negative discharge is seen on photographs can be tested by shortening the voltage pulse duration to $\sim 100 \text{ ns}$ (the transition time of type 3 streamers in a 10 mm point-plane gap) and thus avoiding the transition to a glow. However, when such short pulses are used the jitter of the voltage pulse in the setup must be less than 100 ns else the laser can not be synchronized with the voltage pulse. This cannot be obtained in our setup where the jitter is at least $2.5 \mu\text{s}$ because of the use of the laser. Literature about laser-triggered-sparkgaps reports jitter down to sub-100 ps [62] at a pressure of 1.5 bar with laser pulse energies of $700 \mu\text{J}$ where a voltage of 10 kV is applied over a 2.3 mm electrode gap. Therefore, it could be possible that even in a non-ideal situation as our parallel plane gap ($p \leq 1 \text{ bar}$, laser pulse energy 4.8 mJ, 10 mm gap and $V \sim 20 \text{ kV}/\text{cm}$) jitter of the order of 100 ns can be obtained. However, when the jitter and the voltage pulse duration have been reduced it may still not be possible to observe primary streamers since the bright light spot can still be visible on the photographs since this light may be a recombining plasma cloud which is created by the laser (the actual laserspot lasts only 8 ns). Since the typical recombination time is $\sim 10 \mu\text{s}$ the light will remain for times longer than the streamer propagation time ($\sim 100 \text{ ns}$). This is also observed in the measurements where the bright spot is still visible after a camera delay of 500 ns.

When the negative discharge observed in the photographs is indeed a glow the discharge is still different from the negative discharges observed in a point-plane gap because in a point-plane gap a glowing channel is not observed at 1000 mbar. Since in plane-plane gaps

larger than 10 mm no discharge is visible on the camera, it cannot be verified if the 10 mm gap is too small for the discharge to develop and show some structures (cf. streamers in a point-plane gap at 100 mbar) or that the single channel arises because of the fast streamer evolution in a high background field (cf. the positive streamer that is as thick as the cloud while propagating through the gap and evolving to glow, figure 3.5).

Chapter 8

Analysis and synthesis

In this chapter the experimental results discussed in previous chapters are reviewed and compared with other measurements reported in the literature as well as with theory and simulations as far as available. An overall synthesis is presented as far as possible. The results are discussed along the following questions for streamers in a point-plane gap in air:

- 1) What is the streamer diameter?
- 2) What is the streamer velocity?
- 3) How much energy is dissipated?
- 4) When do streamers branch?
- 5) How do streamers depend on the oxygen:nitrogen ratio?
- 6) Do streamers scale with air density or pressure?
- 7) How do streamers start up and propagate?
- 8) What is the electric field and the average electron energy in the streamer head?

8.1 Diameter

Introduction

The question of the streamer diameter has played a classical role in streamer theory. In particular, for a long time, the diameter was not a result of a simulation, but it was used as an input for so-called 1.5D dynamical streamer computations. The first to perform such a calculation were Dawson and Winn [24] who thought 0.06 mm to be reasonable. Later

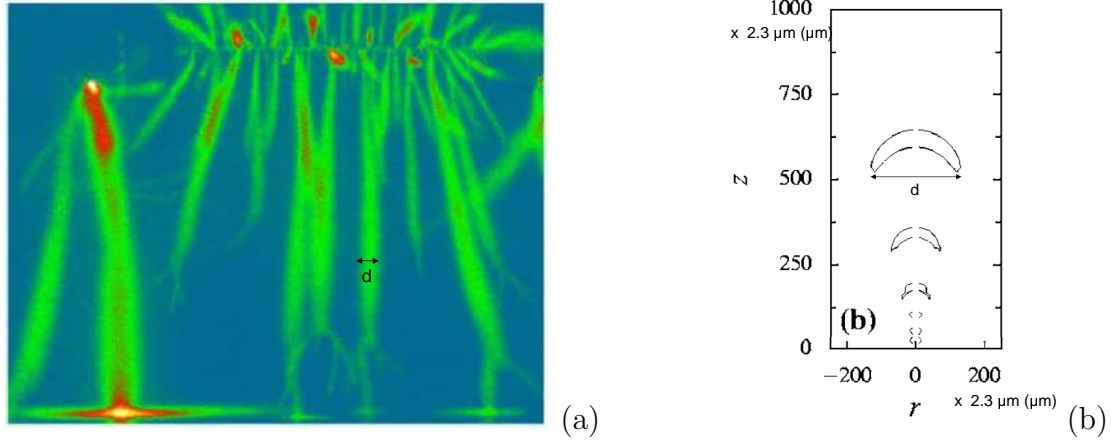


Figure 8.1: (a) Positive streamers in a 40 mm wire-plane gap at 40 kV and 1000 mbar. This picture is taken from Grabowski *et al.* [37]. d is added to the picture to show what in this thesis is meant by the optical diameter as found in experiments. (b) A negative streamer in a homogeneous electric field of 100 kV/cm in air at 1000 mbar. Plotted is the contour of the half maximum of the space charge at different times. The time interval between two consecutive snapshots is $t = 150$ ps. This picture is taken from Luque *et al.* [59]. d is added to the picture to show what in this thesis is meant by the diameter as found in simulations. Note that the simulation is given in dimensionless units. The values at the axes should be multiplied by $2.3 \mu\text{m}$ to obtain the dimensional units at standard pressure and temperature.

a fixed streamer diameter was predicted by minimization arguments by D'yakonov and Kachorovskii [29] and Simakov and Raizer [92] though these arguments seem to violate the physical law of charge conservation [34]. These theoretical approaches were, of course, motivated by experiments where the diameter was found to be (roughly) constant during propagation. However, the diameters reported in literature vary widely. A diameter of 0.04 mm is reported in pure oxygen at 500 mbar in a gap of 10 mm at a voltage of about 11 kV by Bastien and Marode [7]. However, in ambient air, a diameter of 0.2 mm in a wire-plane gap of 35 mm at 30 kV is reported by Creighton *et al.* [19] and a diameter of 0.5 mm in a point-plane gap of 20 mm at 25 kV by Pancheshnyi *et al.* [80]. In larger gaps limited information is available. Blom *et al.* [8; 9] report diameters of 10 mm in a wire-cylinder gap of 290 mm diameter using a voltage pulse of 100 kV at 480 mbar (figure 1.2b).

Already forty years ago, it was shown by Waters and Jones in experiments where a voltage of 270 kV was applied to a 2 m gap that this diameter is not necessarily a fixed value. They report a diameter of up to 20 mm near the anode, that decreases further in the gap to ~ 2 mm [114]. Only recently it was found that also in small gaps the streamer diameter

el. config.	gas	pol.	field (kV/cm)	d_{start} (mm)	d_{end} (mm)	x (mm)	t (ns)	v (mm/ns)	ref.
pl-pl	air	-	$100 \cdot P$	0.1	0.6	15	$0.6 \cdot P$		Luque <i>et al.</i> [59]
		-	$40 \cdot P$	0.1	0.2	15	$5 \cdot P$		
		-			0.7	35	$14 \cdot P$		
p-p	air	+	10 kV/2 cm	0.4	0.8	6	29		Kulikovsky [51]
		+	15 kV/2 cm	0.4	2	5	9		
~p-p or ~pr-p	air	+	a	1	2	8		1	Babaeva and Naidis [6]
		-	a	3	2	8		1.5	
		+	b	1	2.2	8		2.3	
		-	b	2	2.2	8		3	

Table 8.1: *Estimated values of the increase in diameter in air as found in simulations. El. config. = electrode configuration, pol. = streamer polarity, d = diameter, x = propagation distance, t = propagation time, v = velocity, pl-pl = parallel plane, p-p = point-plane, pr-p = protrusion-plane, $P = (p/1 \text{ bar})$, a = 115 kV/cm at sphere with radius 0.1 cm and 15 kV/cm homogeneous background field, b = 115 kV/cm at sphere with radius 0.1 cm and 25 kV/cm homogeneous background field.*

is not fixed. Grabowski *et al.* [37] show a very abrupt change from 4 mm to ≤ 0.5 mm in a wire-plane discharge of 40 mm with short voltage pulses up to 45 kV (figure 8.1a); the thin streamers probably occur after the voltage has collapsed. Winands [119] and Grabowski *et al.* [37] observe that the diameter increases during propagation, although in [37] the effect is less pronounced. Also recent 2D-computations (where the diameter is not an input but a result of the computation) show that in gaps longer than 5 mm the diameter of both positive and negative single streamers can vary between simulations and through the gap. One might conclude that the applied voltage or the background field determine the different outcomes [50; 55; 56; 59; 70; 71; 78], however, it also should be noted that the electron distribution assumed as an initial condition and the boundary conditions on the electrode can play a decisive role for the results, and this is not always discussed carefully. In homogeneous [5; 49; 55; 56; 59; 68; 70; 71; 93] and in inhomogeneous fields [6; 51], the streamers are seen to expand in overvolted gaps, see e.g. figure 8.1b and table 8.1. Diameter values of recent experimental literature are given in tables 8.2 and 8.3.

Note however that in simulations not the width of the space charge density layer should be used but the density profile of the $N_2(C)$ -state when a good comparison with (optical) diameters in experiments is desired.

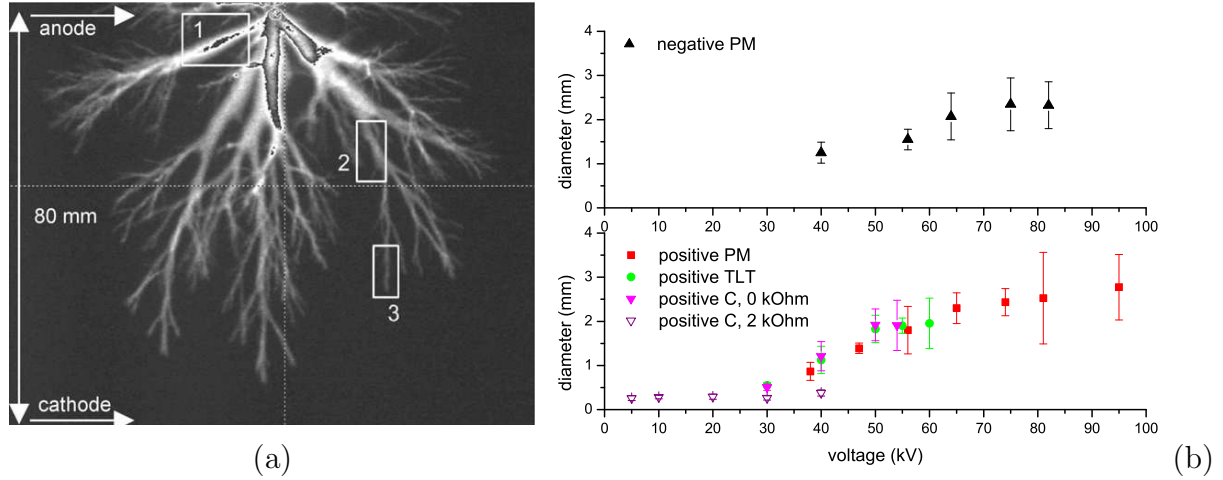


Figure 8.2: a) Positive streamers in an 80 mm gap at 60 kV. This picture is taken from chapter 4. The number of the box corresponds to the number of the streamer type. Late, type 4, streamers are not shown in this picture. b) Diameters of positive and negative streamers in a 40 mm gap. This graph is taken from chapter 7. The streamers obtained in the C-supply with 2 k Ω are also plotted. They show the thinnest possible channels at the respective voltage.

Our results

Diameters of positive streamers in ambient air

Our measurements in an 80 mm point-plane gap have shown that the previously observed extremely large variation of streamer diameters is neither an artifact, nor is there a phase transition between different streamer types. Rather the diameters of positive streamers in atmospheric pressure air can vary by a factor of 10 (!) within a single discharge provided that the gap is long enough (chapter 4). Different streamer regimes are distinguished based on their diameter and their time of occurrence; the three that occur during the initial stage of the discharge are shown in figure 8.2a.

- 1) *Thick streamers* (type 1) are very thick with a diameter of about 2.5 mm, their velocity is over 1 mm/ns and they carry currents with a temporal maximum of up to 12 A. Their current density is about 2.4 A/mm². They are created when $V > 40$ kV and the internal resistance in the discharging circuit is low (< 1 k Ω) so that the voltage rise time is short and the streamers start propagating when the total voltage is applied to the gap. They propagate much longer than thinner streamers before they branch. Whether their diameter is the maximal possible value or whether even thicker streamers can be produced with higher voltages applied, has not been explored yet. It must be noted, however, that one could argue in figure 8.2b that a

diameter saturation sets in above $V \geq 60$ kV.

- 2) *Intermediate streamers* (type 2) have an average diameter of 1.2 mm, a velocity of 0.5 mm/ns and currents of the order of 1 A. Their current density is about 2.4 A/mm². They are created when $V \approx 40$ kV and the resistance is low. They can also be obtained when the resistance is higher (and hence the voltage rise time is longer), but then the saturation voltage has to be increased as well.
- 3) *Minimal streamers* (type 3) are thin; they are called minimal because we never have observed thinner streamers; their diameter is 0.2 mm; their velocity is ~ 0.1 mm/ns and their current ~ 10 mA. Their current density is about 0.5 A/mm². They are created for $5 \text{ kV} \lesssim V < 40 \text{ kV}$ and/or when the internal resistance in the discharging circuit is high and the voltage rise time is long ($\geq 1 \text{ k}\Omega$, $\geq 60 \text{ ns}$, respectively) since then the streamers start in the rising slope of the voltage, thus at a lower voltage than the saturation value. These streamers branch often except when $V \approx V^+$ ($\approx 5 \text{ kV}$ at atmospheric pressure). Then they have trouble crossing the gap at all and hardly branch.
- 4) *Late streamers* (type 4) incept late, they start to propagate after thick or intermediate streamers have crossed the gap. They seem to start at some surface roughness higher up on the anode or somewhere along an existing streamer path; their path largely seems to avoid that of the previous streamers. Their diameter is similar to that of minimal streamers. Their velocity and current could not be determined but it is plausible that they are similar to minimal streamers. Late streamers occasionally connect to the already existing streamer paths of thick or intermediate streamers. Note that these late streamers should not be confused with secondary streamers that propagate along the same path as the primary ones (chapter 3).

Thick and intermediate streamers may branch into thinner ones provided that the gap size is long enough. Minimal streamers branch often but keep their diameter. Occasionally thin streamers are seen to branch off from a thick or intermediate streamer. Then the thick or intermediate streamer usually keeps its diameter. In our point-plane gap, the streamer diameter never increases during propagation, although at high applied voltages the streamer is occasionally observed to be slightly thinner (but within the same regime) near the electrodes (chapter 4). Thick and intermediate streamers extend much further in the gap before they branch than the thinner ones. More information about branching is given in section 8.4.

Diameters of positive and negative streamers in ambient air

The classification above is also applied to streamers in gaps ≤ 40 mm. Such gaps are so short that we do not see a change of diameter, nor of velocity (to be discussed in section 8.2) while the streamer crosses it.

Our measurements indicate that the inception of a negative streamer is determined by a critical voltage V^- , and that this inception voltage is considerably higher than the inception voltage $V^+ \approx 5$ kV of a positive streamer. In our 40 mm point-plane gap at atmospheric pressure air this value is about 40 kV which is around the DC-breakdown voltage of the gap, while the inception voltage of positive streamers lies at about 5 kV (section 8.7.1). Therefore one needs to distinguish two regimes of the applied voltage for streamers created in a 40 mm point-plane gap in air at 1000 mbar as shown in figure 8.2b.

- 1) $V^+ < V < V^-$ (≈ 40 kV): The positive streamers start at $V^+ \approx 5$ kV. Their diameters increase from 0.2 mm at 5 kV to 1 mm at 40 kV, they bridge the complete electrode gap when $V > 20$ kV and they branch. A sign of a negative discharge is only visible above 20 kV as a glowing cloud near the electrode tip; no negative streamers are formed.
- 2) $V > V^-$: Negative streamers appear, but they do not bridge the gap until a voltage of 56 kV is applied. Positive and negative streamers have a similar thickness of 1 mm at 40 kV that increases up to 3 mm for 96 kV.

Another, quite remarkable, observation in figure 8.2b is that the diameter of positive streamers increases by a factor of 10 when the voltage increases only by a factor of two, i.e. from 0.2 mm at 25 kV to 2 mm at 55 kV.

Conclusions

Our results in gaps ≤ 40 mm show that the diameter of positive and negative streamers increases with increasing voltage provided that the voltage rise time is fast enough (≤ 30 ns). The fast rise time assures that the streamers start propagating only after the voltage has reached its saturation value. The observation that the diameter increases continuously with voltage indicates that thin and thick streamers, e.g. the 0.2 mm thin positive streamers at 25 kV in a point-wire gap by Van Veldhuizen and Rutgers [106] and the 2.8 mm thick ones at 77 kV in a wire-plane gap by Winands [119], are related by a continuous transition rather than by an abrupt phase transition between different types of streamers. Negative streamers, however, form only at much higher voltages than positive streamers, but are then quite similar.

gap (mm)	gas	polarity	d (mm)	v (mm/ns)	V (kV)	ref.
40 p-p	air	+	0.2-2.5	0.1-3.5	5-83	chapter 7
		-	1-2.4	1-2.4	40-83	
35 w-p	air	+		0.5(w)-1(w)	20-30	Creyghton [20]
		+		0.2(h)-0.6(h)	20-30	
		+		0.25(p)-0.7(p)	20-30	
57 w-p	air	+	0.7 (w)-1.8 (p)	~ 0.5	57	Winands [119]
		+	0.8 (w)-2.6 (p)	~ 0.7	70	
130 pr-p	N ₂	+	≤ 2 (@ 98 kV)	0.2-0.7	82-123	Yi and Williams [123]
	90%N ₂ :10%O ₂	-	4 (@ 123 kV)	0.6-1.4	82-123	
		+	6	0.8-3.4	82-123	
		-	8	0.8-1.7	82-123	

Table 8.2: Overview of experimentally found diameters and velocities of positive and negative streamers at 1000 mbar. *p-p* = point-plane, *w-p* = wire-plane, *pr-p* = protrusion-plane, (*w*) = at the wire, (*h*) = halfway, (*p*) = at the plane.

Gaps ≥ 80 mm are long enough to observe that thick streamers branch into thinner ones, so that different diameters varying by up to a factor 10 can be seen in different spatial regions of *one* single discharge. One reason for the variety of diameters could be that the thick streamers start in a high background electric field near the tip that decreases further away from the point electrode. This would mean that the streamer diameter would be determined by the background field, which, however, is strongly modified by the streamer itself. Another way to characterize the streamer is by the voltage and the charge content of the streamer tip. While such a theory is appealing (Ebert *et al.* [33]) and strongly motivated by the present results, it is not worked out yet.

Calculations and measurements of the diameter are still difficult to compare as they use different voltage pulse parameters and initial and boundary conditions. A recent attempt by Pancheshnyi *et al.* [80] to compare measurements and calculations for single positive streamers in air shows that this is still not a straightforward task.

8.2 Velocity

Introduction

We now address the propagation velocity of the streamers. Recent experiments and simulations show that streamer velocities in air are in the order of 1 mm/ns [6; 20; 80; 109; 119] (table 8.2, table 8.3). Experiments by Winands [119] in a 57 mm wire-plane gap and voltages between 40-90 kV show that positive streamers are slightly faster than negative ones but they both have typical velocities of ~ 1 mm/ns. He also observes an acceleration near the plate electrode for both polarities. This is also observed by Van Veldhuizen and Rutgers [109] at *both* electrodes in a 25 mm point-plane gap and for voltages of 9 kV in N₂ and 16 kV in air. Investigations on this subject by Creighton [20] in a 35 mm wire-plane gap show that the velocity growth near the plate depends on the applied voltage: at 20 kV almost no increase is observed, while at 30 kV an increase of 0.2 mm/ns near the plate is observed, see table 8.2.

Simulations on velocities of positive and negative streamers are performed by Babaeva and Naidis [6] in a geometry that resembles a gap in which streamers form in the region of strong electric field (115 kV/cm) near a spherical electrode with a radius of 0.1 cm and then propagate in a uniform field between parallel plane electrodes. This uniform electric field can have values of 15, 25 and 35 kV/cm [6], respectively. They observe that negative streamers are faster than positive ones when they have propagated over the same distance (table 8.1). The values, however, are close together. These simulation results can be understood as follows. The streamer velocity is the velocity of the thin ionization front at its tip. This velocity is determined by the local enhanced electric field and by the spatial profile of free electrons in the leading edge of the front. This profile is determined by electron diffusion, background ionization and photoionization. The velocity of the front is the electron drift velocity in the locally enhanced electric field augmented by the nonlocal effects due to the electron density profile in the leading edge. As these nonlocal effects are isotropic, the negative front is always faster than the positive one, if the overall geometry and voltages are the same, as the negative front propagates with the electron drift while the positive one propagates against it. This general argument is substantiated for planar fronts by Ebert *et al.* [30] for fronts in simple gases, but is easily extended along the general mathematical lines as discussed in Ebert *et al.* [31].

The streamer velocity furthermore increases with increasing applied background electric field. That the velocity increases with the background field is also found by simulations in a homogeneous electric field as performed by e.g. Luque *et al.* [59] for negative streamers in N₂ and air and by Kulikovsky [51] for positive streamers in air.

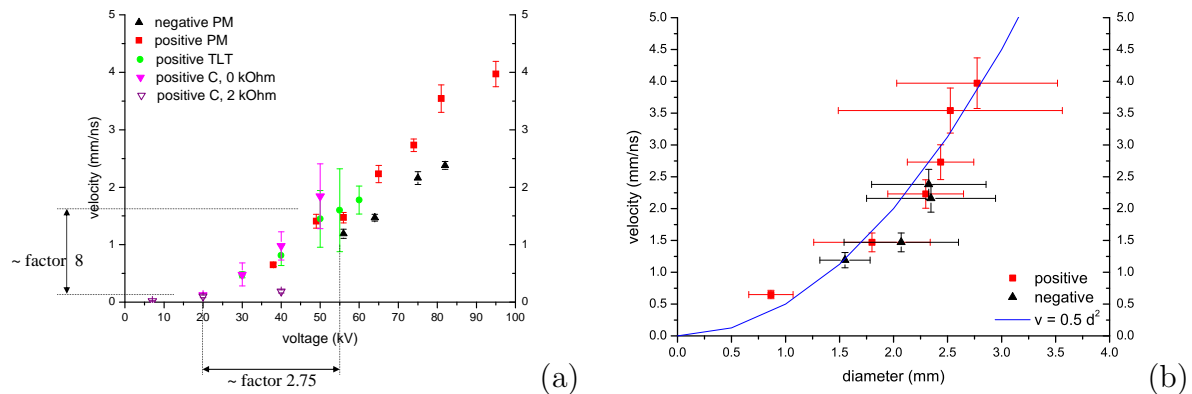


Figure 8.3: a) Velocities of positive and negative streamers in a 40 mm gap in air at 1000 mbar. The streamers obtained in the C-supply with 2 k Ω are intentionally kept slow to show the lowest possible velocity at the respective voltage. b) A fit through the diameter and velocity data obtained with the PM-supply. Both graphs are taken from chapter 7.

Our results

We have measured the velocities of positive and negative streamers in a 40 mm gap since in gaps ≤ 40 mm the velocity is rather constant during propagation when measuring not immediately at the electrodes (cf. the discussion of longer gaps in section 8.1). The velocity of a streamer channel can only be evaluated if they propagate over a certain distance. Therefore, velocities of negative streamers can only be measured when the applied voltage is well above its inception value V^- (section 8.1 and 8.7.1). The results are shown in figure 8.3a. The data shows that the velocity of a positive streamer increases rapidly from 0.1 to 1.5 mm/ns for voltages from 5 to 56 kV while at these voltages no velocities of negative streamers can be measured. At voltages higher than 56 kV, the velocity of the positive streamer increases from 1.5 to 4 mm/ns for voltages from 56 to 96 kV which is about 20% higher than the velocity of the negative streamers that increases from 1.2 to 2.4 mm/ns for voltages from 56 to 83 kV. Both velocities increase with increasing voltage.

In section 8.1 it was observed that thick streamers have higher velocities than thin streamers. This hypothesis is tested by plotting the diameter d and velocity v obtained under similar conditions in figure 8.3b. A fit of $v = 0.5 \cdot d^2 \cdot \text{mm}^{-1} \text{ns}^{-1}$ is drawn through the data points. This rough approximation works quite well to estimate the velocity from a given diameter.

Conclusions

The velocity of positive streamers increases rapidly by a factor of 8, when the voltage increases by a factor of 2.75. Velocities of negative streamers can only be measured well above their inception voltage V^- . Then positive streamers are 20% faster than negative ones which is very surprising in view of the theoretical arguments given above. Velocity and diameter of positive and negative streamers in our measurements are roughly related as $v = 0.5 \cdot d^2 \cdot \text{mm}^{-1} \text{ns}^{-1}$. However, for the minimal streamers with a diameter of 0.2 mm this approximation gives a too low velocity value of 0.02 mm/ns; the velocity of minimal streamers should be ~ 0.1 mm/ns as is given in section 8.1. The approximation is also tested for other experiments of streamers in atmospheric pressure air [80; 106; 109; 119]. The approximation still works quite well for intermediate diameters as found in Winands [119]. The velocities of the thin streamers in [80; 106; 109] are also overestimated by the approximation.

Finally, we speculate that the following mechanism might explain the observed dependence of the streamer velocity on its diameter. Suppose that photoionization and/or background ionization supply electrons for local avalanches in all regions where the electric is sufficiently high. Then the electron density profile in the leading edge of the ionization front is largely influenced by the profile of the electric field. The electric field is created predominantly by a thin space charge layer that screens the field from the interior and enhances it ahead of it. This field enhancement decays approximately like R^2/r^2 where R is the local radius of curvature of the space charge layer and $r - R$ is the distance from the layer. Therefore the electron density profile will also decay roughly like $1/R^2$. As the electron density profile in a pulled front can dominate the velocity [30; 31; 53], a larger streamer radius can create higher velocities. Whether this mechanism actually can lead to velocities that increase like the square of the diameter for realistic values of photo and background ionization, will be a matter of future investigation.

8.3 Dissipated energy

Introduction

A third quantity that can be monitored during experiments is the amount of energy that is dissipated by the discharge. This energy can be used to create e.g. radicals for gas and water cleaning, Winands [119], Grabowski [40]. Measurements in air in wire-plane gaps of 32 to 77 mm for voltages of 40 to 90 kV performed by Winands [119] (also table 8.2) show that the energy efficiency transfer from their power supply into the streamers is about 70% to 80% at 40 to 70 kV for positive streamers while it is 20% to 60% at 60 to 80 kV for

negative ones. These results indicate that the energy efficiency transfer becomes similar for positive and negative streamers with increasing voltage, hence the energy dissipated by positive and negative streamers becomes more similar.

The energy that is dissipated by the streamer can heat up the gas inside the streamer and inside the complete vacuum vessel. However, in literature the gas temperature for a pulsed discharge is found to be around 300-350 K from rotational spectra, so it remains close to room temperature [20; 104].

Our results

We have measured the dissipated energy for positive and negative streamers in a 40 mm gap in air. These results are given in figure 8.4. They show that primary positive and negative streamers dissipate the same amount of energy of 20-50 mJ at voltages of 74-90 kV (chapter 7). This is in agreement with observations by Winands [119] that the energy efficiency transfer becomes similar for both polarities. The maximum increase in gas temperature inside the streamer can be estimated from the dissipated energy. Hereby it is assumed that *all* energy will be used to heat the streamer channel whereas in reality the main part of the energy is used for chemical processes [119]. Therefore, an upper limit of the temperature increase inside the streamer channel is calculated below. For a discharge at 90 kV in a 40 mm gap which consists of 10 streamers with a diameter of ~ 3 mm and a total primary streamer energy of 50 mJ (hence 5 mJ/streamer channel), the maximum increase in temperature in one channel is estimated to be ~ 13 K by

$$\Delta T = Q/C, \quad (8.1)$$

in which ΔT is the increase in temperature, Q the dissipated energy and C the specific heat capacity which is 10^3 J/kg·K for air. Thus the gas temperature inside our streamers remains indeed close to room temperature. The gas temperature inside a glowing channel can increase considerably since the duration of such a glow regime, e.g. as shown in figure 7.15b, is very long (~ 20 μ s). An estimate of the temperature of the glowing channel can be made when a channel diameter of 3 mm is assumed with an energy of ~ 10 mJ. This gives an upper limit of the heating of the glowing channel of ~ 340 K which is $30\times$ more than the maximum heating of a thick primary streamer.

Conclusions

Our results show that the energy of the primary positive and negative streamers is similar and increases with voltage above a critical value. Furthermore the data leads to the conclusion that the gas temperature rise within a primary streamer channel is negligible.

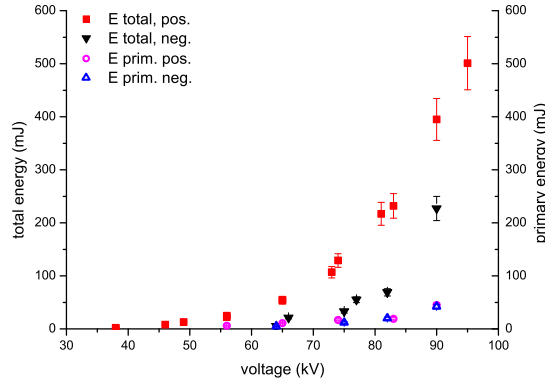


Figure 8.4: *Dissipated streamer energy in a 40 mm gap in air at 1000 mbar. This graph is taken from chapter 7.*

8.4 Branching and multiple streamers

Introduction

The photographs show that streamers branch frequently. This topic is underexposed in literature. Most simulations investigate only one non-branching streamer [6; 80]. Investigations of branching streamers [5; 33; 51; 59; 68] have to stop at the moment of branching since then the numerically implemented cylindrical symmetry (allowing essentially 2D simulations) at that moment becomes non-physical. While branching streamers were observed in simulations earlier, they were typically thought to be numerical artifacts and not published. Therefore the observation of streamer branching by Ebert's group in a minimal fluid model [5; 33; 59; 68] was not immediately accepted [5; 32; 52]. Of course, such an effect cannot be established on the basis of mere numerical simulations, but nonlinear analysis and the mathematical similarity with tip splitting events in two fluid flow [5; 66] clearly indicate that streamers branch even in fluid models.

Another point of interest is that only now the first theoretical studies of several streamers propagating next to each other are being submitted [60; 61]. These studies show how strongly streamers can interact electrostatically and through photoionization. They indicate that a group of streamers can have quite different characteristics than a single streamer.

The experimental literature also pays little attention to streamer branching. Only Yi and Williams [123] observe in atmospheric pressure nitrogen that positive streamers branch after ~ 3 mm, while the mean branching distance for negative ones is ~ 10 mm. This indicates that positive streamers branch more than negative streamers. Additions of small amounts of O_2 reduce the branching rate. Simulations based on fluid theory by Luque *et al.*

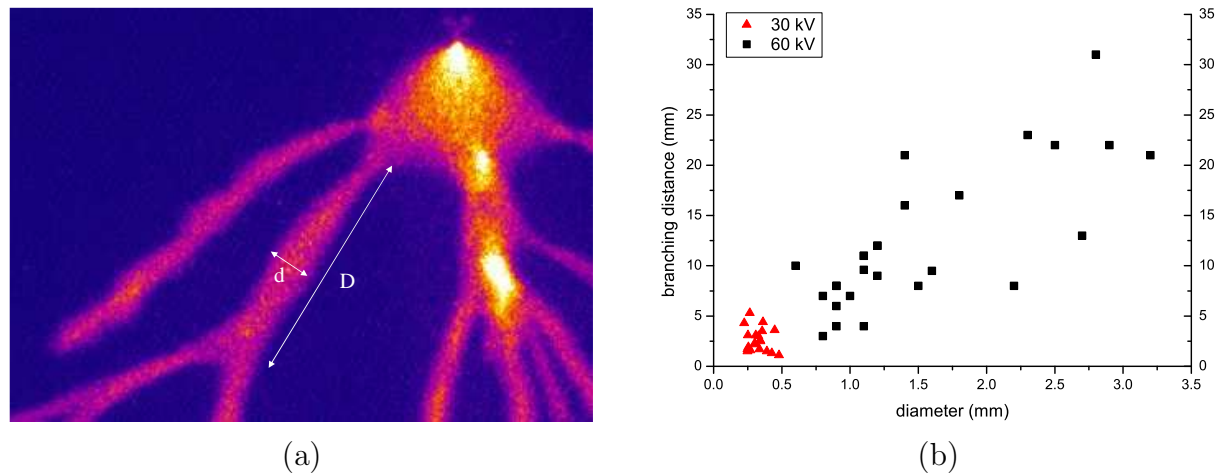


Figure 8.5: a) Definition of the branching structure D/d . b) The distance between branches as function of the voltage in an 80 mm gap in 1000 mbar air. This graph is taken from chapter 6.

[59] show that photoionization (that is strong in oxygen:nitrogen mixtures like air) makes a negative streamer smoother and can suppress branching. However, this effect should also be reinvestigated within a particle model [54] with its inherent particle density fluctuations.

Our results

Our measurements in air show that positive streamers branch more than negative ones (chapter 7). Furthermore, measurements on the thinnest positive streamers in air and nitrogen¹ show that streamers in N_2 branch more frequently (e.g. roughly every 4 to 5 mm at 400 mbar and 16 kV, figure 6.13b) than streamers in air (roughly every 12 to 13 mm, idem). Over the pressure range of 100-1000 mbar the branching structure, as defined by the ratio D/d in figure 8.5a, is independent of pressure and is found to be 11.6 ± 1.5 for air and 9.1 ± 3.3 for N_2 .

The measurements on streamers in N_2 and air also show that the streamer head in N_2 is more diffuse than the streamer head in air as is shown in figure 8.6 (chapter 6). The distance of the tip over which the intensity drops to 50% of its maximum is measured to be ~ 4 times longer in N_2 . This observation in relation with the knowledge that streamers in N_2 branch more may indicate that a stable front results in less branching.

¹The purity of the nitrogen in this thesis is 99.9%. The impurities are expected to be mainly water and oxygen. At the time that the measurements were performed the purity was expected to be 99.999%.

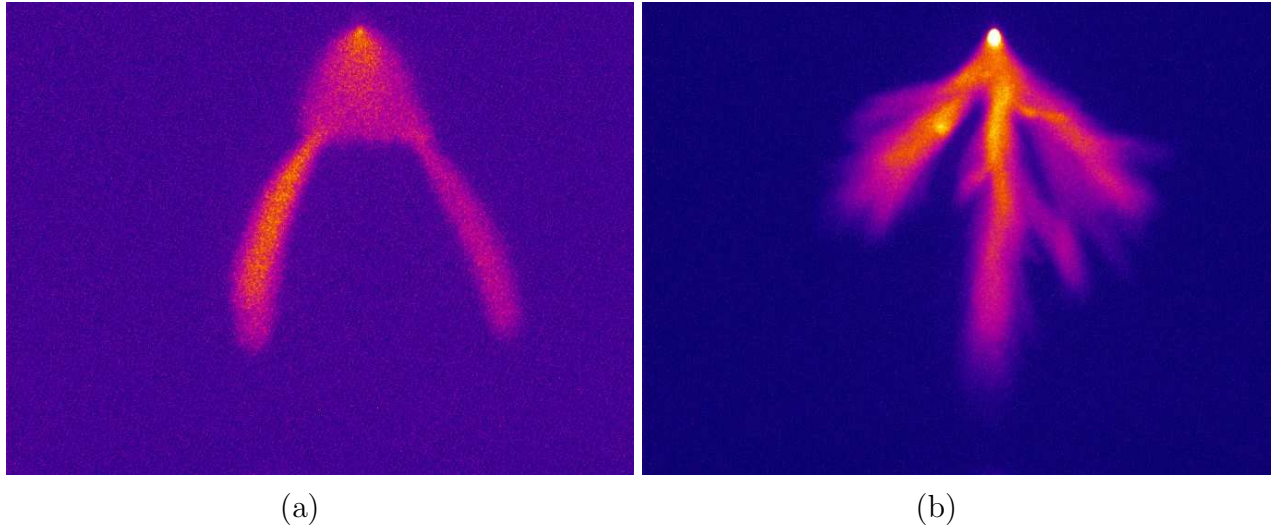


Figure 8.6: *Streamers in a 40 mm gap at 100 mbar in a) air, 5 kV and b) N_2 , 15 kV. Camera delay is 0, the exposure time and pulse frequency are: a) $0.7 \mu s$, 1 Hz and b) $0.37 \mu s$, 10 Hz. These photographs are taken from chapter 6.*

Figure 8.2a shows that thick streamers can branch into thinner ones. Another observation is that thick channels branch less than thin channels. These observations are investigated in detail in chapter 6. The data indeed shows that the distance between branches D increases with increasing diameter d , figure 8.5b. However, when the branching parameter, i.e. ratio D/d , is calculated for thick positive streamers at voltages higher than 30 kV in atmospheric pressure air a value of 7.6 ± 3.6 is found while for thin streamers at voltages below 10 kV a value of 11.6 ± 1.5 is found. These results indicate that although thick streamers branch further away from the previous branch than thinner ones, they propagate over a shorter distance with respect to their diameter before branching.

Other observations that are done concerning branching include that streamer channels almost always seem to branch in two: one main channel that propagates further and one channel that bends away from this channel. This observation is more pronounced in N_2 than in air. Occasionally branching in three channels is seen e.g. in the white circle in figure 8.7. Furthermore, branching seems not to start directly at the needle: the main channel first propagates a certain distance before it branches or the streamers emerge from a cloud (figure 5.2).

A last observation is that the angle between streamer branches often appears to be approximately 30° . Of course, this angle is subject to projection onto the 2D image plane, and it is further examined at present by means of stereophotography.

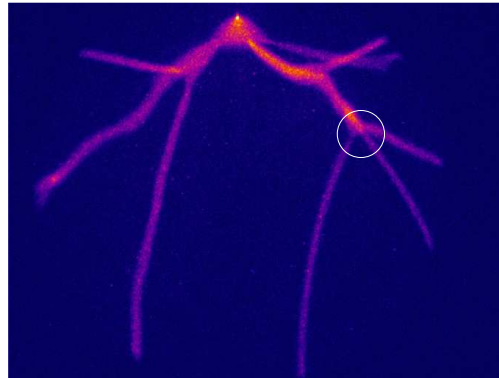


Figure 8.7: *Positive streamers in a 160 mm gap in air at 62.5 mbar, 5 kV, 1 Hz, 0 ns delay and 70 μ s exposure time (settings of table 6.1).*

Conclusions

The branching structure D/d of streamers appears to scale over the pressure range of 100 to 1000 mbar; it gives a value of 11.6 ± 1.5 for thin streamers in air and 9.1 ± 3.3 for thin streamers in nitrogen. A decrease in oxygen concentration increases the branching rate when parameters such as pressure, voltage, gap distance and streamer diameter have the same value, as is observed in our experiments. Most likely the branching rate increases when the rate of photoionization in the gas decreases.

A possible explanation for the observation that thick streamers branch less than thin ones can be as follows. Since the electric field in front of a thick streamer decays less fast than the field in front of a thin streamer, the electron density in the direction of propagation decreases less rapidly for a thick streamer, if the electron profile due to background or photoionization is dominated by the profile of the electric field in the leading edge of the front. This would stabilize thick streamers and suppress branching.

8.5 Streamer dependence on the oxygen:nitrogen ratio

Introduction

Ambient air is a frequently used gas in experiments since it is most commonly found in nature and used in most applications. A complication of air is that it is a compound gas in which many processes can occur such as photoionization and attachment; where it also

should be noted that there is recently a serious concern about commonly used parameters for photoionization. For understanding the physical mechanisms and for comparing with a simple theory with a decent number of reactions it is useful to perform experiments in simple gases as well. Therefore, measurements are done in nitrogen which, besides being the main component of air, is a simple single molecular gas in which photoionization or attachment is suppressed. However, experiments can never obtain 100% gas purity. Therefore, always some impurities will be present in the gas that may influence the streamer behavior.

Up to now, there is only one set of experiments [123] (also table 8.2, 8.3) where the nitrogen:oxygen ratio was varied systematically. These experiments in a 130 mm protrusion-plane gap show that in a voltage range of 82 to 123 kV, the velocity of positive and negative streamers at 1000 mbar increases when 10% oxygen is added to rather pure N_2 . The increase in velocity is more pronounced for positive streamers (roughly a factor 3) than for negative ones (\sim factor 1.2). Furthermore, they observe that the diameter increases and the number of streamers reduces with increasing oxygen concentration. Van Veldhuizen and Rutgers [109] also observe an increase in velocity with increasing oxygen concentration for positive streamers in a 25 mm point-plane gap for voltages between 3 and 30 kV at atmospheric pressure. They observe an average velocity of 0.012 mm/ns at 9 kV for N_2 and 0.2 mm/ns at 16 kV for air [109]. Their velocity of 0.2 mm/ns is found for positive streamers with a diameter of \sim 0.2 mm at 1000 mbar [106].

Van Veldhuizen and Rutgers [109] furthermore observe that streamers in N_2 need a lower voltage to transit a 25 mm point-plane gap compared to air (\sim 7 kV and \sim 9 kV, respectively). The applied voltage divided by the maximal streamer length has the dimension of an electric field and in the literature this empirical quantity is called the "stability field". Van Veldhuizen and Rutgers [109] as well as our own experiments (section 8.7.2) indicate that this stability field is lower in nitrogen than in air. Raizer [90] suggests that this effect is related to the lack of electron attachment in nitrogen. Since electrons are removed by the attachment in electronegative gases, higher energies and electric fields are necessary to free the attached electrons from the O_2 molecules and to obtain the same amount of free electrons as in an electropositive gas. Van Veldhuizen and Rutgers [109] also report that the breakdown voltage at which the streamers transit into sparks occurs at lower voltages in N_2 (9 kV for N_2 and 27 kV for air at 1000 mbar in a 25 mm point-plane gap). The value for air is similar to our observation in a 20 mm gap where sparking occurs at 27 kV (not shown in this thesis). The stability field will be further discussed in section 8.7.2.

gap (mm)	type	gas	p (mbar)	d (mm)	v (mm/ns)	V (kV)	ref.
160 p-p	3	air	1000	~ 0.3 (@ 5-40 kV)*	0.1-0.2	30-50	chapter 6
	2,3	air	400	0.8-1.7 (@ 10-25 kV)*	0.15-0.27	20-40	
	3	N ₂	1000	~ 0.2 (@ 15-28 kV)*	0.02-0.05	20-40	
	2,3	N ₂	400	0.5-0.7 (@ 8-10 kV)*	0.08-0.35	10-40	
	2,3	a	400		0.05-0.27	10-30	
25 p-p	3	air	1000	0.2 [106] (pr-p, p-w)	0.2	16	Van Veldhuizen and Rutgers [109]
		N ₂	1000		0.012	9	
130 pr-p	1	b	1000	6 ≤ 2 (@ 98 kV)	0.8-3.4	82-123	Yi and Williams [123]
	1	N ₂	1000		0.2-0.7	82-123	
	1	N ₂	400		4	98	
30 pr-p	3	c	1000	0.5	0.4	22	Pancheshnyi <i>et al.</i> [80]
	2	c	455	2.5	1.4	22	
-	1	air	0.1	60-145 m			Gerken <i>et al.</i> [35]
	3	air	0.01	20-50 m			
-		air			0.2- ≥ 30		Moudry <i>et al.</i> [72]

Table 8.3: Overview of positive streamers in N₂ and air. *a* indicates 99.8%N₂:0.2%O₂, *b* indicates 90%N₂:10%O₂ and *c* indicates 80%N₂:20%O₂ (= synthetic air). p is the pressure, d the diameter, v the velocity and V the applied voltage. *p-p* = point-plane, *p-w* = point-wire and *pr-p* = protrusion-plane gap. The values indicated by * are from measurements in a 40 mm gap.

Our results

Our positive streamers in air and N₂ (99.9% purity) have different structures as is illustrated in figure 8.8 (chapter 6). The differences are summarized as follows: the streamers in N₂ are 1) thinner, 2) curlier, 3) more intense and 4) less diffuse than streamers in air. They also 5) branch more resulting in 6) a shorter distance between branching events and 7) they propagate further down the electrode gap at the same applied voltage. The branches that deviate from the main channel, however, 8) die out after a shorter distance. 9) The voltage at which sparking occurs is lower for N₂. Furthermore, 10) the current pulse duration in N₂ is longer than in air, which leads to an easier transition into the spark phase. At 1000 mbar, the difference in current pulse duration is a factor $\sim 30^2$. The streamer propagation time in both gases is roughly similar therefore this difference is ascribed to the "glow"

²This factor however depends strongly on the power supply; when very short pulses are used the glow regime may not arise.

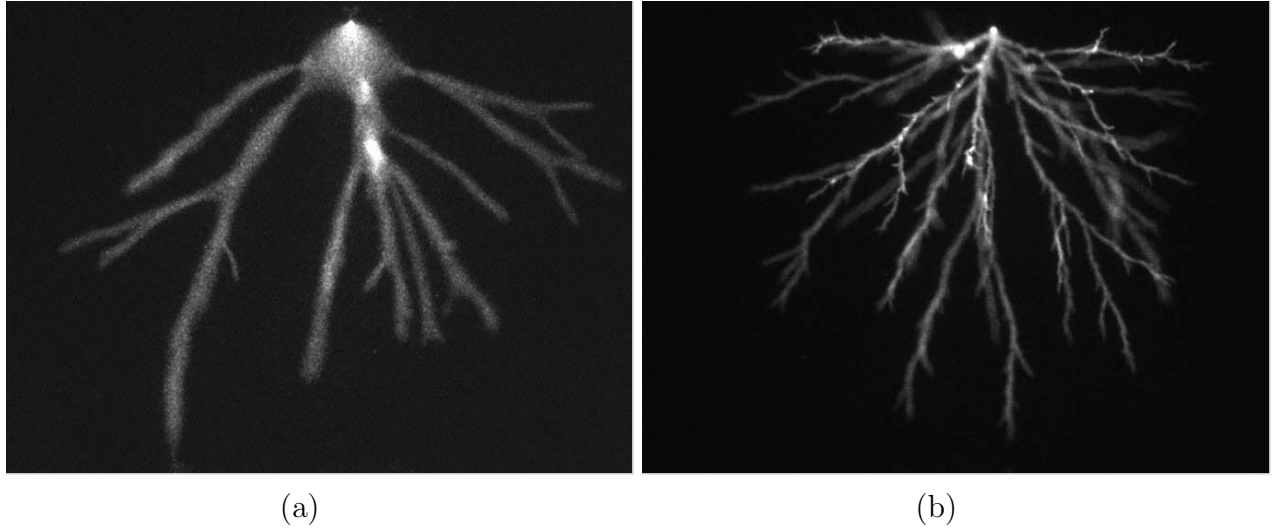


Figure 8.8: *Streamers in a 40 mm gap at 400 mbar and 16 kV in a) air and b) N₂. Camera delay is 0, exposure time is a) 0.6 μ s and b) 2 μ s. These pictures are taken from chapter 6.*

regime which is easier to obtain in N₂ because of the absence of attachment. Therefore, the factor will decrease when in air also a glow regime is found. This occurs mainly at low pressures. A current pulse duration of $> 15 \mu$ s, as found in N₂ at 1000 mbar, is found in air only at a low pressure of 100 mbar and 8 kV.

The diameter and velocity of streamers in air and N₂ increase with decreasing pressure when evaluations are done at a fixed voltage, as will be explained in the next section 8.6 on the dependence on gas density. This is also observed in data for synthetic air (80% N₂: 20% O₂) by Pancheshnyi *et al.* [80]. At 1000 mbar we observe that the velocity in our thinnest streamers increases by a factor 2 to 5 when air is used instead of N₂. However, at 400 mbar we do not observe a difference in the velocity of streamers in air and N₂; the velocity is similar within the error margins (table 8.3, figure 6.11 and 6.12). Why this is so is unknown and other measurements performed at 400 mbar in air and N₂ have not been found in the literature.

The diameter d , ratio D/d and velocity v as function of pressure for air and N₂ are given below in section 8.6 "scaling with gas density or pressure".

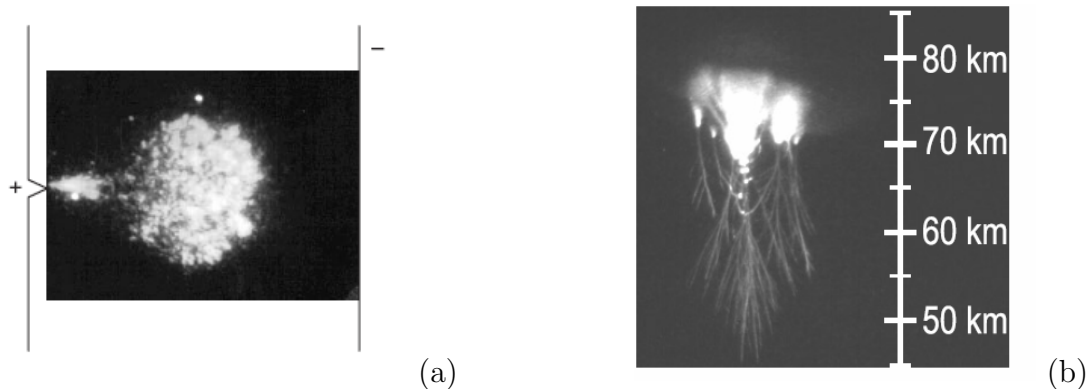


Figure 8.9: a) *Positive streamers in a 130 mm gap in pure N_2 . The picture is taken from Yi and Williams [123].* b) *Example of a sprite discharge. This picture is taken from Cummer et al. [22].*

Conclusions

The question whether the photoionization characteristic for air or other oxygen:nitrogen mixtures is mandatory for the propagation of positive streamers cannot be answered. We as well as other authors [63; 109; 123] observe positive streamers in N_2 . But whether they propagate due to a minor contamination (as experimental nitrogen is never 100% pure) that creates some minor amount of photoionization, or due to other processes, such as cosmic particles or radioactivity, cannot be decided on the basis of the present experiments.

Our observations have shown that the streamers in nitrogen with $\sim 0.1\%$ impurities behave very differently than streamers in ambient air. Some of the characteristics can be explained by photoionization (e.g. branching), others by attachment (e.g. the lower stability field and lower sparking voltage in N_2). Experiments performed by Brandenburg *et al.* [10] in a diffuse barrier discharge with an interelectrode gap of 1.1 mm at atmospheric pressure nitrogen (99.999% pure) with small admixtures of oxygen have shown that the homogeneous glow regime shows a transition into the filamentary mode at an oxygen concentration of about 450 ppm. At higher admixtures of about 1000 ppm, micro-discharges are generated. When these observations are used as a rough estimate for streamer experiments, a nitrogen purity of at least 99.95% is necessary to neglect the contribution of oxygen.

We finally remark that figure 8.9a by Yi and Williams [123] shows a discharge in N_2 that appears more like a cloud than as single streamers. This discharge is very different from our discharge in N_2 , e.g. figure 8.8. We could not reproduce the cloud, possibly due to the 0.1% contamination in our N_2 .

8.6 Scaling with gas density or pressure

Introduction

High altitude discharge phenomena (40-90 km altitude) have become a subject of study since their discovery in 1989, see e.g. Sentman *et al.* [97] and Pasko *et al.* [83]. These transient luminous events are referred to as sprites, elves, blue jets etc. Sprites, in particular, are thought to be a type of streamer discharge and their diameter, which ranges from 20 to 150 m [35], corresponds to the much lower gas density at high altitudes. This scaling with air density follows simply from the fact that the basic length scale of the discharge is set by the mean free path of the electron between collisions with neutral molecules, and that the mean free path is inversely proportional to the gas density [33]. This relates experiments at low or high density to each other, e.g. Pasko *et al.* [82; 84]. The results are somewhat modified by photoionization [55; 59; 126]. As the gas density according to the ideal gas law is proportional to the ratio of pressure over temperature, and as the temperature is fixed to around 20°C during our experiments, we will discuss scaling with pressure rather than scaling with density since pressure is directly measured.

Observations used for comparing sprites (e.g. figure 8.9b) with laboratory scale streamers are done in the tendril region³ of the sprite since this region consists of densely-packed branching streamers, Gerken *et al.* [35]. They observe that there are thick and thin sprite channels. The transverse scale of filamentary structures shown in figure 1.5b by Gerken *et al.* [35] ranges from 60 to 145 m (± 12 m) in the altitude range of 60-64 km (± 4.5 km) which is at an estimated pressure of ~ 0.1 mbar and a temperature of 2°C. This gives a scaled diameter of ~ 6 mm·bar at laboratory conditions which is considerably thicker than our thickest streamers. Minimal sprite diameters are found with transverse extents of 20-50 m (± 13 m) in the altitude range 76-80 km (± 5 km). This is at an estimated pressure of $\sim 10^{-2}$ mbar and temperature of -83°C giving a scaled diameter at 20° of 0.1-0.3 mm·bar. However it must be noted that the pressure is an estimate and therefore this scaled diameter can vary considerably. Downward tendril development of sprites occurs at velocities that vary by more than two orders of magnitude, ranging from ~ 0.1 mm/ns to ≥ 30 mm/ns as was observed by Moudry *et al.* [72]. The tendrils progress through multiple velocity regimes, typically in the order fast-slow or slow-fast-slow. The minimal velocity of sprites is similar to the minimal streamer velocity of ~ 0.2 mm/ns in air. However, it is unknown if this minimal sprite velocity is observed for minimal sprite diameters as occurs in streamers. When the observations by Gerken *et al.* [35] are combined with observations by Cummer [23] it appears that the sprites generally have velocities of the order of 10

³The tendril region is the bottom part of the sprite; the region around the white box, between 50-80 km altitude in figure 1.5.

mm/ns at the altitude where the minimal sprite diameters are observed.

Our results

The similarity law that states that all lengths and times scale inversely with pressure is tested experimentally for the minimal positive streamers in the pressure range from 13 to 1000 mbar in gaps of 10 to 160 mm (chapter 6). We have chosen to test the minimal streamers for several reasons. First, since there is a distribution of diameters for the thicker streamers, only the minimal ones at each pressure are appropriate to compare. Second, the minimal streamers are furthest away from the electrodes that might break the scaling laws locally, cf. chapter 2. Third, these streamers do not evolve into glow and/or spark as easily at low pressures and in small gaps as the thick streamers, and therefore they can be imaged more easily.

We have observed that the diameter d scales inversely with pressure p resulting in an $p \cdot d = 0.20 \pm 0.02$ mm·bar in air and $p \cdot d = 0.12 \pm 0.02$ mm·bar in N_2 at room temperature (293 K) as is shown in figure 8.10a. The velocity v was expected to remain constant with pressure since the scaling law states that both time and distance are inversely proportional to pressure. We, however, observed that the velocity increases slightly with decreasing p , see e.g. figure 8.10b or table 8.3. Here it must be noted that v is determined from thin and thick streamers since under some conditions (especially at low pressures) no minimal streamers could be found because the voltage could not be lowered enough. Although the results show that v increases with p all values lie within a band of $v \approx 0.2 \pm 0.1$ mm/ns over the whole pressure range. This "average" velocity is much smaller than the velocity for the very thick streamers ($v \geq 1$ mm/ns). Therefore, a velocity of 0.2 mm/ns for thin streamers in air over the whole pressure range can be used as a first approximation. The velocity difference with pressure within N_2 is larger, therefore an estimate of the "average" velocity does not seem to be appropriate.

The dependence of the branching parameter D/d on pressure is tested in a 40 mm gap over the pressure range from 100 to 1000 mbar, where D is the distance between branching events and d is the diameter (figure 8.5a). A ratio of $D/d = 11.6 \pm 1.5$ for air and $D/d = 9.1 \pm 3.3$ for N_2 is found. These values indicate that the relative distance between branching events in air is larger when the diameters in air and N_2 are the same.

Measurements in a plane-plane gap where the discharge is triggered by a laser (chapter 7) have shown that positive and negative discharges in air and N_2 can only be created in a small band around 20 ± 5 kV/(cm·bar) of reduced electric field.

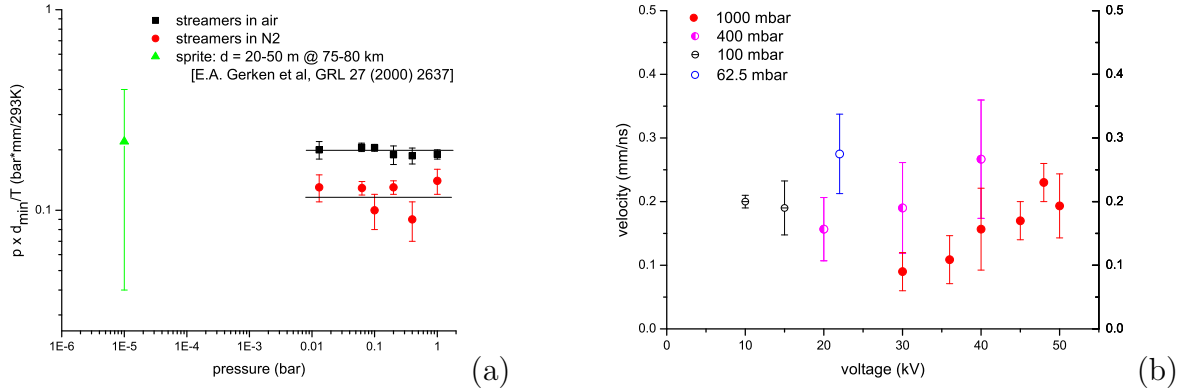


Figure 8.10: a) Scaling with pressure of streamer diameter in air and N₂. b) Velocity of thick and thin streamers in a 160 mm gap at different pressures in air. Both graphs are taken from chapter 6.

Conclusions

Our measurements have shown that the theoretically predicted approximate scaling with pressure of the streamer diameter and velocity agree with experiments. It even holds for positive streamers in air of up to 1 bar while photoionization is expected to lead to corrections to scaling above ≈ 0.1 bar. A quite remarkable observation is that the laboratory data on the minimal streamer diameter even coincides with the minimal diameter observed in sprites when the sprite data is calculated back to a temperature of 20°C, as shown in figure 8.10a. Streamer and sprite velocities, however, seem to vary generally by a factor ~ 10 . However, the trend that thick streamers have higher velocities is also observed for sprites since diameters in sprites are usually larger than in laboratory streamers and velocities also. Although it is assumed that sprites are an upscaled version of streamers (e.g. Pasko *et al.* [82; 84]), it must be noted that the background ionization at sprite altitude is much higher than in the laboratory due to the higher cosmic radiation rate; a term that is not found back in the scaling law. Furthermore, streamers are created between electrodes while in the atmosphere electrodes are absent. When one assumes that structures like clouds function as electrodes, then these electrodes will probably give a more homogeneous electric field than our point-plane gap.

Scaling with pressure in air is allowed, as mentioned above and observed in chapter 6. Scaling with pressure in N₂ must be handled with care since the averaged $p \cdot d$ -line is just outside the error margins, especially the value at 400 mbar (figure 8.10a). Furthermore,

the velocity of streamers in N_2 depends more on pressure than the velocity of streamers in air.

Values of the branching parameter D/d as function of pressure are not reported in literature. Yi and Williams [123] report an average branching distance of 3 mm for positive streamers in N_2 at 1000 mbar with a diameter of about 2 mm at 98 kV. This gives an D/d of 1.5 which is in qualitative agreement with our observation that the ratio D/d decreases with increasing voltage at a fixed pressure (chapter 6).

8.7 Start and propagation of streamers

8.7.1 The start of positive and negative streamers

Introduction

A streamer starts always from an initial seed of ionization that eventually develops its own field enhancement (see also chapter 2). The initial seed is typically built up by an ionization avalanche: free electrons propagate through a sufficiently strong electric field where they gain sufficient energy to ionize molecules by impact. If the field is so high that the ionization rate is higher than the lost rate due to attachment or recombination, an electron avalanche is created, as was first described by Townsend [69; 91; 101; 104]. The avalanche can form either in free space between the electrodes or in the high field zone next to a strongly curved electrode where processes on the electrode surface also can play a role. The question rises how the streamer start looks in experiments. This is a question that to our knowledge has not yet been investigated, most likely since it requires an intensified CCD-camera with short exposure times down to several nanoseconds which have just become available at the end of the last century.

The inception voltage is investigated by Van Veldhuizen and Rutgers [109] in a 25 mm point-plane gap at 1 bar for positive streamers in air and N_2 . They observe that this voltage is ~ 5.5 -6 kV for both gases. They were not able to create negative streamers in their setup; the negative discharge appeared more as a cloud near the tip without any channels [107]. This is in agreement with Raizer [90] who argues that the applied electric field must be higher to ignite negative streamers. Also Yi and Williams [123] observe that negative streamers propagate less far in the electrode gap than positive streamers (~ 60 mm at 123 kV for negative streamers and at least 130 mm at 82 kV, their lowest obtained voltage, for positive ones).

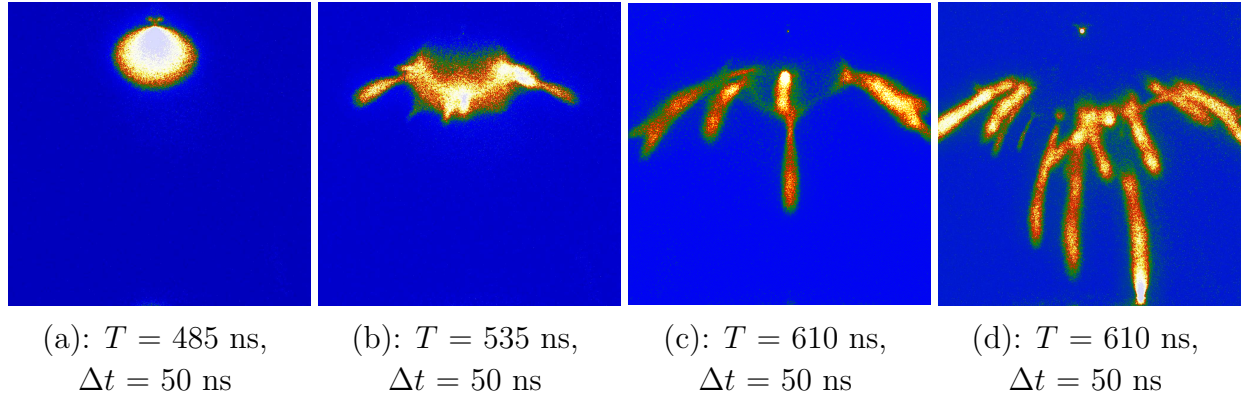


Figure 8.11: *The start and propagation of a positive streamer in a 40 mm gap at 400 mbar and 25 kV in ambient air. Setting c in table 3.1. The camera's delay T and exposure time Δt are given. These pictures are taken from chapter 3.*

Our results

The positive (cathode directed) and negative (anode directed) primary streamer evolution consists of four stages as shown in figure 8.11 (chapter 3 and 7):

- 1) a light emitting cloud at the electrode tip that evolves into
- 2) a thin expanding shell from which
- 3) one or more streamers emerge that
- 4) propagate towards the plate electrode.

This process occurs for positive streamers when $V \geq V^+$, which is around 5 kV at 1000 mbar in our 40 mm point-plane gap. The negative streamer propagation needs a higher voltage V^- of about 40 kV (which happens to be about the DC-breakdown voltage in our 40 mm point-plane gap at 1 bar) to proceed beyond the expanding shell (stage 2) as shown in figure 8.12. When the inception voltage V^- for negative streamers is related to the DC-breakdown voltage, this would imply that the formation of negative streamers depends on the interelectrode distance while for positive streamers the electric field at the electrode tip is dominant and the position of the plate electrode has not much influence.

When looking at the discharge by eye rather than by iCCD-camera, the streamers appear to come from the outer edge of the shell and not from its interior as shown in figure 8.13. This, however, is difficult to observe on 2 dimensional iCCD-photographs, maybe 3D-reconstructions can give an answer.

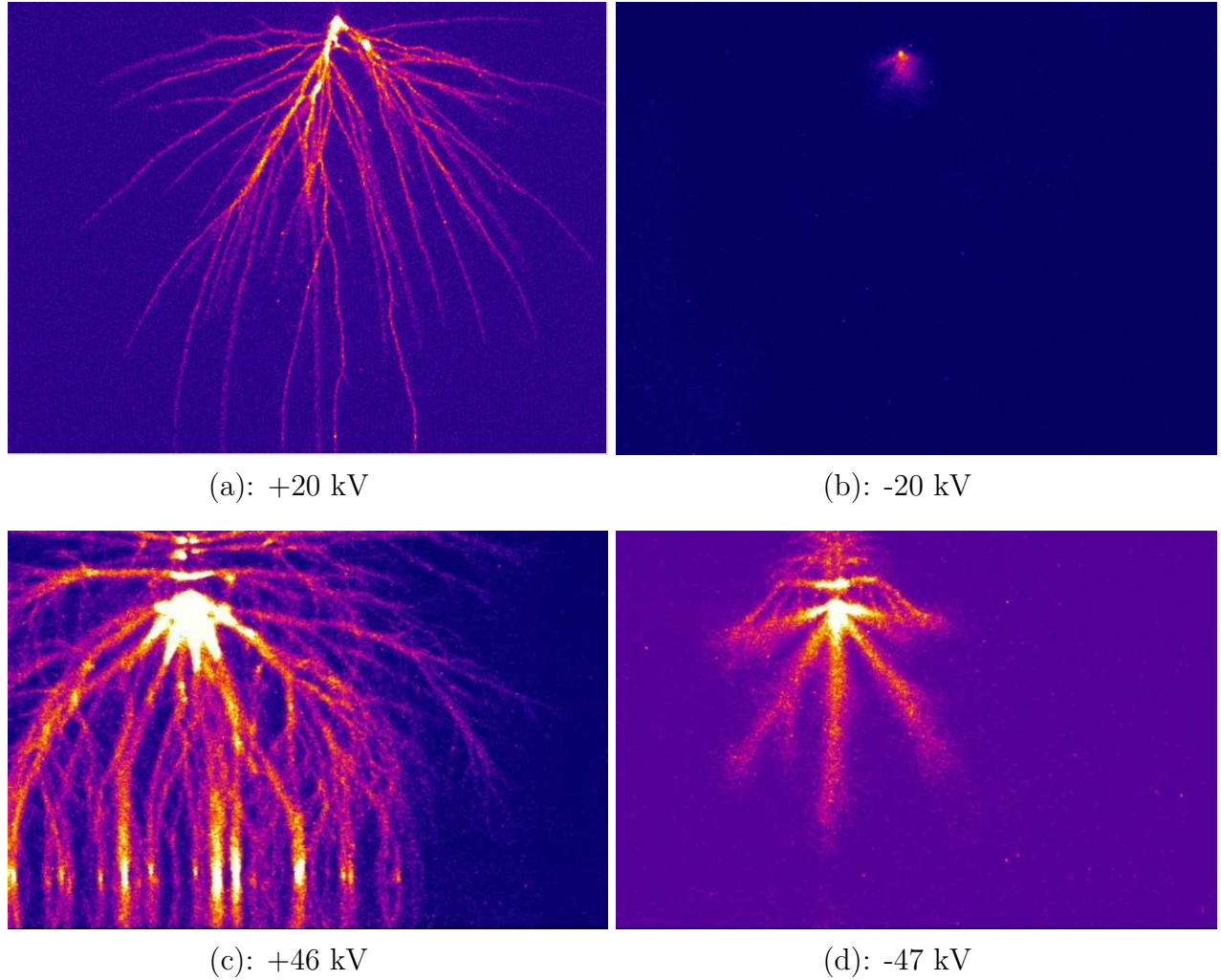


Figure 8.12: *Time integrated photographs of positive (left) and negative (right) streamers in a 40 mm gap in air at 1000 mbar. The delay is 0 ns, the exposure time and supply are a) 1 μ s, C-SC-supply with $R_2 = 2$ k Ω , b) 100 μ s, C-SG-supply with $R_2 = 2$ k Ω and c,d) 160 ns with the PM-supply. These pictures are taken from chapter 7.*

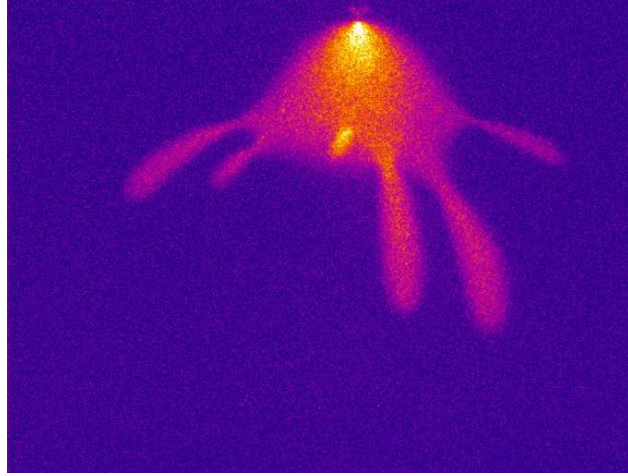


Figure 8.13: *Positive streamers in a 40 mm gap in air at 200 mbar, 10 kV, 0 ns delay and 0.8 μ s exposure time (settings of table 3.1).*

8.7.2 Propagation of positive and negative streamers

Introduction

An empirical observation mentioned earlier is that applied voltage over maximal streamer length gives similar values for streamers in the same gas with the same polarity. It is argued that this so-called stability field is necessary to maintain the streamer, and that the stability field needs to increase with the electron attachment rate in the streamer [90]. However, while a single simulated streamer has a non-vanishing electric field in its ionized interior that is argued to be the stability field, a group of streamers can completely screen the electric field from their interior by the sum of net charges in their heads, as found by Luque *et al.* [60]. The simulation, however, results on single streamers and therefore cannot be applied to a group of streamers, and the concept of the stability field at this point must be seen as purely empirical.

Experiments by Raizer [90] and Allen and Ghaffar [4], and references therein, show that for plane-plane and point-plane gaps of 5 to 600 mm, the stability field for positive streamers in air is 4.4 to 5 kV/cm. Raizer furthermore reports that positive streamers in N_2 (with up to 2% oxygen) have a stability field of ~ 1.5 kV/cm. Stability fields for positive streamers in a 25 mm point-plane gap by Van Veldhuizen and Rutgers [109] are 2.8 kV/cm for N_2 and 3.6 kV/cm for air. Simulations by Babaeva and Naidis [6] in an electrode geometry that resembles an inhomogeneous electric field show stability fields for negative streamers in air that are 2-3 times higher than for positive streamers. In Yi and Williams [123] negative streamers in N_2 , created in a 130 mm protrusion-plane gap, propagate roughly 60 mm at

123 kV. This results in a stability field of 20.5 kV/cm. Their positive streamers in N₂ already bridge the complete 130 mm gap at their lowest voltage used of 82 kV.

Our results

We have calculated the stability field in our measurements as the applied voltage divided by the streamer length. In this way we observed a stability field of ~ 5 kV/cm (chapter 6) for positive streamers and ~ 15 kV/cm for negative streamers in air in a 40 mm point-plane gap (chapter 7). Positive streamers in N₂ in a 40 mm point-plane gap have a stability field of 2 to 3 kV/cm. In a smaller point-plane gap of 10 mm slightly higher values of the stability field are observed, namely 5 kV/cm for positive streamers in air and N₂ and 18 kV/cm and 12.5 kV/cm for negative streamers in air and N₂, respectively. Most likely the higher values are caused by the fact that the streamers generally bridged the complete gap or did not ignite at all. Therefore some upper limit of the voltage (and thus the stability field) is found.

Igniting streamers in short point-plane gaps is sometimes difficult since the inception voltage V^+ and the DC breakdown voltage are close together, and breakdown must be avoided to protect the camera and other components in the setup. The inception voltage can sometimes be lowered by a pulse repetition rate of 1 or 10 Hz. Simulations by Pancheshnyi [79] suggest that pre-ionization can facilitate subsequent discharges when frequencies higher than 10^{-2} Hz at 1000 mbar or 0.1 Hz at 100 mbar are used in a 20 mm point-plane electrode gap in air. This is in qualitative agreement with our observations. Although pulse repetition facilitates subsequent discharges, we observed no differences in streamer pattern between a single shot pulse or pulses with a frequency of 1 Hz. When a frequency of 10 Hz is used, the streamer pattern usually looks like a single shot discharge at ~ 3 kV lower voltage.

Conclusions

The results on start and propagation of positive and negative streamers have shown that both polarities become more and more alike well above the inception voltage for negative streamers. This conclusion applies to the diameter (section 8.1), velocity (section 8.2) and energy (section 8.3) and also from the photographs in figure 8.12

A possible reason why positive and negative streamers propagate in a different way at low voltages and are more similar at high voltages is the following: in the positive case, the electrons propagate towards the needle or streamer tip. The electrons thus go from a large

volume to a small region where the electric field is high and thus the ionization is enhanced. In this way enough electrons are created for the positive streamer to keep on going. In the case of the negative streamer, the electrons start at the small needle and propagate into the large background volume where the electric field is low. The avalanche, which runs through a decreasing electric field, dies out. At very high applied voltages the electric field in the volume is higher than the stability field (≥ 15 kV/cm in air, ≥ 12.5 kV/cm in N₂ at 1000 mbar, chapter 7) and the negative discharge can keep propagating. Then the positive and negative streamers look more alike.

8.8 Electric field and average electron energy

Introduction

The electric field in a discharge containing N₂ can be determined from the spectral bands of N₂ when the N₂ molecules are excited dominantly from the ground state directly by electron impact, Paris *et al.* [81], which is the case in the streamer head. Measured curves of the reduced field strengths against the ratio of the intensities of the spectral bands of N₂ (337 nm and 394 nm) and N₂⁺ (391 nm) are given in Paris *et al.* [81] where these curves are experimentally obtained by using a non-self-sustaining dc discharge in a parallel-plane gap for the excitation of the gas molecules and by varying the reduced field strength. In Li *et al.* [54] and Creighton [20] computed plots of the field strength against average electron energy are given for negative streamers in N₂ and positive streamers in air, respectively. The values from Li *et al.* [54] run from ~ 5 to 15 eV for fields between ~ 50 and 200 kV/cm; the values from Creighton [20] from ~ 5.5 to 14 eV for fields from ~ 50 to 200 kV/cm.

Our results

We have measured and added the spectral lines of 1800 discharges in air at ~ 60 mbar and 10 kV. In this way a good signal-to-noise ratio is obtained. The same is done for the spectrum in N₂ (chapter 6). The ratio of the intensities of the spectral bands of N₂ (337 nm and 394 nm) and N₂⁺ (394 nm) are obtained from these spectra. They are used to estimate the reduced field strength in the light emitting streamer head via the measured curves of intensity ratio against field strength by Paris *et al.* [81]. The reduced electric fields are found to be $|\mathbf{E}|/p \approx 128 \pm 25$ kV/(cm·bar) in N₂ and $|\mathbf{E}|/p \approx 82 \pm 19$ kV/(cm·bar) in air. The average electron energy corresponding to these field strengths can be obtained via the curve given by Creighton for positive streamers in air (figure 4.10 in [20]). When

it is assumed that this curve can also roughly be applied to N_2 , average electron energies are found of $\sim 11 \pm 2$ eV for N_2 and $\sim 8 \pm 2$ eV for air. These values are similar to values found in Li *et al.* [54] who simulated negative streamers in N_2 . In their curves of average electron energy versus reduced electric field for N_2 values are found of $\sim 10 \pm 2$ eV for N_2 and, when assuming that the curve is roughly similar in air, $\sim 8 \pm 2$ eV for air. These values show that the electrons in N_2 are more energetic than those in air. This may explain why we observe a higher light intensity for streamers in N_2 than in air. Note however that these values are only a rough estimate since the spectrum is obtained from a time integrated discharge, thus from primary streamers where the electric field at the tip must be above the ionization threshold (order 100 kV/cm) and secondary streamers where the electric field can be as low as the stability field (order 5 kV/cm). Therefore the values found may be lower than that would be found when only the primary streamer propagation is used.

Conclusions

Our measurements have shown that the electric field in the streamer head and the average electron temperature for streamers in N_2 is higher than for streamers in air. We expect that then the streamer velocity in N_2 will also be higher since when fields and energies are higher the ionization rate is also higher. This expectation is confirmed by the observation that the streamer velocities in N_2 at 65 mbar and 10 kV are indeed $\sim 20\%$ higher than those in air (chapter 6). Similar measurements at 400 mbar indicate that the intensity ratio of the spectral lines in air is equal to or slightly higher than in N_2 which indeed corresponds to the observation that streamers in air and N_2 at 400 mbar have similar velocities (figure 6.11). It would, however, contradict the observation that streamers in N_2 are more intense than in air (figure 6.7). It must be remarked though that at 400 mbar both spectrum ratios have a worse signal-to-noise ratio than the measurements at ~ 60 mbar, especially in air where the 391 nm-line cannot be resolved from the background noise with certainty. Therefore, no real conclusion can be drawn from the measurements at 400 mbar.

Chapter 9

Conclusions and outlook

The main conclusions of this thesis are that

1. There is *one* kind of streamer whose properties vary gradually with voltage, pressure and circuit impedance as long as measurements are done in *one* gas and with *one* polarity. It is also noted that differences in polarity decrease at voltages higher than a critical voltage which in our experiments appeared to be around the DC-breakdown voltage. Other properties as the inception voltage, breakdown voltage, minimal diameter, distance between branching events can be different as summarized in chapter 8.
2. Pressure scaling is indeed allowed and the results are better than expected on the basis of theory since the electrodes were not scaled with pressure and pressures higher than 40 mbar were used where photoionization becomes more quenched with increasing pressure.
3. Concerning the power supplies used it is shown that different supplies will create similar streamer patterns and velocities if their voltage rise time, peak voltage and internal resistance are similar. The internal resistance appears to play a decisive role.
4. The systematically obtained results of this thesis are also in good agreement with recent streamer and sprite experiments found in literature which makes this broad parameter study reliable and suitable for comparison with simulations and theory.

This thesis has linked the streamers as found in small-gap experiments to the streamers used in large-gaps for industrial purposes. The results even showed that when caution is taken the streamers can be upscaled to sprite phenomena. However, more knowledge about the physical processes that drive the streamers (e.g. about the difference in propagation mechanisms of streamers in N_2 and air, the streamer branching or the interconnecting of

streamer channels) will be gained when experiments and simulations under similar conditions can be compared. For a good comparison of results with theory a clear physical picture must be pursued. Therefore, it is advisable for future experiments to keep the following items in mind.

1. Fast pulses with rise times ≤ 25 ns should be used to avoid that streamers start when the voltage is still rising since then the actual applied voltage is difficult to determine.
2. The voltage pulse duration should be made similar to the streamer transit time since then only primary streamers can propagate and the picture will not be influenced by events that occur later (e.g. return strokes, secondary and/or late streamers, glow, spark). This means that a setup is preferred where a coaxial cable is charged since then short and fast pulses can be made. An extra benefit will be that also higher voltages can be obtained without having breakdown.
3. The influence of the voltage pulse repetition rate and of the background ionization on the streamer propagation should be determined. A high pulse repetition rate or an increase in background ionization by e.g. a UV-lamp may cause that the streamer propagates through a pre-ionized medium which can facilitate streamer inception.
4. A very clean vacuum vessel is required when streamers are made in different gases to avoid even the smallest amount of pollution. Only then a clear picture of the propagation mechanisms in each gas can be obtained.
5. When the 3D streamers are imaged onto a 2D photograph spatial information becomes lost. Therefore, 3D-reconstructions as can be made via stereophotography will be a nice addendum to the 2D photographs.
6. The electric field and the electron density in the streamer head are parameters that characterize and drive a discharge. These parameters can be measured by Stark spectroscopy [113] or Thomson scattering [96], respectively. Note however that these diagnostics are not easily implemented on streamers at high pressures since these streamers usually do not appear on the same position in the electrode gap.

Appendix A

Overview of the parameter regimes in the setups

A.1 Experimental setups

Four pulsed power supplies are used to generate streamers. They are called the C-supply which can be triggered by a sparkgap (SG) or semiconductor (SC) switch (Physics Department), the TLT-supply (Physics Department), the PM-supply (Electrical Engineering Department) and the MIPT-supply (MIPT-Moscow). Their working mechanisms are based on one of the following two principles: a charged coupled capacitor (C, TLT) or a charged coaxial cable (PM, MIPT).

An overview of the main properties of the supplies is given in table A.1 with a reference to the chapter where the supply is explained in more detail.

A.2 Intensified CCD-cameras

Five cameras (an Andor Technology ICCD-452, an analogue and a digital 4QuikE from Stanford Computer Optics, a Princeton Instruments 576G/RB and a PicoStar HR12 from La Vision) and three different lenses (Nikon UV-Nikkor, Sigma 180 and Industar 61L/3) are used, table A.2. All cameras make *one* photograph per discharge (the shutter opens and closes). Only the Picostar camera can switch its intensifier on and off several times during one photograph with a minimal time interval between the exposures of several ns (stroboscopic mode). Reading out the Andor camera by the computer takes several seconds and therefore only a few photographs per minute can be made. Both Stanford cameras are quicker. They can obtain a photograph repetition rate of 2 Hz. The Princeton camera can make one photograph every ~ 30 s.

	C-SC-supply	TLT-supply	PM-supply	MIPT-supply
Shape vessel	cylindrical	cylindrical	no vessel	cubic
Dimensions vessel (cm)	$\varnothing = 50$ height = 30	$\varnothing = 50$ height = 30	–	22 x 22 x 22
Electrode gap (mm)	10 - 160	40, 80	40	30, 40
Pressure (mbar)	10 - 1000	1000	1000	465 - 1000
Gases	ambient air nitrogen 99.8%N ₂ :0.2%O ₂	ambient air	ambient air	ambient air 80%N ₂ :20%O ₂
Polarity	+ and –	+	+ and –	+
Voltage rise time (ns) from 10% to 90% in a 40 mm gap	30, 60, 150	25	15	12
Voltage duration (ns)	> 1000	50	100	400
Min. voltage (kV)	1 ^a	30	40	20
Max. voltage (kV)	60	60	90	40
HV switch	sparkgap Behlke HTS 301 Behlke HTS 361 Behlke HTS 651	sparkgap	sparkgap	thyatron
Current via	divided cathode	Pearson 6585	DI-system	shunt
Voltage via	Tektronix P6015 Northstar PVM4	Tektr. P6015	DI-system	shunt
Oscilloscope	LeCroy Waverunner 6100A 1 GHz, 5 GS/s	LeCroy Waver. 6100A 1 GHz, 5 GS/s	LeCroy Waver. 2 1 GHz, 4 GS/s	Tektronix TDS3054 0.5 GHz, 5 GS/s
Explained in	chapter 4	chapter 4	chapter 7	chapter 3
Used in	chapter 3 chapter 4 chapter 5 chapter 6 chapter 7	chapter 4 chapter 7	chapter 7	chapter 3

Table A.1: *Main properties of the experimental setups used.* ^a *When the sparkgap switch is used (C-SG-supply) the minimal voltage is 5 kV.*

Camera	Andor ICCD-452	4QuikE analogue	4QuikE digital	Princeton 576G/RB	PicoStar HR12
Pixels	1024 x 1024	736 x 572	1360 x 1024	576 x 384	640 x 480
Pixel size (μm)	13 x 13	8.6 x 8.3	4.7 x 4.7	23 x 23	?
Minimum optical gate (ns)	2	2	2	~ 5	0.2
Lens	Nikon UV Nikkor	Nikon UV Nikkor	Nikon UV Nikkor	Sigma 180	Industar 61L/3
Wavelength range camera (nm)	180-850	300-800	300-800	180-800	300-700
Supply	C-supply	C-supply TLT-supply	C-supply	PM-supply	MIPT-supply
Wavelength range total setup (nm)	300-850	300-800	300-800	UV ^a -800	400 ^a -700
Used in chapter	3	4 7	3 5 6 7	7	3

Table A.2: Overview of the *iCCD*-camera - lens combinations used. ^aThis value is an estimate.

Bibliography

- [1] A. Abou-Ghazala, S. Katsuki, K.H. Schoenbach, F.C. Dobbs and K.R. Moreira, *Bacterial decontamination of water by means of pulsed-corona discharges*, IEEE Trans. Plasma Sci. **30** (2002) 1449.
- [2] S. Achat, Y. Teisseyre and E. Marode, *The scaling of the streamer-to-arc transition in a positive point-to-plane gap with pressure*, J. Phys. D.: Appl. Phys. **25** (1992) 661.
- [3] H. Akiyama, *Streamer discharges in liquids and their applications*, IEEE Trans. Dielect. Elect. Insul. **7** (2000) 646.
- [4] N.L. Allen and A. Ghaffar, *The conditions required for the propagation of a cathode-directed positive streamer in air*, J. Phys. D.: Appl. Phys. **28** (1995) 331.
- [5] M. Arrayás, U. Ebert and W. Hundsdorfer, *Spontaneous Branching of Anode-Directed Streamers between Planar Electrodes*, Phys. Rev. Lett. **88** (2002) 174502.
- [6] N.Y. Babaeva and G.V. Naidis, *Dynamics of positive and negative streamers in air in weak uniform electric fields*, IEEE Trans. Plasma Sci. **25** (1997) 375.
- [7] F. Bastien and E. Marode, *The determination of basic quantities during glow-to-arc transition in a positive point-to-plane discharge*, J. Phys. D: Appl. Phys. **12** (1979) 249.
- [8] P.P.M. Blom, C. Smit, R.H.P. Lemmens and E.J.M. van Heesch, *Combined Optical and Electrical Measurements on Pulsed Corona Discharges*, Gaseous Dielectrics VII, Edited by L.G. Christophorou and D.R. James, New York: Plenum Press (1994).
- [9] P.P.M. Blom, *High-Power Pulsed Coronas*, Ph.D. thesis, Eindhoven University of Technology, The Netherlands (1997). Available on www.tue.nl/bib.
- [10] R. Brandenburg, V.A. Maiorov, Yu.B. Golubovskii, H.-E. Wagner, J. Behnke and J.F. Behnke, *Diffuse barrier discharge in nitrogen with small admixtures of oxygen: discharge mechanism and transition to the filamentary regime*, J. Phys. D.: Appl. Phys. **38** (2005) 2187.

- [11] T.M.P. Briels, E.M. van Veldhuizen and U. Ebert, *Experiments on propagating and branching positive streamers in air*, Proc. XVth International Conference on Gas Discharges and their Applications, Toulouse, France (2004) 323.
- [12] T.M.P. Briels, E.M. van Veldhuizen and U. Ebert, *Experiments on the diameter of positive streamers in air*, XXVIIth International Conference on Phenomena in Ionized Gases (ICPIG), Eindhoven, the Netherlands, (2005) file 04-418. Available on www.icpig2005.nl.
- [13] T.M.P. Briels, E.M. van Veldhuizen and U. Ebert, *Branching of Positive Discharge Streamers in Air at Varying Pressures*, IEEE Trans. Plasma Sci. **33** (2005) 264.
- [14] T.M.P. Briels, J. Kos, E.M. van Veldhuizen, C. Montijn, A. Luque and U. Ebert, *Experiments and calculations on pulsed streamers in air and N₂*, Proc. 5th Int. Symp. Non Thermal Plasma Technology, Ile d'Oléron, France (2006).
- [15] T.M.P. Briels, J. Kos, E.M. van Veldhuizen and U. Ebert, *Circuit dependence of the diameter of pulsed positive streamers in air*, J. Phys. D.: Appl. Phys. **39** (2006) 5201.
- [16] T.M.P. Briels, E.M. van Veldhuizen, A.J.M. Pemen, G.J.J. Winands and U. Ebert, *Pulsed corona investigations with a wide parameter range*, XXVIIIth International Conference on Phenomena in Ionized Gases (ICPIG), Prague, Czech Republic, (2007) file 3P10-86. Available on <http://icpig2007.ipp.cas.cz/>.
- [17] J.S. Clements, A. Mizuno, W.C. Finney and R.H. Davis, *Combined removal of SO₂, NO_x, and fly ash from simulated flue gas using pulsed streamer corona*, IEEE Trans. Ind. Appl. **25** (1989) 62.
- [18] D. Comtois, H. Ppin, F. Vidal, F.A.M. Rizk, C.-Y. Chien, T. Wyatt Johnston, J.-C. Kieffer, B. La Fontaine, F. Martin, C. Potvin, P. Couture, H.P. Mercure, A. Bondiou-Clergerie, P. Lalande and I. Gallimberti, *Triggering and Guiding of an Upward Positive Leader From a Ground Rod With an Ultrashort Laser Pulse I: Experimental Results*, IEEE Trans. Plasma Sci. **31** (2003) 377.
- [19] Y.L.M. Creighton, E.M. van Veldhuizen and W.R. Rutgers, *Electrical and optical study of pulsed positive corona in Non-Thermal Plasmas for Pollution Control*, ed. by B.M. Penetrante and S.E. Schultheis, NATO ASI Series, Springer, subseries G, vol. 34, part A, (1993) 205.
- [20] Y.L.M. Creighton, *Pulsed positive corona discharges: Fundamental study and application to flue gas treatment*, Ph.D. thesis, Eindhoven University of Technology, The Netherlands (1994). Available on www.tue.nl/bib.

- [21] L.G. Christophorou, *Electron-Molecule Interactions and Their Applications*, New York: Academic (1984).
- [22] S.A. Cummer, N. Jaugey, J. Li, W.A. Lyons, T.E. Nelson and E.A. Gerken, *Submillisecond imaging of sprite development and structure*, Geophys. Res. Lett. **33** (2006) L04104.
- [23] S.A. Cummer, *Currents, Charges, and Electromagnetic Fields Associated With Sprite Initiation and Development*, presentation at the workshop: "Streamers, sprites, leaders, lightning: from micro- to macroscales", Leiden, The Netherlands, (2007). Available on www.lorentzcenter.nl.
- [24] G.A. Dawson and W.P. Winn, *A model for streamer propagation*, Z. Phys. **183** (1965) 159.
- [25] S.K. Dhali and P.F. Williams, *Numerical simulation of streamer propagation in nitrogen at atmospheric pressure*, Phys. Rev. A **31** (1985) 1219.
- [26] S.K. Dhali and P.F. Williams, *Two-dimensional studies of streamers in gases*, J. Appl. Phys. **62** (1987) 4696.
- [27] G. Dinelli, L. Civitano and M. Rea, *Industrial experiments on pulse corona simultaneous removal of NO_x and SO_2 from flue gas*, IEEE Trans. Ind. Appl. **26** (1990) 535.
- [28] R.A. Dougal and P.F. Williams, *Fundamental processes in laser-triggered electrical breakdown of gases*, J. Phys. D: Appl. Phys. **7** (1984) 903.
- [29] M.I. D'yakonov and V.Yu. Kachorovskii, *Theory of streamer discharge in semiconductors*, Sov. Phys. JETP **67** (1998) 1049.
- [30] U. Ebert, W. van Saarloos and C. Caroli, *Propagation and structure of planar streamer fronts*, Phys. Rev. E **55** (1997) 1530.
- [31] U. Ebert and W. van Saarloos, *Front propagation into unstable states: Universal algebraic convergence towards uniformly translating pulled fronts*, Physica D **146** (2000) 1.
- [32] U. Ebert and W. Hundsdorfer, *Reply to: Spontaneous branching of anode-directed streamers between planar electrodes by M. Arrayás, U. Ebert and W. Hundsdorfer*, Phys. Rev. Lett. **88** (2002) 174502., Phys. Rev. Lett. **89** (2002) 229402.

- [33] U. Ebert, C. Montijn, T.M.P. Briels, W. Hundsdorfer, B. Meulenbroek, A. Rocco and E.M. van Veldhuizen, *The multiscale nature of streamers*, Plasma Sources Sci. Technol. **15** (2006) S118.
- [34] U. Ebert, unpublished work (2007).
- [35] E.A. Gerken, U.S. Inan and C.P. Barrington-Leigh, *Telescopic imaging of sprites*, Geophys. Res. Lett. **27** (2000) 2637.
- [36] E.A. Gerken and U.S. Inan, *Streamers and Diffuse Glow Observed in Upper Atmospheric Electrical Discharges*, IEEE Trans. Plasma Sci. **33** (2005) 282.
- [37] L.R. Grabowski, T.M.P. Briels, E.M. van Veldhuizen and A.J.M. Pemen, *Streamers in pulsed positive corona: low and high current regimes*, Proc. XVIIth International Conference on Phenomena in Ionized Gases (ICPIG), Eindhoven, the Netherlands, file 04-425 (2005). Available on www.icpig2005.nl.
- [38] L.R. Grabowski, E.M. van Veldhuizen and W.R. Rutgers, *Removal of Phenol from Water: A Comparison of Energization Methods*, J. Adv. Oxid. Technol. **8** (2005) 142.
- [39] L.R. Grabowski, E.M. van Veldhuizen, A.J.M. Pemen and W.R. Rutgers, *Corona Above Water Reactor for Systematic Study of Aqueous Phenol Degradation*, Plasma Chem. Plasma Procs. **26** (2006) 3.
- [40] L.R. Grabowski, *Pulsed corona in air for water treatment*, Ph.D. thesis, Eindhoven University of Technology, The Netherlands (2006). Available on www.tue.nl/bib.
- [41] B. Gravendeel, *Negative corona discharges: A fundamental study*, Ph.D. thesis, Eindhoven University of Technology, The Netherlands (1987). Available on www.tue.nl/bib.
- [42] A.H. Guenther and J.R. Bettis, *The laser triggering of high-voltage switches*, J. Phys. D: Appl. Phys. **11** (1978) 123.
- [43] Handbook of Chemistry and Physics, 87th edition 2006-2007, on <http://hbcnetbase.com>.
- [44] J. Hermann, C. Boulmer-Leborgne and D. Hong, *Diagnostics of the early phase of an ultraviolet laser induced plasma by spectral line analysis considering self-absorption*, J. Appl. Phys. **83** (1998) 691.
- [45] M.A. van Houten, *Electromagnetic compatibility in high voltage engineering*, Ph.D. thesis, Eindhoven University of Technology, the Netherlands (1990). Available on www.tue.nl/bib.

- [46] U. Kogelschatz, *Atmospheric-pressure plasma technology*, Plasma Phys. Control. Fusion **46** (2004) B63.
- [47] J. Kos, *Parameter dependence of streamer discharges*, Masters thesis, EPG 06-14, Eindhoven University of Technology, The Netherlands (2006).
- [48] A.V. Krasnochub, E.I. Mintousov, M.M. Nudnova and A.Yu. Starikovskii, *Flame Blow-off Velocity Control: the Importance of Proper Organization of Nanosecond Barrier Discharge*, Proc. XXVII International Conference on Phenomena in Ionized Gases (ICPIG), Eindhoven, The Netherlands (2005) file 18-311. Available on www.icpig2005.nl.
- [49] A.A. Kulikovsky, *Positive streamer between parallel plate electrodes*, J. Phys. D: Appl. Phys. **30** (1997) 441.
- [50] A.A. Kulikovsky, *Positive streamer in a weak field in air: A moving avalanche-to-streamer transition*, Phys. Rev. E **57** (1998) 7066.
- [51] A.A. Kulikovsky, *The role of photoionization in positive streamer dynamics*, J. Phys. D: Appl. Phys. **33** (2000) 1514.
- [52] A.A. Kulikovsky, *Comment on: Spontaneous branching of anode-directed streamers between planar electrodes by M. Arrayás, U. Ebert and W. Hundsdorfer*, Phys. Rev. Lett. **88** (2002) 174502., Phys. Rev. Lett. **89** (2002) 229401.
- [53] A.N. Lagarkov and I.M. Rutkevich, *Ionization waves in electrical breakdown of gases*, Berlin: Springer (1994).
- [54] C. Li, W.J.M. Brok, U. Ebert and J.J.A.M. van der Mullen, *Deviations from the local field approximation in negative streamer heads*, J. Appl. Phys. **101** (2007) 123305.
- [55] N. Liu and V.P. Pasko, *Effects of photoionization on propagation and branching of positive and negative streamers in sprites*, J Geophys. Res. **109** (2004) A04301.
- [56] N. Liu and V.P. Pasko, *Effects of photoionization on similarity properties of streamers at various pressures in air*, J. Phys. D.: Appl. Phys. **39** (2006) 327.
- [57] L.B. Loeb, *Basic processes of gaseous electronics*, Berkeley: University of California Press (1961).
- [58] Y-F. Lu, Z-B. Tao and M-H. Hong, *Characteristics of excimer laser induced plasma from an Aluminum target by spectroscopic study*, Jpn J. Appl. Phys. **38** (1999) 2958.

- [59] A. Luque, U. Ebert, C. Montijn and W. Hundsdorfer, *Photoionization in negative streamers: Fast computations and two propagation modes*, Appl. Phys. Lett. **90** (2007) 081501.
- [60] A. Luque, F. Brau and U. Ebert, *Saffman-Taylor streamer discharges: a study on interacting streamers*, submitted to Phys. Rev. Lett. (2007). Available on arxiv.org, article arXiv:0708.1722v1.
- [61] A. Luque, U. Ebert, C. Montijn and W. Hundsdorfer, *Pseudo-spectral 3D simulations of streamers with adaptively refined grids*, XXVIIIth International Conference on Phenomena in Ionized Gases (ICPIG), Prague, Czech Republic, (2007) file 2P05-36. Available on <http://icpig2007.ipp.cas.cz/>.
- [62] B.M. Luther, L. Furfaro, A. Klix, and J.J. Rocca, *Femtosecond laser triggering of a sub-100 picosecond jitter high-voltage spark gap*, Appl. Phys. Lett. **79** (2001) 3248.
- [63] G.C.G.M. Manders, *Conductor to insulator transition and insulator to conductor transition, studied by gas discharges and breakjunctions*, Ph.D. thesis, Radboud University Nijmegen, The Netherlands (2004).
- [64] H.S.W. Massey, E.H.S. Burhop and H.B. Gilbody, *Electronic and ionic impact phenomena: Electron collisions with molecules and photo-ionization*, Oxford: Oxford University Press (1969).
- [65] J.M. Meek and J.D. Craggs, *Electrical breakdown of gases*, Oxford: Clarendon press (1953).
- [66] B. Meulenbroek, A. Rocco and U. Ebert, *Streamer branching rationalized by conformal mapping techniques*, Phys. Rev. E **69** (2004) 067402.
- [67] B. Meulenbroek, *Streamer branching: conformal mapping and regularization*, Ph.D. thesis, Eindhoven University of Technology, The Netherlands (2006). Available on www.tue.nl/bib.
- [68] C. Montijn, *Evolution of negative streamers in nitrogen: a numerical investigation on adaptive grids*, Ph.D. thesis, Eindhoven University of Technology, The Netherlands (2005).
- [69] C. Montijn and U. Ebert, *Diffusion correction to the Raether-Meek criterion for the avalanche-to-streamer transition*, J. Phys. D: Appl. Phys. **39** (2006) 2979.
- [70] C. Montijn, U. Ebert and W. Hundsdorfer, *Numerical convergence of the branching time of negative streamers*, Phys. Rev. E **73** (2006) 065401(R).

- [71] C. Montijn, W. Hundsdorfer and U. Ebert, *An adaptive grid refinement strategy for the simulation of negative streamers*, J. Comp. Phys. **219** (2006) 801.
- [72] D.R. Moudry, H.C. Stenbaek-Nielsen, D.D. Sentman and E.M. Wescott, *Velocities of sprite tendrils*, Geophys. Res. Lett **29** (2002) 1992.
- [73] S.A. Nair, K. Yan, A.J.M. Pemen, G.J.J. Winands, F.M. van Gompel, H.E.M. van Leuken, E.J.M. van Heesch, K.J. Ptasinski and A.A.H. Drinkenburg, *A high-temperature pulsed corona plasma system for fuel gas cleaning*, J. Electrostatics **61** (2004) 117.
- [74] M.M. Nudnova and A.Yu. Starikovskii, private communication (2005).
- [75] M.M. Nudnova, N.B. Anikin, T. Briels, A.A. Kirpichnikov, S.M. Starikovskaia, N.A. Zavialova and A.Yu. Starikovskii, *Streamer and fast ionisation wave: control of development and electron density*, Proc. XVIII European Conference on the Atomic and Molecular Physics of Ionized Gases (ESCAMPIG), Lecce, Italy (2006).
- [76] M.M. Nudnova and A.Yu. Starikovskii, *Cathode-directed streamer head fine structure*, Proc. XVI International Conference on Gas Discharges and their Applications, Xian, China (2006) 289.
- [77] S.V. Pancheshnyi and A.Yu. Starikovskii, *Role of photoionization processes in propagation of cathode-directed streamer*, J. Phys. D: Appl. Phys. **34** (2001) 248.
- [78] S.V. Pancheshnyi and A.Yu. Starikovskii, *Two-dimensional numerical modelling of the cathode-directed streamer development in a long gap at high voltage*, J. Phys. D: Appl. Phys. **36** (2003) 2683.
- [79] S.V. Pancheshnyi, *Role of electronegative gas admixtures in streamer start, propagation and branching phenomena*, Plasma Sources Sci. Technol. **14** (2005) 645.
- [80] S.V. Pancheshnyi, M.M. Nudnova and A.Yu. Starikovskii, *Development of a cathode-directed streamer discharge in air at different pressures: Experiment and comparison with direct numerical simulation*, Phys. Rev. E **71** (2005) 016407.
- [81] P. Paris, M. Aints, F. Valk, T. Plank, A. Haljaste, K.V. Kozlov and H.-E. Wagner, *Intensity ratio of spectral bands of nitrogen as a measure of electric field strength in plasmas*, J. Phys. D: Appl. Phys. **38** (2005) 3894.
- [82] V.P. Pasko, U.S. Inan and T.F. Bell, *Spatial structure of sprites*, Geophys. Res. Lett. **25** (1998) 2123.

- [83] V.P. Pasko, M.A. Stanley, J.D. Mathews, U.S. Inan and T.G. Wood, *Electrical discharge from a thundercloud top to the lower ionosphere*, Nature **416** (2002) 152.
- [84] V.P. Pasko, *Red sprite discharges in the atmosphere at high altitude: the molecular physics and the similarity with laboratory discharges*, Plasma Sources Sci. Technol. **16** (2007) S13.
- [85] R.W.B. Pearse and A.G. Gaydon, *The identification of molecular spectra*, London: Chapman and Hall (1984).
- [86] G.W. Penney and G.T. Hummert, *Photoionization measurements in air, oxygen and nitrogen*, J. Appl. Phys. **41** (1970) 572.
- [87] S. Pleslić and Ž. Andreić, *Laser produced plasmas on Mg, Al and Si surfaces*, Fyzika A **14** (2005) 107118.
- [88] H. Raether, *The development of electron avalanche in a spark channel (from observations in a cloud chamber)*, Z. Phys. **112** (1939) 464.
- [89] H. Raether, *Electron avalanches and breakdown in gases*, S.I.: Butterworth (1964).
- [90] Yu.P. Raizer, *Gas Discharge Physics*, Berlin: Springer (1991).
- [91] Yu.P. Raizer and E.M. Bazelyan, *Spark discharge*, Boca Raton: CRC Press (1998).
- [92] Yu.P. Raizer and A.N. Simakov, *Main Factors Determining the Radius of the Head of a Long Streamer and the Maximum Electric Field near the Head*, Plasma Phys. Rep. **24** (1998) 700.
- [93] A. Rocco, U. Ebert and W. Hundsdorfer, *Branching of negative streamers in free flight*, Phys. Rev. E **66** (2002) 035102.
- [94] L.A. Rosocha, D.M. Coates, D. Plattis and S. Stange, *Plasma-enhanced combustion of propane using a silent discharge*, Phys. Plasmas **11** (2004) 2950.
- [95] J.R. Roth, *Industrial plasma engineering, Vol. 1: Principles*, Bristol: Institute of Physics (1995-2001).
- [96] M.J. van de Sande and J.J.A.M. van der Mullen, *Thomson scattering on a low-pressure, inductively-coupled gas discharge lamp*, J. Phys. D: Appl. Phys. **35** (2002) 1381.
- [97] D.D. Sentman, E.M. Wescott, D.L. Osborne and M.J. Heavner, *Preliminary results from the Sprites94 aircraft campaign: 1. Red Sprites*, Geophys. Res. Lett. **22** (1995) 1205.

- [98] R.S. Sigmond, *The residual streamer channel: Return strokes and secondary streamers*, J. Appl. Phys. **56** (1984) 1355.
- [99] E. Stoffels, W.W. Stoffels, D. Vender, M. Kando, G.M.W. Kroesen and F.J. de Hoog, *Negative ions in a radio-frequency oxygen plasma*, Phys. Rev. E **51** (1995) 2425.
- [100] P. Tardiveau, E. Marode and A. Agneray, *Tracking an individual streamer branch among others in a pulsed induced discharge*, J. Phys. D: Appl. Phys. **35** (2002) 2823.
- [101] J.S.E. Townsend, *Electrons in gases*, London: Hutchinson's Scientific and Technical Publications (1947).
- [102] N.G. Trinh, *Electrode Design for Testing in Uniform Field Gaps*, IEEE Trans. Power Apparatus and Systems **PAS-99** (1980) 1235.
- [103] E.M. van Veldhuizen, W.R. Rutgers and V.A. Bityurin, *Energy efficiency of NO removal by pulsed corona discharges*, Plasma Chem. Plasma Process. **16** (1996) 227.
- [104] E.M. van Veldhuizen (ed.), *Electrical Discharges for Environmental Purposes: Fundamentals and Applications*, Huntington: Nova Science Publishers (2000).
- [105] E.M. van Veldhuizen, P.C.M. Kemps and W.R. Rutgers, *Streamer branching in a short gap: the influence of the power supply*, IEEE Trans. Plasma Sci. **30** (2002) 162.
- [106] E.M. van Veldhuizen and W.R. Rutgers, *Pulsed positive corona streamer propagation and branching*, J. Phys. D: Appl. Phys. **35** (2002) 2169.
- [107] E.M. van Veldhuizen, unpublished work (2002).
- [108] E.M. van Veldhuizen, W.R. Rutgers and U. Ebert, *Branching of streamer type corona discharge*, Proc. XIV International Conference on Gas Discharges and their Applications, Liverpool, United Kingdom (2002).
- [109] E.M. van Veldhuizen and W.R. Rutgers, *Inception behaviour of pulsed positive corona in several gases*, J. Phys. D: Appl. Phys. **36** (2003) 2692.
- [110] E.M. van Veldhuizen, T.M.P. Briels, L.R. Grabowski, A.J.M. Pemen and U. Ebert, *Influences of the pulsed power supply on corona streamer appearance*, Proc. IInd International Workshop on Cold Atmospheric Pressure Plasmas: Sources and Applications (CAPPSPA), Bruges, Belgium (2005).
- [111] E.M. van Veldhuizen, T.M.P. Briels, J. Kos and U. Ebert, *Pulsed positive corona in different gaps in air*, Proc. XVIth International Conference on Gas Discharges and their Applications, Xi'an, China (2006).

- [112] G. Verkerk, J.B. Broens, W. Kranendonk, F.J. van der Puijl, J.L. Sikkema and C.W. Stam, *Binas: informatieboek vwo/havo voor het onderwijs in de natuurwetenschappen*, Groningen: Wolters-Noordhoff (1992).
- [113] E. Wagenaars, M.D. Bowden and G.M.W. Kroesen, *Measurements of Electric-Field Strengths in Ionization Fronts during Breakdown*, Phys. Rev. Lett. **98** (2007) 075002.
- [114] R.T. Waters and R.E. Jones, *The Impulse Breakdown Voltage and Time-Lag Characteristics of Long Gaps in Air. I. The Positive Discharge*, Phil. Trans. Roy. Soc. London Ser. A **256** (1964) 185.
- [115] J.M. Wetzter and P.C.T. van der Laan, *Prebreakdown Currents: Basic Interpretation and Time-resolved Measurements*, IEEE Trans. Electrical Insulation **24** (1989) 297.
- [116] E.R. Williams, *Problems in lightning physics: the role of polarity asymmetry*, Plasma Sources Sci. Technol. **15** (2006) S91.
- [117] G.J.J. Winands, Z. Liu, A.J.M. Pemen, E.J.M. van Heesch, K. Yan and E.M. van Veldhuizen, *Temporal development and chemical efficiency of positive streamers in a large scale wire-plate reactor as a function of voltage waveform parameters*, J. Phys. D: Appl. Phys. **39** (2006) 3010.
- [118] G.J.J. Winands, K. Yan, A.J.M. Pemen, S.A. Nair, Z. Liu and E.J.M. van Heesch, *An industrial streamer corona plasma system for gas cleaning*, IEEE Trans. Plasma Sci. **34** (2006) 2426.
- [119] G.J.J. Winands, *Efficient streamer plasma generation*, Ph.D. thesis, Eindhoven University of Technology, The Netherlands (2007). Available on www.tue.nl/bib.
- [120] G.J.J. Winands, private communication (2007).
- [121] C. Wu and E.E. Kunhardt, *Formation and propagation of streamers in N_2 and N_2 - SF_6 mixtures*, Phys. Rev. A **37** (1988) 4396.
- [122] K. Yan, E.J.M. van Heesch, A.J.M. Pemen, P.A.H.J. Huijbrechts and P.C.T. van der Laan, *A 10 kW high-voltage pulse generator for corona plasma generation*, Rev. Sci. Instr. **72** (2001) 2443.
- [123] W.J. Yi and P.F. Williams, *Experimental study of streamers in pure N_2 and N_2/O_2 mixtures and a ≈ 13 cm gap*, J. Phys. D: Appl. Phys. **35** (2002) 205.
- [124] M. Yousfi, P. Segur and T. Vassiliadis, *Solution of the Boltzmann equation with ionisation and attachment: application to SF_6* , J. Phys. D: Appl. Phys. **18** (1985) 359.

[125] www.lenntech.com.

[126] M.B. Zheleznyak, A. Kh. Mnatsakanyan and S.V. Sizykh, *Photoionization of nitrogen and oxygen mixtures by radiation from a gas discharge*, High Temp. **20** (1982) 357.

Related publications

Publications associated with this thesis are:

Journal Publications

2006

- T.M.P. Briels, J. Kos, E.M. van Veldhuizen, U. Ebert, *Circuit dependence of the diameter of pulsed positive streamers in air*, J. Phys. D: Appl. Phys. **39** (2006) 5201-5210.
- U. Ebert, C. Montijn, T.M.P. Briels, W. Hundsdorfer, B. Meulenbroek, A. Rocco, E.M. van Veldhuizen, *The Multiscale Nature of Streamers*, Plasma Sources Sci. Technol. **15** (2006) S118-S129.

2005

- T.M.P. Briels, E.M. van Veldhuizen, U. Ebert, *Branching of Positive Discharge Streamers in Air at Varying Pressures*, IEEE Plasma Sci. **33** (2005) 264-265.

Conference contributions

2007

- T.M.P. Briels, E.M. van Veldhuizen, A.J.M. Pemen, G.J.J. Winands and U. Ebert, *Pulsed corona investigations with a wide parameter range*, XVIIIth International Conference on Phenomena in Ionised Gases, Prague, Czech Republic (proceedings and poster presentation).
- T.M.P. Briels, G.J.J. Winands, S. Nijdam, E.M. van Veldhuizen, U. Ebert, *Exploring streamer variability in experiments*, Workshop: Streamers, sprites, leaders, lightning: from micro- to macroscales, Leiden, the Netherlands (oral and poster presentation).
- S. Nijdam, J.S. Moerman, T.M.P. Briels, E.M. van Veldhuizen, U. Ebert, *Stereophotographs of point-plane streamers in air*, Workshop: Streamers, sprites, leaders, lightning: from micro- to macroscales, Leiden, the Netherlands (oral and poster presentation).

- T.M.P. Briels, S. Nijdam, J. Kos, G.J.J. Winands, E.M. van Veldhuizen, U. Ebert, *Effects of polarity on streamer propagation and branching*, 19th Symposium Plasma Physics & Radiation Technology, Lunteren, The Netherlands (poster presentation).
- T.M.P. Briels, G.J.J. Winands, S. Nijdam, E.M. van Veldhuizen, U. Ebert, *Exploring streamer variability in experiments*, 10th Euregional Workshop on the Exploration of Low Temperature Plasma Physics (WELT-PP), Kerkrade, the Netherlands (poster presentation).
- S. Nijdam, J.S. Moerman, T.M.P. Briels, E.M. van Veldhuizen, U. Ebert, *Stereophotographs of point-plane streamers in air*, 10th Euregional Workshop on the Exploration of Low Temperature Plasma Physics (WELT-PP), Kerkrade, the Netherlands (poster presentation).

2006

- T.M.P. Briels, J. Kos, E.M. van Veldhuizen, A. Luque and U. Ebert, *Experiments and calculations on pulsed streamers in air and N₂*, Vth International Symposium on Non Thermal Plasma Technology, Saint Pierre d'Oléron, France (proceedings and oral presentation).
- E.M. van Veldhuizen, T.M.P. Briels, J. Kos and U. Ebert, *Pulsed positive corona in different gaps in air*, XVIth International Conference on Gas Discharges and their Applications, Xi'an, China (proceedings and oral presentation).
- M.M. Nudnova, N.B. Anikin, T. Briels, A.A. Kirpichnikov, S.M. Starikovskaia, N.A. Zavialova, A.Yu. Starikovskii, *Streamer and fast ionisation wave: control of development and electron density*, XVIII European Conference on the Atomic and Molecular Physics of Ionized Gases (ESCAMPIG), Lecce, Italy (proceedings and poster presentation).
- T.M.P. Briels, J. Kos, E.M. van Veldhuizen, and U. Ebert, *Experiments on pulsed positive streamers in air*, 18th Symposium Plasma Physics & Radiation Technology, Lunteren, The Netherlands (oral presentation).
- J. Kos, G.J.J. Winands, T.M.P. Briels, E.M. van Veldhuizen, U. Ebert, *The behaviour of pulsed negative streamers in air and nitrogen*, 9th Euregional Workshop on the Exploration of Low Temperature Plasma Physics (WELT-PP), Kerkrade, the Netherlands (poster presentation).

2005

- T.M.P. Briels, E.M. van Veldhuizen, U. Ebert, *Experiments on the diameter of positive streamers in air*, XVIIth International Conference on Phenomena in Ionised Gases, Veldhoven, the Netherlands, 04-418 (proceedings and poster presentation).
- L.R. Grabowski, T.M.P. Briels, E.M. van Veldhuizen, A.J.M. Pemen, *Streamers in pulsed positive corona: low and high current regimes*, XVIIth International Conference on Phenomena in Ionised Gases, Veldhoven, the Netherlands, 04-425 (proceedings and poster presentation).

- E.M. van Veldhuizen, T.M.P. Briels, L.R. Grabowski, A.J.M. Pemen, U. Ebert, *Influences of the pulsed power supply on corona streamer appearance*, IInd International Workshop on Cold Atmospheric Pressure Plasmas: Sources and Applications, Bruges, Belgium (proceedings).
- T.M.P. Briels, E.M. van Veldhuizen, U. Ebert, *Experimental investigation and nanosecond imaging of streamers*, Workshop: The multiscale nature of spark precursors and high altitude lightning, Leiden, the Netherlands (oral presentation).
- T.M.P. Briels, E.M. van Veldhuizen, U. Ebert, *Time-resolved measurements on positive streamers in air at different pressures*, 17th Symposium Plasma Physics & Radiation Technology, Lunteren, the Netherlands (poster presentation).
- J. Kos, T.M.P. Briels, E.M. van Veldhuizen, U. Ebert, *The diameter of pulsed positive streamers in air*, 8th Euregional Workshop on the Exploration of Low Temperature Plasma Physics (WELT-PP), Kerkrade, The Netherlands (poster presentation).

2004

- T.M.P. Briels, E.M. van Veldhuizen, U. Ebert, *Experiments on propagating and branching positive streamers in air*, XVth International Conference on Gas Discharges and their Applications, Toulouse, France, 323-326 (proceedings and oral presentation).
- T.M.P. Briels, E.M. van Veldhuizen, U. Ebert, *Experimental investigation of propagating and branching discharge channels*, 16th Symposium Plasma Physics & Radiation Technology, Lunteren, The Netherlands (poster presentation).
- T.M.P. Briels, E.M. van Veldhuizen, and U. Ebert, *Experiments on growing positive ionization channels in air*, Symposium on Nonlinear Systems, Technische Universiteit Enschede, The Netherlands (poster presentation).
- T.M.P. Briels, E.M. van Veldhuizen, and U. Ebert, *Experiments on positive streamers in air at varying pressures and electrode distances*, School/Master class for molecular physics and plasma physics, Eindhoven, The Netherlands (poster presentation).
- T.M.P. Briels, E.M. van Veldhuizen, U. Ebert, *Experiments on positive streamers in air at varying pressures and electrode distances*, 7th Eurogional Workshop on the Exploration of Low Temperature Plasma Physics (WELT-PP), Kerkrade, The Netherlands (poster presentation).

2003

- T.M.P. Briels, E.M. van Veldhuizen, and U. Ebert, *Experimental investigation of propagating and branching discharges channels*, International WE-Heraeus Summer School "Low Temperature Plasma Physics: Basics and Applications" and Master Class: "Electronegative Plasmas", Physikzentrum Bad Honnef, Germany (poster presentation).
- T.M.P. Briels, E.M. van Veldhuizen, and U. Ebert, *Experimental investigation of propagating and branching discharges channels*, Workshop: Trends in Pattern Formation From

Amplitude Equations to Applications, Dresden, Germany (poster presentation).

Populair Scientific

2005

- *Bliksems onder de loep, het laatste nieuws*, interview with Tanja Briels and Ute Ebert by Bruno van Wayenburg, *Natuurwetenschap en Techniek*, volume 73, June 2005.
- *Mysteries van omhoog flitsende engelen*, interview with Tanja Briels, Eddie van Veldhuizen and Ute Ebert by Michael Persson, *Volkskrant*, Saturday 7 May 2005.

Dankwoord

Als eerste wil ik mijn dagelijkse begeleider Eddie van Veldhuizen en eerste promotor Ute Ebert bedanken voor de mogelijkheid om op dit onderwerp te kunnen promoveren, voor hun enthousiasme voor het overbrengen van kennis van streamers en andere relevante zaken en het geduld dat daar soms voor nodig was, voor de correcties op het proefschrift die me weer hebben aanzet tot nadenken over de stof en de vele dingen die ik nu vergeet op te noemen. Verder wil ik ook graag mijn tweede promotor en de overige leden van de leescommissie bedanken voor hun input ter verbetering van het proefschrift; Gerrit Kroesen, GertJan van Heijst, Hans-Erich Wagner en Klaus Boller: bedankt! En Freddy Manders, ik vond het leuk dat je mijn promotiecommissie compleet wilde maken.

Ook wil ik graag Marius Bogers, Frank van Hoof, Henk van Helvoirt, Ginny Fransenter Plegt en Han den Dekker van de werkplaats van de faculteit natuurkunde bedanken want zonder hen hadden de diverse stukken van mijn opstelling nooit zo goed in elkaar gepast. Ook de (oud)technici van de vakgroep, Charlotte Groothuis, Evert Ridderhof, Huib Schouten en Loek Baede bedankt voor het helpen met o.a. de (aansluiting van de) gassen, de computers, de electronica en de optiek in de opstelling. Charlotte, ik vind het leuk dat we ook buiten het werk nog contact hebben gehouden. Verder wil ik Eddie hier nogmaals bedanken maar nu voor zijn gigantische kennis van wat wel en niet handig is in de opstelling. Het heeft de metingen aanzienlijk verbeterd en het onderzoek versneld.

Alle (oud)medewerkers en (oud)studenten van de vakgroep EPG van de TU Eindhoven en van de groep MAS3 op het Centrum voor Wiskunde en Informatica in Amsterdam bedankt voor de gezelligheid in de afgelopen jaren. Ingrid Kieft en Tanya Nimalasuriya, ik vond het erg fijn dat ik jullie het merendeel van mijn promotie als kamergenoten heb gehad. Ik vond het leuk dat we over alledaagse dingen konden kletsen maar ook over de natuurkundige verschijnselen die ons bezig hielden. Rina Boom als secretaresse ben je natuurlijk onmisbaar maar ik vond het ook gezellig om zomaar je kamer binnen te kunnen lopen. Verder wil ik met name "mijn" afstudeerder Joost Kos en stagiaires Bert Lodewijks en Rob Schiffeleers bedanken voor de leuke tijd in het lab, voor het uitvoeren van de diverse experimenten, het meebouwen aan de opstelling en zelfs voor alle lastige vragen :-). Ik vond het fijn om

jullie begeleider te mogen zijn en ik heb veel van jullie geleerd. Ook wil ik Joost K. en Hans Winands bedanken voor het doen van aanvullende metingen terwijl ik met verlof was. Lukas Grabowski thank you for lending me your TLT-supply and for your cooperation with the first experiments on thick streamers. Sander Nijdam, bedankt voor je handige programmaatje voor het uitrekenen van diameters en snelheden. Succes met je promotie en ik ben erg benieuwd naar jouw toekomstige streamer resultaten. Hans W. en Guus Pemen, ik vond het erg fijn dat ik met al mijn vragen over hoogspanningstechniek en opstellingen bij jullie terecht kon. Bedankt! I would also like to thank Andrei Starikovskii for giving me the opportunity to come to MIPT in Dolgoprudny (near Moscow) and perform measurements in your laboratory. Also thanks to Masha Nudnova and all the other (Ph.D.) students who showed me Moscow, learned me how make a campfire and bake sausages above it, helped me in the supermarket, translated Russian to English and vice versa, cooked lunch and made my stay a time that I will never forget. Svetlana Starikovskaia, thank you for helping me when I went to Moscow all by myself and thanks to your daughter for showing me the Moscow State University.

Als laatste wil ik mijn (schoon)familie en vrienden bedanken. Sorry dat ik de laatste periode weinig tijd voor jullie heb gehad. Ik vond het erg fijn dat jullie er toch altijd waren als ik zin had om te kletsen. Mama, papa en Iris bedankt voor de eeuwige en onvoorwaardelijke liefde en steun bij alles wat ik in mijn leven heb ondernomen. Mam, ook nog bedankt voor het vele extra babysitten de afgelopen maanden zodat ik het proefschrift op tijd af kon krijgen. Menno bedankt voor de liefde, steun en hulp, zowel in de natuurkunde als daarbuiten, in de afgelopen 10.5 jaar en ook bedankt voor onze prachtige Sterre. Sterre, ik verwonder me steeds weer wat je iedere dag bij leert of opeens kunt; je laat zien dat je alles kunt bereiken als je maar doorzet. Ook bedankt voor het herontdekken van de wereld, niets is even logisch als het lijkt. Ik kan (en wil) me geen leven zonder jullie voorstellen!

Bedankt!

Tanja Briels, september 2007

Curriculum Vitae

5 January 1978

Born in Weert, the Netherlands

1990-1996

Secondary education at Bisschoppelijk College Weert

1996-2003

M.Sc. in Applied Physics at the Eindhoven University of Technology (TU/e):

-Traineeship at the Eindhoven University of Technology in the group Fluid Dynamics.

Subject: *Monopolen in een shear-stroming* (Monopolar vortices in a shear-flow), supervised by dr.ir. R.R. Trieling and prof.dr.ir. G.J.F. van Heijst.

-Traineeship at the University of Tromsø, Norway in the group Cosmic Geophysics.

Subject: *Nitrogen plasmas in Blaumann for rocket probe testing*, supervised by prof. Å. Fredriksen and prof. O. Havnes.

-Master's thesis project at the Royal Netherlands Meteorological Institute (KNMI) in the group Atmospheric Composition.

Subject: *Planetary wave propagation into the stratosphere*, supervised by dr.ir. P.C. Siegmund (KNMI), dr.ir. L.P.J. Kamp (TU/e) and prof.dr. H.M. Kelder (KNMI & TU/e).

Extracurricular activities include the membership of the Education Committee (OCN), the membership of the board of the student association of Applied Physics "J.D. van der Waals" and a student assistantship of the Student Education Organisation (STOOR), all of the Department of Applied Physics at TU/e.

2003-2007

Ph.D project at the Eindhoven University of Technology in the group Elementary Processes in Gas Discharges of the Department of Applied Physics.

Subject: *Exploring streamer variability in experiments*, supervised by dr.ir. E.M. van Veldhuizen and prof.dr. U. Ebert.

